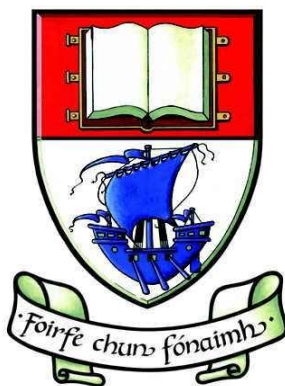


# **The Development and Characterisation of Microemulsions for the Separation of Pharmaceutical Analytes by HPLC and CE**



By  
Richie Ryan

Dept of Chemical & Life Sciences  
School of Science  
Waterford Institute of Technology  
Waterford, Ireland

Under the Supervision of  
Dr. Sheila Donegan, Dr. Kevin Altria & Dr. Joe Power

A dissertation submitted to Waterford Institute of Technology in partial fulfilment for  
the degree of Doctor of Philosophy, October 2011

**Declaration**

I hereby declare that this thesis, in partial fulfilment of the requirements for the Degree of Doctor of Philosophy, is my own work based on research carried out at the department of Chemical and Life Sciences, Waterford Institute of Technology between October 2006 and October 2011.

Richie Ryan

Date

## Acknowledgments

I would like to express a sincere thanks to my supervisors Sheila, Kevin and Joe who gave me excellent opportunities, guidance and support during this work. I have greatly enjoyed conducting my research, and owe much to their direction and confidence in me. I have learned a great deal from their expertise and feel truly honoured to have had the opportunity.

Thanks also to my separations colleague Eamon McEvoy for his help and informed discussions on all things science.

I would also like to thank the technicians for their assistance and for finding all the materials I needed throughout the years. Many thanks as well to my friends and colleagues in B21, and along the science corridor, they helped to make this a truly enjoyable experience.

Finally, the biggest thanks goes to my family. To my parents Edward and Helena, and brothers, William and Patrick for their constant support all along, especially throughout all my years in college. I owe them more than can ever be repaid. A special thanks also to Marlene for her support and encouragement, and putting up with talk of microemulsions and separation science since my research began.

To all who have accompanied and helped me along this journey, I express sincere thanks and can only hope to be of similar assistance to them in the future.

***'Ever tried. Ever failed. No matter. Try again. Fail again. Fail better.'***

*Samuel Beckett*

## **Abstract**

Microemulsions are unique dispersions of oil in water or water in oil which are stabilised by a surfactant and co-surfactant. The formation of such a mixture was first reported by Hoar and Schulman in the 1940s when they noticed a mixture of hydrocarbon and surfactant turned from milky to clear on the addition of alcohol. The ability of microemulsions to simultaneously solubilise either aqueous or organic components while remaining isotropically clear and thermodynamically stable attracted much attention, particularly in the 1970s for use in tertiary oil recovery. During the early 1990s these surfactant based systems were reported in separation science as mobile phases in HPLC and background electrolytes in CE.

Given the capability of microemulsions to dissolve both aqueous and non-aqueous compounds, their use as eluents in HPLC (MELC) and background electrolytes in CE (MEEKC) was further examined. In order to effectively test the ability of microemulsions to separate a diverse range of compounds, they were applied to the simultaneous analysis of oil- and water-soluble vitamins. A novel MELC method was developed for the simultaneous isocratic separation of oil- and water-soluble vitamins. Similarly, a MEEKC method was also developed for separating the same range of vitamins. In addition to separation, all microemulsion compositions examined in the development of the MEEKC method were characterised in terms of droplet size, surface tension, conductivity, and refractive index. When cross correlated with the MEEKC vitamin separation, relationships between choice of microemulsion components, physicochemical measurements and separation were observed.

Also, a commonly reported SDS based microemulsion was characterised and applied to the MEEKC separation of pharmaceutical analytes. Initially a pseudoternary phase diagram was constructed to establish a range of possible compositions. Microemulsions across an aqueous dilution line were prepared and physicochemical measurements conducted to establish microemulsion phase type and transition. Results indicated that the measurement techniques employed were capable of describing microemulsion phase type. Furthermore, it was seen that the microemulsion phase type could be correlated with a MEEKC separation.

<b>Contents</b>	<b>Page</b>
<b>Theoretical aspects and literature review</b>	<b>1</b>
<b>1.0 Surface tension and microemulsion formation</b>	<b>2</b>
1.1 Surface Activity and Interfacial Tension	3
1.2 Surface active agents (surfactants) and Gibbs' adsorption isotherm	4
1.3 Surfactants	5
1.3.1 Anionic surfactants	6
1.3.2 Cationic Surfactants	6
1.3.3 Non-ionic surfactants	7
1.3.4 Zwitterionic surfactants	8
1.4 Surfactant interaction at the interface and micellisation	9
1.5 The Micelle	9
1.6 The Critical Micelle Concentration (CMC)	10
1.7 Microemulsion formation	11
1.7.1 O/W and W/O microemulsions	13
1.8 References	15
<b>2.0 Application of microemulsion in HPLC</b>	<b>16</b>
2.1 Introduction	17
2.2 Advantages of MELC	18
2.3 Current separation application in O/W MELC	18
2.3.1 Calculation of partition coefficients (log P)	20
2.4 Operating parameters and optimisation of O/W MELC	23
2.4.1 Column Temperature	23
2.4.2 Column conditioning and equilibration	23
2.4.3 Oil content	24
2.4.4 Oil type	24
2.4.5 Surfactant concentration	25
2.4.6 Surfactant type	26
2.4.7 Microemulsion pH	27
2.4.8 Co-surfactant concentration	28
2.4.9 Co-surfactant type	28
2.5 Operating parameters and optimisation of W/O MELC	29
2.6 MELC Robustness	29
2.7 Gradient MELC	30
2.8 Eluent flow rate and column type	32
2.9 Conclusion	33
2.10 References	34

<b>3.0</b>	<b>Applications of microemulsion in CE</b>	<b>37</b>
3.1	Introduction	38
3.2	Principles of MEEKC	38
3.3	Comparison of MEEKC to MEKC	40
3.4	Online sample concentration techniques	41
3.4.1	FASI with high level salt matrices and ACN stacking	42
3.4.2	Borate complexation and acetonitrile sweeping	44
3.4.3	FASI-sweeping MEEKC with ASEI and CSEI	45
3.4.4	Effect of water and acid/basic plugs on online sample concentration	47
3.4.5	Online sample concentration and analyte functional group	48
3.4.6	FASI with suppressed EOF	48
3.4.7	Effect of microemulsion composition on online sample concentration	49
3.5	Operating Parameters in MEEKC	50
3.5.1	Buffer concentration and pH	52
3.6	Advances in chiral separations utilising MEEKC	52
3.6.1	Novel chiral selector complex	53
3.6.2	Effect of ME component purity on chiral separation	54
3.6.3	Chiral co-surfactant Vs achiral co-surfactant	54
3.6.4	Chiral separation using cyclodextrin-modified MEEKC	56
3.7	Recent developments in MEEKC-MS	57
3.7.1	MEEKC-ICP-MS	57
3.8	Improved Limits of Detection	58
3.9	Prediction of solute characteristics and partitioning mechanisms	58
3.9.1	Experimental design strategy	58
3.9.2	Microemulsion Structure	59
3.9.3	Calculating partition coefficients in MEEKC	60
3.10	Recent applications in MEEKC	61
3.10.1	Water analysis	64
3.10.2	Vitamin Analysis	64
3.10.3	Bioanalysis by MEEKC	65
3.10.4	Natural products analysis by MEEKC	66
3.10.5	Detection of antibiotics by MEEKC	66
3.11	W/O MEEKC	67
3.12	Conclusion	67
3.13	References	69
<b>4.0</b>	<b>Microemulsion characterisation</b>	<b>75</b>
4.1	Introduction	76
4.2	Scattering techniques	76
4.2.1	The basic principle	77

4.2.2	Small angle scattering models	78
4.2.2.1	Particulate Model	78
4.2.2.2	Concentrated systems and generalised indirect Fourier transform method (GIFT)	79
4.2.2.3	Teubner-Strey model and bicontinuous systems	80
4.3	SANS and SAXS Applications	81
4.4	Dynamic Light Scattering (DLS)	84
4.5	DLS applications	85
4.6	NMR	86
4.7	NMR applications	88
4.8	Scanning and Transmission electron microscopy (SEM/TEM)	88
4.9	Differential scanning calorimetry (DSC)	91
4.10	Conductivity	93
4.11	Density and surface tension	96
4.12	Empirical calculations	97
4.13	Conclusion	97
4.14	References	99

## **Experimental** **103**

### **5.0 Analysis of oil- and water-soluble vitamins by MELC** **104**

5.1	Introduction	105
5.2	Experimental	106
5.2.1	Chemicals	106
5.2.2	Microemulsion components	106
5.2.3	Instrumentation	108
5.3	Method development	108
5.3.1	Microemulsion preparation	108
5.3.2	Vitamin solubility	108
5.3.3	Preparation of vitamin standards and UV spectra	109
5.3.4	Analysis of vitamins using standard microemulsion	109
5.3.4.1	Chromatographic conditions	109
5.3.5	Analysis of vitamin E on the HP1050 with traditional aqueous/organic solvents	109
5.3.5.1	Chromatographic conditions	109
5.3.6	Analysis of vitamins using THF modified microemulsion	110
5.3.6.1	Sample preparation	110
5.3.6.2	Chromatographic conditions	110
5.3.7	Variation of oil phase for separation of water and oil-soluble vitamins	111
5.3.7.1	Chromatographic conditions	111
5.3.8	Effect of pH on the separation of water soluble vitamins	111
5.3.8.1	Chromatographic conditions	112

5.3.9	Effect of co-surfactant on the vitamin separation	112
5.3.9.1	Chromatographic conditions	112
5.3.10	Effect of column length on vitamin separation	112
5.3.10.1	Chromatographic conditions	112
5.3.11	Validation of vitamin preparation	113
5.3.11.1	Specificity	113
5.3.11.2	Linearity	113
5.3.11.3	Assay	114
5.3.11.4	Precision and Repeatability	114
5.3.11.5	Accuracy	115
5.3.11.6	Limit of Detection (LOD)	115
5.3.11.7	Limit of Quantitation (LOQ)	115
5.4	Results	115
5.4.1	Solubility of vitamins and UV detection	115
5.4.2	Analysis of vitamins using standard microemulsion	116
5.4.3	Analysis of vitamin E on the 1050LC with traditional aqueous/organic solvents	117
5.4.4	Analysis of vitamins using THF modified microemulsion	117
5.4.5	Variation of oil phase for separation of water and oil- soluble vitamins	118
5.4.6	Effect of pH on the separation of water soluble vitamins	119
5.4.7	Effect of co-surfactant on the vitamin separation	120
5.4.8	Effect of column length on vitamin separation	122
5.4.9	Validation	122
5.5	Discussion	124
5.5.1	Solubility of vitamins	124
5.5.2	Analysis of vitamins using MELC with the standard microemulsion	124
5.5.3	Analysis of vitamin E on the HP1050 with traditional aqueous/organic solvents	125
5.5.4	Analysis of vitamins using THF modified microemulsion	125
5.5.5	Variation of oil phase for separation of water soluble vitamins	126
5.5.6	Effect of pH on water soluble vitamins	126
5.5.7	Effect of co-surfactant on the vitamin separation	127
5.5.8	Analytical column length	127
5.5.9	Validation of vitamin preparation	128
5.5.9.1	Gradient Elution Option	128
5.5.9.2	Development of method for oil- or water- soluble vitamins	129
5.6	Conclusion	129
5.7	References	130

<b>6.0</b>	<b>Analysis of oil and water-soluble vitamins by MEEKC</b>	<b>132</b>
6.1	Introduction	133
6.2	Experimental	133
6.2.1	Chemicals	133
6.2.2	Microemulsion components	134
6.2.3	Instrumentation	135
6.3	Method development	135
6.3.1	Microemulsion preparation	137
6.3.2	Sample preparation	135
6.3.3	Initial conditions	135
6.3.4	Variation of oil phase type	136
6.3.5	Variation of co-surfactant type	136
6.3.6	Variation of SDS concentration	136
6.3.7	Co-surfactant concentration	136
6.3.8	Addition of organic modifiers	136
6.3.9	Addition of $\alpha$ -cyclodextrin	136
6.3.10	Addition of sodium cholate	137
6.3.11	Variation of surfactant type	137
6.3.12	Mixed surfactant system	137
6.3.13	CTAB microemulsion with addition mixed of organic modifiers	137
6.3.14	Sodium cholate microemulsion	137
	6.3.14.1 Sodium cholate microemulsion with the addition of organic modifiers	138
	6.3.14.2 Sodium cholate ME with SDS and increased butanol concentration	138
	6.3.14.3 Sodium cholate ME with increased butanol and addition of organic modifiers	138
6.4	Results and discussion	138
6.4.1	Optimising initial conditions	138
6.4.1.1	Sodium tetraborate concentration	138
6.4.1.2	Applied voltage	138
6.4.1.3	Capillary cassette temperature	140
6.4.1.4	Rinsing procedure	141
6.4.2	Variation of oil phase type	142
6.4.3	Variation of co-surfactant type	145
6.4.4	SDS concentration	148
6.4.5	Addition of organic modifiers	150
6.4.6	Addition of mixed modifiers	154
6.4.7	Addition of $\alpha$ -CD	154
6.4.8	Surfactant type	154
6.4.8.1	Sodium cholate	154
6.4.8.2	Mixed surfactant system	155

	6.4.8.3 CTAB	155
	6.4.8.4 CTAB microemulsion with addition of organic modifiers	156
	6.4.8.5 Sodium cholate microemulsion with the addition of organic modifiers	156
	6.4.8.6 Sodium cholate ME with increased butanol concentration	157
	6.4.8.7 Sodium cholate ME with increased butanol and addition of organic modifiers	158
6.5	Conclusion	159
6.6	References	161

## **7.0 Characterisation of microemulsion for the separation of oil and water-soluble vitamins by MEEKC 163**

7.1	Introduction	164
7.2	Experimental	164
	7.2.1 Microemulsion components	164
	7.2.2 Microemulsion preparation	165
	7.2.2.1 Variation of oil phase type	165
	7.2.2.2 Variation of co-surfactant type	165
	7.2.2.3 Variation of SDS concentration	165
	7.2.2.4 Co-surfactant concentration	165
	7.2.2.5 Addition of organic modifiers	166
	7.2.2.6 Variation of surfactant type	166
	7.2.2.7 Mixed surfactant system	166
	7.2.3 Instrumentation	166
	7.2.3.1 Droplet Size	166
	7.2.3.2 Conductivity	166
	7.2.3.3 Surface Tension	166
	7.2.3.4 Refractive Index	167
7.3	Results and discussion	167
	7.3.1 Variation of oil phase type	167
	7.3.1.1 Surface tension	167
	7.3.1.2 Droplet size	168
	7.3.1.3 Conductivity	169
	7.3.1.4 Correlation with separation	169
	7.3.2 Variation of co-surfactant type	170
	7.3.2.1 Surface tension	170
	7.3.2.3 Droplet size	170
	7.3.2.4 Conductivity	171
	7.3.2.5 Correlation with separation	171
	7.3.3 SDS concentration	172
	7.3.3.1 Surface tension	172

	7.3.3.2 Droplet size	172
	7.3.3.3 Conductivity	173
	7.3.3.4 Correlation with separation	173
7.3.4	Co-surfactant concentration	174
	7.3.4.1 Surface tension	174
	7.3.4.2 Droplet size	174
	7.3.4.3 Conductivity	175
	7.3.4.4 Correlation with separation	175
7.3.5	Addition of ACN	175
	7.3.5.1 Surface Tension	175
	7.3.5.2 Droplet size	176
	7.3.5.3 Conductivity	177
	7.3.5.4 Correlations with separation	177
7.3.6	Addition of methanol	177
	7.3.6.1 Surface Tension	177
	7.3.6.2 Droplet size	178
	7.3.6.3 Conductivity	178
	7.3.6.4 Correlations with separation	178
7.3.7	Addition of IPA	178
	7.3.7.1 Surface Tension	178
	7.3.7.2 Droplet size	179
	7.3.7.3 Conductivity	180
	7.3.7.4 Correlations with separation	180
7.3.8	Addition of mixed modifiers	180
7.3.9	Surfactant type	181
	7.3.9.1 Surface tension	181
	7.3.9.2 Droplet size	182
	7.3.9.3 Conductivity	183
	7.3.9.4 Correlations with separation	183
7.4.	Conclusion	184
	7.4.2 Surface tension	184
	7.4.1 Droplet size	185
	7.4.3 Conductivity	186
	7.4.4 General correlations and limitations	187
7.5	References	189
<b>8.0</b>	<b>Characterisation of SDS based microemulsion</b>	<b>190</b>
8.1	Introduction	191
8.2	Experimental	191
	8.2.1 Phase Diagram	191
	8.2.2 Sample preparation	193
	8.2.3 Droplet Size	193
	8.2.4 Surface Tension	194

8.2.5	Conductivity	194
8.2.6	Refractive index	194
8.2.7	DSC	194
8.2.8	MEEKC separation	194
8.3	Results and discussion	195
8.3.1	Particle size	195
8.3.2	Surface Tension	196
8.3.3	Refractive index	197
8.3.4	Conductivity	198
8.3.5	DSC	198
8.3.6	MEEKC separation	200
8.4	Conclusions	203
8.5	References	205
<b>9.0</b>	<b>Conclusions and future work</b>	<b>206</b>
9.1	Microemulsion liquid chromatography (MELC)	207
9.2	Microemulsion electrokinetic chromatography (MEEKC)	208
9.3	Comparison of MELC and MEEKC	209
9.4	Microemulsion characterisation	209
9.5	Future Work	211
9.5.1	MELC	211
9.5.1.2	Gradient onset	211
9.5.1.3	Robustness testing Experimental design (QbD)	211
9.5.1.4	Compatibility of MELC with different stationary phases	211
9.5.1.5	Rapid Resolution MELC	212
9.5.1.6	Method for extremes or intermediate polarity analytes	212
9.5.2	MEEKC	213
9.5.2.1	Online sample concentration/MS/fluorescence	213
9.5.2.2	Streamlining method development	213
9.5.3	Microemulsion characterisation	213
<b>Appendix</b>		<b>214</b>

### **Publications**

Microemulsion HPLC, Ryan, R., Donegan, S., Power, J., McEvoy, E., Altria, K., LCGC, October (2008) 504-513.

Recent advances in the methodology, optimisation and application of MEEKC, Ryan, R., Donegan, S., Power, J., McEvoy, E., Altria, K., Electrophoresis, 30 (2009) 65-82.

Advances in the theory and application of MEEKC, Ryan, R., Donegan, S., Power, J., Altria, K., Electrophoresis, 31 (2010) 755-767.

Recent developments in the methodology and optimisation of MEEKC, Ryan, R., Donegan, S., Power, J., McEvoy, E., Altria, K., *Electrophoresis*, 32 (2011) 184-201

## **Section 1**

### **Theoretical aspects and literature review**

# **Chapter One**

## **Surface tension and microemulsion formation**

## 1.1 Surface Activity and Interfacial Tension

All surface activity is based on and studied at the interface between two phases. An interphase is the boundary between two bulk phases.

Since this body of work is concerned with liquid phases the discussion will be centred mainly on liquid-air and liquid-liquid interphases.

For a stable interface between two phases to exist the free energy of formation must be positive. A zero or negative free energy would result in the continuous expansion of the surface until one region disperses into another e.g. two miscible liquids [1].

Surface tension and interfacial tension are used in conjunction with Gibbs free energy to describe the action occurring at the interface. Surface tension refers to the energy required to expand the surface of a liquid by unit area at the liquid air interface. Interfacial tension refers to the surface tension at the interface separating two non-miscible liquids. Surface tension is the result of excess free energy created by un-bonded or non-interacting parts of a molecule at the surface of a liquid compared to the bulk phase. The surface area of such a liquid is reduced in order to minimise this excess free energy [1].

Surface tension is directly related to the cohesive energy of a substance, the higher the cohesive properties the higher the surface tension. Hence, solid materials have a very high surface tension compared to liquids, and a gas has no surface tension as molecules in the gas phase have no cohesive energy. Cohesive energy between molecules becomes smaller with increasing temperature and hence surface tension decreases with increasing temperature [1;2].

The relationship between surface tension, interfacial tension and free energy can be described when two liquids A and B come together and form an interface. The attractive forces between A and B offset against the excess free energy and lower the surface tension of both liquids. This relationship is summarised in Equation 1.1[1].

$$\gamma_{AB} = \gamma_A + \gamma_B - 2\sigma_{AB} \quad \text{Equation 1.1[1]}$$

Where  $\gamma_{AB}$  is the interfacial tension between A and B,  $\gamma_A$  and  $\gamma_B$  represent the surface tension of A and B respectively and the  $\sigma_{AB}$  is attractive cohesive energy between A and B.

When the two liquids A and B possess similar intermolecular interactions (e.g. Van der Waals) then  $\sigma_{AB} = (\gamma_A\gamma_B)^{1/2}$ . This allows the interfacial tension at the interface to be calculated from the surface tension of A and B respectively. When  $\sigma_{AB}$  is equal to either  $\gamma_A$  or  $\gamma_B$  then  $\gamma_{AB}$  is the difference in surface tension between A and B (e.g. water and octane). In water and octane the intermolecular interactions in both liquids are Van der Waals forces. The interfacial tension,  $\gamma_{AB}$ , is caused by the imbalance in hydrogen bonding within the water molecules and this is not offset by interaction with the organic octane molecules.

In the case between some alcohols and water, the interfacial tension is very low. The OH group of the alcohol orientates towards the water phase and hydrogen bonding occurs. Strong H-bonding leads to an increase in  $\sigma_{AB}$  and hence a decrease in  $\gamma_{AB}$ , if  $\sigma_{AB}$  was to become sufficiently large then  $\gamma_{AB}$  would become negative with the implication of no interface and result in a true solution (miscibility)[3].

## 1.2 Surface active agents (surfactants) and Gibbs' adsorption isotherm

Any additive to a liquid can have an effect on the surface tension. For example inorganic salts have the effect of increasing the surface tension of water while methanol lowers it. Additives that lower the surface tension are known as surface-active agents and are commonly called surfactants [1;3].

Surfactants act by adsorbing onto the surface of the solution or at the interface between two solutions. The amount of surfactant that adsorbs onto the solution is given by Gibbs' adsorption isotherm in equation 1.2[1].

$$\frac{d\gamma}{d\mu} = \frac{-1}{RT} \frac{d\gamma}{d \ln a} = \Gamma \quad \text{Equation 1.2 [1]}$$

Where,

$\gamma$  = surface tension of solution.

$\mu$  and  $a$  = chemical potential and activity of the solute in solution.

$\Gamma$  = adsorption amount at the surface.

R and T = ideal gas and temperature constants respectively.

If the concentration of surfactant, C, is low enough the equation can be written as Equation 1.3 [1];

$$\frac{-1}{RT} \frac{d\gamma}{d \ln C} = \Gamma \quad \text{Equation 1.3 [1]}$$

Equation 1.3 implies that the more efficiently the surfactant adsorbs onto the surface of the solution the greater the drop in surface tension (the less concentration of surfactant required to bring about the desired effect). The adsorption of surfactant occurs due to the free energy gain (energy decrease in system) which can be achieved, in this case by lowering the surface tension.

Lowering of surface tension results in the  $\Gamma$  term being more positive. Conversely, a rise in surface tension results in a negative value for  $\Gamma$ . [1]

### 1.3 Surfactants

A surfactant is a chemical compound known technically as an amphiphile. An amphiphilic compound contains two parts, a hydrophilic head group (a dipole or charged group) and a hydrophobic tail (usually a hydrocarbon chain). Each part of the molecule has therefore very different solubility characteristics and in solution partitions itself at the interface between two phases. The polar head group partitions in the polar phase and the non-polar tail partitions in the more non-polar phase.

There are various different types of surfactant and they are classified by the charge on the polar head group. The general classes are;

Anionics  $\Rightarrow$  negatively charged

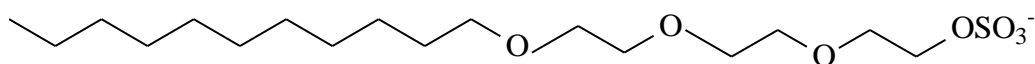
Cationics  $\Rightarrow$  positively charged

Non-ionics  $\Rightarrow$  no net charge

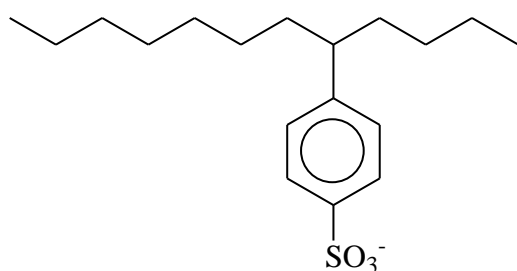
Zwitterionics  $\Rightarrow$  both positively and negatively charged [3]

### 1.3.1 Anionic surfactants

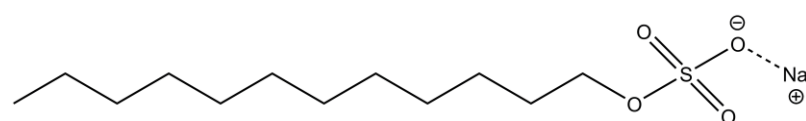
These surfactants are a type of electrolyte and when they dissociate in aqueous solution the surface active ion is negative (anion). They are used as strong detergents and as high foaming agents. They are the largest class of surfactant and generally not compatible with cationics, although there are exceptions. While they are sensitive to hard water a short polyoxyethylene chain between the anionic group and hydrocarbon tail improves salt tolerance. Their solubility in organic solvents is improved by the addition of a polyoxypropylene chain between the head group and the hydrocarbon chain. The most common counterions used are sodium, potassium, calcium and various protonated alkyl amines. Sodium and potassium are used to give water solubility while calcium and magnesium promote oil solubility. Figure 1.1 shows a schematic representation of some anionic surfactants. [1;3]



**Alkyl ethersulphate**



**Alkylbenzene sulphonate**



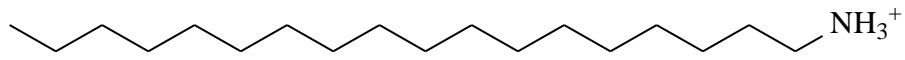
**Sodium dodecyl sulphate**

**Figure 1.1 General structure of anionic surfactants. [3]**

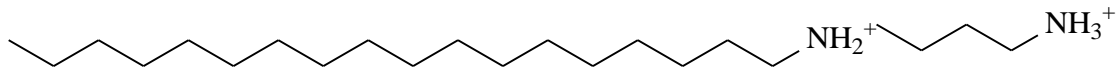
### 1.3.2 Cationic Surfactants

Cationic surfactants are electrolytes with a positive charge. Their hydrophilic head group acts by orientating itself towards the surface of the material interface. They adsorb strongly to negatively charged materials and are derivatives of alkylamines.

They are generally not compatible with anionics, but there are exceptions. Figure 1.2 shows a schematic representation of some cationic surfactants. [3]



**Fatty amine salt**



**Fatty diamine Salt**

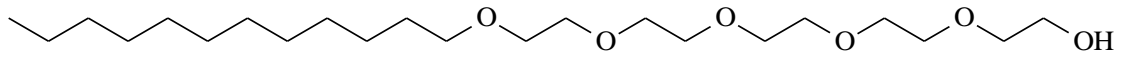


**CTAB**

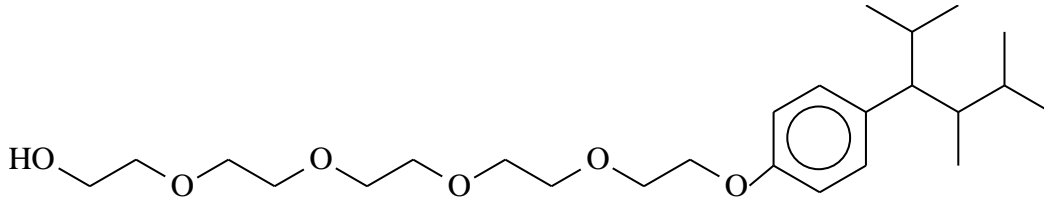
**Figure 1.2 General structure of cationic surfactants. [3]**

### 1.3.3 Non-ionic surfactants

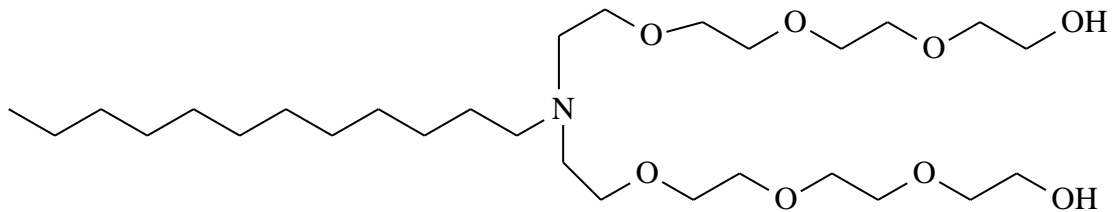
Non-ionic surfactants are not electrolytes and their hydrophilic head group does not dissociate in solution. They are tolerant to aqueous solutions, salts and hard water conditions. They generally have a polyether or polyhydroxyl as their polar group. The polar polyether head group is synthesised from the polymerisation of ethylene oxide. Unlike anionic and cationic surfactants non-ionics are compatible with all other types of surfactant. Also their physicochemical properties are not affected by electrolytes. Figure 1.3 shows a schematic representation of some non-ionic surfactants. [3]



**Fatty alcohol ethoxylate**



**Alkylphenol ethoxylate**



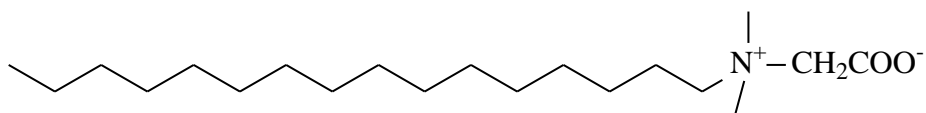
**Fatty amine ethoxylate**

**Figure 1.3 General structure of non-ionic surfactants. [3]**

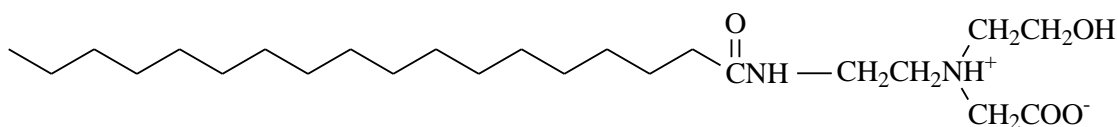
### 1.3.4 Zwitterionic surfactants

Zwitterionic surfactants are composed of two charged groups with a different charge. The positive charge is usually an ammonium ion and the negative charge is generally a carboxylate group. Like non-ionics they are compatible with all classes of surfactant and are not sensitive to hard water. They are relatively stable in acidic and basic solutions.

Often referred to as amphoteric surfactants, but this is somewhat misleading. In an amphoteric surfactant the nature of the ion changes with the pH of the solution and therefore an amphoteric surfactant can be anionic, non-ionic, cationic or zwitterionic. A zwitterionic surfactant only exists within a certain pH range depending on the pKa of that particular surfactant. Figure 1.4 shows the schematic representation of some zwitterionic surfactants. [3]



**Betaine**



**Imidazoline**

**Figure 1.4** General structures of zwitterionic surfactants. [3]

### 1.4 Surfactant interaction at the interface and micellisation

As mentioned in section 1.2, surfactants act by adsorbing at the interface and the amount adsorbed is a function of Gibbs' adsorption isotherm. As explained in the nature of the surfactant, the part of the surfactant which adsorbs onto the interface is dependent on the nature of the bulk phase and the type of surfactant being used. Depending on the concentration of surfactant in the aqueous solution different types of structures may form, such as micelles.

Taking an anionic surfactant added to water (bulk phase) as a model, the surfactant will adsorb at the air water interface as an orientated monolayer. The hydrophilic head will be orientated towards the aqueous phase while the hydrophobic tail will be orientated towards the air phase. This occurs to avoid unfavourable interactions and minimise the free energy of the system. Figure 1.5 shows a schematic of the anionic surfactants orientation in the aqueous phase. Aggregation among surfactant molecules also occurs in order to minimise the free energy of the system. Aggregation occurs because the interface becomes packed with surfactant monomer, this aggregation results in the formation of micelles. In a micelle the hydrophobic tails associate together in order to avoid interaction with the aqueous bulk phase, the hydrophilic heads orientate towards the bulk phase. Figure 1.6 shows a schematic of a micelle.

### 1.5 The Micelle

The micelle is a separated liquid phase and proof of this is obtained from Gibbs' adsorption isotherm. The ' $\Gamma$ ' term in the equation measures the amount of surfactant adsorbed at the interface and up to a certain point there is a drop in surface tension. At

a certain concentration (break point) the graph levels off, but at this point further addition of surfactant shows  $\Gamma$  to be zero. The fact that surfactant concentration does not appear to increase when surfactant is added is thermodynamic proof of surfactant separation. [3]

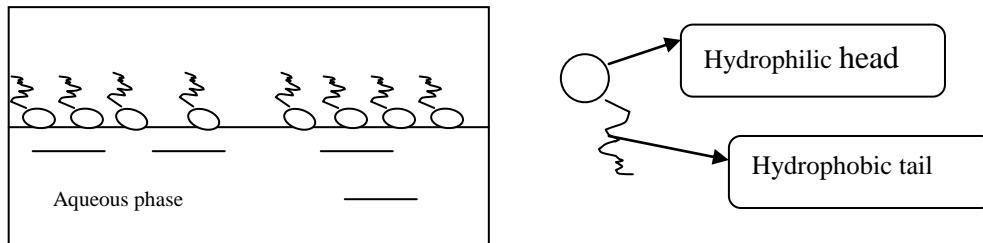


**Figure 1.5** Anionic surfactant orientating as a monolayer when added to an aqueous phase.

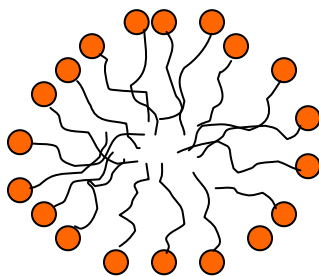


**Figure 1.6** Schematic of micelle

## 1.6 The Critical Micelle Concentration (CMC)

Gibbs' isotherm is used to calculate the amount of surfactant adsorbed at the interface. Up to a certain concentration there is a drop in surface tension. However, at a certain concentration there is no further drop in surface tension. After this point Gibbs' isotherm cannot be used to measure the amount of surfactant adsorbed, as it will give a result of zero, which is not possible, if it is known that more surfactant is being added. This point represents a critical concentration of surfactant, where there are enough micelles present in the bulk phase to change the overall nature of the system. This concentration of surfactant is known as the critical micelle concentration (CMC) and its changes on the physicochemical characteristics of the system have been well documented.

## 1.7 Microemulsion formation

Microemulsions can be seen as an extension of the micellar system. The formation of a microemulsion was first observed about 60 years ago when Schulman and Hoar [4] noted a mixture of water, surfactant and hydrocarbon turned from cloudy to clear on the addition of alcohol. Some years later Schulman coined the term microemulsion to describe this unique mixture of oil and water.

The microemulsion (ME) results from the mixture of oil, water, surfactant and co-surfactant. Microemulsions have a complicated phase behaviour [5] and the formation of an oil-in-water (O/W) or water-in-oil (W/O) system is possible. Either occurs when each component is present at a specific concentration. There are three general classifications of microemulsion based on the system proposed by Winsor [6].

Phase 1: Oil -in -water (O/W) where the surfactant is more soluble in water and is labelled as Winsor I.

Phase 2: Water- in -oil (W/O) where surfactant has a greater solubility in the oil phase, labelled as Winsor II.

Phase 3: This is a middle (bicontinuous) phase microemulsion and the surfactant is equally soluble in both the water and oil phases. This type is labelled as Winsor III.

Figure 1.7 shows a typical phase diagram indicating the regions where all three compositions occur [7] .

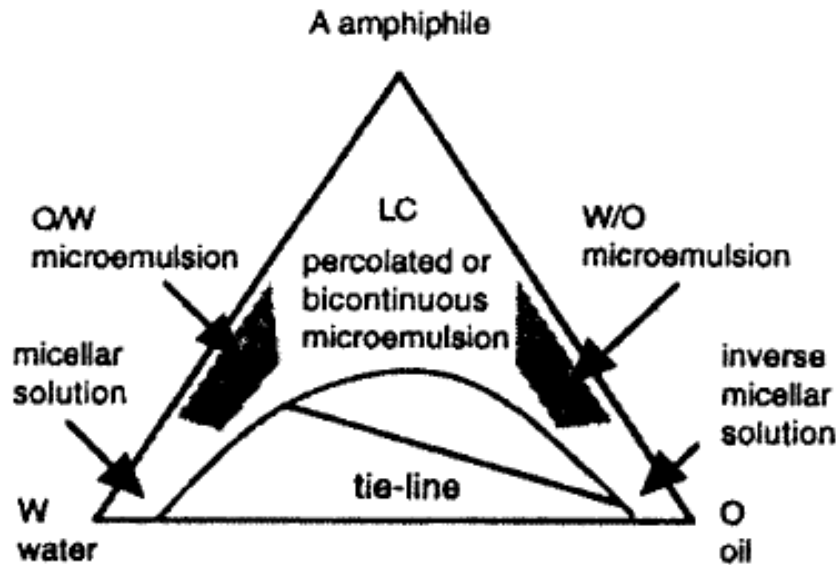


Figure 1.7 Phase diagram of water, surfactant (amphiphile) and oil system. [7]

Equation 1.4 was put forward by Ruckenstein [8] to explain the thermodynamics of microemulsion formation based on Gibbs' free energy equation.

$$\Delta G_m = \Delta G_1 + \Delta G_2 + \Delta G_3 - T\Delta S \quad \text{Equation 1.4 [8]}$$

$\Delta G_m$  is the free energy of microemulsion formation

$\Delta G_1$  is the free energy change due to the increase in surface area

$\Delta G_2$  is the free energy change due to the interaction between droplets

$\Delta G_3$  is the free energy change due to adsorption of surfactant molecules at the oil water interface

T = temperature

$\Delta S$  = the increase in entropy due to the dispersion of droplets.

The overall sum of the free energy changes on the right hand side of Equation 1.4 will determine if microemulsion formation will occur. If  $\Delta G_m$  is negative then spontaneous dispersion will lead to formation of microemulsion droplets. An increase in overall free energy of the system due to decreasing particle size may be offset by the  $T\Delta S$  term. Since the number of microemulsion particles increases with decreasing particle size,  $T\Delta S$  becomes more favourable with decreasing size [9]. The spontaneous dispersion of one phase into another liquid phase can only occur if the interfacial tension between the

two phases is so low that  $\Delta S$  can dominate the total energy of the system. Although surfactants can lower the interfacial tension between oil and water substantially, the nature of the head group will usually lead to the formation of fairly rigid interfacial films and limited surfactant mobility in the film, and hence reduce the curvature of the droplet, preventing the formation of small droplets [3]. The addition of a co-surfactant usually in the form of a short or medium chain length alcohol can reduce the rigidity of the interfacial film and increase adsorption at the surface.

Equation 1.5 relates the amount of surfactant material adsorbed at the interface to the interfacial tension of the system.

$$\delta\sigma = -\Gamma_i RT \delta(\ln C_i) \quad \text{Equation 1.5}$$

$\sigma$  = interfacial tension of a system

$\Gamma_i$  = the surface excess of component i at the interface

$C_i$  = concentration of component i in bulk solution

R = gas constant

T = temperature

The maximum value of  $\Gamma_i$  possible for a single surfactant system is usually limited by solubility and/or CMC so that the amount of surfactant adsorbed onto the interface is not usually enough to reduce the interfacial tension adequately for spontaneous microemulsion formation. The addition of medium chain alcohols (co-surfactants) to surfactant systems results in an increase in their CMC and water solubility, thereby increasing the amount of surfactant molecules at the interface. Because of the relatively small size of the alcohol molecules compared to the surfactant molecules, they can efficiently pack themselves between the surfactant molecules at the interface, reducing the electrostatic and steric interactions between the surfactant head groups. This results in a densely packed interfacial layer and a much higher value of  $\Gamma_i$  making the interfacial energy sufficiently low for spontaneous microemulsion formation.

### 1.7.1 O/W and W/O microemulsions

In an O/W microemulsion the dispersed oil is stabilised by the surfactant molecules and co-surfactant molecules. A typical and widely used O/W system [5;10] is that of octanol (oil phase), water (bulk phase) sodium dodecyl sulphate (SDS surfactant) and butanol (short chain alcohol co-surfactant). The surfactant is present well in excess of

its critical micelle concentration (CMC) and the oil phase partitions itself inside the resultant surfactant micelles. This ensures that the interfacial tension between the oil and water is reduced sufficiently. The co-surfactant molecules position themselves between the head groups of the surfactant micelles which reduces the electrostatic repulsion and results in the overall ultra-low surface tension required for the spontaneous formation of the microemulsion. Figure 1.8 shows a schematic representation of an O/W microemulsion droplet. For the W/O microemulsion the water droplet positions itself inside the resultant reversed micelles.

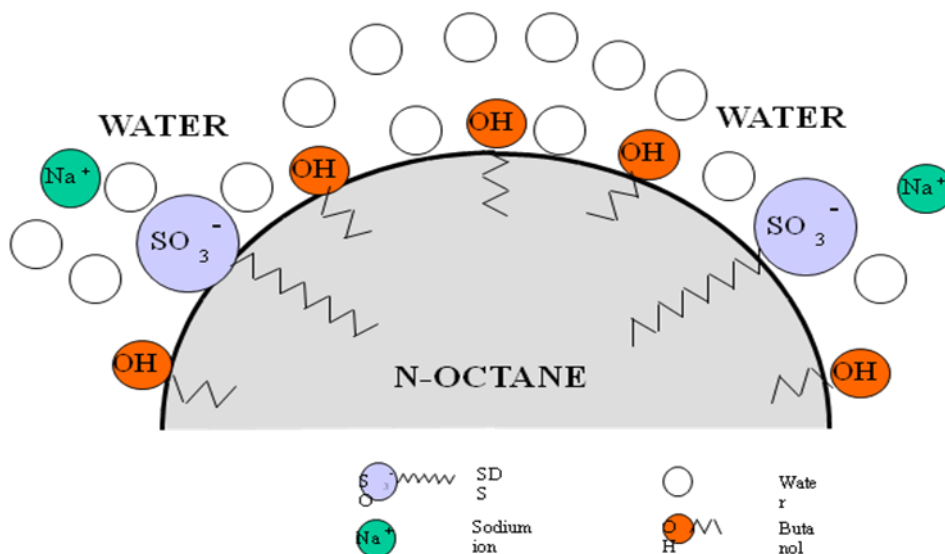


**Figure 1.8** Schematic representation of an O/W microemulsion droplet.

In comparison to micellar systems where neither co-surfactant nor oil are present, microemulsion systems offer many advantages. The presence of the co-surfactant and particularly the oil result in microemulsions having greater solubilising power for both polar and non polar compounds. They therefore offer the ability to directly solubilise hydrophobic samples and matrices, such as creams and waxes, without lengthy pre-extraction steps. The water insoluble samples are dissolved by the hydrophobic oil core of the microemulsion droplet, aided by the non polar surfactant and co-surfactant components while the water soluble samples are simultaneously dissolved into the aqueous region of the microemulsion.

## 1.8 References

- [1] Tsujii, K Surface Activity, Principles, Phenomena, and Applications. Academic Press, San Diego, 1998.
- [2] Iampietro, D.J., and Kaler, E.W., *Langmuir*, 15 (1999) 8590-8601.
- [3] Myers, D Surfaces, Interfaces, and Colloids. John Wiley & Sons, New York, 1999.
- [4] Hoar, T.P., and Schulman, J.H., *Nature*, 152 (1943) 102-103.
- [5] Altria, K., Broderick, M., Donegan, S., Power, J., *Chromatographia*, 62 (2005) 341-348.
- [6] Winsor, P.A., *Transactions of the Faraday Society*, 44 (1948) 376-398.
- [7] Altria, K.D., Mahuzier, P.E., Clark, B.J., *Electrophoresis*, 24 (2003) 315-324.
- [8] Ruckenstein, E., and Chi, J.C., *Journal of the Chemical Society-Faraday Transactions II*, 71 (1975) 1690-1707.
- [9] Heimenz, P.C. and Rajagopalan, R., (1997) Principles of Colloid and Surface Chemistry. Marcel Decker, New York.
- [10] Marsh, A., Clark, B.J., Altria, K.D., *Journal of Separation Science*, 28 (2005) 2023-2032.

## **Chapter Two**

### **Application of microemulsions in HPLC**

## 2.1 Introduction

Microemulsions have been employed as novel eluents in HPLC systems giving rise to the technique Microemulsion Liquid Chromatography (MELC) [1-4]. In MELC a microemulsion mobile phase is used with conventional HPLC columns. Generally O/W microemulsions are used with reverse phase columns, while W/O microemulsions are used with normal phase columns.

W/O MELC was first reported in 1986 by Hernandez-Torres et al. [5] using normal phase LC, however, there was no subsequent reports of its use until a more in depth investigation was conducted by Broderick et al. [1]. They optimised a W/O MELC method which was found to be suitable for the separation of compounds in a complex hydrophobic matrix and results compared well with an established reverse phase HPLC method [6].

O/W MELC using reversed phase columns has been more widely documented since it first appeared in literature in 1992, when its use was reported by Berthod et al. [7;8]. More recently, Marsh et al. [9] outlined the effects of changing various operating and microemulsion parameters on MELC separations.

MELC is an extension of micellar liquid chromatography (MLC) which was introduced by Armstrong and Henry in 1980 [10]. In MLC a surfactant is added in excess of the critical micelle concentration (CMC) with the result that the mobile phase contains a large amount of micelles. The micelles affect the chromatography as analytes partition with the micelles rather than adsorb onto the stationary phase. In the O/W microemulsion the dispersed oil droplets are stabilised by the surfactant molecules and co-surfactant molecules. The surfactant is present at concentrations well in excess of its CMC and the oil phase positions itself inside the resultant surfactant micelles. This reduces the interfacial tension between the oil and water. The co-surfactant molecules position themselves between the head groups of the surfactant molecules which reduces the electrostatic repulsion between them and results in the overall ultra-low surface tension required for the spontaneous formation of the microemulsion. Sodium dodecyl sulphate (SDS) is a common and widely used [3;4;9] surfactant, with medium chain alcohols such as butanol or pentanol common co-surfactants.

## **2.2 Advantages of MELC**

Microemulsions have the ability to dissolve hydrophobic samples and matrices without lengthy pre-extraction steps required in conventional HPLC. This characteristic has been widely exploited by several authors [1;3;4;9;11;12]. O/W MELC also offers alternative partitioning mechanisms. As in MLC, the stationary phase of the RP-HPLC column is coated with the surfactant present in the microemulsion which affects the stationary phase interactions. A secondary partitioning mechanism is created by the presence of the oil droplets, and solutes partition between the aqueous phase, the oil droplets and the stationary phase of the column. Water insoluble compounds tend to reside in the oil droplet, while water soluble compounds reside mainly in the aqueous phase. Separation is also affected the stationary phase interactions. MELC does not appear to suffer from the same efficiency problems encountered in MLC [10]. Also, as many compounds do not have strong chromophores they need to be analysed at low wavelengths. MELC can be used to analyse compounds at wavelengths as low as 190 nm. This property showed a significant advantage over conventional HPLC where most mobile phases absorb in this region.

## **2.3 Current separation application in O/W MELC**

While there has been a relatively large amount of publications on the potential use of microemulsions as a separation media in HPLC [1;5;7-10], there have been only a few papers published on fully optimised and validated methods [2;3;12;13]. Table 2.1 provides a summary of current applications and the microemulsion compositions used. McEvoy et al. [3] optimised an O/W MELC method for the determination of paracetamol content in a suppository formulation. This method gave excellent results and extremely fast analysis time when compared to the British Pharmacopeia method [14]. Figure 2.1 shows a sample chromatogram of the suppository spiked with the internal standard propyl paraben.

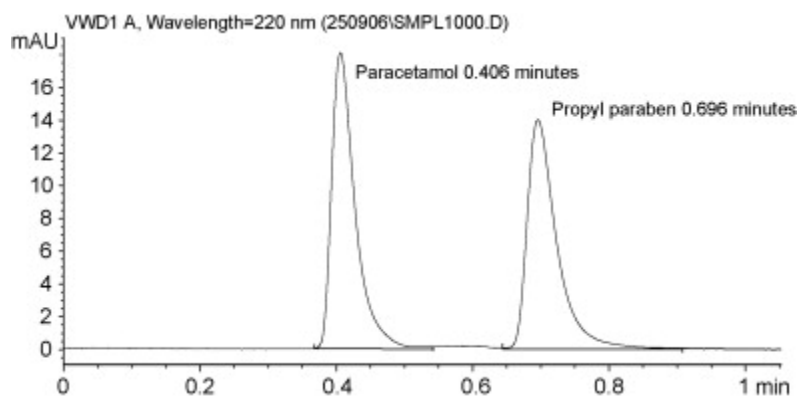


**Figure 2.1** Sample chromatogram of paracetamol suppository spiked with propyl paraben internal standard. The optimised microemulsion consisted of 66g butanol, 8g octane, 33g SDS, 1 litre 0.05% trifluoroacetic acid and 3% (v/v) acetonitrile. The separation was performed on a Waters Symmetryshield RP18 150mm x 4.6mm column with 3.5 micron packing. [3]

Another group, Jancic et al. [15] developed and validated an O/W MELC method for the determination of the angiotension- converting- enzyme (ACE) inhibitor, fosinoprilat in human plasma resulting from the breakdown fosinopril. The optimum mobile phase used is given in Table 2.1. The MELC method avoided pre-treatment of the sample and minimised errors and losses, which makes bio analysis very difficult. This method was also simpler and less time consuming than previously reported methods. The same group [11], also used a microemulsion eluent to characterise and model the retention behaviour of fosinopril sodium and fosinoprilat.

Malenovic et al. [16] developed a microemulsion method to analyse the cholesterol lowering statin drug simvastatin and its impurities. Resolution of simvastatin and its impurities in a single isocratic conventional HPLC run is virtually impossible due to its structurally similar impurities which have a wide range of polarities [17]. Until the group published this paper gradient HPLC was the only established separation method [17]. Figure 2.2 shows a representative chromatogram of the optimised separation.

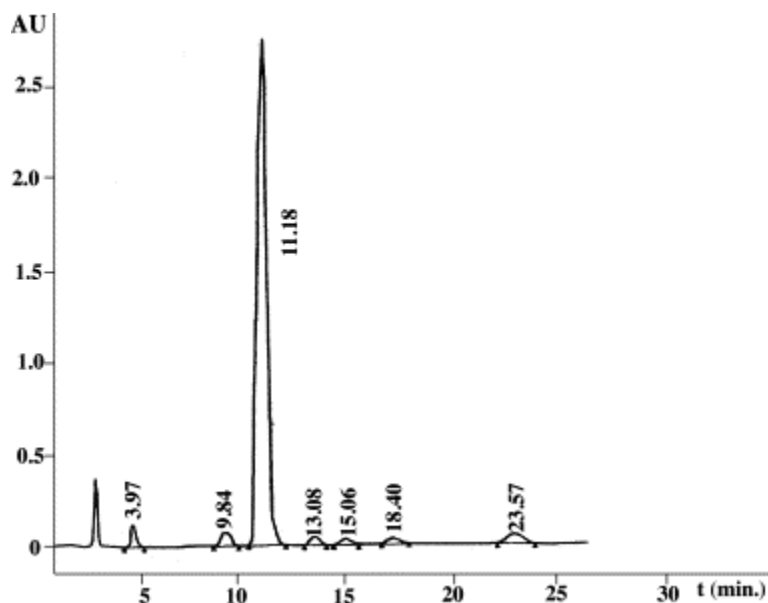


**Figure 2.2** Representative Chromatogram of Simvastatin and its impurities. Conditions; Xterra column at 30°C. Mobile phase composition; 0.9% diisopropylether, 2.2%SDS, 7% butan-1-ol, 89.9% 25mM Na<sub>2</sub>HPO<sub>4</sub> pH 7. [16]

EL-Sherbiny et al. [2] developed a MELC method for the simultaneous determination of the antihistaminic drug, loratadine and its analog desloratadine in pharmaceutical preparations. The method was fully validated and on comparison to a previous HPLC method developed by Qi et al. [18], the analysis time was only slightly longer but the need for organic solvents was greatly reduced.

### 2.3.1 Calculation of partition coefficients (log P)

MELC has found use in the high throughput screening of drug compound log P values [19;20]. The retention time of an analyte in a MELC separation can be related to the log P value through equation 2.1. Initially a calibration curve is constructed using a series of compounds with known log P values and the curve is then used to estimate the partition coefficients of unknown compounds.

$$\text{Log P} = \log \left( \frac{(t_r - t_0)}{t_0} \right) \quad \text{Equation 2.1}$$

Where;  $t_0$  represents the dead volume and  $t_r$  is the retention time of the solute.

Liu et al. [20] optimised a microemulsion composition for modelling the blood brain barrier (log BB) penetration for a series of 32 drug compounds. Results for test compounds were found to be in good agreement with other experimental techniques

and literature values, with regression coefficients greater than 0.7. The optimised microemulsion was composed of 3.3% SDS, 6.6% butanol, 1.6% heptane and 88.5% phosphate buffer pH 7.0.

Similar work was conducted by Li et al. [19] where a non-ionic microemulsion composed of 6.0% Brij-35, 6.6% butanol, 0.8% octanol and 86.6% phosphate buffer was used to predict the log P values for a number of pharmaceutical drugs. Comparison of predicted values to literature values showed excellent correlation ( $r = 0.96$ ).

**Table 2.1 Applications of MELC, with their corresponding microemulsion mobile phase composition.**

<i>Application</i>	<i>Composition</i>	Reference
Paracetamol analysis	33g SDS, 66g butan-1-ol, 8g n-octane in 1 litre 0.05% TFA +3% v/v ACN.	[3]
Study of W/O ME	8.33% w/w SDS, 16.6% w/w pentan-1-ol, 70% w/w heptane and 5% w/w (70mM) sodium acetate pH 7.5.	[1]
Determination of loratadine and desloratadine	0.1M SDS, 1% octanol, 10% n-propanol and 0.3% triethylamine in 0.02M phosphoric acid, pH 3.0.	[2]
Analysis of pharmaceuticals	33g SDS, 66g butan-1-ol, 8g n-octane in 1 0.05% TFA.	[9]
Analysis of fosinopril and fosinoprilat	0.9% w/w cyclohexane, 2.2% w/w SDS, 8.0% w/w n-butanol and 88.9% aqueous 25mM disodium phosphate adjusted to pH 2.8 with 85% orthophosphoric acid.	[11]
Analysis of simvastatin	0.9 w/w diisopropylether, 1.7% w/w SDS, 7.0% w/w n-butanol, and 90.4% w/w aqueous 25mM di-sodium phosphate (pH 7.0).	[12]
Developed determination of fosinoprilat	1.0% w/v diisopropyl ether, 2.0% w/v SDS, 6% w/v n-propanol and 91% w/v aqueous 25mM di-sodium hydrogen phosphate adjusted to pH 2.8 with 85% orthophosphoric acid.	[15]
Separation of furosemide, bumetanide, naproxen, ibuprofen, atenolol, acebutolol, nadolol, timolol and naphthalene.	2% SDS, 10% butanol, 1% octanol, 0.3% TEA in 0.02M phosphoric acid.	[21]

## 2.4 Operating parameters and optimisation of O/W MELC

### 2.4.1 Column Temperature

Marsh et al. [9] used an O/W microemulsion to separate methyl paraben, ethyl paraben, propyl paraben, oxibendazole and BDP. Chromatographic performance was examined at 20-60°C. It was found that increasing temperatures did not greatly affect analyte retention times, but an increase in peak-to-peak resolution was observed for the last two peaks. The peak efficiency increased for all solute peaks over the temperature range 40 to 60°C. Figure 2.3 shows a chromatogram of the separation at 60°C achieved by Marsh et al. [9]. In the optimisation of the MELC assay for paracetamol in a suppository, McEvoy et al. [3] examined the operating temperature range between 25-60°C. A similar result was noted with a small reduction in retention time and an insignificant increase in peak efficiencies. However, due to the increase in column temperature a large drop in column back pressure was noted.

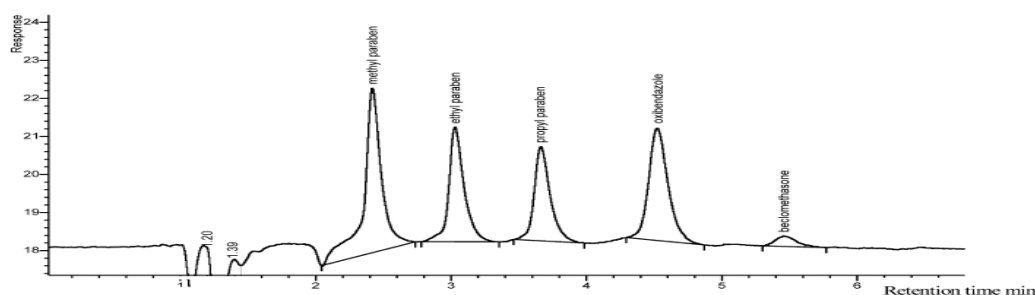


**Figure 2.3** Separation of methylparaben, ethylparaben, propylparaben, oxibendazole and BDP in a test mixture at 60°C. Conditions: detection 215nm; flowrate 1mL min<sup>-1</sup>; waters Symmetryshield C18 3.5 x 150x 4.6 column. [9]

### 2.4.2 Column conditioning and equilibration

Columns require conditioning with the mobile phase before use and up to 30 column volumes may be needed to equilibrate columns with traditional HPLC solvents. Microemulsions are more viscous and contain less organics and it can take much longer for steady base line to be achieved. Approximately one hour was required at a flow rate of 1mL min<sup>-1</sup> to equilibrate (340 column volumes) the 150 x 4.6 mm C18 packed column used by McEvoy et al. in the analysis of paracetamol [3]. When changing parameters such as microemulsion composition or temperature, longer conditioning times are required. Also there is a considerable amount of time required to clean the microemulsion out of the column after use. These disadvantages are reduced when methods are continuously employed in routine operations.

### 2.4.3 Oil content

The oil content was varied by Marsh et al. [9] from zero w/w to 1.2% w/w. At 1% w/w and above, chromatographic reproducibility became poor as the microemulsion became unstable. It was observed that the effect of the oil content on the separation was largely dependent on the nature of solute. For very hydrophobic solutes the retention time decreased with increasing oil content, as the solubilising power of the eluent increased for the hydrophobic analytes. The resolution however, suffered with the decrease in retention time. Figure 2.4 shows a graph of the change in retention time with a variation in oil content.

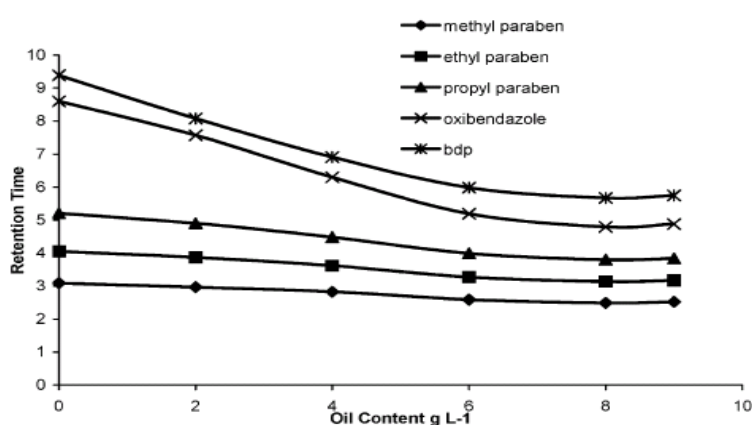


Figure 2.4 Effect of increasing oil in the microemulsion on the retention time of methylparaben, ethylparaben, propylparaben, oxibendazole and BDP. Conditions: temperature 60°C; detection 215nm; flowrate 1mL min<sup>-1</sup>; waters Symmetryshield C18 3.5 x 150x 4.6 column. [9]

### 2.4.4 Oil type

When studying a series of water insoluble alkanes and alcohols with differing chain lengths as the oil phase, Marsh et al. [9] found that peak to peak resolution and retention increased when an alcohol was used as the oil phase. An increase in the chain length of the alkane or alcohol decreased retention time with a corresponding increase in peak resolution.

In evaluating the use of microemulsions as eluents, El-Sherbiny et al. [21] separated the test solutes, furosmide, bumetanide, naproxen, ibuprofen, atenolol, acebutolol, nadolol, timolol, and naphthalene. The influence of the oil phase was examined by replacing 1-octanol with diisopropyl ether, 2-octanone, n-octane, and butyl acetate. Only the retention of the neutral hydrophobic solute naphthalene varied greatly with

changes in the oil phase. When 1-octanol was replaced with diisopropyl ether, butyl acetate or 2-octanone the retention times increased slightly, as the solutes did not partition as strongly into the oil droplets. Replacement with the more lipophilic n-octane decreased the retention time of all solutes except the hydrophobic naphthalene.

While developing a method for the separation of loratadine and desloratadine El-Sherbiny et al [2] used butyl acetate and diisopropyl ether as the oil phase in place of 1-octanol. Butyl acetate gave the shortest retention time and diisopropyl ether gave an intermediate retention time, but 1-octanol gave the best separation in terms of selectivity and detection.

Jancic et al. [15] noted when developing the method for the determination of fosinoprilat in plasma, that the separation and selectivity was not significantly influenced by the type and concentration of the oil phase.

#### 2.4.5 Surfactant concentration

Variation in the concentration of SDS from 1.75 to 5% w/w by Marsh et al. [9] showed the chromatography was not stable below 3% w/w. Increasing the SDS concentration from 3-4% w/w decreased solute retention times. Further increases to 5% had no further effect on the first three peaks and slightly increased the retention times of the last two. Figure 2.5 illustrates the relationship between the retention times of the solutes and the concentration of SDS.

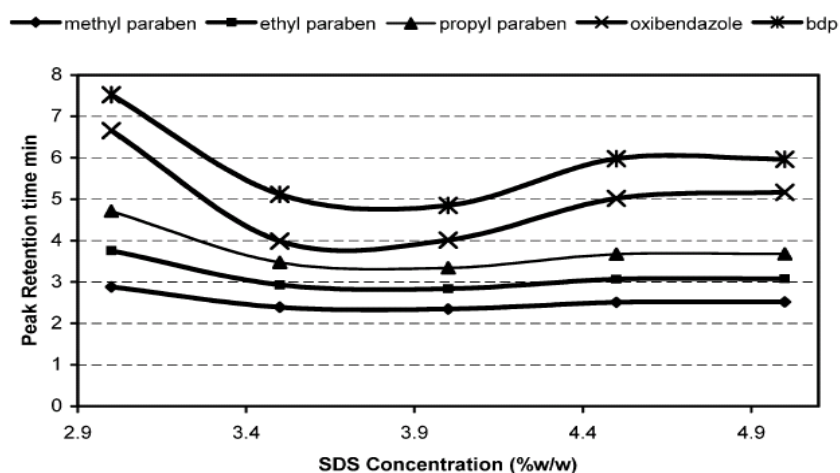


Figure 2.5 Effect of SDS concentration on the retention time of methylparaben, ethylparaben, propylparaben, oxibendazole and BDP. Conditions: temperature 60°C; detection 215nm; flowrate 1mL min<sup>-1</sup>; waters Symmetryshield C18 150x 4.6 column with 3.5µ packing. [9]

El-Sherbiny et al. [21] in evaluating MELC separations also varied the surfactant concentration from 1-4% w/w to assess the effect on selectivity and retention time. They too noted that an increase in SDS concentration led to a decrease in retention time. No significant affect in selectivity was observed. The same type of result was noted by El-Sherbiny et al. [2] when determining loratadine and desloratadine in a pharmaceutical preparation.

Malenovic et al. [12] in the monitoring of simvastatin and its impurities varied the SDS concentration and stated that when using the content of surfactant and co-surfactant as selectivity modifiers the concentration had to be strictly controlled to achieve reproducible results. The developed method proved robust for SDS concentrations between 1.5-2.5% w/w.

Jancic et al. [15] when determining fosinoprilat in human plasma noted a decrease in retention time when the SDS concentration was increased from 1% w/v to 3% w/v. 2% w/v SDS achieved the optimum separation with 3 % w/v leading to co-elution with components in the plasma.

#### **2.4.6 Surfactant type**

When replacing SDS by the similar anionic STS, Marsh et al. [9] noted there was no dramatic changes in chromatography. Changing the surfactant type to the cationic CTAB, TTAB or DTAB resulted in very poor chromatographic peaks and a relationship between surfactant type and retention or selectivity could not be established.

In the MELC evaluation, El-Sherbiny et al. [21] substituted SDS with mixtures containing SDS and the anionic surfactant SDOSS or SDS and any of the three non-ionic surfactants, Brij 35, Tween 21 or Tween 80. The most dramatic result observed was the increase in retention time for the solutes containing a carboxylic acid group when the SDS and Tween mixture was used. Similarly, while characterising the separation of fosinopril sodium and fosinoprilat, Jancic et al. [11] noted an increase in retention time when an SDS/SDOSS mixture was used in place of SDS.

### 2.4.7 Microemulsion pH

The charge of a solute molecule can be changed and influenced by the pH of the microemulsion mobile phase due to electrostatic repulsion, attraction and hydrophobic forces between the microemulsion droplets and the functional groups of the solute. Marsh et al. [9] examined the influence of pH over the range 9.7 to 1.5 for naproxen ( $pK_a = 4.4$ ). The retention time was increased from 1.18 to 4.37 minutes as the mobile phase pH was lowered.

El-Sherbiny et al. [21], while evaluating a MELC system varied pH from 2.5 to 5. Cationic solutes were not ionised in this range and as the microemulsion droplet was negatively charged the separation of these solutes was not really changed. The carboxylic acid compounds (furosemide, bumetanide, naproxen and ibuprofen) had  $pK_a$  values of 3.5 to 5, and therefore became increasingly ionised in the pH range being investigated. The authors saw a decrease in the retention time for the carboxylic acid compounds as the pH increased. The neutral compound naphthalene was naturally unaffected by a change in the pH.

For the simultaneous determination of loratadine and desloratadine, El-Sherbiny et al. [2] saw an increase in retention time for both drugs with increases in pH from 3 to 7. Figure 2.6 shows a plot of retention factors for both drugs with increasing pH. The authors explained the results in terms of the difference in hydrophobicity and dissociation constant as reflected in the  $\log P$  and  $pK_a$  values.

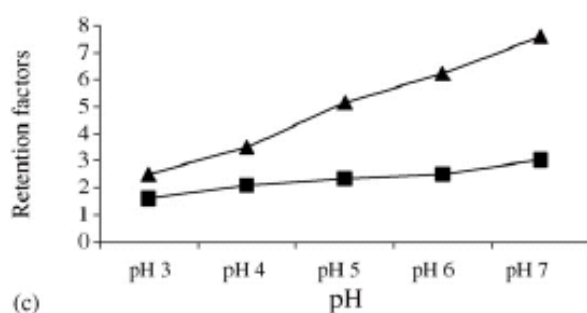


Figure 2.6 Effect of varying pH on loratadine and desloratadine. ■ Represents loratadine and ▲ represents desloratadine. [2]

In developing a method for fosinoprilat determination, Jancic et al. [15] observed how lowering the pH of the mobile phase from 4.5 to 2.5 doubled the retention time. The same group [11], when characterising fosinopril sodium and fosinoprilat noted a major

reduction in retention time for fosinopril sodium when increasing the pH from 4.5 to 7 (from 15.46min to 2.72min).

#### **2.4.8 Co-surfactant concentration**

El-Sherbiny [21] changed the co-surfactant concentration of n-propanol from 6-15% v/v, in evaluating MELC. They noted a decrease in the retention times for increasing co-surfactant concentration, but the decrease was less than that observed when changing the SDS concentration from 1 to 4 %. No significant effect was observed for the selectivity. A similar result was observed by the same group in the determination of loratadine and desloratadine [2].

Marsh et al. [9] varied the concentration of 1-butanol from 6.6% to 16.5% w/w. Up to 9% w/w no affect was observed on the separation, above 9% the chromatogram was compressed with the retention of the first peak remaining constant and a decrease in retention time of all the other peaks.

Jancic et al. [11], when characterising the fosinopril sodium and fosinoprilat separation, varied the co-surfactant concentration from 6-10% w/w, and noted that for increasing content of co-surfactant there was a decrease in retention time.

When Malenovic et al. [12] analysed simvastatin and its impurities, they concluded that in order to achieve the optimum separation the co-surfactant (1-butanol) concentration had to be between 7-7.5% w/w as it had a pronounced effect on selectivity.

#### **2.4.9 Co-surfactant type**

El-Sherbiny et al. [21] observed the importance of varying the nature of the co-surfactant as a selectivity modifier in their evaluation of MELC. The effect on separation selectivity was investigated by replacing propanol with 1-butanol, tetrahydrofuran, acetonitrile and ethanol. They highlighted the fact that the late eluting peaks had a decrease in retention time when using 1-butanol and tetrahydrofuran. The group performed a similar investigation when determining loratadine and desloratadine [2]. Figure 2.7 graphs the effect of co-surfactant on the separation. 1-butanol, propanol and tetrahydrofuran resulted in good resolution between the peaks, however acetonitrile resulted in co-elution.

Jancic et al [15], when developing the fosinoprilat determination stated the greatest influence on the separation was the type and concentration of the co-surfactant.

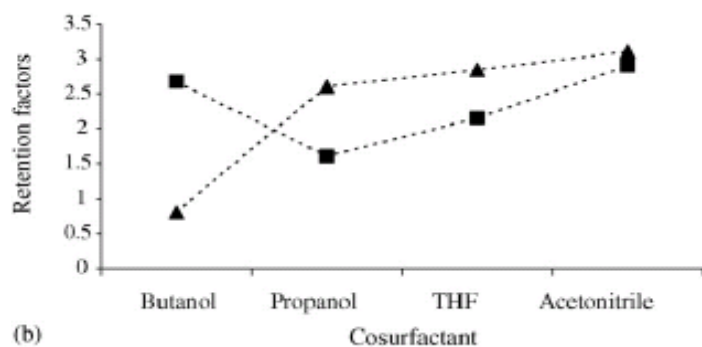


**Figure 2.7** Effect of co-surfactant type on the retention of loratadine and desloratadine. ■ Represents loratadine and ▲ represents desloratadine. [2]

## 2.5 Operating parameters and optimisation of W/O MELC

To date, the main body of investigations carried out in MELC have been focussed on the O/W microemulsion. However, Altria et al. [1] performed a preliminary study on the use of W/O microemulsions as eluents in HPLC. They examined a range of microemulsion compositions to separate a test mixture (naphthalene, 4-hydroxyacetophenone, paracetamol and niacinamide) consisting of basic, neutral and acidic analytes in isocratic MELC mode. In optimising the separation they varied the oil type, co-surfactant type, surfactant type, water concentration, pH, flow rate and temperature.

## 2.6 MELC Robustness

Jancic et al. [22] examined the benefits of Central Composite Design (CCD) in testing the robustness of a related substances assay for carbamazepine (anticonvulsant) and its related substances. CCD is an experimental design capable of forming a second order polynomial which is used to map response factors. The CCD approach utilises less experiments than a full factorial design. In addition the design was tested using analysis of variance (ANOVA) and artificial neural networks (ANNs). The microemulsion was composed of SDS, n-propanol, diisopropyl ether and 1% TEA aqueous buffer. With respect to robustness, only SDS concentration, n-propanol concentration and pH were examined. From the three parameters investigated ANOVA and ANNs predicted SDS and n-propanol concentration to have the greatest impact on

the robustness of the method. The use of such programs are advantageous in MELC, given the greater number of parameters available compared to traditional LC. The same group [23] also employed ANNs to model the chromatographic behaviour for separation of atorvastatin and its related substances utilising a modified micellar phase as the eluent. The optimum micellar phase consisted of 32% v/v acetonitrile, 2% v/v ethylene glycol and 6.4 mmols of AOT in 20 mM ammonium acetate buffer pH 5.5 (adjusted with acetic acid). The optimised ANN was seen to have excellent predictive abilities with tests showing correlation coefficients of greater than 0.97.

Maskovic et al. [24] developed a validated an O/W method for the separation of perindopril tert-butylamine (ACE inhibitor) from its related substances. In order to conduct robustness testing the authors employed the Plackett-Burman design, which was capable of investigating the relationship between a measured quantity (e.g. retention) with respect to a number of dependent variables (e.g. surfactant/co-surfactant/oil concentration).

Momenbeik et al. [25] employed a design approach comprising multiple linear regression (MLR) and a genetic algorithm (GL) to optimise the microemulsion composition for the separation of five oil-soluble vitamins. MLR (examines correlation of two or more independent variables with a dependent variable) was implemented to determine which microemulsion components had the greatest influence on the separation. It was found that co-surfactant and oil concentration had the most important effect on the quality of the vitamin separation. A genetic algorithm, which utilised an iterative learning process, was used to predict the optimum composition. The optimised microemulsion contained 73.6 mM SDS, 13.64% v/v 1-butanol, 0.48% v/v diethyl ether and 85.88 % v/v 0.02 M phosphate buffer pH 6.99.

## **2.7 Gradient MELC**

There have been few reports of microemulsions used in gradient elution [3;4;26-28]. Bryant et al. [27] performed an initial assessment on the use of gradient elution in microemulsion and micellar LC. As in isocratic MELC the oil, surfactant, co-surfactant type/concentration, as well the pH, all have an influence on selectivity. Bryant et al. [27] initially tried to separate a number of components (caffeine, paracetamol, methyl paraben, ethyl paraben, propyl paraben and butyl paraben) in a mixture using gradient MELC. The same components when separated in isocratic MELC showed poor

resolution and separation efficiency. The initial program pumped 100% water and linearly increased the percentage of microemulsion until it reached 100%. The method was unsuccessful as the water disrupted the microemulsion in the pump and led to the formation of an immiscible 2-phase suspension. This problem was solved by adding a salt to the water (0.5M NaCl), which facilitated mixing by increasing the ionic strength, allowing the microemulsion to remain as a single phase at high water concentrations and a successful efficient separation resulted. Figure 2.8 shows a comparison of the separation in isocratic and gradient mode.

More recently, Marsh et al. [28] completed an in-depth analysis of gradient MELC mode to assess its potential for routine pharmaceutical analysis. A test mixture of 15 acidic, basic, and neutral compounds was separated. The operating parameters varied included gradient profile, eluent flow rate, sample dissolving solvent, temperature and microemulsion oil content. The effect on separation with regard to type of reversed phase column, low detection wavelength and addition of organic solvents was also examined. Unlike Bryant et al. [27], no phase separation was observed during the start of the gradient with the mixing of the microemulsion and aqueous phase. For this reason no salt was added to the aqueous solution to aid mixing. However, it was acknowledged that the phase separation encountered by Bryant could have been due to the nature of the solvent pump on the HPLC, as the two groups used different HPLC systems. In order to have a ground for comparison preliminary experiments were conducted on a test mixture to establish an initial set of gradient conditions. The separation was also performed in isocratic MELC mode and while all compounds were separated in the gradient elution, the two most hydrophilic compounds were not separated in isocratic mode. It was noted that this result showed gradient MELC offered potential for greater separation selectivity compared to the isocratic mode.

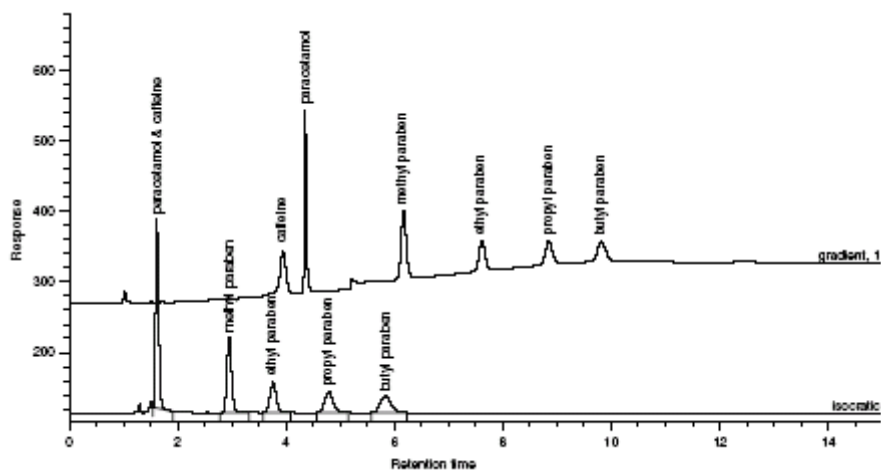


**Figure 2.8** Gradient and isocratic MELC separation of caffeine, paracetamol, methyl paraben, ethyl paraben, propyl paraben and butyl paraben. [27]

Another investigation into the use of the gradient microemulsion system was reported [3] in the MELC method for the determination of paracetamol in a suppository. In the assessment of the stability indicating capability of the MELC method, a number of gradient modes were attempted to separate paracetamol and five of its related substances. While separation of all the impurities was achieved, peak retention times and resolution were irreproducible. More recently the same group [4] carried out a similar investigation and concluded that reproducible separations could only be achieved using isocratic MELC. The irreproducible retention times in gradient LC was found to be due to the nature of the adsorbed layer on the column packing. To achieve reproducibility the column has to be completely equilibrated with the microemulsion mobile phase and a constant adsorbed layer on the packing. This is achievable in isocratic MELC but when a concentration gradient is employed equilibration is not possible due to the dynamic nature of the surfactant adsorbed onto the column.

## 2.8 Eluent flow rate and column type

Altria et al. [26] carried out extensive studies on isocratic and gradient MELC mode using a monolithic column. As microemulsions have high viscosities, this results in high back pressures, which limit the flow rate to 1 or 1.5 mL min<sup>-1</sup> when using conventional C18 packed columns. When the group used monolithic columns they reported a threefold decrease in back pressure, which allowed the use of flow rates up

to 4 mL.min<sup>-1</sup>. The high flow rates resulted in rapid separations with no loss in efficiency or resolution.

## **2.9 Conclusion**

MELC can offer some advantages over conventional HPLC methods in terms of reduced sample pre-treatment needs for complex samples. Generic MELC conditions can be directly applied to a wide range of compounds due to the ability of microemulsions to solubilise a wide range of both water-soluble and -insoluble solutes. Separations can be optimised using a variety of parameters and the use of microemulsion gradients also extends the selectivity optimisation possibilities. To date MELC has been applied to a limited number of complicated pharmaceutical analysis problems, including quantitative analysis and separation of related impurities. MELC has also been shown to offer value in the area of bioanalysis.

The area of MELC offers great possibilities for extending the current applications and moving into other application areas such as agrochemical and vitamin analysis.

## 2.10 References

- [1] Altria, K., Broderick, M., Donegan, S. and Power, J., *Chromatographia*, 62 (2005) 341-348.
- [2] El-Sherbiny, D.T., El-Enany, N., Belal, F.F. and Hansen, S.H., *Journal of Pharmaceutical and Biomedical Analysis*, 43 (2007) 1236-1242.
- [3] McEvoy, E., Donegan, S., Power, J. and Altria, K., *Journal of Pharmaceutical and Biomedical Analysis*, 44 (2007) 137-143.
- [4] McEvoy, E., Donegan, S., Power, J. and Altria, K., *Chromatographia*, 68 (2008) 49-56.
- [5] Hernandeztorres, M.A., Landy, J.S. and Dorsey, J.G., *Analytical Chemistry*, 58 (1986) 744-747.
- [6] Legorburu, M.J., Alonso, R.M., Jimenez, R.M. and Ortiz, E., *Journal of Chromatographic Science*, 39 (2001) 425-430.
- [7] Berthod, A., Laserna, J.J. and Carretero, I., *Journal of Liquid Chromatography*, 15 (1992) 3115-3127.
- [8] Berthod, A. and Decarvalho, M., *Analytical Chemistry*, 64 (1992) 2267-2272.
- [9] Marsh, A., Clark, B.J. and Altria, K.D., A., *Journal of Separation Science*, 28 (2005) 2023-2032.
- [10] Armstrong, D.W. and Henry, S.J., *Journal of Liquid Chromatography*, 3 (1980) 657-662.
- [11] Jancic, B., Medenica, M., Ivanovic, D., Malenovic, A. and Markovic, S., *Analytical and Bioanalytical Chemistry*, 383 (2005) 687-694.
- [12] Malenovic, A., Medenica, M., Ivanovic, D. and Jancic, B., *Chromatographia*, 63 (2006) S95-S100.
- [13] Ivanovic, D., Medenica, M., Jancic, B., Malenovic, A. and Markovic, S., *Chromatographia*, 60 (2004) S87-S92.

- [14] British Pharmacopoeia (2005) Vol. III, pp 2701-2702, 2009.
- [15] Jancic, B., Ivanovic, D., Medenica, M., Malenovic, A. and Dimkovic, N., *Journal of Chromatography A*, 1088 (2005) 187-192.
- [16] Malenovic, A., Ivanovic, D., Medenica, M., Jancic, B. and Markovic, S., *Journal of Separation Science*, 27 (2004) 1087-1092.
- [17] European Pharmacopoeia, 4th edition (2002), Council of Europe, Strasburg Cedex., 2009.
- [18] Qi, M.L., Wang, P. and Geng, Y.S., *Journal of Pharmaceutical and Biomedical Analysis*, 38 (2005) 355-359.
- [19] Li, N., Huang, J.Y., Huang, S.J. and Gao, C.K., *Acta Chimica Sinica*, 67 (2009) 2116-2120.
- [20] Liu, J.F., Sun, J., Sui, X., Wang, Y., Hou, Y. and He, Z.G., *Journal of Chromatography A*, 1198 (2008) 164-172.
- [21] El-Sherbiny, D.T.M., El-Ashrya, S.M., Mustafa, M.A., El-Emam, A.A. and Hansen, S.H., *Journal of Separation Science*, 26 (2003) 503-509.
- [22] Jancic-Stojanovic, B., Malenovic, A., Ivanovic, D. and Medenica, M., *Acta Chim. Slov.*, 56 (2009) 507-512.
- [23] Malenovic, A., Jancic-Stojanovic, B., Kostic, N., Ivanovic, D. and Medenica, M., *Chromatographia*, 73 (2011) 993-998.
- [24] Maskovic, M., Dotsikas, Y., Malenovic, A., Jancic-Stojanovic, B., Ivanovic, D. and Medenica, M., *Journal of AOAC International*, 94 (2011) 723-734.
- [25] Momenbeik, F., Roosta, M. and Akbar Nikoukar, A., *Journal of Chromatography A*, 1217 (2010) 3770-3773.
- [26] Altria, K.D., Marsh, A. and Clark, B.J., *Chromatographia*, 63 (2006) 309-314.
- [27] Bryant, S.M. and Altria, K.D., *Journal of Separation Science*, 27 (2004) 1498-1502.

[28] Marsh, A., Clark, B.J. and Altria, K.D., *Chromatographia*, 61 (2005) 539-547.

## **Chapter Three**

### **Application of microemulsions in CE**

### **3.1 Introduction**

Microemulsion electrokinetic chromatography (MEEKC) is a mode of CE, which utilises MEs as separation media. The two principal types of microemulsion utilised in MEEKC are oil-in-water (O/W) microemulsion where water makes up the bulk phase and water-in-oil (W/O) microemulsions where oil makes up the bulk phase, although the W/O type is far less commonly used.

This chapter details advances in the methodology, optimisation and application of MEEKC from 2006 –2010. Areas where practical advancement and novel theories have been reported include online sample concentration, method optimisation, chiral analysis, MEEKC-MS and MEEKC-ICP-MS. In addition to separating analytes of pharmaceutical and biotechnological interest, MEEKC has been used for the determination of the physicochemical properties (log P) of drug compounds. Previous reviews have covered advances and applications from the periods 2006-2008 [1] 2004-2006 [2], 2002-2005 [3;4] and from 1996-2002 [5]. Reviews covering the background theory have been published by Altria et al. [6;7].

### **3.2 Principles of MEEKC**

MEEKC utilises MEs as carrier electrolytes in place of the common aqueous CZE buffers like borate and acetate. An electroosmotic flow (EOF) of liquid occurs when a voltage is applied across the capillary. The magnitude of the EOF is based on the nature of the capillary and ionisation of its inner surface. Charged particles in an electric field experience an attractive force and cationic sample components migrate towards the negatively charged cathode while anions migrate towards the anode. At low pH, ionisation is suppressed and EOF does not occur. At high pH values the EOF is strong and sweeps all solutes, even anions to the cathode and through the detector. The microemulsion droplet acts as a pseudostationary phase (PSP) and allows separation of neutral as well as charged analytes. The oil droplets can be positively or negatively charged depending on whether anionic or cationic surfactants have been utilised for microemulsion formation. Zwitterionic and neutral surfactants have also been employed to improve the separation of charged analytes [8], while addition of cyclodextrins allows chiral analytes to be separated [9]. Anionic SDS is the most commonly used microemulsion surfactant in MEEKC applications, although some cationic surfactants have also been used. The ME droplets migrate when a voltage is applied. Solute selectively partition between the aqueous phase and moving oil

droplets. The more hydrophobic the solute is; the more it will partition into the microemulsion droplet and the longer it will take to migrate. Uncharged, highly hydrophilic solutes reside in the aqueous phase of the microemulsion and migrate quickly with the EOF towards the detector. Charged species are also electrophoretically separated based on their number of charges, size and how they interact with the droplet. Positively charged solutes may form an ion pair interaction with the surface of a negatively charged droplet while negatively charged solutes in general will be repelled by the droplet. Figure 3.1 shows a schematic representation of a MEEKC separation.

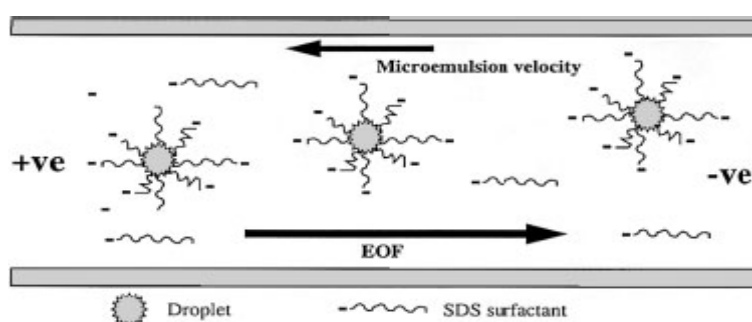


**Figure 3.1** Schematic representation of MEEKC separation. [7]

Equations have been developed [6;10-12] to quantify and reflect the mechanisms in a MEEKC separation.

The migration time  $t_m$  of a neutral species is always between  $t_0$  and  $t_{ME}$  such that:

$$t_m = \left( \frac{1+k}{1 + \frac{t_0}{t_{ME}} k} \right) t_0 \quad [12] (3.1)$$

Where  $t_0$  is the time taken for the electroosmotic flow marker (such as methanol) to travel from the injection capillary tip to the detector,  $t_{ME}$  is the time taken for the microemulsion (ME) marker (such as octanophenone which is very water insoluble) to pass through the capillary and  $k$  is the retention factor. The difference in time between  $t_0$  and  $t_{ME}$  defines the migration window.

The mass distribution ratios or retention factors of the solutes ( $k$  values) in a MEEKC system are calculated from:

$$k = \frac{t_m - t_o}{t_o * \left( \frac{1 - t_r}{t_{ME}} \right)} \quad [12] \quad (3.2)$$

The distribution ratio (k) indicates the migration behaviour of the analytes and defines the total moles of analyte in the PSP relative to the aqueous phase. The higher distribution ratio indicates slower migration and stronger partitioning of the analyte into the microemulsion droplet.

### 3.3 Comparison of MEEKC to MEKC

Micellar electrokinetic chromatography (MEKC) was introduced by Terabe in 1984 [12] and the operating principles are similar to MEEKC except a micelle is used instead of a ME droplet as the PSP. The micelle in MEKC can also be positively or negatively charged, and has the ability to separate charged and neutral analytes.

Since MEEKC was introduced in 1991 [13] there have been many comparisons between the two techniques [14-17]. It has been observed that highly lipophilic compounds are better separated in MEEKC [18]. It has been suggested that solutes can partition more effectively with the MEEKC ME droplet than the rigid micelle in MEKC [19-21]. Greater partition between the ME droplet and the aqueous phase leads to a higher rate of mass transfer and a more efficient separation. Yin et al. [18] proposed that highly lipophilic compounds have an extreme affinity to the micelles which results in long migration times and poor resolution. Work by Hansen et al. [22] found that MEKC modified with the addition of 1-butanol delivered similar separation efficiencies to MEEKC for separation of neutral aromatic compounds. Debate exists as to the advantages between solvent modified MEKC and MEEKC [23]. Ortner et al. [24] recently examined CZE, MEKC, solvent modified MEKC and MEEKC for the separation of insulin and five of its analogues. Only solvent modified MEKC was capable of achieving full separation. The modified MEKC system was composed of 35 mM SDS and 15 % ACN in a 10 mM sodium borate buffer adjusted to pH 9.2.

In the online sample concentration of six flavonoids using MEKC and MEEKC [17] it was seen that enrichment factors in MEEKC were higher. It was noted that the retention factors were higher in MEEKC which may have led to the analytes partitioning with the ME droplets to a greater extent, thus increasing online enrichment in the sweeping stage. Similarly, higher enrichment factors (28 – 33) were observed in the stacking of urinary porphyrins [15] when the MEEKC method was compared to

enrichment factors (12 - 32) obtained with MEKC. With regard to the separation of the porphyrins, MEEKC provided superior resolution and efficiency for the more hydrophobic analytes. While the MEKC mode separated the more hydrophilic analytes with good resolution in a shorter time, MEEKC provided better peak shapes.

The separation of isoquinoline alkaloids (berberine, palmatine, jatrorrhizine, sinomenine and homoharringtonine) was performed in CZE, MEKC and MEEKC [16] prior to online sample concentration and it was found that MEEKC provided better resolution values compared to the other two techniques.

Angkanasiriporn et al. [25] compared the prediction of retention factors in MEKC and MEEKC for a range of disubstituted benzenes. Similar to previous work [26] the 'retention factor' ( $k$ ) and 'retention index' ( $I$ ) were used to analyse the migration behaviour. While similar to retention factor, the retention index is independent of the phase ratio and concentration of surfactant in MEEKC and MEKC systems. This property allowed the comparison of relative solute affinity to different PSPs or phase ratios. The authors found that for various concentrations of SDS similar relative  $I$  values were obtained for each solute in a range of benzene (BZ) standards in both the MEEKC and MEKC systems, while differing  $k$  values were obtained. Also, similar  $I$  values in MEKC and MEEKC were obtained for xylenes, dihalogenated benzenes and halogenated toluenes, while significantly smaller  $I$  values were obtained in MEEKC for dibenzaldehyde, dimethoxybenzene and methoxybenzene/benzaldehyde. Slightly smaller  $I$  values in MEEKC were observed for disubstituted benzenes containing a methoxy or aldehyde moiety. The difference in  $I$  values between MEEKC and MEKC was explained in terms of the analytes interaction with the PSP. Since the dominant interaction between the solute and PSP was hydrophobic, highly non-polar analytes such as the xylenes and dihalogenated benzenes had a similar affinity for the micelles and microemulsion droplets. However, analytes with methoxy or aldehyde functionalities were more polar and partitioned with the 1-butanol co-surfactant in the aqueous region/droplet surface of the microemulsion reducing the affinity for the PSP and resulting in lower  $I$  values.

### **3.4 Online sample concentration techniques**

All CE techniques which use a short optical path length and low sample volume suffer from poor detection sensitivity, particularly when UV detection is employed. Online sample concentration techniques have been developed in MEEKC to increase sample

concentration within the capillary and improve detection. Online sample enrichment can involve an injection process such as field amplified sample injection (FASI) where sample stacking occurs. This injection process allows analytes of interest in a large injected sample volume (e.g. 1000 nL) be focussed into a tight sample zone (e.g. 5 nL) resulting in heavily increased sample concentrations. FASI techniques include; transient isotachopheresis (ITP) [27], dynamic pH junction [28], sweeping and stacking with reverse migrating pseudostationary phase (SRMP) [17] as well as a combination of these techniques. Sample stacking is the result of sample ions moving across a boundary which is formed inside the capillary between the sample and separation zone. The solutes have different migration velocities in a high electric-field strength (low-conductivity) sample region and in a low electric-field strength (high conductivity) separation region. The molecules in the rear part of the plug migrate quicker than the front zone resulting in a narrow, more concentrated sample zone [29].

Injection processes can also be further optimised by using approaches such as anion selective exhaustive injection (ASEI) sweeping [30;31] and cation selective exhaustive injection (CSEI) sweeping [32]. Offline pre-concentration methods such as solid phase extraction have been implemented but this increases time and cost.

#### **3.4.1 FASI with high level salt matrices and ACN stacking**

The use of acetonitrile as a stacking medium has been reported since its introduction to CE in 1993 [33;34]. The addition of ACN to the sample matrix causes stacking due to its low conductivity in a high field strength region, hence the solute molecule has a greater velocity in the injection medium than in the separation medium. The presence of ACN also leads to de-proteinisation, which reduces protein adsorption to the walls of the capillary and also minimises the effect of harmful inorganic ions [15;16].

The effect of ACN stacking has recently been applied to samples containing both a high and low level of salt [15;16]. The application of FASI MEEKC to sample matrices containing a high level of salt was found to suffer from band broadening, poor sensitivity and poor resolution [35]. Yu et al. [16] found that in the separation and detection of isoquinoline alkaloids (berberine, palmatine, jatrorrhizine, sinomenine and homoharringtonine), the addition of ACN to the sample matrix containing a high level of salt, improved separation and detection sensitivity.

In the optimisation and separation of urinary porphyrins, Li et al. [15] established that the addition of ACN with an appropriate salt concentration (1.1% NaCl) led to an enhancement factor of 12-32 in detection sensitivity. Stacking of the negatively charged porphyrins occurred by a mechanism similar to the isotachopheresis process (ITP), with the chlorine from the salt acting as the leading ion and the acetonitrile acting as the trailing ion. The salt ions moved rapidly in the low conductivity injection region when a positive voltage was applied, followed by the porphyrin ions. Once the salt ions migrated into the separation buffer their migration velocity decreased and the porphyrins ions also slowed and remained behind. The porphyrins ions in the injection zone continued to migrate with high speed, therefore concentrating the total injected sample to give high intensity signals. The sample matrix required a co-ion with a higher intrinsic electrophoretic mobility than that of the surfactant of the pseudostationary phase in order to maintain a high electric field strength sample zone. The presence of the salt ensured the formation of a pseudo-steady-state boundary between the pseudostationary phase and the co-ion. A decrease in resolution and a poor peak shape was observed when salt concentrations exceeded 1.1%. The authors postulated that this was due to the disappearance of the pseudo-steady-state boundary.

Cao et al. [36] noted that at a certain concentration, the addition of salt to the sample matrix improved the stacking ability for the analysis of neutral saponins (notoginsenoside R<sub>1</sub>, ginsenoside Rg<sub>1</sub>, ginsenoside Rf, ginsenoside Rh<sub>1</sub>, ginsenoside Rd and ginsenoside Rg<sub>3</sub>). The group examined the effect of salt when using pressure and electrokinetic injection processes, coupled with increased injection volumes. Similar to the work by Li et al. [15], the presence of the salt ensured the ionic strength of the sample zone was higher than that of the running buffer. For both injection processes the greatest peak area was realised at different salt concentrations and injection lengths. For both injection types the less hydrophobic analytes experienced a peak broadening at longer injection times, while the more hydrophobic analytes experienced less broadening. This result indicated that the sample stacking was dependent on the analyte/microemulsion interaction within the sample zone. The optimum interaction between the analyte and microemulsion droplet was found through varying surfactant concentration, oil type, pH and the addition of organic modifiers.

### 3.4.2 Borate complexation and acetonitrile sweeping

Cao et al. [37] recently reported the separation and online sample concentration of a range of neutral glucosides (ginsenoside Rf, ginsenoside Rb2, and ginsenoside Re) using a non-ionic microemulsion with borate complexation and ACN sweeping. Generally neutral surfactants such as Brij-35 alone are not capable of separating neutral analytes. However, the authors utilised the property of the borate buffer which is capable of selective complexation with compounds containing a vicinal diol functionality such as nucleosides, catechols, glycosides, dicarboxylic acids and polyols [38;39]. The separation occurred due to the formation of anionic complexes based on the cis-diol moiety of the neutral analytes and concentration of borate ions. The capillary was initially filled with the high-conductivity BGE before injection of the low viscosity sample, prepared with sodium phosphate solution in the absence of borate. On the application of positive voltage a proportionally greater electric field was experienced in the sample zone and complexation between the analytes and borate ions occurred before migration of the analyte complexes towards the anode due to their electrophoretic velocities exceeding that of the EOF. A degree of sample concentration took place on the boundary due to the solvent viscosity difference during sweeping with the non-ionic ME. Following sweeping, the separation proceeded according to MEEKC principles. The borate concentration was also found to have a marked effect on the separation due to its role in complexation. The borate concentration was examined between 10 and 50 mM. At low concentrations (10-20 mM) co-migration was observed. 40 mM borate was found to be the optimum concentration, however it was noted that since the buffer concentration has a large effect on the EOF and the level of complexation that the optimum concentration is analyte dependent. The pre-concentration efficiency was further improved with ACN sweeping in the MEEKC system. ACN was added to the sample in the range of 0-70 % (w/v) and injection volume was increased from 3s to 50s. Generally, an increased injection volume leads to broad peaks and poor separation; however a 60-110 fold increase in sensitivity was reported when compared to normal injection process. Also at 60 % ACN the peaks were found to be sharp and well resolved. The authors also attributed the improved sensitivity to differences in the solvent viscosity between the sample and BGE and not differences in conductivity. Figure 3.2 shows the effect of various concentrations of ACN on the separation.

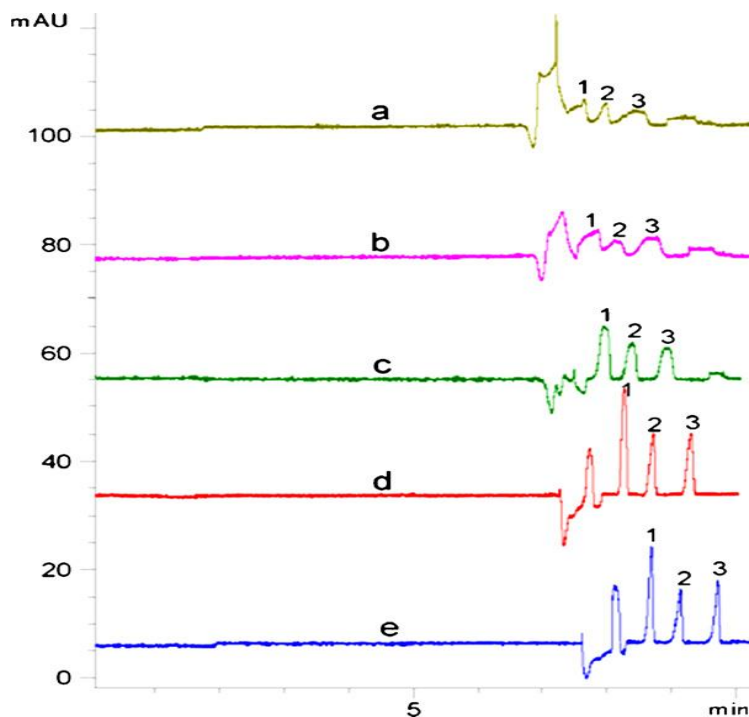


**Figure 3.2** Effect of sample matrix ACN concentration on sample sweeping. Conditions: running buffer: 3% w/v Brij-35, 0.6% heptane, 20% w/v ACN and 40 mM sodium borate pH 9.2. All samples contain 0-70 % ACN in 40 mM sodium borate buffer, (a) 0% ACN, (b) 10% ACN, (c) 30% ACN, (d) 60% ACN and (e) &0 % ACN. Peak identification 1, RF; 2, Rb2 and 3, Re. [37]

### 3.4.3 FASI-sweeping MEEKC with ASEI and CSEI

Sample enrichment by sweeping occurs when analytes are picked up and concentrated by the microemulsion that penetrates the sample zone. Techniques such as sweeping and stacking with reversed migrating pseudostationary phase (SRMP) [40] and reversed electrode polarity stacking mode (REPSM) [41] involve the injection of a large amount of sample to achieve sample concentration. This can cause instability in the ME phase when sweeping analytes in the longer sample zone and result in a failed separation. However, in anion selective exhaustive injection (ASEI) [30] or cation selective exhaustive injection (CSEI) [32] only the ions of interest are electrokinetically injected into the capillary, which reduces the amount of sample matrix and results in a continuously stable ME.

Zhu et al. [17] employed anion selective electrokinetic injection and sweeping with reverse migrating microemulsion for the online concentration of six flavanoids.

Previous work by Huang et al. [30;32] applied ASEI and CSEI to the analysis of phenolic acid compounds and tobacco alkaloids respectively. Recently the group has

combined ASEI and CSEI injection with the ME sweeping method for the analysis of eight penicillin compounds (nafcillin, dicloxacillin, ampicillin, penicillin V, cloxacillin, penicillin G and amoxicillin) [42]. All penicillins had a pKa of approximately 2.6; however ampicillin and amoxicillin existed as zwitterions in a weak acid or neutral solution. Figure 3.3 shows a schematic diagram of the ASEI, CSEI, and successive anion/cation selective sweeping modes. When the separation was carried out using ASEI sweeping MEEKC all penicillins except ampicillin and amoxicillin experienced a concentration effect. Alternatively, when the separation was carried out in CSEI mode ampicillin and amoxicillin were enriched but the other six penicillins were not detected. Using either CSEI or ASEI alone was unsuccessful because the amount of sample introduced in FASI is dependent on the degree of analyte dissociation, which is determined by the pH of the sample matrix and the analyte pKa. Hence, a combination of successive anion- and cation-selective injection (SACSI) was developed. The SACSI method allowed a simultaneous separation and a 260-3050 fold detection limit enhancement for all penicillins and improved resolution when compared to normal injection MEEKC.

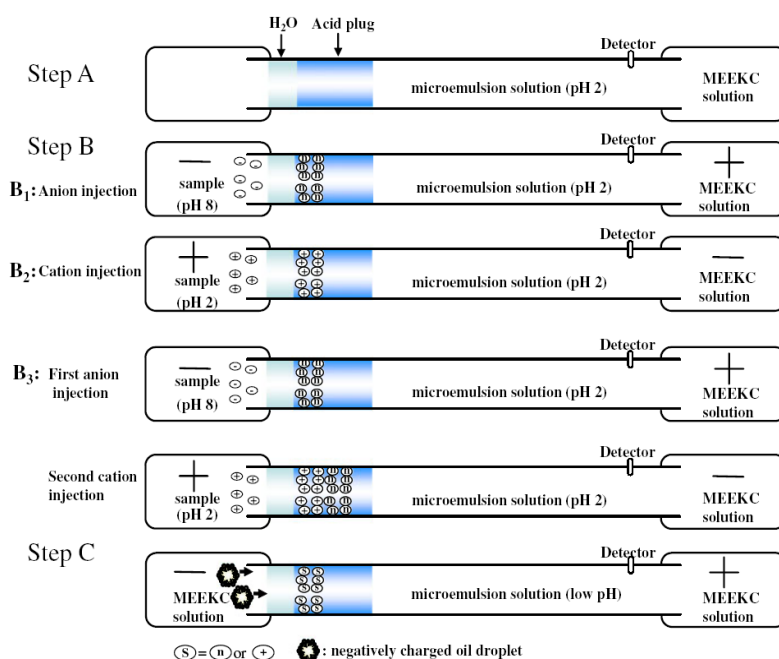


**Figure 3.3 Schematic diagram of FASI-sweeping MEEKC model.** Step A: A capillary was conditioned with a microemulsion solution of pH 2.0. An acidic plug (50 mM phosphoric acid) and a deionised water plug were then introduced hydrodynamically. Step B: ASEI mode: electrokinetic injection for 600 s at negative polarity (-10 kV) of the penicillin analytes prepared in a phosphate solution of pH 8 (step B1); CSEI mode: electrokinetic injection for 300 s at positive polarity (110 kV) of the penicillin analytes prepared in a phosphate solution of pH 2 (step B2); SACSI mode: anionic analytes were first introduced into the capillary by an anion-selective injection mode followed by a cation-selective injection mode for the introduction of cationic analytes (step B3). Step C: Microemulsion solution was placed at the inlet end of the capillary followed by the application of voltage at negative polarity (-20 kV). Reproduced with permission from [42].

### 3.4.4 Effect of water and acid/basic plugs on online sample concentration

It has been shown that the introduction of a deionised water plug prior to sample introduction improves sample stacking in FASI, by providing a high electric field at the tip of the capillary [43]. Huang et al. [42] assessed the role of water and acid plugs in ASEI and CSEI sample stacking of penicillins. It was found that increasing the length of water plug from 0-60 seconds improved signal intensities, but increasing to 90 seconds resulted in no further enhancement. Generally for CSEI a shorter water plug is favoured due to the adsorption of cation analytes to the negatively charged inner surface of the capillary wall. When optimising the online concentration of another set of isoquinoline alkaloids Yu et al. [44] found the introduction of a water plug resulted in improved absorbance and higher reproducibility. When stacking aromatic acid

impurities [45] the presence of a water or acid plug did not result in a significant sensitivity enhancement, however the presence of a water and/or acid increased the peak height reproducibility between runs.

During ASEI the presence of an acid plug can prevent the sample analytes from partitioning with the ME droplets before sample concentration occurs [31]. During the ASEI stacking of penicillins [42], the presence of an acidic plug (pH 2) in front of the ME buffer converted the anionic analytes into neutral form and prevented their migration towards the detector end during sample injection. It was noted that increasing the acid plug from 30 to 90s markedly enhanced the stacking ability and also improved separation.

#### **3.4.5 Online sample concentration and analyte functional group**

Huang et al. [45] assessed the online sample concentration for a range of aromatic acids to investigate a correlation between analyte functional group and sensitivity enhancement. It had previously been noted that the CSEI concentration of tobacco alkaloids [32] had been modest (10-540 fold) in comparison to the ASEI concentration of phenolic acid compounds (96000-238000)[31]. It was postulated that the cationic alkaloids may have been partially adsorbed onto the capillary wall during sample injection. For the online concentration of phenolic acid [31] compounds and polyphenols [31], it was noted that the presence of the carboxyl group in the former led to an increase in sensitivity enhancement over the polyphenols. In the latest study of online sample concentration [45] the aromatic acids under investigation had between 1-3 carboxyl groups. The use of a matrix buffer of pH 8 resulted in the aromatic acids with two or three carboxyl groups becoming divalent or trivalent anions. During electrokinetic injection these divalent or trivalent anions migrated into the capillary faster than the monovalent anions, thus, resulting in higher concentration sensitivities. Also the solubility of the aromatic acids increased in the acid plug with an increasing number of carboxyl groups leading to increased stacking. The results indicated that there was a correlation between analyte functional group and online concentration enhancement.

#### **3.4.6 FASI with suppressed EOF**

Suppression of EOF has been employed in MEEKC to reduce the migration time of neutral compounds [26;44;46-48]. Under normal MEEKC conditions, employing a

negatively charged surfactant such as SDS and a strong EOF flow with a positive applied voltage, neutral hydrophobic compounds partition strongly into the ME droplet and migrate towards the anode. However, the EOF is higher than the electrophoretic mobility of the oil droplets and all species are eventually swept towards the cathode. Suppressing the EOF and using a negative applied voltage results in a reversal of migration order. Hence, neutral compounds, which partition strongly with the negatively charged ME droplet, migrate quicker under a reduced EOF.

Yu et al. [44] used a suppressed EOF to achieve separation, and FASI for the detection, of quinolizidine alkaloids (sophoridine, matrine, oxymatrine, oxysophcarpine and cystine) in the Chinese herbal medicine *S.flavescens*. Instead of using a low pH running buffer to suppress the EOF, the divalent cation  $Mg^{2+}$  was added to the buffer. The presence of cations within the compact double layer reduced the effective charge on the capillary wall, thereby lowering the zeta potential and EOF. The addition of  $Mg^{2+}$  in the concentration range 1-4 mM to the running buffer was found to improve resolution, with 4 mM resulting in the separation of all alkaloids. Resolution decreased at concentrations above 4 mM. It was also noted that the migration time repeatability improved at 4 mM  $Mg^{2+}$ , due possibly, to a decrease in the adsorption of analytes to the capillary wall. FASI injection was achieved by preparing the analytes in pure water and injecting a water plug prior to the electrokinetic sample injection. The length of the water plug was optimised and an injection time of 5 seconds was found to provide the highest absorbance for the analytes under investigation. The FASI resulted in a 60-2000 fold improvement in detection sensitivity over normal hydrodynamic injection, with no loss in resolution.

#### **3.4.7 Effect of microemulsion composition on online sample concentration**

The effects of oil phase type and SDS concentration on stacking efficiency were examined in the separation of six neutral saponins [36]. With respect to oil phase type, six organic solvents were examined (chloroform, ethyl acetate, octanol, cyclohexane, octane and heptane). All six saponins had similar migration times and separation resolutions in all oil types, which indicated that changes in the oil phase did not cause a significant change in the separation of the analytes. However, the use of cyclohexane, octane and heptane as the oil phase resulted in superior stacking ability of the analytes. The more hydrophobic oil phases resulted in a stronger affinity between the

microemulsion droplet and analyte, demonstrating that there was a correlation between oil type and stacking. Since the concentration of surfactant affects the droplet charge and size, it plays a significant role in the affinity between the analyte and ME droplet. Changes in the SDS concentration between 2.5 to 4.0 % w/v resulted in a maximum stacking ability at 3.0% w/v.

Cao et al. [49] investigated the effect of oil phase type and non-ionic surfactant concentration on the online enrichment of five phenolic acids, in terms of stacking and sweeping. Heptane, octane, cyclohexane, ethyl acetate, chloroform and octanol were examined as oil phase types. Similar to separation of six neutral saponins [36], the oil phase type had little effect on the separation resolution. The stacking ability of the phenolic acids showed no great difference with variation in oil phase. However, a higher pre-concentration effect was realised in the sweeping mode when heptane and octane were employed. The use of the non-ionic surfactant Brij-35 did not contribute to the overall ionic strength of the buffer, and therefore could be used at high concentration without causing excessive joule heating. The concentration was varied from 1 to 4 % w/v. Results indicated that while the surfactant content played a minor role in the affinity between the analyte and ME droplet, the effect on stacking and sweeping was unimportant. The influence of buffer ionic strength was explored by varying the borate buffer concentration from 10-40 mM and an enhancement in both stacking and sweeping was seen at 40 mM.

### **3.5 Operating Parameters in MEEKC**

The complex nature of the microemulsion systems utilised in MEEKC separations lend themselves to numerous method development options when compared to other more conventional modes of CE. Changes in the type and/or concentration of surfactant, co-surfactant, oil phase along with buffer pH and the addition of organic modifiers can have a striking affect on separation selectivity and quality.

Before examining the online concentration of six flavonoids (tangeretin, nobiletin, naringenin, hesperidin and naringin), Zhu et al. [17] optimised the separation conditions in terms of the type of oil phase, organic modifier and the concentration of microemulsion components.

SDS is the most common surfactant used in MEEKC and its concentration (1.3 to 4.3%) in the separation of esbiothrin enantiomers was assessed [14]. The surfactant has a substantial role in lowering the surface tension between the oil and aqueous phase of

the microemulsion, and hence the stability of the system. Decreasing the SDS concentration below 1.3% resulted in the breakdown of the microemulsion. Conversely, a more stable system as well as improved solubility for esbiothrin was realised with an increase in surfactant concentration. Given that SDS was anionic, an increase in concentration resulted in a higher negative charge density on ME droplets and higher migration mobility in the opposite direction to the EOF. Hence an increase in analyte migration time from 14 to 30 minutes was seen with increasing concentrations of SDS from 1.8 to 4.3%.

However, SDS may not always be the optimum surfactant. The type of surfactant affects oil droplet charge and size, the level and direction of the EOF, and ion pair interactions. Positively charged surfactants, such as CTAB, have been used for the analysis of basic analytes to eliminate ion-pair interactions. Non-ionic surfactants, such as Brij-35, have also found use in MEEKC [49]. While they cannot be used to separate neutral solutes, non-ionic surfactants can be added to the ME buffer in higher concentrations than ionic surfactants without increasing the overall operating current. Mixed surfactant systems have also been investigated. In the separation of five isoquinoline alkaloids [16], the surfactant SDS was replaced by sodium cholate (SC), Brij 35 and a mixture of SDS & SC. SDS was incapable of producing a separation while the use of SC was found to be the most favourable. The authors noted that co-surfactant had the greatest influence on separation and selectivity. Migration times are altered with an increase in co-surfactant concentration because the buffer viscosity and EOF rate change, and the microemulsion droplets increase in size which reduces their ability to oppose the EOF. A concentration of 2.4% v/v 1-butanol was found to be the optimum. The addition of organic modifiers has been seen to improve many MEEKC separations [16;18] and the addition of 10% v/v methanol resulted in full baseline resolution of the isoquinoline alkaloids. Analytes may partition strongly with the ME droplet resulting in poor resolution, however the presence of an organic modifier can alter this interaction and improve resolution [18].

Yu et al. [44] assessed all microemulsion components in the separation of quinolizidine alkaloids. From a range of surfactants (SDS, SDS & SC, SC, Brij 35, SC & Brij 35, SC & Triton x-100), sodium cholate was found to provide the best separation. In addition to surfactant, the oil phase type and co-surfactant were also optimised. Addition of 10% methanol to the ME buffer was also seen to improve resolution.

In optimising the enantioseparation of phenylalanine derivatives [50], changing the oil phase from 0.5% octane to 0.5% ethyl acetate (which has a lower interfacial tension when compared to octane) reduced the migration time of 3,4-dihydroxyphenylalanine from 23 minutes to 6 minutes. This result demonstrated that the choice of oil phase can have a marked effect on an analytes interaction with the ME droplet and its electrophoretic mobility.

### **3.5.1 Buffer concentration and pH**

High pH buffers such as borate or phosphate at low ionic strength (5-10 mM) are generally used in MEEKC as they generate a high EOF with a low current when voltage is applied across the capillary. Alternatively, zwitterionic organic buffers such as tris-(hydroxymethyl)-aminomethane (TRIS) may be used [51]. An increase in buffer concentration has been shown to enhance resolution factors. Wu et al. [52] noted that in the separation of structurally related corticosteroids, an increase in phosphate buffer concentration from 10 to 50 mM improved resolution.

As the pH of the buffer has a pronounced effect on both the EOF velocity and degree of solute ionisation [53], it plays an important role in the separation. Generally pH is optimised between 7-9 [18;52;54], and this results in a high EOF with a fast and efficient separation. However, pH values as high as 12 or as low as 2 may be required [55] depending on the pKa of the analytes under investigation and whether there is a need to eliminate ion pair interactions. When employing a low pH, the EOF is suppressed and a negative voltage is applied across the capillary to move the ME droplets through the detector. Low pH running buffers have been used recently for the separation of aromatic acids [55], phenylalanine derivatives [50] and penicillins [42].

## **3.6 Advances in chiral separations utilising MEEKC**

Chiral MEEKC was introduced by Aiken et al. in 1993 [56], and can be achieved through two different methods. The first is indirect and relies on derivitisation of the enantiomers to form diastereomers, which are no longer chiral and can be separated using traditional MEEKC. The second approach is direct and involves the use of one or more chiral reagents in the ME buffer e.g. the chiral surfactant R- and S-dodecoxycarbonylvaline (DDCV) [10].

Kahle and Foley have completed extensive studies involving the affects of single, dual and triple chiral component microemulsion systems [10;57-60]. A summary of their

findings are covered in previous reviews [1;60]. Interested readers are also encouraged to consult a review by Preinerstorfer et al. [61], dedicated to enantioselective separations in CE, MEKC, MEEKC and CEC.

### 3.6.1 Novel chiral selector complex

An original chiral selector was recently reported by Hu et al. [62] for the enantioseparation of 12 pairs of  $\beta$ -blockers. The novel selector was formed in situ through complexation of the chiral oil di-n-butyl L-tartrate with boric acid (present in the TTAB microemulsion buffer). The complex shows a marked improvement when compared to use of the chiral oil alone. Its improvement in chiral recognition was attributed to the structural differences between di-n-butyl L-tartrate and the boric acid complex. Figure 3.4 shows the reaction of di-n-butyl L-tartrate with boric acid to form the chiral complex.

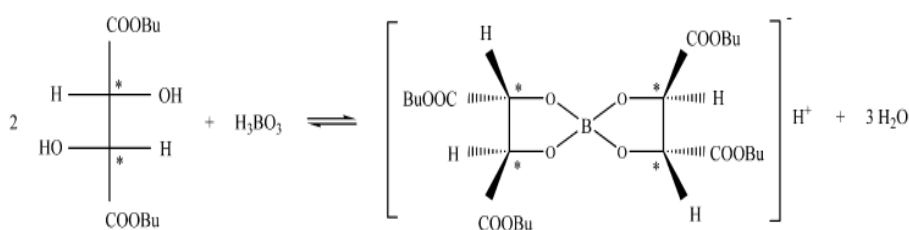


**Figure 3.4** Reaction of di-n-butyl L-tartrate with boric acid to form chiral selector complex. [62]

In di-n-butyl L-tartrate the C-C bond containing the stereogenic centres is free to rotate thereby allowing the chiral groups to fit the steric orientation of the analytes chiral centres and reduce enantiomeric discrimination. By comparison the rotation of the C-C in the di-n-butyl L-tartrate boric acid complex is restricted by the five-membered rings and leads to enhanced chiral recognition. Also, since the chiral complex is negatively charged compared to the neutral di-n-butyl L-tartrate it facilitates electrostatic interaction with positively charged analytes.

The concentration of di-n-butyl L-tartrate and sodium tetraborate was investigated in the range 15 -30 mM and 10-30 mM respectively. While changes in their concentration did not have an obvious effect on efficiency or elution range, an increase in concentration resulted in an increase in retention factor and enantioselectivity. In addition to TTAB, CTAB was also employed as the surfactant. It was noted that TTAB had a better solubility than CTAB and was less inclined to clog the capillary. The

concentration of TTAB also had to be strictly controlled with the optimum being 50 mM. High concentrations resulted in poor enantioselectivity which was ascribed to a decrease in the ratio of oil droplets and a low concentration made the dispersion of oil difficult. Interestingly, addition of the co-surfactant 1-butanol led to a marked decrease in efficiency and resolution while not having an effect on enantioselectivity and elution range. Since dibutyl L-tartrate and its boric acid complex have a low interfacial tension when compared to traditional oil phases such as heptane and octane the addition of co-surfactant was not necessary to form the microemulsion. The effects of pH and the addition of organic modifiers were also investigated. Increasing the pH of the microemulsion influenced the separation in two ways. Firstly, an increase in pH resulted in more chiral selector complex being formed which increased enantioseparation. However, since the analytes were basic ( $pK_a \sim 9$ ), an increase in pH also decreased their ionisation and reduced electrostatic interaction with the anionic chiral complex. The optimum pH of 8 was reached based on a compromise between the two competing effects. Addition of organic modifiers such as methanol, ethanol and ACN did not improve separation.

### **3.6.2 Effect of ME component purity on chiral separation**

In previous studies by Kahle and Foley [10;57-59;61] it was suggested that the chiral surfactant (R- and S- DDCV) may have contained impurities, which would have impacted on the enantioselectivity, resolution, efficiency and migration of enantiomeric ephedrine compounds. Recently Kojtari and Foley [63] investigated the purity of R- and S-DDCV and its impact on the enantioseparation of chiral ephedrine and pseudoephedrine. The purity of R- and S-DDCV was assessed by polarimetry and fast atom bombardment mass spectrometry (FAB-MS), and through enantioselectivity values. Results suggested that R-DDCV was less pure than S-DDCV and this was reflected in enantioselectivity and resolution values.

### **3.6.3 Chiral co-surfactant Vs achiral co-surfactant**

Lately Kojtari et al. [64] investigated the effect of co-surfactant on the chiral separation of a range of chiral ephedrine compounds (ephedrine, pseudoephedrine, N-methylephedrine, and synephrine) in addition to atenolol and metoprolol. The surfactant S-DDCV was used as the principal chiral component while both racemic 2-hexanol and chiral S-2-hexanol, respectively, were employed as the co-surfactant to

prepare the alcohol modified ‘swollen micelles’. The investigation was also carried out through varying the phase ratio in which the chiral surfactant and chiral co-surfactant were employed. Concentrations composed of 3.0% (w/v) S-DDCV/2.48% (v/v) S-2-hexanol (1.5 x phase ratio), 4.0% S-DDCV/3.30% S-2-hexanol (2.0 x phase ratio) and 2.0% S-DDCV/1.65% S-2-hexanol (1.0 x phase ratio) were examined. The authors compared the chromatographic figures of merit and compared them with other aggregate systems. As a starting point for method development 2.0% DDCV and 1.65% 2-hexanol were chosen as these concentrations proved to be optimum from previous chiral microemulsion studies [57]. Table 3.1 details the compositions examined and the enantioselectivities achieved for the eight systems investigated. It was noted that enantioselectivity increased for ephedrine, pseudoephedrine, N-methylephedrine and synephrine with increasing surfactant concentration when the co-surfactant was achiral. When both the surfactant and co-surfactant were chiral maximum enantioselectivity was reached at 3% DDCV and decreased at 4%. Similar trends were also noted for efficiency. The authors postulated that the drop in enantioselectivity, efficiency and resolution was most likely due to an interaction of both chiral components which reduced interaction between the aggregate and analyte. Interestingly, the two chiral component swollen micelle systems had lower resolutions and similar enantioselectivities when compared to the one chiral component systems. This result is in contrast to previous studies of microemulsion systems where enantioselectivity increased with an increased number of chiral components. Also noteworthy was that systems containing 4% DDCV were stable for only 2-3 weeks.

**Table 3.1 Enantioselectivities achieved for the ephedrine compounds and the compositions examined. [64]**

	Racemic 2-hexanol <sup>a)</sup>			(S)-2-hexanol <sup>a)</sup>			Phase ratio <sup>b)</sup>	
	2%	3%	4%	2%(1x)	3%	4%	1.5X	2.0x
Ephedrine	1.091	1.164	1.213	1.110	1.138	1.115	1.082	1.074
Pseudoephedrine	1.179	1.290	1.372	1.209	1.253	1.140	1.171	1.168
N-Methylephedrine	1.104	1.145	1.182	1.120	1.143	1.112	1.043	1.031
Atenolol	1.044	1.035	1.025	1.027	1.040	1.035	1.035	1.028
Metoprolol	1.114	1.062	1.060	1.051	1.147	1.055	1.042	1.040
Synephrine	1.064	1.067	1.075	1.066	1.070	1.053	1.060	1.059
Arithmetic Mean	1.099	1.127	1.154	1.079	1.132	1.085	1.072	1.067

a) Surfactant (S-DDCV) concentration was 2, 3 or 4% w/v; co-surfactant concentration was 1.65% v/v.

b) In total 1.5 x : 3% w/v chiral surfactant (S-DDCV) and 2.48% v/v co-surfactant (S-2-hexanol); 2.0 x : 4% surfactant (S-DDCV) and 3.30% co-surfactant (S-2-hexanol).

### 3.6.4 Chiral separation using cyclodextrin-modified MEEKC

Cyclodextrins (CDs) are additives that do not form aggregate structures and have been predominantly used as chiral selectors in CE. Since CDs are available in a range of shapes and forms (cationic, neutral, anionic, etc), they offer many possibilities as PSPs. CDs behave as secondary PSPs in the ME running buffer and possess the ability to incorporate analytes into their cavity to varying degrees based on hydrophobicity, hydrogen bonding capability and steric hindrance [65;66], thereby separating similar compounds [67]. Other chiral agents such as crown ethers and glycopeptides have also been used in MEEKC to induce chiral recognition [50].

Borst et al. [50] utilised a range of cyclodextrins in MEEKC for the chiral analysis of structurally related phenylalanine derivatives (DL-3,4-dihydroxyphenylalanine (dopa), DL-phenylalanine, DL-tyrosine, and DL-methyldopa). After optimising the microemulsion, a range of cyclodextrins were examined for the enantioseparation of DL-dopa. Initially a range of native cyclodextrins ( $\alpha$ -,  $\beta$ -,  $\gamma$ -CD) were examined in the concentration range 0.75, 1.5 and 3.0%. When no separation was observed, a range of neutral CDs (heptakis (2,6-di-O-methyl)- $\beta$ -CD, heptakis (2,6,6-tri-O-methyl)-  $\beta$ -CD and hydroxypropyl-  $\beta$ -CD) and anionic CDs (heptakis (2,3-di-O-diacetyl-6-O-sulfo)-  $\beta$ -CD (HDAS), heptakis (2,3-di-O-dimethyl-6-O-sulfo)-  $\beta$ -CD (HDMS) and heptakis (6-O-sulfo)-  $\beta$ -CD (HS)) were assessed. HS- $\beta$ -CD resulted in partial enantioseparation while full enantioseparation was achieved with 1.25% sulphated  $\beta$ -CD. Through variation of pH between 2 and 2.5, along with the concentration of sulphated  $\beta$ -CD, chiral separation of the other phenylalanine derivatives was achieved.

Neutral enantiomers of esbiothrin have been separated by CD-MEEKC through variation of CD type and ME buffer pH [14]. The chiral selectors included  $\alpha$ -CD,  $\beta$ -CD, hydroxypropyl- $\beta$ -CD (HP- $\beta$ -CD), methyl- $\beta$ -CD (M- $\beta$ -CD), poly- $\beta$ -CD, sulphated- $\beta$ -CD (S- $\beta$ -CD) and  $\gamma$ -CD at buffer pH 7-11. Both  $\alpha$ - and  $\gamma$ -CD showed poor solubility in the microemulsion and due to their low concentration (1% w/v) did not produce any enantioselectivity. It was noted that S- $\beta$ -CD had the same migration direction (opposite to the EOF) as the negatively charged ME droplets, and this resulted in the problematic migration of the analytes. HP- $\beta$ -CD, M- $\beta$ -CD and poly- $\beta$ -CD resulted in full separation of the enantiomer in the pH range 9-11, with M- $\beta$ -CD (3% w/v) providing the best separation at pH 10.

Giannini et al. [68] developed a cyclodextrin modified MEEKC method for the analysis of oxybutynin and its related impurities. The optimum composition was found to be 89.1% 10 mM borate buffer pH 9.2, 1.7% n-heptane, 9.2% SDS/n-butanol in a 1:2 ratio and 18 mM (2-hydroxypropyl)- $\beta$ -CD.

### **3.7 Recent developments in MEEKC-MS**

MEEKC-MS was first introduced in 2007 [69-71] following the introduction of atmospheric pressure photo ionisation (APPI) [72] and its subsequent coupling to CE [73]. APPI ionises sample molecules using high-energy photons from a krypton lamp, and this overcame the problem of charged surfactants, such as SDS, having a suppressive effect on ESI [74]. The technique has been applied to the separation and detection of acidic, basic and neutral stimulants [71] as well as a range of pharmaceutical compound [69;70]. Interested readers are referred to a review article by Klampfl [75] covering all aspects of CE-MS including MEEKC-MS.

More recently Ortner et al. [24] coupled MEKC to MS using a volatile micelle forming compound in place of SDS. Perfluorooctanoic acid (PFOA) in combination with volatile ammonium acetate buffer was used for the separation and detection of insulin and its analogues through MEKC-ESI-MS. On investigation it was found that while suppression did occur the signals were suitable for qualitative and quantitative analysis. Henchoz et al. [76] utilised MEEKC-APPI-MS for the rapid determination of octanol-water partition coefficients ( $\log P$ ) for a range of basic compounds. The results were compared to MEEKC-UV. It was shown that in MS mode very lipophilic compounds could be separated from the ME marker according to their respective  $m/z$  with a slight sacrifice in efficiency when compared to MEEKC-UV. Due to sample pooling a 21 fold increase in throughput was achieved in MS mode.

#### **3.7.1 MEEKC-ICP-MS**

A novel coupling of MEEKC to ICP-MS was reported by Bytzek et al. [77] for the analysis of platinum (II) and platinum (IV) complexes which are used in anticancer drugs. The migration behaviour and  $\log P_{ow}$ , which reflects the uptake of such metal complexes into the cell, has previously been described in MEEKC [78;79]. Coupling MS to element specific ICP resulted in enhanced sensitivity and selectivity. Also, in contrast to ESI-MS the ICP-MS method was not influenced by ion suppression. DMSO (34S) and 1-bromodecane (79Br) were used as markers for EOF and ME droplets

respectively in ICP-MS mode. The ICP-MS mode was capable of detecting compounds which do not possess a chromophore such as 1-dromodecane. The developed method was compared to MEEKC-UV/vis, and while the ICP-MS provided higher selectivity and sensitivity, MEEKC-UV/vis was found to be more stable in operation and gave high linearity of the calibration curve without the addition of internal standards.

### **3.8 Improved Limits of Detection**

Improved LODs have also been achieved through use of LIF [80] and electrochemical detection [81]. Yu et al. [81] achieved the separation of 14 flavanoids using MEEKC and reported detection limits ranging from 0.02 to 0.5 µg/L with electrochemical detection.

### **3.9 Prediction of solute characteristics and partitioning mechanisms**

Choice of microemulsion components and method conditions is critical to successful separation in MEEKC. An understanding of the interaction between the ME PSP and analytes of interest gives an advantage to the practitioner in allowing the logical choice of microemulsion components. Previous advances in chemometric design [82] have proved useful in predicting optimum ME compositions for separation in MEEKC. Recently Giannini et al. [68] employed experimental design for the analysis of oxybutynin and its impurities. Advances in MEKC structure-migration relationships [83] may also reveal results which have a bearing on MEEKC. Poole et al. [84] published a detailed review covering structure-migration relationships in MEKC. MEEKC has also been used recently to model and predict octanol-water partition coefficients (Log P) with reference to drug-tissue binding [85].

#### **3.9.1 Experimental design strategy**

Giannini et al. [68] developed and optimised a method for the analysis of oxybutynin and its impurities through mixture design. The method involved the chiral separation of five compounds and one achiral compound. Initially the microemulsion composition was optimised according to a previous paper for the analysis of ketorolac and related substances [82]. The approach involved an experimental plan with 13 runs to optimise the elements of the microemulsion (SDS, n-butanol, n-heptane and 10 mM sodium borate buffer at pH 9.2) with an appropriate CD. The composition of the microemulsion was then correlated through the *Scheffe Special Cubic Model* [86] based

on chosen responses (e.g. resolution, migration time). The *Scheffe Special Cubic Model* is a polynomial equation which represents the response. The model was then used to predict the optimal microemulsion. Where there was a conflict in the optimum composition *Derringer's Desirability Function* (D) was employed [86]. The concentration of CD and applied voltage were also assessed by using *Doehlert* experimental design [86] *Doehlert* design allowed an efficient and in-depth analysis of these two factors. The final optimised microemulsion composition allowed full separation of analytes within 12 minutes and was validated according to ICH guidelines.

Recent work in MEKC may also help facilitate the rational choice of PSP in MEEKC. Fu et al. [83] developed a micellar selectivity triangle (MST) to characterise and classify the chemical selectivities of PSPs in EKC. The theory of the MST is similar to the solvent selectivity triangle (SST) [87]. A training set of 35 analytes with various sizes, polarities and hydrogen bonding capabilities, were analysed using MEKC among various surfactants. The results were characterised and classified in terms of the chemical selectivity of the PSP using linear solvation energy relationships (LSERs) [88-90].

### **3.9.2 Microemulsion Structure**

While a lot work has been dedicated to the effect of microemulsion composition on separation, few have correlated the relationship with ME droplet microstructure. Cao et al. [91] recently related changes in microemulsion composition to microemulsion droplet size and surface charge density. The effect on separation with regard to migration window, peak shape, efficiency etc was discussed. A widely utilised microemulsion consisting of SDS, 1-butanol, octane and sodium borate buffer was examined. The influence of the organic modifiers such as ACN and methanol was also assessed. The concentration of all microemulsion components was varied and droplet size was measured by dynamic light scattering (DLS), while the Zeta potential ( $\zeta$ ) was used to infer the charge density on the droplets. Increasing surfactant concentration from 2.4 to 4.6% resulted in a drop in droplet size from 190 to 120 nm respectively. Interestingly, the  $\zeta$  remained unchanged. The authors noted that as the droplet size reduced the aggregation number of the surfactant was correspondingly reduced due to electrostatic repulsion, hence that charge-to-size ratio and hence  $\zeta$  remained unchanged. A decrease in droplet size led to an increase in electrophoretic mobility towards the

anode and increase in the migration window. It was reported that for neutral analytes the migration window had a significant impact on the achievable resolution. Conversely an increase in 1-butanol concentration resulted in an increase in droplet size through swelling and a decrease in  $\zeta$ . With regard to separation a decrease in charge density of the droplets contributes to a shorter migration window which may hinder resolution. However, mass transfer between the analyte and PSP is increased due to the droplet being swollen and this increased efficiency may be offset against the narrower migration window. Variation in the oil phase of the microemulsion revealed little change in either droplet size or  $\zeta$ . The addition of ACN between 0 and 9% had no effect on droplet size but decreased  $\zeta$  which acted to increase the migration window. The addition of modifiers have been vital to the successful separation of many analytes in MEEKC through altering selectivity and improving resolution [15;17;18]. The result demonstrated that ACN resides on the outside of the ME droplet and in addition to influencing partitioning with the PSP, it can also be used to effect EOF and analyte solubility.

### 3.9.3 Calculating partition coefficients in MEEKC

Wan et al. [85] recently developed a method to predict brain tissue binding of central nervous system (CNS) drugs based on the relationship between analyte lipophilicity and migration time in MEEKC.

The octanol-water partition coefficient ( $\log P$ ) is an indicator of analyte solubility or hydrophobicity and can be determined from the relationship with  $\log k$  through a linear plot [47] as given in Equation 3.

$$\text{Log } P = b \log k + a \quad (3.3)$$

Where  $b$  and  $a$  represent the slope and intercept respectively.

Initially the relationship between the  $\log P$  and  $k$  for a set of standards with known  $\log P$  was examined using the MEEKC method according to the relationship described in Equation 3. An excellent correlation was observed ( $R^2=0.991$ ).

The  $\log k$  of 36 CNS drugs and of 26 test compounds was then measured according to MEEKC method. When the relationship between the  $\log P$  values and the fraction of unbound drug in brain tissue was plotted a good correlation ( $R^2=0.79$ ) was observed.

The results indicated that the developed method was applicable for brain tissue binding prediction and lipophilicity screening.

Henchoz et al. [76] used MEEKC to determine the log P for a range of acidic, basic and neutral analytes. The optimised microemulsion consisted of 6.6% w/v 1-butanol, 3.3% w/v SDS and 0.78% w/v heptane and was prepared in two buffering systems, pH 2 which was made up of phosphoric acid and 1 M NaOH and pH 10 which was made up of boric acid and 1 M NaOH. 35 reference compounds were first examined based on their van der Waals volume, polarizability, H-bond donor acidity, H-bond acceptor basicity and log P values. Neutral and basic compounds were analysed at pH 10, while acidic compounds were analysed at pH 2. The data obtained showed excellent agreement between the shake-flask method (actual measured partition coefficient between octanol and water) and HPLC. Analysis times were improved by using short-end injection (reduction in analysis time from 60 min per compound to 25 minutes per compound) under alkaline conditions. A coated capillary was used for the analysis of acidic compounds to impart a negative charge on the capillary wall and stabilise the EOF.

Recent work has also compared the prediction of log P values for a range of disubstituted benzene compounds in MEEKC and MEKC systems [50]. The authors noted good agreement between both modalities and literature values indicating that either MEEKC or MEKC could be used for log P determination.

### **3.10 Recent applications in MEEKC**

Besides the fundamental aspects of previously described reports in this paper, it is relevant to mention advances in MEEKC applications. From late 2008 to June 2010 MEEKC has been applied to the water analysis [92], vitamins [18;93], bioanalysis [54], natural products [94-96] and antibiotics [97]. Table 3.2 specifies the optimised ME composition and separation application for all reports in this paper.

**Table 3.2 MEEKC applications and microemulsion composition**

<b>Application</b>	<b>Composition</b>	<b>Ref.</b>
Separation of urinary porphyrins.	60 mM SDS, 6.61% w/v 1-butanol, 0.82% w/w 1-octanol, 20.0% v/v acetonitrile and 20 mM N-tris(hydroxymethyl)methyl-2-aminoethanesulfonic acid pH 7.5.	[15]
Separation of isoquinoline alkaloids.	18 mM sodium cholate, 2.4% v/v 1-butanol, 0.6% v/v ethyl acetate, 10% v/v methanol and 87% v/v 5 mM sodium tetraborate/ 10 mM sodium phosphate buffer pH 10.2.	[16]
Separation of neutral saponins	3% w/v SDS, 6% w/v 1-butanol, 0.6% w/v heptane, 5% w/v ACN and 85.4% v/v 10 mM sodium tetraborate buffer pH 9.1.	[36]
Separation of flavonoids	80 mM SDS, 0.6% v/v 1-butanol, 1.2% v/v ethyl acetate, 10% v/v ACN and 50 mM phosphoric acid pH 1.8.	[98]
Analysis and online sample concentration of Glucosides	2.0% (w/v) Brij-35, 6.0% (w/v) 1-butanol, 0.6% (w/v) heptanes, 20% (w/v) ACN and 40 mM sodium tetraborate buffer pH 9.2	[37]
Detection and online sample concentration of penicillins.	2.21% w/v SDS, 7.71% w/v 2-propanol, 0.81% w/v propylene glycol monomethyl ether acetate (PGMEA) and 89.27% v/v 50 mM phosphoric acid pH 2.0 and pH 8.0.	[42]
Separation and online concentration of aromatic acid impurities.	3.75% w/v SDS, 5.0% w/v cyclohexanol, 0.975% w/v n-octane and 90.3% v/v 50 mM phosphate buffer pH 3.0.	[45]
Separation of charged phenolic acid compounds in a plant.	3.0% w/v Brij-35, 6.0% w/v 1-butanol, 0.6% w/v octane and 90.4% v/v 40 mM sodium tetraborate buffer pH 9.0.	[49]
Separation of water- and oil-soluble vitamins.	1.2% w/w SDS, 21% v/v 1-butanol, 18% v/v acetonitrile, 0.8% w/w n-hexane and 20 mM borax buffer pH 8.7.	[18]
Analysis of water- and oil-soluble vitamins.	0.8% heptanes, 2.6% SDS, 6.6% 1-butanol, 10 % 2-propanol, 0.4% Brij 35 and 25 mM sodium tetraborate buffer pH 9.2	[93]
Separation and detection of insulin and its related analogues using solvent modified MEKC-MS.	100 mM SDS and 15% acetonitrile in 10 mM sodium borate buffer pH 9.2.	[24]
Determination of Log P values using	3.0% w/v SDS, 6.6% w/v 1-butanol, 0.78%	[76]

MEEKC-MS	w/v heptanes and 20 mM phosphoric acid/sodium hydroxide pH 2.0 or boric acid/sodium hydroxide pH 10.	
Analysis of Platinum complexes utilising MEEKC-ICP-MS	1.43% SDS, 6.57% 1-butanol, 0.85% heptanes and 91.15% 10 mM phosphate buffer pH 7.4.	[77]
CD-modified separation of esbiothrin and its enantiomers.	2.3% w/w SDS, 6.6% w/w n-butanol, 0.8% w/w n-heptane and 96.7% 10 mM sodium tetraborate buffer pH 10 containing 5% w/v $\beta$ -CD.	[14]
CD-modified enantioseparation of phenylalanine and its derivatives.	1.5% SDS, 3% 1-butanol, 0.5% n-octane, 2% 2-propanol, 4% sulphated $\beta$ -CD and 95.0% 20 mM sodium hydrogen phosphate buffer pH 2.5.	[50]
CD-modified enantioseparation of oxybutynin and its impurities.	89.1% 10 mM borate buffer pH 9.2, 1.7% n-heptane, 9.2% SDS/n-butanol in a 1:2 ratio and 18 mM (2-hydroxypropyl)- $\beta$ -CD.	[68]
Separation of highly hydrophobic structurally related corticosteroids.	3.6% w/w SDS, 6.6% w/w 1-butanol, 0.8% w/w n-octane and 89% w/w 40 mM sodium dihydrogen phosphate buffer pH 8.0.	[52]
Enantioseparation of ephedrine and pseudoephedrine.	2% R/S DDCV, 1.65% v/v 2-hexanol, 1.23% v/v diethyl tartrate and 50 mM sodium phosphate buffer pH 7.0.	[63]
Enantioseparation of $\beta$ -blockers and structurally related compounds	50 mM TTAB, 30 mM dibutyl L-tartrate in 30 mM sodium tetraborate and 60 mM dihydrogen phosphate mixed buffer at various pH.	[62]
Enantioseparation of a range of ephedrine compounds.	S-DDCV (2.0, 3.0 or 4.0% w/v), S- and/or racemic 2-hexanol (1.65, 2.48 or 3.30% v/v) in 50 mM sodium dihydrogen phosphate buffer pH 7. -	[64]
Detection and separation of ephedrine and pseudoephedrine employing laser-induced fluorescence detection.	3.24% w/w n-heptane, 3.24% w/w SDS, 26.44% w/w 1-butanol and 95% 50 mM sodium borate buffer containing 16% acetonitrile pH 7	[80]
Separation and determination of flavonoids employing electrochemical detection.	0.9% w/v SDS, 0.9% w/v sodium cholate, 0.9% w/v 1-butanol, 0.6% w/v ethyl acetate and 98.2% v/v 10mM sodium tetraborate buffer pH 7.5.	[81]
Analysis of chlorophenols in water.	15 mM SDS, 112 mM 1-butanol, 10 mM n-	[92]

---

	octane and 20 mM sodium tetraborate buffer pH 9.0.	
Determination of the coenzyme Q10 (2,3-dimethoxy-5methyl-6-decaprenyl-1,4-benzoquinone) in human plasma.	1.4% w/w sodium bis(2-ethylhexyl) sulfosuccinate (AOT), 4% w/w cholic acid, 8.5% w/w butanol, 1% w/w octane, 0.1% w/w PVA and 85% w/w 10 mM Tris buffer pH 9.0.	[54]
Determination of catechols and caffeine in tea.	1.36% (w/v) heptanes, 3.5 % (w/v) SDS, 9.72% (w/v) 1-butanol and 86.5% (v/v) 10 mM buffer solution containing sodium acetate and citric acid	[95]
Fingerprint analysis and extraction of <i>resina draconis</i> .	3.3% w/v SDS, 6.6% w/v 1-butanol, 0.8% w/v n-octane and 10 mM sodium tetraborate buffer pH 9.2.	[94]
Separation and determination of nitrofurans antibiotics in fish.	3.48% w/w SDS, 6.48% w/w 1-butanol, 0.82% w/w octane and 10 mM sodium tetraborate buffer pH 9.70.	[97]
Separation of phenolic acids and diterpenoids using W/O MEEKC.	48 % w/v 1-butanol, 18 % w/v SDS, 8.0 % w/v 2-propanol and 26 % v/v sodium acetate buffer pH 6.0	[99]

---

### 3.10.1 Water analysis

Zhou et al. [92] developed a method for the analysis of 2-chlorophenol, 4-chlorophenol, and 2,4-dichlorophenol in water samples. The optimum microemulsion was composed of 15 mM SDS, 112 mM 1-butanol, 10 mM n-octane and 20 mM sodium tetraborate buffer pH 9.0. The method was optimised in terms of applied voltage, pH, and component concentration. The concentration of SDS, 1-butanol and octane all had an effect on the separation and at optimum concentrations the separation was achieved in less than eight minutes. Water samples were pre-treated with C18 SPE before MEEKC analysis and the method was validated in terms of linearity and precision with limits of detection between 0.5 and 50  $\mu\text{g L}^{-1}$  achieved.

### 3.10.2 Vitamin analysis

Yin et al. [18] simultaneously separated oil and water soluble components in a vitamin preparation containing a range of 13 oil and water soluble vitamins. The novel microemulsion consisted of 1.2% (w/w) SDS, 21% (v/v) 1-butanol, 18% (v/v) acetonitrile and 0.8% (w/w) n-hexane in a 20 mM borax buffer pH 8.7. The authors

noted that the choice of organic modifier, co-surfactant and ME pH had the greatest effect on the separation of the fat-soluble vitamins, water soluble vitamins, and stabilisation of the system respectively. In terms of migration time reproducibility, flushing the capillary between runs with three minutes of water and three minutes of microemulsion was necessary. The optimised ME achieved the baseline separation and detection of all vitamins in the test mixture, however when applied to the multivitamin sample, two water soluble vitamins (B12 and H) and two oil soluble vitamins (A and D3) were below the limit of detection

More recently Svidritskii et al. [93] reported a method for the simultaneous separation of oil- and water-soluble vitamins. The optimised microemulsion was composed of 0.8% heptane, 2.6% SDS, 6.6% 1-butanol, 10 % 2-propanol, 0.4% Brij 35 and 25 mM sodium tetraborate buffer pH 9.2. The authors also compared a range of previously reported microemulsions with respect to the number of vitamins separated, analysis time and disadvantages. The authors stated that MEEKC without the use of suppressed EOF was preferable and that the addition of organic modifiers such as 2-propanol was necessary for the separation of oil-soluble vitamins. Interestingly, it was noted that addition of 2-propanol increased the viscosity and reduced the EOF which resulted in long analysis time. However, the addition of Brij 35 had the opposite effect by reducing the effective charge on the ME droplet thereby reducing the migration window and was used to reduce the overall analysis time.

### **3.10.3 Bioanalysis by MEEKC**

A MEEKC method [54] utilising the double chain surfactant sodium bis(2-ethylhexyl) sulfosuccinate (AOT) and cholic acid was applied to the quantitative determination of the highly hydrophobic coenzyme Q10 (2,3-dimethoxy-5methyl-6-decaprenyl-1,4-benzoquinone) in human plasma. The optimised MEEKC method was validated and compared with a standard HPLC method. Table 3.3 below shows a comparison between the Q10 determined in human plasma by MEEKC and HPLC. The results demonstrated good agreement between the two methods, providing evidence that the MEEKC method could be adopted for clinical studies.

**Table 3.3 Comparison of the mean values of Q10 in plasma samples determined by MEEKC and HPLC. [54]**

<i>Mean Q10 value</i>	<i>MEEKC (<math>\mu\text{g/mL}</math>)</i>	<i>HPLC (<math>\mu\text{g/mL}</math>)</i>	<i>R<sup>a)</sup></i>
<i>in plasma samples (n=5)</i>	1.11 +/- 0.47	0.99 +/- 0.50	0.9938

<sup>a)</sup>R Correlation coefficient between results performed by MEEKC and HPLC methods

### 3.10.4 Natural products analysis by MEEKC

Cao et al. [94] developed a MEEKC method for the fingerprint analysis and extraction of *resina draconis* in four Chinese herbal medicines. The samples contained both water- and fat-soluble analytes with a wide range of polarities. The optimised ME consisted of 3.3% (w/v) SDS, 6.6% (w/v) n-butanol and 0.8% (w/v) n-octane in a 10 mM sodium tetraborate buffer pH 9.2. When compared to an optimised HPLC method, 27 peaks were detected by the MEEKC method compared to 20 in HPLC.

Kartsova et al. [95] utilised MEEKC with suppressed EOF (also termed reverse flow (RF) MEEKC) for the quantitative determination of catechols and caffeine in black and green tea. The optimised MEEKC microemulsion consisted of 1.36% (w/v) heptane, 3.5 % (w/v) SDS, 9.72% (w/v) 1-butanol and 86.5% (v/v) 10 mM buffer solution containing sodium acetate and citric acid. Separations were performed by CZE, normal MEKC, RF-MEKC, normal MEEKC and RF-MEEKC. Under normal separation conditions above pH 7 the polyphenolic catechols were partially oxidised. Since all catechols were negatively charged they co-migrated as a single peak by CZE. In reversed flow mode at pH 2 MEEKC outperformed MEKC in terms of efficiency and LOD, however RF-MEKC resulted in a more rapid separation (11 mins Vs 40 mins). Similar work by the same group [4] developed MEEKC and MEKC methods for the analysis of catechols and catecholamine's in black and green tea samples.

### 3.10.5 Detection of antibiotics by MEEKC

The presence of four nitrofurans (NF) antibiotics (furazolidone, furaltadone, nitrofurazone and nitrofurantoin) in fish was examined using MEEKC [97]. NFs are broad spectrum antibiotics used for the treatment of protozoan infections in both humans and fish. Despite their therapeutic properties, NFs have been shown to be both mutagenic and carcinogenic. The microemulsion was optimised in terms of surfactant, co-surfactant and oil concentration with the optimum buffer being composed of 0.82 %

(w/w) octane, 3.48 % (w/w) SDS and 6.48 % (w/w) butanol in a 10 mM sodium borate buffer pH 9.70. The method was successfully validated and applied to the determination of NF antibiotics in contaminated fish.

### **3.11 W/O MEEKC**

W/O MEEKC was reported in 2004 by Altria et al. [100] for the separation of neutral and acidic compounds. W/O MEs are composed of water droplets surrounded by surfactant and co-surfactant in a nonpolar bulk phase. Since the main component of the bulk phase is oil, a low separation current is generated allowing the application of high voltages. However, high buffer concentrations are required to generate a sufficient operating current. W/O MEEKC offers an alternative separation selectivity and unlike O/W MEEKC solutes do not partition in order of their hydrophobicity.

Cao et al. [99] recently compared O/W and W/O MEEKC for the separation of eight phenolic acids and five diterpenoids. The O/W microemulsion consisted of 0.6 % w/v cyclohexane, 3 % w/v SDS, 6.0 % w/v 1-butanol and 3.0 % w/v ACN in 87.4 % v/v sodium tetraborate buffer at pH 8.0, while the W/O buffer was composed of 48 % w/v 1-butanol, 18 % w/v SDS and 8.0 % 2-propanol in 26 % v/v sodium acetate buffer pH 6.0. Both systems were optimised in terms of oil type and concentration as well as surfactant content. While the two methods allowed complete separation of the 13 analytes, the O/W ME buffer provided superior resolution and peak shape along with quicker analysis time.

### **3.12 Conclusion**

This chapter has demonstrated the continuing application of MEEKC to a wide range of uses where fast and efficient separations for a wide range of acidic, basic and neutral, water-soluble and water-insoluble compounds have been achieved. The components of the microemulsion offer several optimisation options in terms of changes to the surfactant/co-surfactant concentration and type, pH and oil type. Investigations into the fundamental physicochemical characteristics of microemulsions in terms of the affects each component has on these characteristics and on separations are beginning to reveal more information about the interaction of analytes with the microemulsion and will contribute to more rapid method development. Conversely, the increased number of method variables compared to CZE and the relative lack of knowledge about these

physicochemical characteristics and the affects they have on MEEKC separations can result in slower method development for some applications.

Whilst the time period covered by this chapter has seen the publication of articles describing a wide range of developments in MEEKC, the issue of relatively poor UV detection sensitivity of CE techniques in general has been increasingly addressed in articles examining preconcentration techniques. This trend has been reflected in the extended focus of Section 3.4 on these techniques.

While SDS remains the most common surfactant in use for reported MEEKC applications, there has been an increase in the number of reports utilising alternative types of surfactant, such as non-ionic surfactants, bile salts and mixed surfactant systems. Enantioseparation have been achieved through the use of chiral ME components and complexes as well as through the addition of CDs to the microemulsion.

MEEKC has been shown to provide good quantitative results when cross-validated with other techniques such as HPLC and with advances in online sample concentration and MEEKC-MS detection, the sensitivity of MEEKC for the detection of trace solutes has been greatly improved.

MEEKC has also found use in pharmacokinetics by predicting brain tissue binding of central nervous system (CNS) drugs based on the relationship between analyte lipophilicity and migration time in MEEKC. Due to the continuing increase in the number and range of applications along with continuous improvements and additions to the knowledge of the mechanism behind MEEKC separations, this mode of CE is expected to increase in popularity for novel and routine research in analytical method development.

### 3.13 References

- [1] Ryan, R., Donegan, S., Power, J., McEvoy, E. and Altria, K., *Electrophoresis*, 30 (2009) 65-82.
- [2] McEvoy, E., Marsh, A., Altria, K., Donegan, S. and Power, J., *Electrophoresis*, 28 (2007) 193-207.
- [3] Huie, C.W., *Electrophoresis*, 27 (2006) 60-75.
- [4] Marsh, A., Clark, B., Broderick, M., Power, J., Donegan, S. and Altria, K., *Electrophoresis*, 25 (2004) 3970-3980.
- [5] Hansen, S.H., *Electrophoresis*, 24 (2003) 3900-3907.
- [6] Altria, K.D., *Journal of Chromatography A*, 892 (2000) 171-186.
- [7] Altria, K.D., Mahuzier, P.E. and Clark, B.J., *Electrophoresis*, 24 (2003) 315-324.
- [8] Pedersen-Bjergaard, S., Gabel-Jensen, C. and Hansen, S.H., *Journal of Chromatography A*, 897 (2008) 375-381.
- [9] Pomponio, R., Gotti, R., Fiori, J. and Cavrini, V., *Journal of Chromatography A*, 1081 (2005) 24-30.
- [10] Kahle, K.A. and Foley, J.P., *Electrophoresis*, 27 (2006) 4321-4333.
- [11] Peterson, A.G. and Foley, J.P., *Journal of Microcolumn Separations*, 10 (1998) 633-645.
- [12] Terabe, S., Otsuka, K., Ichikawa, K., Tsuchiya, A. and Ando, T., *Analytical Chemistry*, 56 (1984) 111-113.
- [13] Watarai, H., *Chemistry Letters*, (1991) 391-394.
- [14] Chu, B.L., Guo, B.Y., Wang, Z.H. and Lin, J.M., *Journal of Separation Science*, 31 (2008) 3911-3920.
- [15] Li, J.H. and Cai, Z.W., *Talanta*, 77 (2008) 331-339.
- [16] Yu, L.S., Xu, X.Q., Huang, L., Lin, J.M. and Chen, G.N., *Electrophoresis*, 30 (2009) 661-667.
- [17] Zhu, J.H., Qi, S.D., Zhang, H.G., Chen, X.G. and Hu, Z.D., *Journal of Chromatography A*, 1192 (2008) 319-322.
- [18] Yin, C.N., Cao, Y.H., Ding, S.D. and Wang, Y., *Journal of Chromatography A*, 1193 (2008) 172-177.
- [19] Wen, T., Zhao, X., Luo, G.A., Wang, Y.M., Wang, J., Zhu, J. and Yu, Z.S., *Chinese Journal of Analytical Chemistry*, 34 (2006) 1529-1534.

- [20] Wen, T., Zhao, X., Luo, G.A., Wang, J., Wang, Y.M., Yao, B., Zhao, J.Y., Zhu, J. and Yu, Z.S., *Talanta*, 71 (2007) 854-860.
- [21] Yang, X., Xia, Y., Tao, C.J., Liao, Y.P., Zuo, Y.M. and Liu, H.W., *Electrophoresis*, 28 (2007) 1744-1751.
- [22] Hansen, S.H., Gabel-Jensen, C. and Pedersen-Bjergaard, S., *Journal of Separation Science*, 24 (2001) 643-650.
- [23] Hansen, S.H., Gabel-Jensen, C., El-Sherbiny, D.T.M. and Pedersen-Bjergaard, S., *Trac-Trends in Analytical Chemistry*, 20 (2001) 614-619.
- [24] Ortner, K., Buchberger, W. and Himmelsbach, M., *Journal of Chromatography A*, 1216 (2009) 2953-2957.
- [25] Angkanasiriporn, S., Singsung, W., Petsom, A. and Nhujak, T., *Electrophoresis*, 31 (2010) 695-701.
- [26] Poouthree, K., Leepipatpiboon, N., Petsom, A. and Nhujak, T., *Electrophoresis*, 28 (2007) 767-778.
- [27] Olvecka, E., Konikova, M., Grobuschek, N., Kaniansky, D. and Stanislawski, B., *Journal of Separation Science*, 26 (2003) 693-700.
- [28] Busnel, J.M., Lion, N. and Girault, H.H., *Electrophoresis*, 29 (2008) 1565-1572.
- [29] Fischer, J. and Jandera, P., sample stacking. In U. Pyell (Ed.), *Electrokinetic Chromatography*, Wiley, UK, 2006.
- [30] Huang, H.Y., Lien, W.C. and Huang, I.Y., *Electrophoresis*, 27 (2006) 3202-3209.
- [31] Huang, H.Y., Huang, I.Y., Liang, H.H. and Lee, S., *Electrophoresis*, 28 (2007) 1735-1743.
- [32] Huang, H.Y. and Hsieh, S.H., *Journal of Chromatography A*, 1164 (2007) 313-319.
- [33] Garcia, L.L. and Shihabi, Z.K., *Journal of Chromatography A*, 652 (1993) 465-469.
- [34] Shihabi, Z.K., *Electrophoresis*, 19 (1998) 3008-3011.
- [35] So, T.S.K., Jia, L. and Huie, C.W., *Electrophoresis*, 22 (2001) 2159-2166.
- [36] Cao, J., Qi, L.W., Chen, J. and Li, P., *Electrophoresis*, 29 (2008) 4422-4430.
- [37] Cao, J., Yi, L., Li, P. and Chang, Y.X., *Journal of Chromatography A*, 1216 (2009) 5608-5613.

- [38] Britz-McKibbin, P., Otsuka, K. and Terabe, S., *Analytical Chemistry*, 74 (2002) 3736-3743.
- [39] Quirino, J.P. and Terabe, S., *Chromatographia*, 53 (2001) 285-289.
- [40] Macia, A., Borrull, F., Calull, M. and Aguilar, C., *Chromatographia*, 63 (2006) 149-154.
- [41] Puig, P., Borrull, F., Aguilar, C. and Calull, M., *Journal of Chromatography B-Analytical Technologies in the Biomedical and Life Sciences*, 831 (2006) 196-204.
- [42] Huang, H.Y. and Hsieh, S.H., *Electrophoresis*, 29 (2008) 3905-3915.
- [43] Chien, R.L. and Burgi, D.S., *Journal of Chromatography*, 559 (1991) 141-152.
- [44] Yu, L.S., Xu, X.Q., Huang, L., Lin, J.M. and Chen, G.N., *Journal of Chromatography A*, 1198 (2008) 220-225.
- [45] Huang, H.Y., Lin, Y.R. and Hsieh, S.H., *Analytica Chimica Acta*, 632 (2009) 148-155.
- [46] Nhujak, T., Saisuwan, W., Srisa-Art, M. and Petsom, A., *Journal of Separation Science*, 29 (2006) 666-676.
- [47] Poouthree, K., Soonthorntantikul, W., Leepipatpiboon, N., Petsom, A. and Nhujak, T., *Electrophoresis*, 28 (2007) 3705-3711.
- [48] Seelanan, P., Srisa-Art, M., Petsom, A. and Nhujak, T., *Analytica Chimica Acta*, 570 (2006) 8-14.
- [49] Cao, J., Qi, L.W., Liu, E.H., Zhang, W.D. and Li, P., *Journal of Pharmaceutical and Biomedical Analysis*, 49 (2009) 475-480.
- [50] Borst, C. and Holzgrabe, U., *Journal of Chromatography A*, 1204 (2008) 191-196.
- [51] Michalska, K., Pajchel, G. and Tyski, S., *Journal of Pharmaceutical and Biomedical Analysis*, 48 (2008) 321-330.
- [52] Wu, C.H., Chen, T.H., Wang, G.R., Huang, K.P. and Liu, C.Y., *Journal of Liquid Chromatography & Related Technologies*, 32 (2009) 833-848.
- [53] Altria, K.D., Clark, B.J. and Mahuzier, P.E., *Chromatographia*, 52 (2000) 758-768.
- [54] Lucangioli, S., Sabrina, F., Mario, C. and Valeria, T., *Electrophoresis*, 30 (2009) 1899-1905.
- [55] Huang, H.Y., Wei, M., Lin, Y.R. and Lu, P.H., *Journal of Chromatography A*, 1216 (2009) 2560-2566.

- [56] Aiken, J.H. and Huie, C.W., *Chromatographia*, 35 (1993) 448-450.
- [57] Kahle, K.A. and Foley, J.P., *Electrophoresis*, 27 (2006) 896-904.
- [58] Kahle, K.A. and Foley, J.P., *Electrophoresis*, 28 (2007) 2503-2526.
- [59] Kahle, K.A. and Foley, J.P., *Electrophoresis*, 28 (2007) 2644-2657.
- [60] Kahle, K.A. and Foley, J.P., *Electrophoresis*, 28 (2007) 1723-1734.
- [61] Preinerstorfer, B., Lammerhofer, M. and Lindner, W., *Electrophoresis*, 30 (2009) 100-132.
- [62] Hu, S.Q., Chen, Y.L., Zhu, H.D., Zhu, J.H., Yan, N. and Chen, X.G., *Journal of Chromatography A*, 1216 (2009) 7932-7940.
- [63] Kojtari, A.B. and Foley, J.P., *Journal of Chromatography A*, 1216 (2009) 3488-3491.
- [64] Kojtari, A.B., Guetschow, E.D. and Foley, J.P., *Electrophoresis*, 30 (2009) 2829-2836.
- [65] Lin, X.L., Zhu, C. and Hao, A., *Journal of Chromatography A*, 1059 (2004) 181-189.
- [66] Lin, X.L., Zhu, C.F. and Hao, A.Y., *Analytica Chimica Acta*, 517 (2004) 95-101.
- [67] Bitar, Y. and Holzgrabe, U., *Electrophoresis*, 28 (2007) 2693-2700.
- [68] Giannini, I., Orlandini, S., Gotti, R., Pinzauti, S. and Furlanetto, S., *Talanta*, 80 (2009) 781-788.
- [69] Himmelsbach, M., Haunschmidt, M., Buchberger, W. and Klampfl, C.W., *Journal of Chromatography A*, 1159 (2007) 58-62.
- [70] Himmelsbach, M., Haunschmidt, M., Buchberger, W. and Klampfl, C.W., *Analytical Chemistry*, 79 (2007) 1564-1568.
- [71] Schappler, J., Guillaume, D., Rudaz, S. and Veuthey, J.L., *Electrophoresis*, 29 (2008) 11-19.
- [72] Robb, D.B., Covey, T.R. and Bruins, A.P., *Analytical Chemistry*, 72 (2000) 3653-3659.
- [73] Zheng, J. and Shamsi, S.A., *Analytical Chemistry*, 78 (2006) 6921-6927.
- [74] Yang, L.Y. and Lee, C.S., *Journal of Chromatography A*, 780 (1997) 207-218.
- [75] Klampfl, C.W., *Electrophoresis*, 30 (2009) S83-S91.
- [76] Henchoz, Y., Romand, S., Schappler, J., Rudaz, S., Veuthey, J.L. and Carrupt, P.A., *Electrophoresis*, 31 (2010) 952-964.

- [77] Bytzek, A.K., Reithofer, M.R., Galanski, M., Groessl, M., Keppler, B.K. and Hartinger, C.G., *Electrophoresis*, 31 (2010) 1144-1150.
- [78] Oszwaldowski, S. and Timerbaev, A.R., *Journal of Chromatography A*, 1146 (2007) 258-263.
- [79] Oszwaldowski, S. and Timerbaev, A.R., *Electrophoresis*, 29 (2008) 827-834.
- [80] Wang, W.P., Wang, S.M., Luo, Z. and Hu, Z.D., *Chinese Journal of Analytical Chemistry*, 35 (2007) 382-385.
- [81] Yu, C.J., Chang, H.C. and Tseng, W.L., *Electrophoresis*, 29 (2008) 483-490.
- [82] Furlanetto, S., Orlandini, S., Marras, A.M., Mura, P. and Pinzauti, S., *Electrophoresis*, 27 (2006) 805-818.
- [83] Fu, C.X. and Khaledi, M.G., *Journal of Chromatography A*, 1216 (2009) 1891-1900.
- [84] Poole, S.K. and Poole, C.F., *Journal of Chromatography A*, 1182 (2008) 1-24.
- [85] Wan, H., Ahman, M. and Holmen, A.G., *Journal of Medicinal Chemistry*, 52 (2009) 1693-1700.
- [86] Lewis, G., Mathieu, D. and Phan-Tan-Luu, R., *Pharmaceutical Experimental Design*, Marcel Dekker, New York, 1999.
- [87] Snyder, L.R., Carr, P.W. and Rutan, S.C., *Journal of Chromatography A*, 656 (1993) 537-547.
- [88] Kamlet, M.J., Doherty, R.M., Abraham, M.H., Marcus, Y. and Taft, R.W., *Journal of Physical Chemistry*, 92 (1988) 5244-5255.
- [89] Khaledi, M.G., Bumgarner, J.G. and Hadjmohammadi, M., *Journal of Chromatography A*, 802 (1998) 35-47.
- [90] Yang, S.Y. and Khaledi, M.G., *Analytical Chemistry*, 67 (1995) 499-510.
- [91] Cao, Y.H. and Sheng, J.W., *Electrophoresis*, 31 (2010) 672-678.
- [92] Zhou, Q.X., Mao, J.L., Xie, G.H. and Xiao, J.P., *Chromatographia*, 71 (2010) 875-880.
- [93] Svidritskii, E.P., Pashkova, E.B., Pirogov, A.V. and Shpigun, O.A., *Journal of Analytical Chemistry*, 65 (2010) 287-292.
- [94] Cao, Y.H., Gong, W.J., Li, N., Yin, C.N. and Wang, Y., *Analytical and Bioanalytical Chemistry*, 392 (2008) 1003-1010.
- [95] Kartsova, L.A., Ganzha, O.V. and Alekseeva, A.V., *Journal of Analytical Chemistry*, 65 (2010) 209-214.

- [96] Kartsova, L.A. and Ganzha, O.V., *Journal of Analytical Chemistry*, 65 (2010) 280-286.
- [97] Jiang, T.F., Lv, Z.H., Wang, Y.H., Yue, M.E. and Lian, S., *Analytical Sciences*, 25 (2009) 861-864.
- [98] Zhu, J.H., Qi, S.D., Zhang, H.G., Chen, X.G. and Hu, Z.D., *Journal of Chromatography A*, 1192 (2008) 319-322.
- [99] Cao, J., Chen, J., Yi, L., Li, P. and Qi, L.W., *Electrophoresis*, 29 (2008) 2310-2320.
- [100] Altria, K.D., Broderick, M.F., Donegan, S. and Power, J., *Electrophoresis*, 25 (2004) 645-652.

## **Chapter four**

### **Microemulsion characterisation techniques**

## **4.1 Introduction**

As mentioned in Chapter 1, microemulsions present complicated phase behaviour and microstructure. The area of characterisation has been widely studied for the past 40 years with particular interest during the 70s and 80s when use of microemulsions was being researched for tertiary oil recovery and in more recent times for drug delivery. While many techniques have been used to characterise the physicochemical properties, few papers have correlated these properties with analytical separation techniques. This chapter is focussed on highlighting the expansive range of methodologies used to characterise microemulsions along with a brief outline of their application. The techniques mentioned may have reference to microemulsions utilised in separation science.

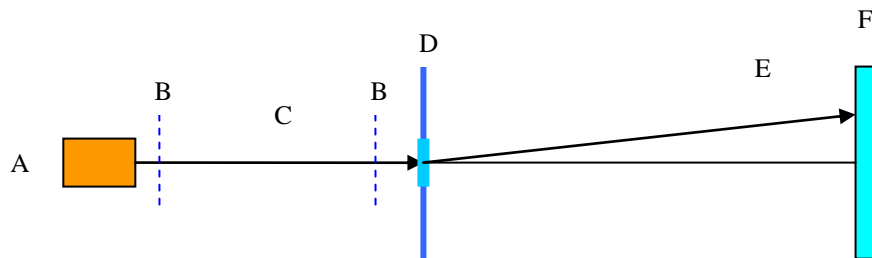
Instrumental techniques employed can be divided into two broad categories. Techniques which are focussed on the microemulsions 'global' properties e.g. viscosity, conductivity, refractive index and surface tension. In tandem with these measurements, techniques have been used to elucidate the 'molecular' properties or internal characteristics of the microemulsion e.g. microemulsion structure, droplet size, interfacial film curvature, position of co-surfactant etc. Techniques used to obtain this information include small angle neutron scattering (SANS), small angle x-ray scattering (SAXS), nuclear magnetic resonance (NMR), light scattering techniques such as dynamic light scattering (DLS), differential scanning calorimetry (DSC) and cryo-transmission electron microscopy (cryo-TEM).

## **4.2 Scattering techniques**

Scattering covers a range of techniques including dynamic light scattering/photon correlation spectroscopy and small angle scattering (SAS) such as SANS and SAXS. In all techniques the radiation wavelength can be used to obtain information about materials whose dimensions are of the same order of magnitude. Of these, SANS and SAXS use radiation wavelengths between 0.4 and 1 nm and are therefore capable of probing not only size but the structural connectivity of microemulsions. By comparison, the wavelength of light is much greater and is used predominantly to give information on size distribution.

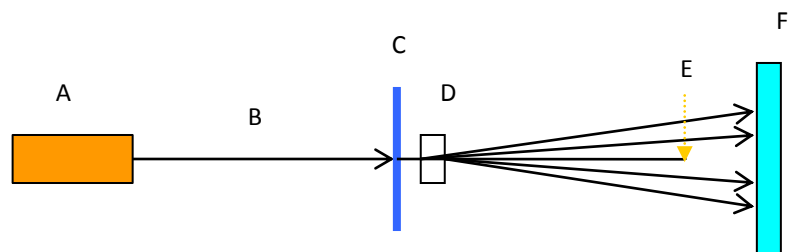
### 4.2.1 The basic principle

An incident beam of radiation from a source (light, x-ray or neutron) is collimated and directed towards a sample. Particles in a sample scatter the incident beam and the resulting intensity can be measured as a function of the angle between the incoming beam and scattered beam. The scattering pattern results from secondary waves emitted from structures within the sample when irradiated by the incoming beam, leading to constructive and destructive interference. Scattering of x-rays is caused by differences in electron density, while that of neutrons results from differences in the scattering power of dissimilar nuclei and light scattering originates from differences in refractive index [1;2]. Figure 4.1 and figure 4.2 show a general schematic for SANS and SAXS measurement systems respectively.



A – Neutron Velocity Selector      C – Incident Neutrons      E – Diffracted Neutrons  
 B – Collimation Slits              D – Magnet & Sample      F – 2D Neutron Detector

**Figure 4.1:** Schematic diagram of a SANS spectrometer. Redrawn from [3]



A – X-Ray Source & Monochromator      C – Sample Plate      E – Beam Stop  
 B – X-Ray Beam                              D – Glassy Carbon      F - Detector

**Figure 4.2** Schematic of a SAXS spectrometer. Redrawn from [4]

The scattering intensity depends on the scattering length densities of the particles and solvent. In SANS, the scattering length density is a complex function of atomic number and must be calculated experimentally. However, the scattering length density in SAXS is proportional to the electron density, which is a linear function of the number of electrons [5]. As a result, SAXS is particularly useful for examining the interfacial region of microemulsions where the polar headgroups and water regions possess a higher electron density compared to oil [1]. By comparison the scattering length of a nucleus varies between isotopes of the same element. Therefore, the scattering length of a molecule can be varied by replacing an element with its deuterated counterpart. This technique is called *contrast variation* and allows the establishment of a background, thereby allowing the examination of a specific microemulsion region [6].

The scattering pattern is used to obtain information about the structure and size of the particles in the sample. However, such a pattern can very complex due to the many particles present. Through Fourier transform operations or fitting the resultant data to mathematical models representing various known shapes, information on size, structure and connectivity can be obtained.

#### **4.2.2 Small angle scattering models**

The interference pattern produced by the structures in the sample result in an angle dependent scattering curve  $I(q)$ , in which  $q$  is the length of the scattering vector, defined by  $q = (4\pi/\lambda) \sin \theta/2$  where  $\lambda$  is the wavelength and  $\theta$  is the scattering angle [7]

The scattering data from either a SANS or SAXS experiment is only as meaningful as the mathematical model to which it is fit. The choice of fit is dependent on which microemulsion phase is perceived i.e. particulate polydisperse /concentrated droplet phase (O/W or W/O), or bicontinuous [8].

##### **4.2.2.1 Particulate Model**

Two cases arise in the particulate model

- 1 Particles in a dilute monodisperse system.
- 2 Concentrated system taking into account particle-particle interactions.

The scattering intensity  $I(q)$  can be written as the product of the form factor  $P(q)$  and the structure factor  $S(q)$ . There is no analytical restrictions used for the form factor and the structure factor is governed by up to four parameters for a given interaction model.  $S(q)$  describes interparticle interference and for dilute monodisperse systems  $S(q)$  is constant [1;9].

In a dilute monodisperse system the scattering generated is independent of the particles position and shape. Scattering intensity curve  $I(q)$  represents the form factor  $P(q)$  (equation 4.1) of the droplets [10] and indirect Fourier transform (IFT) of  $P(q)$  yields the pair distance distribution function (PDDF)  $p(r)$  (equation 4.2) [9]. The PDDF describes the probability of finding a distance ‘ $r$ ’ between two atoms in the material being examined and is a real space interpretation of the scattering pattern. Also, scattering length density profile  $\rho(r)$  (e.g. radially averaged length density across a micelle, assuming spherical symmetry) can be determined by deconvolution of  $p(r)$ . The PDDF represents a histogram of distances inside the particle weighted with scattering length density differences and goes to zero at the maximum particle dimension. The particle diameter can be obtained directly from the shape of the  $p(r)$  curve[9]. Equations have also been developed to express the form factor  $P(q)$  as a sphere, prolate ellipsoid or a oblate ellipsoid [11].

$$P(q) = \left[ \frac{3[\sin(qR) - qR\cos(qR)]}{(qR)^3} \right]^2 \quad \text{EQ 4.1}$$

$$p(r) = \frac{1}{2\pi^2} \int I(q)(qr)\sin(qr)dq \quad \text{EQ 4.2}$$

#### **4.2.2.2 Concentrated systems and generalised indirect Fourier transform method (GIFT)**

In a concentrated system, interpretation of the scattering data by IFT breaks down as  $I(q)$  deviates from the ideal form factor due to interactions between the particles, represented by  $S(q)$ . A generalised indirect Fourier transform (GIFT) [7] method has been developed which allows simultaneous determination of the form factor and structure factor for concentrated systems. The GIFT method is model free with respect to the form factor and is based on the hard sphere model with respect to the structure

factor. However, it has been shown that the GIFT method can be used outside its theoretical limits and has been applied to polydisperse systems as well as following the sphere-to-rod transition in binary and ternary systems[1;7].

#### 4.2.2.3 Teubner-Strey model and bicontinuous systems

Teubner and Strey model considered a fluid ternary microemulsion system to be composed of an oil and water region coupled together by a flexible surfactant film [10;12;13] . In such a model the structure of the oil and water phase was taken not to be independent. Such a model would show good correlation with a bicontinuous phase microemulsion.

The scattering data is fit to the Teubner-Strey expression in equation 4.3 which can be used to describe small angle scattering from flexible microemulsions [10;12-14].

$$I(q) = \frac{1}{a_2 + c_1 q^2 + c_2 q^4} b \quad \text{EQ 4.3}$$

Where,  $a_2$ ,  $c_1$ ,  $c_2$  and  $b$  are obtained using the Levenburg-Marquardt procedure[14;15].

The Teubner-Strey equation expresses the scattering intensity as a real space correlation function  $\gamma(r)$  of the form given in equation 4.4[14].

$$\gamma(r) = \frac{\sin kr}{kr} e^{-r/\xi} \quad \text{EQ 4.4}$$

Where;  $k$  and  $\xi$  are given by equations 4.5[10;14;16] and 4.6 [10;14;16] respectively.

$$k = [(1/2)((a_2 / c_2))^{\frac{1}{2}} - (c_1 / 4c_2)]^{-1/2} \quad \text{EQ 4.5}$$

$$\xi = [(1/2)((a_2 / c_2))^{\frac{1}{2}} + (c_1 / 4c_2)]^{-1/2} \quad \text{EQ 4.6}$$

From the correlation function two length scales are derived; the periodicity  $d$  ( $=2\pi/k$ ), which represents domain size and  $\xi$  which represents a correlation length (characteristic

length of a bicontinuous ME [16]). A third parameter  $f_a$ , given by equation 4.7 [14], reflects the ability of the surfactant to impose order on the microemulsion.

$$f_a = \frac{c_1}{[4a_2c_2]^{1/2}} \quad \text{EQ 4.7}$$

Comparison of  $d$  and  $\xi$  values allows information about size and structure to be deduced [10].

### 4.3 SANS and SAXS Applications

Freiberger et al. [8] employed SANS to determine phase type transition for a well characterised microemulsion system. The principle involved fitting the scattering data using two different models; the GIFT method, based on the particulate system and the Teubner and Strey (TS) model which was developed for bicontinuous phases. While it was expected that the data from the bicontinuous systems would show a good fit to the TS model, a poor fit would be obtained for the GIFT method. Results indicated that while the TS model showed a reduced fit for particulate systems the GIFT method was capable of accurately characterising the bicontinuous phase also.

Fanun et al. [14] examined a Winsor IV type microemulsion employing sucrose esters as a non-ionic surfactant. Sucrose esters are advantageous as surfactants due to their non-toxic nature and biodegradability. SAXS data was analysed according to the Teubner-Strey model and the microemulsion composition was assessed in terms of the quantity of surfactant, chain length of surfactant and oil, presence of an alcohol (1-butanol) and the concentration of water. From a pseudoternary phase diagram a dilution line was chosen and an increase in water content examined. It was seen that the domain size ( $d$ ) increased from 3.7-9.7 nm with an increase in water content. Changing the oil type in the bulk phase from n-dodecane to n-hexadecane resulted in an increase in  $d$  from 4 to 7 nm and 4 to 10.7 nm respectively. The degree of order in the system was also inferred by monitoring the correlation length ( $\xi$ ) and amphiphilicity factor ( $f_a$ ). It was seen that when n-hexadecane was employed as the oil, addition of water resulted in an increase in  $\xi$  (more ordered system). However, when water becomes the bulk phase a decrease in  $\xi$  was observed. The authors postulated that the correlation

length maxima corresponded to phase inversion. Interestingly it was seen the systems solubilisation of water was close to zero without the presence of 1-butanol.

Fanun also conducted SAXS experiments to investigate mixed non-ionic surfactant systems without the presence of a co-surfactant [5]. The microemulsion system was composed of water sucrose laurate/ethoxylated mono-di-glyceride (surfactants) and R (+)-limonene (oil). The results indicated that the mixed surfactant system was capable of solubilising an increased volume of water when compared to single surfactant counterparts. An increase in  $d$  was also observed for the mixed surfactant system.

Acosta et al. [16] employed SANS to test the net-average curvature (NAC) model [17-19]. The NAC model involved a set of semi-empirical equations used to predict solubilisation capacity of oils, phase transitions, phase volumes and interfacial tension of microemulsion systems. The NAC model was used to predict the average curvature and droplet size for an ionic microemulsion composed of sodium dihexyl sulfosuccinate (surfactant), toluene and aqueous electrolyte (sodium chloride solution). While the inverse of the average curvature predicted by the NAC model reflected the average size of the microemulsion aggregates, the solubilisation radii did not represent the actual size of oil or water droplets.

A combination of SANS and SAXS have also been used to assess the affect of ionic liquids on the curvature of microemulsion systems [10]. Interfacial rigidity and spontaneous curvature of the surfactant film are fundamental in dictating the stability, properties and structure of microemulsion systems. Non-ionic surfactant systems possess a flexible interfacial film and disordered domains where temperature can be used to tune interfacial curvature. By comparison, ionic surfactant systems have a more rigid interfacial film and contain well defined dispersions of spheres, cylinders or lamellae structures. Interfacial curvature of ionic systems can be controlled by addition of electrolytes or co-surfactants. Liu et al. [10] studied the effect of 1-butyl-3-methylimidazoliumtetrafluoroborate ([bmim][BF<sub>4</sub>]) ionic liquid on the interfacial curvature of a microemulsion system composed of mixed ionic surfactants (DODMAC and SDS), n-heptane and 1-butanol. Analysis of scattering data allowed comparison of  $d$  and  $\zeta$  values, thereby facilitating structural information. Based on the obtained shape and agreement of fit, the direction of curvature was derived. The authors concluded

that a low concentration of ionic liquid was required to induce phase transition when compared to an aqueous salt solution, thereby offering an efficient additive with which to control ME curvature. Similar work was conducted by Monkenbusch et al. [20], where SANS was utilised to examine the effect of diblock copolymers on the bending moduli of bicontinuous non-ionic microemulsions composed of polyglycol ether (surfactant), water and decane.

Walderhaug and Knudsen [11] employed SANS and NMR diffusion experiments to examine the microstructure of silicone (polymeric) surfactant systems. Changes in microstructure with changes in surfactant concentration, co-surfactant, water and temperature were investigated. Lowering the surfactant concentration to create a dilute micellar system, it was expected that aggregates were spherical. However, comparison of SANS and NMR data revealed a difference in radius. The discrepancy in obtained values was attributed to a deviation in shape. The SANS data when fitted to the ellipsoidal model suggested that even at low surfactant concentrations, the micelles were not completely spherical. The authors concluded that with respect to structure SANS may be more sensitive to deviations in shape compared to NMR.

Frank et al. [21] synthesised a range of non-ionic surfactants (alcohol ethoxylates) with varying hydrocarbon chain length and alcohol position used for the formation of bicontinuous microemulsions. SANS data was used to characterise the microstructure of the resultant systems as well as phase behaviour and film properties. From the TS model, domain size ( $d$ ) and correlation length were obtained. In addition to information from the TS model [13] the Roux expression [22] was used to calculate the thickness, rigidity and curvature of the interfacial film. The authors concluded that linear alcohol ethoxylates allowed parallel alignment of surfactant molecules and resulted in the most rigid interfacial films. Conversely, branched chain surfactants had more bulky hydrophobic tails and resulted in a less rigid interfacial film.

Balogh et al. [6] studied droplet growth in non-ionic microemulsions by using SANS to assess the effects of temperature on the spontaneous curvature of the surfactant film.

#### 4.4 Dynamic Light Scattering (DLS)

Dynamic light scattering (DLS) or photon correlation spectroscopy (PCS) encompasses a range of techniques used to estimate the size and distribution of submicron particles in solution. The technique has been routinely employed to measure the droplet size of microemulsions.

The theory is based on the principle that nano-sized particles in solution undergo Brownian motion due to their thermal energy and bombardment from solvent molecules.

The sample to be analysed is placed in a cuvette and thermostatted to a set temperature. A beam of light generated by a helium-neon laser is directed towards the sample. The intensity of the light scattered by the sample is collected by the detector. The particle diffusion coefficient ( $D$ ) and hence the particle size are obtained from a measure of the time dependent fluctuations and scattering intensity produced by the particles. Figure 4.3 shows a schematic diagram of the DLS setup.

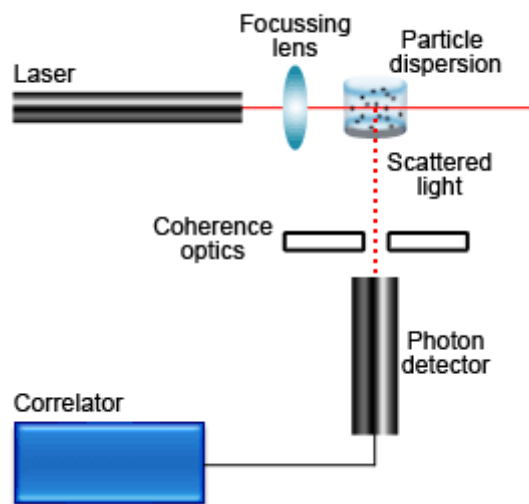


Figure 4.3 Schematic representation of DLS set-up. [23]

The size of the droplet is inferred from the hydrodynamic diameter ( $d(H)$ ) obtained from the Stokes-Einstein equation (EQ 4.8).

$$d(H) = kT/3\pi\eta D \quad \text{EQ 4.8}$$

Where;  $k$  is the Boltzmann's constant,  $T$  is the absolute temperature and  $\eta$  is the viscosity of the bulk phase.

From equation 4.8 the key parameter measured by DLS is the particle's diffusion coefficient, which is obtained from the intensity of the scattered light and its fluctuation over time. Based on the premise that small particles move faster under Brownian motion than larger ones, a relative change in light intensity can be observed. This change in light intensity is compared to give a correlation function and can be expressed as an exponential decay curve over time. The rate of decay expressed in the correlation function is used to calculate the diffusion coefficient. The intensity distribution is converted to a volume distribution by Mie theory.

#### **4.5 DLS applications**

While not as sensitive as neutron or x-ray scattering, light scattering experiments have been frequently reported in the literature. Acharya et al. [24-27] examined a range of microemulsion compositions involving microemulsification of natural oils which may have use in pharmaceutical formulations. In all cases DLS measurements were performed to estimate microemulsion droplet size, polydispersity and diffusion coefficient. Investigations into the microemulsification of eucalyptol (oil) and water in the presence of Brij-30 (non-ionic surfactant) and ethanol (co-surfactant) were conducted at various phase ratios [24]. DLS measurements for five systems in the O/W or W/O region were performed at different temperatures. In the case of one W/O microemulsion system an increase in diameter (hydrodynamic radius) from 8nm to 34.6nm was observed with an increase in temperature from 30 to 35°C. The authors postulated that this increase droplet size may have resulted from coalescence or fusion of droplets, and indicate a system proceeding towards instability. A corresponding increase in polydispersity was also noted with increasing temperature. In another report [25] investigating the pharmaceutically acceptable oil isopropylmyristate, an O/W system was seen to show a decrease in droplet size with a corresponding increase in temperature. The decrease in size was attributed to droplet declustering due to increased thermal energy which overcame attractive forces. Similar work performed on the microemulsification of coconut oil by the same group [27] revealed the limitations of DLS. Since the systems investigated were very concentrated, they deviated from the ideal model where interaction between droplets is limited. The authors concluded that

reporting droplet size or polydispersity would not be meaningful and form no grounds for comparison between different systems. However diffusion coefficient at different temperatures were reported and used to infer interaction behaviour based on different compositions.

Work by Hait et al. [28] examined the dynamics of percolation in W/O microemulsions through performing conductance experiments. DLS measurements were then performed above and below the percolation threshold. Results indicated that hydrodynamic radius, polydispersity and diffusion coefficients did not change before or after the onset of percolation.

An exceptionally detailed investigation into light scattering experiments was conducted by Goddeeris et al. [29]. The group examined a unique O/W surfactant system capable of self- microemulsifying upon dilution. Such systems are capable of transporting drugs and controlling release properties and are referred to self- microemulsifying drug delivery systems (SMEDDS). In addition to traditional DLS, a range of complimentary light scattering techniques including multiple angle light scattering and static light scattering were investigated and the results correlated. Also a detailed study on sample preparation and data handling was conducted. The authors found that sample preparation and detection angle could have a marked effect on particle size. In a similar study Saintruth et al. [30] examined the droplet size of microemulsions composed of isopropyl myristate, water and ethanol. In comparing both static and dynamic light scattering, the authors noted that data had to be corrected for interparticle interactions at high droplet concentrations.

#### **4.6 NMR**

NMR is based on the characteristic spin of different nuclei and has proved a powerful technique in the characterisation of surfactant and microemulsion systems. Use of  $^1\text{H}$ ,  $^2\text{H}$  and  $^{13}\text{C}$  NMR have been used to study the connectivity within microemulsion systems and reveal information on critical micellar concentration (CMC), aggregation number, counterion binding, aggregate shape, size and hydration, solution structure, solubilisation equilibria, etc. Parameters investigated have included chemical shift values, relaxation rates, quadrupole splittings, shift anisotropy and self diffusion [2].

Of the parameters which can be investigated, self diffusion coefficients (D) have been the most widely reported. Monitoring the molecular self-diffusion coefficient of microemulsion components in their pure state and in the microemulsion mixture reveals details on connectivity and allows information about Winsor phase, size, and shape to be extrapolated [31].

Information by comparison of diffusion coefficients is based on the fact that the self diffusion coefficient of a molecule in a closed domain, such as oil in an O/W microemulsion droplet, differs by orders of magnitude when compared to its diffusion coefficient as a neat solvent. The reverse is the case for a W/O system. For a bicontinuous structure, where both solvents form domains that extend over macroscopic distances, the diffusion coefficients of each are have similar orders of magnitude to that of their neat counterparts [14].

The pulsed gradient spin-echo (PGSE) NMR approach has been demonstrated as a suitable and reliable way to calculate molecular diffusion coefficients for surfactant systems. Lindman and Olsson [31] have published detailed NMR experimental methods on the calculation of diffusion coefficients. Briefly, the displacement of nuclear spins is controlled by a magnetic field gradient and the resultant NMR signals (spin-echo) monitored. By Fourier transformation the contributions of different components are resolved. The PGSE method involves the two equal and rectangular gradient pulses of magnitude G and duration d, sandwiched on either side of the 180° rf pulse.

The diffusion coefficient can be obtained from the slope of equation, given in 4.9 [31;32].

$$\ln\left(\frac{I_g}{I_o}\right) = -[\gamma^2 d^2 G^2 (\Delta - d/3)]D \quad \text{EQ 4.9}$$

Where  $I_g$  and  $I_o$  are intensities of the NMR signal in the presence and absence of field gradient pulses;  $\gamma$  is the gyromagnetic constant for  $^1\text{H}$ ; d is the duration of the z-gradient pulse; G is the gradient strength; and  $\Delta$  is the time interval between the gradient pulses.

#### **4.7 NMR applications**

Rozner et al. [33] examined the solubilisation capacity of non-ionic microemulsions containing cholesterol using PGSE NMR. The microemulsion was composed of Tween 60 (surfactant), limonene (oil), propylene glycol (co-solvent), ethanol (co-surfactant) and water. The objective of the work was to elucidate structural changes within the ME with respect to dilution with water and define the location of solubilised sterols in order to make a correlation between the two. A phase diagram was first constructed and a dilution line chosen. Using PGSE NMR self diffusion coefficients were calculated for each ME constituent along a particular dilution line without addition of cholesterol. The  $H^1$  shift for each constituent was calculated in both the neat form and in the microemulsion system. From equation 4.9 the self diffusion coefficient for each constituent was calculated. Comparing the changes in self-diffusion coefficients for each component allowed phase types to be assigned to the 'empty emulsions'. A similar approach was adapted after the microemulsions had been loaded with cholesterol. Through comparison of self diffusion coefficients changes in the microstructure caused by the addition of cholesterol were analysed. The effect of cholesterol allowed information about surfactant curvature, solubilisation locus and microstructural shape to be determined.

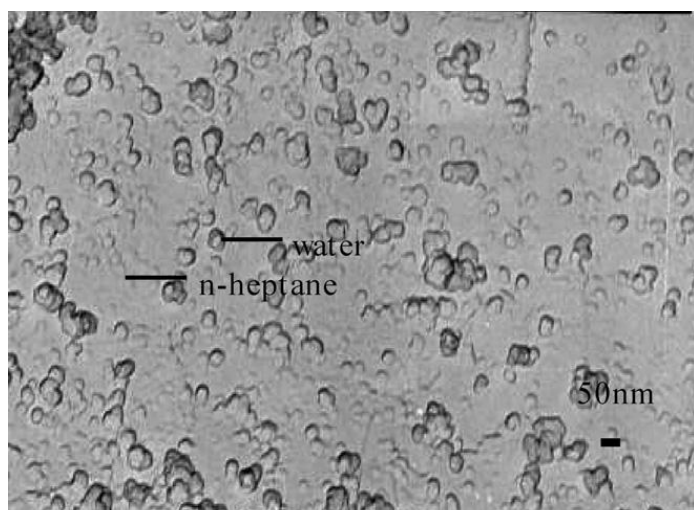
When investigating sucrose esters as non-ionic surfactants Fanun et al. [14] correlated changes in microstructure monitored by SAXS with PGSE NMR measurements. Good agreement between the two techniques was achieved with an increase in water content corresponding to an increase in droplet size. However, severe spectral overlap was observed for signals of the oil and alkyl portion of the surfactant. The problem was overcome by implementing a mathematical model developed by Windig [34;35] known as the direct exponential curve resolution algorithm (DECRA). Fanun [5] also studied mixed non-ionic surfactant system through PGSE NMR.

#### **4.8 Scanning and Transmission electron microscopy (SEM/TEM)**

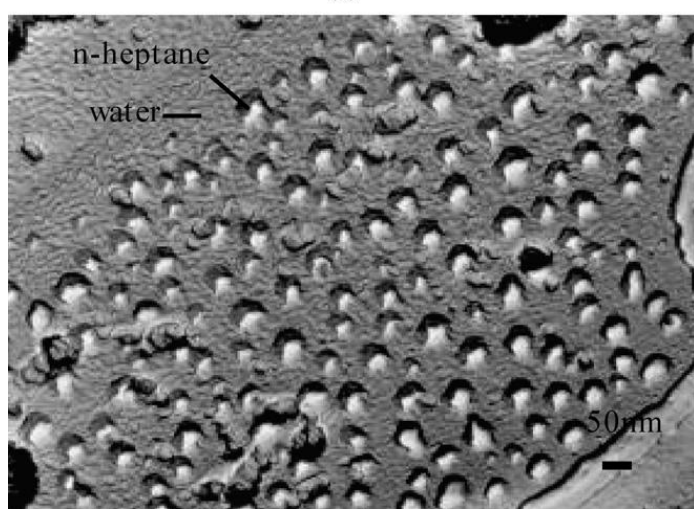
Use of electron microscopy to obtain images of microemulsions and examine the effect of composition on phase behaviour has been reported [32;36-38]. However, unlike examining a solid substrate, examination of liquids such as microemulsions involves the creating of an image of the microemulsion on a solid metal disc. Techniques such as freeze fracture TEM (FF-TEM) and Cryo-SEM have been developed, which involve

freezing the microemulsion and etching the resultant image on a metal surface which can be shadowed and viewed with electron microscopy. A typical Freeze fracture procedure reported by Alany et al. [36] involved placing the microemulsion in a mesh and sandwiching it between two flat copper discs. The sandwich was then flash frozen using liquid propane ( $-180^{\circ}\text{C}$ ) before being loaded into a double-replica device immersed in liquid nitrogen. The double replica device was then mounted on an etching device and fracturing was carried out under a vacuum. The fractured surfaces were then shadowed with platinum and carbon before being washed and finally viewed with the TEM.

Xie et al. [38] employed FF-TEM to characterise the microstructure and phase transitions of a microemulsion composed of rhamnolipid (biosurfactant), butanol, water and heptane. The authors examined the effects of aqueous dilution on microemulsion system. FF-TEM images in figure 4.4 clearly demonstrated the difference in size between O/W and W/O droplets.



(a)



(b)

**Figure 4.4** FF-TEM image of (a) W/O and (b) O/W microemulsion. [38]

Note et al. [37] obtained images of the bicontinuous phase using Cryo-SEM in a microemulsion composed of SDS, toluene, pentanol and aqueous PEI. The authors observed a sponge-like structure for the bicontinuous region and correlated changes in the region with concentration of PEI in the aqueous phase.

Boonme et al. [32] employed Cryo-SEM to characterise the phase and structure of colloidal samples formed in a microemulsion composed of isopropyl palmitate, water, Brij 97 and 1-butanol. The authors fixed the ratio of surfactant to co-surfactant and constructed a phase diagram by titration of various oil/surfactant mixture ratios with water. From the resultant phase diagram a region of the microemulsion area was examined with water concentrations between 0 and 55% (w/w). The authors noted that in regions with water concentrations less than 15% (w/w), no globular structures were observed. While reversed micelles were expected to be present at low water

concentrations, it was thought their size was too small to be detected. While globular structures were observed at water concentrations above 15% (w/w), it was not possible to differentiate between O/W or W/O type based solely on the photomicrographs. It was also noted that interpretation of the Cryo-SEM images required careful interpretation as ice contamination may appear as microemulsion structure. Figure 4.5 demonstrates the difference between images containing microemulsion structures and an ice contaminated artefact respectively.

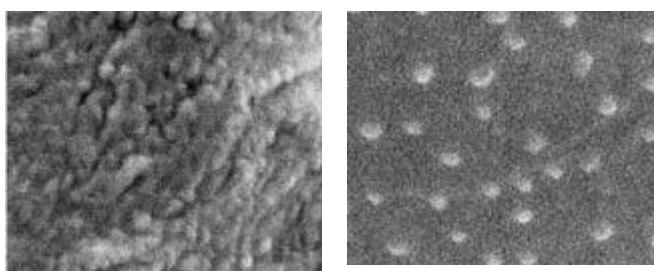


**Figure 4.5** The image on the left shows a typical microemulsion structure, while the image on the right demonstrates an image contaminated by ice artefacts.[32]

#### **4.9 Differential scanning calorimetry (DSC)**

DSC involves the controlled cooling and heating of a solution. Such measurements allow the generation of heating and cooling curves for microemulsion systems. From these curves, exothermic and endothermic peaks are plotted and can be related to properties such as phase type, percolation, droplet interaction and structural correlations. Similar to the procedure in PGSE-NMR, microemulsion components are analysed individually and as part of the system. Differences observed in peak intensities and positions can be attributed to microemulsion characteristics.

In microemulsion systems, monitoring the water is particularly advantageous as it departs considerably from its average behaviour when present at liquid interfaces [39]. Garti et al. [40] employed DSC measurements in optimising the amount of solubilised water in W/O microemulsions consisting of sucrose esters (non-ionic surfactant), butanol (co-surfactant) and a range of n-alkanes ( $C_{12}$ - $C_{16}$ ). The authors utilised the unique behaviour of water in its 'bulk' (free) and 'bound' (interfacial) state to evaluate and optimise microemulsion composition. Bulk water is assumed to have physicochemical properties similar to that of pure water (i.e. freezes at zero). However, bound water is influenced by its interaction with surfactant self-assemblies which alter its thermodynamic properties (freezing point, melting point, enthalpy, heat capacity

etc). The studies allowed the determination of bulk and/or bound water to be detected in microemulsions and correlate composition with the concentration of solubilised water and its binding capacities. It was seen that the water molecules were strongly bound by the surfactant hydroxyl groups at the interface and beyond a saturation point additional solubilised water migrated to the micelle core. A greater amount of water was solubilised with increasing chain length of the oil phase. It was thought that the longer chain oils allowed stronger hydrophobic interactions with the surfactant tails and kept the head groups further apart from one another, which in turn allowed a larger core for water to partition into. Figure 4.6 shows a DSC thermogram for microemulsion systems.

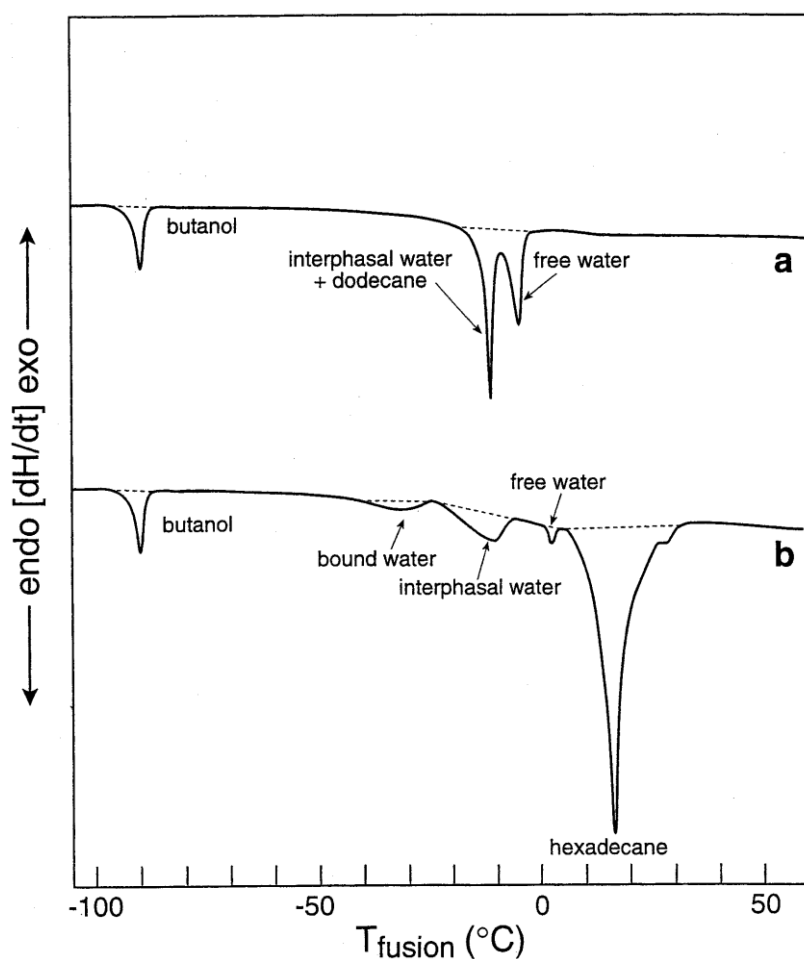


**Figure 4.6** DSC thermogram demonstrating the difference in endotherm observed for bound, free and interphasal water in a microemulsion. [40]

Spemath et al. [41] examined the phase transition induced by water dilution on phospholipid food grade microemulsions by DSC. Differences in water state melting point were used to track phase transitions upon dilution. A distinction was made for

three water states. Free water was seen to melt at approximately 0°C, interfacial water at -10°C and bound water (water associated with the hydrophilic head groups at the surfactant film) at < -10°C. It has been reported that no free water may be detected in similar O/W type microemulsions due to a binding interaction with the surfactant and co-solvent (propylene glycol) [42]. Also, only a single peak may be detected for bound and interfacial water. However, in the systems investigated distinct peaks were observed for all water melting points. Information on surfactant packing and the rigidity of the interfacial film was obtained through comparing water behaviour for various compositions. It was noted that at certain compositions, water was more confined to the droplet core inferring that, water-soluble analyte would be better protected and therefore more stable. The results were seen to be in good agreement when correlated with NMR and conductivity studies.

Podlogar et al. [43] examined a range of techniques including DSC when characterising the structure and phase transitions of a pharmaceutically usable microemulsion. The microemulsion was composed of Tween 40, water and isopropyl myristate. It was seen that water interacted strongly with the surfactant and the transition to the O/W phase was difficult to detect at high surfactant concentrations. However, in combination with SAXS data it was concluded that above 50 % (w/w) water, an O/W microemulsion with strongly interacting oil droplets was expected to form. At a water concentrations below 20% a W/O type system was observed and at concentrations in between the system was bicontinuous.

#### **4.10 Conductivity**

Conductivity measurements have been applied to a range of microemulsion systems to investigate transport effects brought about by percolation. Percolation is believed to occur when droplets cluster or fuse and enable the movement of ions from one region to another thereby enhancing conductance [44;45]. Such measurements allow information about droplet interaction, phase type and polydispersity to be obtained. Since the conductivity for O/W microemulsions remains relatively constant with respect to water [2], studies have mostly focussed on changes in W/O and bicontinuous microemulsion systems. In a W/O system, addition of water results in an exponential increase in conductivity as the onset of percolation occurs. The conductivity reaches a maximum in the bicontinuous phase before levelling out as the system inverts to the O/W phase

[43;46]. However, conductivity curves are strongly dependent on the percolation process and the type of surfactant. For non-ionic microemulsion systems a bell shape curve is generally observed, while an ionic system frequently yields an exponential type curve.

Fanun et al. [46] examined phase behaviour, transport, diffusion and structure properties for a microemulsion system composed of water, sucrose laurate (surfactant), propylene glycol (co-solvent), ethanol (co-surfactant) and benzaldehyde (oil). In addition to PGSE-NMR and viscosity, the authors performed conductivity experiments. As in the case of all non-ionic microemulsion systems utilising a non-ionic surfactant, a dilute aqueous electrolyte (0.05M NaCl) was used in place of pure water to induce conductivity. While it was accepted that NaCl may result in changes to size and shape on the microscopic level, these variations should not be significant when the salt solution is suitably dilute. Figure 4.7 displays the influence of water volume fraction on conductivity. Analysis of conductivity results revealed the establishment of a percolation threshold and indicated the structural transition from W/O to a percolated system prior to the formation of a bicontinuous microstructure.

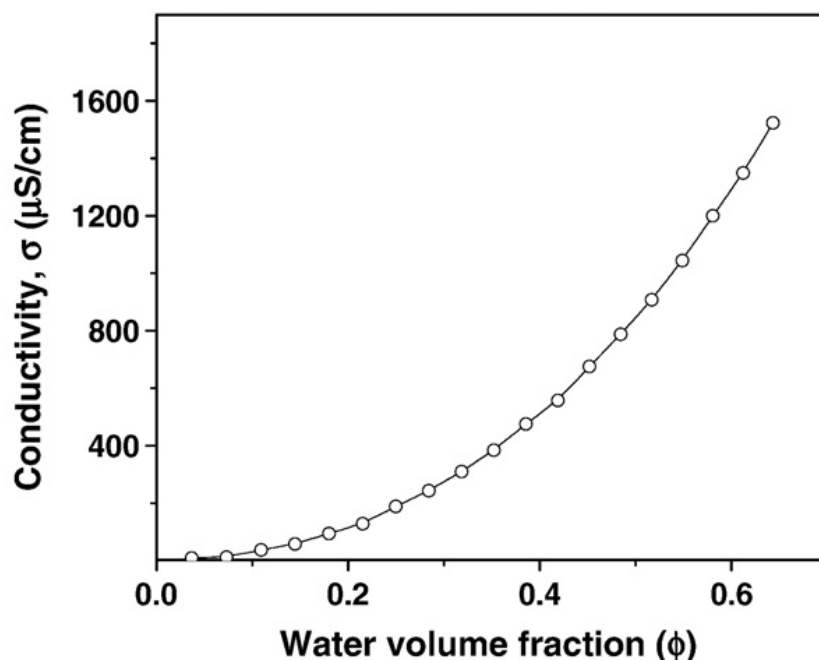


Figure 4.7 Effect of water volume fraction on microemulsion conductivity.[46]

Podlogar et al. [43] correlated the results obtained from conductivity and viscosity for various non-ionic microemulsions composed of Tween 40, water and isopropyl myristate. Increasing the water concentration from 0 to 70% (w/w) with a fixed

surfactant and oil ratio saw electrical conductivity follow a bell shaped curve. A percolation threshold was observed at approximately 30% (w/w) water as the system changed from an isolated W/O droplet system to an interconnected bicontinuous structure. The percolation threshold corresponded with a slight decrease in viscosity; however viscosity remained relatively constant up to a concentration of 52% (w/w) where a sharp increase was observed. In comparison, conductivity increased up to approximately 52% before it began to decrease. The reduction in conductivity was attributed to the increased viscosity and formation of an O/W phase transition.

Note et al. [37] studied an ionic microemulsion system by examining the influence of replacing water with an aqueous polymer solution of polyethyleneimine (PEI). The microemulsion was composed of SDS, toluene, pentanol and aqueous PEI. The authors correlated a range of techniques including viscosity, conductivity and DSC. Conductivity was measured as a function of increasing aqueous PEI (30% w/v) concentration. Upon initially increasing the aqueous phase an increase in conductivity was observed. The moderate slope corresponded to weak percolation of charges in the W/O phase. By comparison much stronger percolation was observed when water was used as the aqueous phase. At 40% w/w a pseudo-plateau was observed which corresponded to transition from O/W to bicontinuous and at 60% w/w; a further increase in conductivity was recorded indicating transition to an O/W phase. When correlated with viscosity measurements an increase in viscosity was seen for all additions of aqueous phase. Interestingly, Newtonian flow behaviour was only observed in the W/O phase prior to the percolation threshold. In addition to composition, the effect of temperature was also examined. Generally temperature is not expected to influence the surfactant film of ionic microemulsion systems, however replacing water with aqueous PEI resulted in a significant increase in the W/O region of the phase diagram with an increase in temperature indicating an increased water solubilisation capacity.

Hait et al. [28] employed conductivity to examine the effect of additives on the dynamics of percolation in ionic microemulsion systems composed water, AOT and isooctane or decane. Additives such as sodium salicylate, aromatic solutes and the bile salt sodium cholate were assessed with respect to their effect on the percolation threshold volume and temperature. In each case the percolation threshold was obtained from conductivity curves. It was seen that the aromatic compounds such as benzene,

anthracene and naphthalene reduce the onset of percolation. Such additives impede percolation by causing a blocking effect which reduces adherence and subsequent fusing of droplets. By comparison it was seen that additives with more than one hydroxyl group, such as sodium cholate, promote the formation of channels between adjacent droplets by adhering to their surface and thereby reduce the percolation threshold.

#### **4.11 Density and surface tension**

In addition to other techniques, measurement of density and surface tension can reveal information about structural changes within the microemulsion system. Podlogar et al. [43] examined compositional changes in a non-ionic pharmaceutical microemulsion using both techniques. In each case, measurements were made with respect to increasing water concentration (5 to 65% w/w). A relatively linear increase in density from 0.9 to 1.02 Kg dm<sup>-3</sup> was noted with increasing water content. Surface tension remained constant at approximately 29.3 dynes cm<sup>-1</sup> with additions of water up to 20% w/w. A decrease from 29.3 to 28 dynes cm<sup>-1</sup> was observed on increasing water concentration to 55%. A sharp increase to 31.5 dynes cm<sup>-1</sup> was noted as water concentration increased from 55 to 65%. Interestingly, similar changes in the slope of the density graph were noted in the same regions as changes in the surface tension of the microemulsion systems. When compared with results from more specific techniques such as SAXS and DSC, the changes in surface tension and density correlated with changes in microemulsion phase type. Below 20% water was found to be W/O, 20 – 50% water was deemed to be bicontinuous and 50-65% water was taken to be an O/W type phase.

Xie et al. [38] employed surface tension measurements in characterising a novel biosurfactant microemulsion composed rhamnolipid (surfactant), butanol, water and heptane. The authors varied the surfactant concentration and noted some interesting observations. In addition to the CMC, denoted by a sharp change in the graph, an initial secondary change in the graph was noted after a certain concentration of surfactant was added. The authors proposed a number of reasons for this observation, among them was that, at certain concentration the rhamnolipid surfactant may have two structural conformations.

Liu et al. [10] employed spinning drop tensiometry to calculate the interfacial tension between oil and aqueous phases of a middle phase microemulsion in which the curvature of the surfactant film was controlled by the addition of the ionic liquid (IL) (bmim)(BF<sub>4</sub>).

#### **4.12 Empirical calculations**

In addition to measuring physical properties of microemulsion systems to gain information on microstructure, mathematical predicative approaches based on surfactant and solvent molecular architecture have been used [47].

Andelija et al. [47] employed lattice fluid self-consistent field theory [48] in conjunction with new classical thermodynamic expressions [49] to calculate fundamental interfacial properties for a O/W microemulsion. The microemulsion was composed of 2% (w/w) SDS, 6.6% (w/w) butanol, 1% (w/w) diisopropyl ether and 90.4% (w/w) 25 mM disodium phosphate buffer pH 7.0. Once optimised, the microemulsion buffer was successfully used for the MELC separation of simvastatin and its related substances. The authors examined a range of microemulsion compositions which were applied to the separation and based on the success of the separation calculated the predicted properties which would have the greatest impact on MELC chromatography. Properties such as predicted droplet radii, area per surfactant, film thickness, interfacial tension and bending moment were calculated and used to characterise the separation.

#### **4.13 Conclusion**

The chapter gives a brief description of the principal techniques used to characterise microemulsion systems and an overview of the applications reported in the literature. While small angle light scattering and NMR infer the most information with respect to microstructure, less involved techniques such as DSC and conductivity impart useful information with respect to phase type. In nearly all reports, a number of methods were employed and the correlation of results allowed a measurement of agreement between techniques to be made.

The application of microstructural studies was focussed mostly on the use of microemulsions with a view to drug delivery, where knowledge of specific interactions between drug-microemulsion-membrane-environment may prove beneficial. Only two reports focussed on characterising microemulsions for separation science. Of these,

one focussed on theoretical aspects while the other was mainly concerned with droplet size and zeta potential. There remains quite a gap in terms reports relating microemulsion physicochemical characteristics to separation.

The void of information in this area may not be overly surprising when the main techniques are considered. Both MELC and particularly MEEKC exhibit complicated separation mechanisms when microemulsion buffers are employed. Apart from changes in the microemulsion composition (i.e. surfactant, co-surfactant, oil type/concentration etc), it may prove difficult to directly compare changes in microstructure with changes in separation. Taking MEEKC as an example, a change in the surfactant concentration may influence microemulsion size and hence analyte interaction, which can be related to the separation of a given set of compounds. However, such a change may also effect ionisation on the capillary wall, EOF and current level which would also influence the observed separation. Such are the number of method development options, it can take a long time to optimise a microemulsion separation method. None-the-less, a detailed study into microemulsion structure and an attempt to relate the microstructure to separation may reveal effects in selectivity which facilitates the judicious selection of sufficient separation conditions within a limited number of exploratory runs.

#### 4.14 References

- [1] Glatter, O., Orthaber, D., Stradner, A., Scherf, G., Fanun, M., Garti, N., Clement, V. and Leser, M.E., 241 (2001) 215-225.
- [2] Moulik, S.P. and Paul, B.K., *Advances in Colloid and Interface Science* 78 (1998) 99-195.
- [3] [www.unifr.ch/physics/fk/research/neut.html](http://www.unifr.ch/physics/fk/research/neut.html). 2011. Accessed 08-12-10
- [4] [www.ipfdd.de/x-ray-lab.197.0.html](http://www.ipfdd.de/x-ray-lab.197.0.html). 2011. Accessed 08-12-10
- [5] Fanun, M., *Journal of molecular liquids*, 142 (2008) 103-110.
- [6] Balogh, J., Olsson, U. and Pedersen, J.S., *Journal of Physical Chemistry B*, 111 (2007) 682-689.
- [7] Yaghmur, A., de Campo, L., Aserin, A., Garti, N. and Glatter, O., *Physical Chemistry Chemical Physics*, 6 (2004) 1524-1533.
- [8] Freiburger, N., Moitzi, C., de Campo, L. and Glatter, O., *Journal of Colloid and Interface Science*, 312 (2007) 59-67.
- [9] Brunner-Popela, J., Mittelbach, R., Strey, R., Schubert, K.V., Kaler, E.W. and Glatter, O., *Journal of Chemical Physics*, 110 (1999) 10623-10632.
- [10] Liu, L.P., Bauduin, P., Zemb, T., Eastoe, J. and Hao, J.C., *Langmuir*, 25 (2009) 2055-2059.
- [11] Walderhaug, H. and Knudsen, K.D., *Langmuir*, 24 (2008) 10637-10645.
- [12] Chen, S.H., Chang, S.L., Strey, R., Samseth, J. and Mortensen, K., *Journal of Physical Chemistry*, 95 (1991) 7427-7432.
- [13] Teubner, M. and Strey, R., *Journal of Chemical Physics* 87 (1987) 3195-3200.

- [14] Fanun, M., Wachtel, E., Antalek, B., Aserin, A. and Garti, N., *Colloids and Surfaces A-Physicochemical and Engineering Aspects*, 180 (2001) 173-186.
- [15] S.A. Teukolsky, W.T. Vetterling and B.P. Flannery, *Numerical Recipes in C: The Art of Scientific Computing*, Cambridge University Press, New York, 1992, 683-688 pp.
- [16] Acosta, E.J., Szekeres, E., Harwell, J.H., Grady, B.P. and Sabatini, D.A., *Soft Matter*, 5 (2009) 551-561.
- [17] Acosta, E., Szekeres, E., Sabatini, D.A. and Harwell, J.H., *Langmuir*, 19 (2003) 186-195.
- [18] Szekeres, E., Acosta, E., Sabatini, D.A. and Harwell, J.H., *Langmuir*, 20 (2004) 6560-6569.
- [19] Szekeres, E., Acosta, E., Sabatini, D.A. and Harwell, J.H., *Journal of Colloid and Interface Science*, 287 (2005) 273-287.
- [20] Monkenbusch, M., Holderer, O., Freilinghaus, H., Byelov, D., Allgaier, J. and Richter, D., *Journal of Physics: Condensed Matter*, 17 (2011) 2903-2909.
- [21] Frank, C., Frielinghaus, H., Allgaier, J. and Prast, H., *Langmuir*, 23 (2007) 6526-6535.
- [22] Roux, D., Nallet, F., Freyssingas, E., Porte, G., Bassereau, P., Skouri, M. and Marignan, J., *Europhysics Letters*, 17 (1992) 575-581.
- [23] [www.malvern.com/LabEng/technology/dynamic\\_light\\_scattering/classical\\_90\\_degree\\_scattering.htm](http://www.malvern.com/LabEng/technology/dynamic_light_scattering/classical_90_degree_scattering.htm). Accessed 10-01-11.
- [24] Acharya, A., Sanyal, S.K. and Moulik, S.P., *International Journal of Pharmaceutics*, 229 (2001) 213-226.
- [25] Acharya, A., Sanyal, S.K. and Moulik, S.P., *Current Science*, 81 (2001) 362-370.

- [26] Acharya, A., Sanyal, S.K. and Moulik, S.P., *Journal of Dispersion Science and Technology*, 22 (2001) 551-561.
- [27] Acharya, A., Moulik, S.P., Sanyal, S.K., Mishra, B.K. and Puri, P.M., *Journal of Colloid and Interface Science*, 245 (2002) 163-170.
- [28] Hait, S.K., Moulik, S.P., Rodgers, M.P., Burke, S.E. and Palepu, R., *Journal of Physical Chemistry B*, 105 (2001) 7145-7154.
- [29] Goddeeris, C., Cuppo, F., Reynaers, H., Bouwman, W.G. and Van den Mooter, G., *International Journal of Pharmaceutics*, 312 (2006) 187-195.
- [30] Saintruth, H., Attwood, D., Ktistis, G. and Taylor, C.J., *International Journal of Pharmaceutics*, 116 (1995) 253-261.
- [31] Lindman, B. and Olsson, U., *Berichte der Bunsen-Gesellschaft-Physical Chemistry Chemical Physics*, 100 (1996) 344-363.
- [32] Boonme, P., Krauel, K., Graf, A., Rades, T. and Junyaprasert, V.B., *Apps Pharmscitech*, 7 (2006).
- [33] Rozner, S., Aserin, A. and Garti, N., *Journal of Colloid and Interface Science*, 321 (2008) 418-425.
- [34] Antalek, B., Hornak, J.P. and Windig, W., *Journal of Magnetic Resonance*, 132 (1998) 307-315.
- [35] Windig, W., Hornak, J.P. and Antalek, B., *Journal of Magnetic Resonance*, 132 (1998) 298-306.
- [36] Alany, R.G., Tucker, I.G., Davies, N.M. and Rades, T., *Drug Development and Industrial Pharmacy*, 27 (2001) 31-38.
- [37] Note, C., Koetz, J. and Kosmella, S., *Journal of Colloid and Interface Science*, 302 (2006) 662-668.
- [38] Xie, Y.W., Ye, R.Q. and Liu, H.L., *Colloids and Surfaces A-Physicochemical and Engineering Aspects*, 292 (2007) 189-195.

- [39] Kunieda, H., Ushio, N., Nakano, A. and Miura, M., *Journal of Colloid and Interface Science*, 159 (1993) 37-44.
- [40] Garti, N., Aserin, A., Tiunova, I. and Fanun, M., *Colloids and Surfaces A-Physicochemical and Engineering Aspects*, 170 (2000) 1-18.
- [41] Spornath, A., Aserin, A. and Garti, N., *Journal of Thermal Analysis and Calorimetry*, 83 (2006) 297-308.
- [42] Yaghmur, A., Aserin, A., Tiunova, I. and Garti, N., *Journal of Thermal Analysis and Calorimetry*, 69 (2002) 163-177.
- [43] Podlogar, F., Gagperlin, M., Tomsic, M., Jamnik, A. and Rogac, M.B., *International Journal of Pharmaceutics*, 276 (2004) 115-128.
- [44] Bug, A.L.R., Safran, S.A., Grest, G.S. and Webman, I., *Physical Review Letters*, 55 (1985) 1896-1899.
- [45] Bug, A.L.R., Safran, S.A. and Webman, I., *Physical Review Letters*, 54 (1985) 1412-1415.
- [46] Fanun, M., *Journal of Molecular Liquids*, 139 (2008) 14-22.
- [47] Andelija, M., Darko, I., Mirjana, M., Biljana, J. and Slavko, M., *Journal of Chromatography A*, 1131 (2006) 67-73.
- [48] Peck, D.G. and Johnston, K.P., *Journal of Physical Chemistry*, 97 (1993) 5661-5667.
- [49] Nagarajan, R. and Ruckenstein, E., *Langmuir*, 16 (2000) 6400-6415.

## **Section Two**

### **Experimental**

## **Chapter Five**

### **Analysis of Oil- and Water-Soluble Vitamins by MELC**

## 5.1 Introduction

Vitamins present a diverse range of essential dietary compounds. They are needed in small amounts and are obtained primarily through diet and various vitamin supplements. In view of the fact that vitamins are so crucial for good health, there is a wide range of fortified foods and supplements on the market giving rise to the need for specific techniques to analyse them [1].

Generally vitamins are categorised as either water-soluble (C or B complex- B<sub>1</sub>, B<sub>2</sub>, B<sub>3</sub>, B<sub>5</sub>, B<sub>6</sub>, B<sub>8</sub>, B<sub>9</sub> and B<sub>12</sub>) or fat-soluble (A, D, E and K). However, even within these groups they possess a wide range of functionalities. For this reason a broad range of techniques have been applied to the analysis of vitamins such as UV-Vis and near-infrared spectrophotometry [2;3], fluorimetry [4], CE [5;6] and HPLC [7;8]. In spite of these many techniques the simultaneous analysis of water and oil soluble vitamins has proven difficult. Areas which have shown promise involve the use of micelles or microemulsions. CE techniques such as MEKC [9] and MEEKC [10] along with HPLC techniques such as MLC [11] and oil-in-water (O/W) MELC [12] have demonstrated the ability to analyse sample matrices containing both oil soluble and water-soluble analytes.

Chapters 1 and 2 give a detailed account of microemulsion formation and MELC.

O/W MELC offers alternative partitioning mechanisms to traditional HPLC. The stationary phase of the RP-HPLC column is coated with the surfactant present in the microemulsion which affects the stationary phase interactions. Solutes partition as in traditional HPLC between the mobile phase and stationary phase. However, in MELC, a secondary partitioning mechanism is created by the presence of the oil droplets, and solutes partition between the aqueous phase, the oil droplets and the stationary phase of the column. Water insoluble compounds tend to reside in the oil droplet, while water soluble compounds reside mainly in the aqueous phase. Separation is also affected by stationary phase interactions. The type and concentration of the oil, surfactant, co-surfactant, as well as pH and the addition of organic modifiers can be used to optimise separation selectivity.

The aim of this study was to develop a MELC method capable of simultaneously separating a mixture of water and oil soluble vitamins. As the starting point for the method development a previously reported microemulsion [13-15], hereafter referred to as the 'standard microemulsion', consisting of 2.98% (w/w) SDS, 5.96% (w/w) 1-butanol, 0.72% (w/w) n-octane and 90.33% (w/w) 0.05% TFA was used as the sample solvent and mobile phase. The method was developed and optimised through variation of oil phase, co-surfactant, addition of organic modifier, and pH. Also different columns, flow rates and injection volumes were examined to assess their effect on separation. Validation of the optimised method was carried out for the analysis of vitamins B<sub>6</sub>, B<sub>1</sub>, niacin and E in a pharmaceutical liquid formulation.

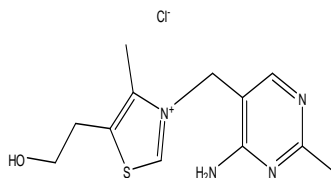
## **5.2 Experimental**

### **5.2.1 Chemicals**

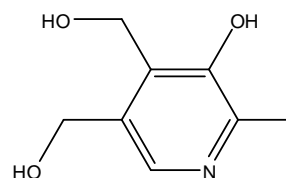
Vitamin standards retinol acetate (vitamin A), tocopherol acetate (vitamin E), cholecalciferol (vitamin D), thiamine hydrochloride (vitamin B<sub>1</sub>), riboflavin (vitamin B<sub>2</sub>), pyridoxine (vitamin B<sub>6</sub>), niacin and ascorbic acid (vitamin C) were purchased from Sigma Aldrich (Ireland). Figure 5.1 shows the chemical structure of the water and oil-soluble vitamins, along with Log P and pK<sub>a</sub> values where available.

### **5.2.2 Microemulsion components**

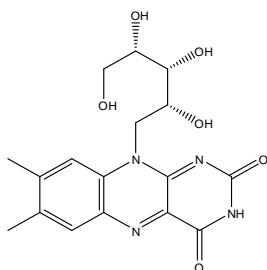
HPLC grade water, n-octane, trifluoroacetic acid (TFA), 1-butanol (all Romil) and 99% sodium dodecyl sulphate (SDS) were obtained from Lennox Laboratory Supplies (Ireland). 5% sodium hydroxide solution, 2-octanol, 1-pentanol, hexane, nonane and dodecane were obtained from the chemical stores at WIT. Organic additives: tetrahydrofuran (THF), 1-propanol, 2-propanol and methanol were also obtained from Lennox.



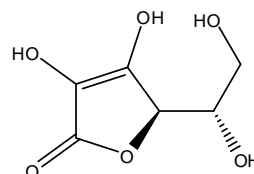
**Thiamine  
hydrochloride (B<sub>1</sub>)**  
**Log P: -3.93**  
**pKa<sub>1</sub>: 4.8**  
**pKa<sub>2</sub>: 9.20**



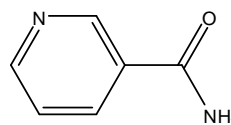
**Pyridoxine (B<sub>6</sub>)**  
**Log P: -0.8**  
**pKa<sub>1</sub>: 5.0**  
**pKa<sub>2</sub>: 8.96**



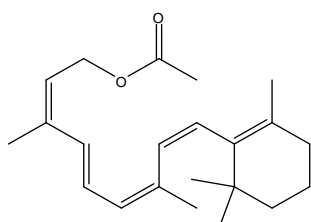
**Riboflavin (B<sub>2</sub>)**  
**Log P: -1.5**  
**pKa<sub>1</sub>: 1.9**  
**pKa<sub>2</sub>: 9.69**



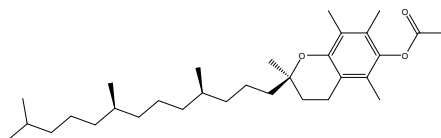
**Ascorbic acid (C)**  
**Log P: -1.8**  
**pKa<sub>1</sub>: 4.19**  
**pKa<sub>2</sub>: 11.57**



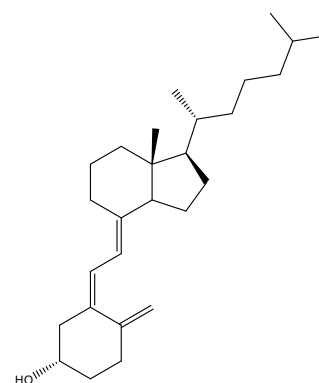
**Niacin**  
**Log P: -0.4**  
**pKa<sub>1</sub>: 0.5**  
**pKa<sub>2</sub>: 3.35**



**Retinol  
Acetate (A)**  
**Log P: 6.3**



**Tocopherol acetate (E)**  
**Log P: 10.8**



**Cholecalciferol (D)**  
**Log P: 7.9**

**Figure 5.1** Structure and physical data of the water and oil-soluble vitamins [16-18].

### **5.2.3 Instrumentation**

Analysis of vitamin E with aqueous/organic solvents was performed on a Hewlett Packard 1050 HPLC system equipped with variable wavelength UV detector, column heater, autosampler and quaternary pumping system coupled to an Agilent Chemstation data management system. All other HPLC analysis was performed on a Hewlett Packard 1090 HPLC equipped with photo diode array UV detector, column heater, autosampler and tertiary pumping system coupled to an Agilent Chemstation data management system. UV scans were carried out on a Shimadzu UV-2401PC.

Separations were carried out using the following columns:

- Waters Symmetryshield RP18 150 mm x 4.6 mm with 3.5 $\mu$ m packing material.
- Hewlett Packard Zorbax RP18 250 mm x 4.6 mm with 5 $\mu$ m packing material.
- Phenomenex RP18 100 mm x 4.6 mm monolith column.

All pH adjustments were made on a Thermo Orion 4 Star pH meter.

## **5.3 Method development**

### **5.3.1 Microemulsion preparation**

The standard microemulsion was prepared by mixing 33g of SDS, 66g of 1-butanol, and 8g of n-octane in a 1L duran bottle. This mixture was stirred for 10 minutes using a magnetic stirrer to ensure a homogenous solution was formed. 1 litre of 0.05% TFA was then added, sonicated for 30 minutes and filtered.

### **5.3.2 Vitamin solubility**

The solubility of each vitamin standard was assessed in water, methanol and standard microemulsion. 20 mg of each vitamin standard was placed in 5 ml of solvent and subjected to sonication for 1 hour. When the mixtures had reached room temperature after sonication the degree of solubility was determined visually. Where a vitamin was deemed to be in solution a further quantity of vitamin standard was added. In a case where the vitamin was not in solution a further quantity of solvent was added and the mixture sonicated until solubility was reached.

### **5.3.3 Preparation of vitamin standards and UV spectra**

A stock solution of each vitamin was prepared by dissolving 25 mg of each vitamin in 50 ml of standard microemulsion. The stock solutions were stored in amber bottles and kept in a fridge at 4°C to protect against light and heat degradation. Dilute solutions with a concentration of 0.01 mg ml<sup>-1</sup> were prepared from the stock solution. The UV spectrum for each vitamin was obtained to determine its wavelength of maximum absorbance in the 190 nm to 400 nm range.

### **5.3.4 Analysis of vitamins using standard microemulsion**

#### **5.3.4.1 Chromatographic conditions**

For the initial study employing the standard MELC microemulsion, analysis was carried out on the HP 1090 using the 150 mm C18 RP packed column. The PDA detector was set at the wavelength of maximum absorbance for each vitamin. The injection volume was 5 µl, temperature was set at 35°C and flow rate was 1 ml min<sup>-1</sup>. The pH of the microemulsion was 2.8. Each vitamin was run separately at a concentration of 0.05 mg ml<sup>-1</sup>.

Since vitamin E could not be eluted using the standard microemulsion it was analysed separately.

### **5.3.5 Analysis of vitamin E on the HP 1050 with traditional aqueous/organic solvents**

Vitamin E was analysed on the HP1050 using traditional aqueous/organic solvents in order to determine which organic solvent could be used as a modifier in the microemulsion to elute the very hydrophobic vitamin.

#### **5.3.5.1 Chromatographic conditions**

Analysis of vitamin E was carried out on the HP 1050 using 150 mm C18 RP packed column. The variable wavelength detector was set at 268 nm. Injection volume was 10 µL and column temperature was 35°C. Based on the Snyder polarity index [19] solvents of increasing hydrophobicity; methanol, 2-propanol (IPA), 1-propanol (nPA), and tetrahydrofuran (THF) were prepared individually with various proportions of water and used as eluents. Table 5.1 shows the eluent compositions, pH, flow rates and

sample solvents examined. Prior to injection, a quantity of vitamin E standard was dissolved in a vial containing the organic component of the running eluent.

THF was chosen as the optimum modifier and analysis of all vitamins was carried out using the THF modified microemulsion.

**Table 5.1** Eluent composition, pH, flow rate and sample solvent used to analyse vitamin E.

<i>Eluent composition</i>	<i>pH</i>	<i>Flow (ml min<sup>-1</sup>)</i>	<i>Sample solvent</i>
50/50 MeOH/H <sub>2</sub> O	6.25	1	MeOH
95/10 MeOH/H <sub>2</sub> O	6.25	2	MeOH
50/50 IPA/H <sub>2</sub> O	7.12	1	IPA
50/50 nPA/H <sub>2</sub> O	6.90	1	nPA
50/50 THF/H <sub>2</sub> O	6.43	1	THF

### 5.3.6 Analysis of vitamins using THF modified microemulsion

The standard microemulsion was modified with a range of THF concentrations from 0-50% v/v. The analysis was performed with decreasing concentrations of THF (50, 40, 20, 30, 10 and 5% v/v).

#### 5.3.6.1 Sample preparation

Stock solutions of vitamins B<sub>1</sub>, B<sub>2</sub>, B<sub>6</sub>, niacin and C were prepared to a concentration of 0.5 mg ml<sup>-1</sup> in standard microemulsion, while vitamins A, D and E were prepared to a similar concentration in THF. Solutions were stored in amber bottles and kept in a fridge at 4°C to protect against light and heat degradation. Vitamin C was unstable in solution and was prepared daily. A working test mixture was prepared daily by mixing a portion of the individual stock solutions.

#### 5.3.6.2 Chromatographic conditions

The investigation was carried out on the HP 1090 using the 100 mm C18 RP monolith column. The PDA detector was set at the wavelength of maximum absorbance for each vitamin. The injection volume was 20 µl, temperature was set at 35°C and flow rate

was 2 ml min<sup>-1</sup>. The pH of each microemulsion was adjusted to 7.0 as previous results suggested sharper peaks could be obtained at this pH.

The THF modified microemulsion was capable of eluting all vitamins, however, the water soluble vitamins eluted with the solvent peak. It was decided to analyse the water soluble vitamins separately with respect to the oil phase of the microemulsion.

### **5.3.7 Variation of oil phase for separation of water and oil-soluble vitamins**

For the analysis of vitamins, the oil phase of the standard microemulsion was varied with respect to hydrophobicity. Three oil phases less hydrophobic than octane (hexane, 2-octanol and 1-pentanol) and two oil phases more hydrophobic (nonane and dodecane) were examined. 2-octanol, 1-pentanol and hexane were used to prepare the microemulsion in equal weight % to octane (0.72%). Nonane and dodecane were added at 7g (0.62% w/w) and 3g (0.27% w/w) respectively as this was the maximum concentration at which they could be integrated into the microemulsion. The microemulsion containing nonane broke at temperatures above 35°C, and was therefore eliminated from the rest of the study.

#### **5.3.7.1 Chromatographic conditions**

Analysis was performed on the HP 1090 using the 100 mm C18 RP monolith column. The PDA detector was set at the wavelength of maximum absorbance for each vitamin. The injection volume was 20 µl, temperature was set at 35°C and flow rate was 0.5 ml min<sup>-1</sup>. The pH of each microemulsion was 7.0. Prior to injection, a quantity of each vitamin standard was dissolved in a vial containing the running eluent. Any of the oil phases examined were not capable of separating vitamins A and D or eluting E. 2-octanol was found to give a slightly better separation for the water soluble vitamins and was used instead of octane for the rest of the study.

### **5.3.8 Effect of pH on the separation of water soluble vitamins**

Using 2-octanol as the oil phase of the microemulsion the pH was varied from 2.8 to 9. 5% NaOH and 1% TFA were used to adjust the pH.

#### **5.3.8.1 Chromatographic conditions**

Analysis was performed on the 1090 LC using the 100 mm C18 RP monolith column. The PDA detector was set at the wavelength of maximum absorbance for each vitamin. The injection volume was 20  $\mu\text{l}$ , temperature was set at 35°C and flow rate was 1.0 ml  $\text{min}^{-1}$ . The sample for injection was prepared by dissolving a quantity of each vitamin standard in a vial of the running eluent.

A pH of 2.8 was found to be the optimum and this pH was used for the rest of the study.

#### **5.3.9 Effect of co-surfactant on the separation of water and oil soluble vitamins**

The effect of the co-surfactant was examined by replacing 1-butanol with an equal weight % of 1-pentanol. It was thought that since 1-pentanol was more hydrophobic than 1-butanol it may better elute the oil soluble vitamins.

#### **5.3.9.1 Chromatographic conditions**

Analysis was performed on the 1090 LC using the 100 mm C18 RP monolith column. The PDA detector was set at the wavelength of maximum absorbance for each vitamin. The injection volume was 20  $\mu\text{l}$ , temperature was set at 35°C and flow rate was 1.0 ml  $\text{min}^{-1}$ . The sample for injection was prepared by dissolving a quantity of each vitamin standard in a vial of the running eluent.

#### **5.3.10 Effect of column length on vitamin separation**

The effect of column length was examined by performing the separation on the 100 mm C18 monolith column and a 250mm C18 packed column. It was accepted that a direct comparison was not possible as the structure of these stationary phase would be very different.

#### **5.3.10.1 Chromatographic conditions**

Conditions were as described in section 5.3.9.1.

### 5.3.11 Validation of vitamin preparation

#### 5.3.11.1 Specificity

The vitamin preparation contained water, glycerol, citric acid, sodium chloride, pantothenic acid and xanthan gum in addition to the vitamins of interest. Specificity was examined through spiking blank and sample solutions with vitamin standards. Also, peak purity was examined using the PDA.

#### 5.3.11.2 Linearity

Stock solutions of vitamins B<sub>1</sub>, B<sub>2</sub>, B<sub>6</sub>, niacin, C, A, D and E were prepared in a microemulsion containing 2.98% (w/w) SDS, 5.96% (w/w) pentanol, 0.72 % (w/w) 2-octanol and 90.33% (w/w) 0.05% TFA. Dilution of each vitamin stock solution was performed to create a range of standard solutions for injection. Table 5.2 shows the concentration of each stock solution and the final concentration of working standard solution.

**Table 5.2** Preparation of vitamin standard solutions

<i>Vitamin</i>	<i>Stock solution concentration mg ml<sup>-1</sup></i>	<i>Working standard Concentration mg ml<sup>-1</sup></i>
A	0.2165	0.035, 0.039, 0.043, 0.048 and 0.052.
D	0.3058	0.00056, 0.00063, 0.00070, 0.00077 and 0.00084.
E	0.5	0.32, 0.36, 0.4, 0.44 and 0.48.
B1	0.1	0.04, 0.05, 0.06, 0.07 and 0.08.
B2	0.15	0.03, 0.06, 0.09, 0.12 and 0.15.
B6	0.12	0.024, 0.048, 0.072, 0.096, and 0.12.
N	4	0.8, 0.96, 1.12, 1.28 and 1.44.
C	5	4, 4.5, 5, 5.5 and 6.

10 µl of each standard solution was injected and run in triplicate using the optimised chromatographic conditions. Mean peak areas for each vitamin standard were calculated and a calibration curve for peak area against concentration was plotted.

### 5.3.11.3 Assay

An assay of the vitamin preparation was performed by quantitatively transferring 5ml of the vitamin preparation into a 25ml volumetric flask. The solution was then made up to the mark with microemulsion. This solution was sonicated at 25°C for 15 minutes before being filtered with a 0.45 µm nylon filter into a HPLC vial. 10 µl of this solution was injected and run in triplicate. A sample chromatogram is shown in Figure 5.2. Where possible mean peak areas for each vitamin were found and the concentration calculated from the calibration curve equation. Assay values were compared to label claim as percent vitamin recovered.

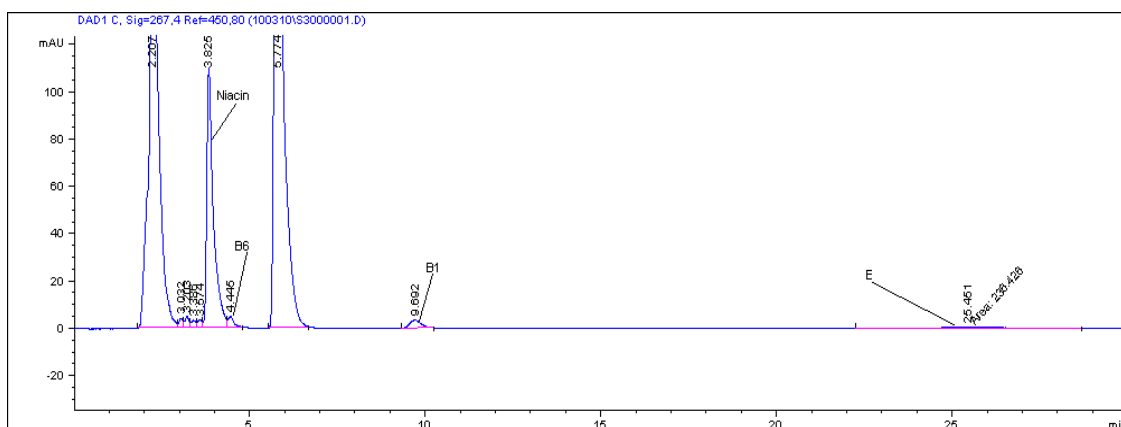


**Figure 5.2** Separation of oil and water soluble vitamins in a commercial liquid formulation on 250mm C18 RP packed column. Microemulsion composition: 2.98% (w/w) SDS, 5.96% (w/w) 1-pentanol 0.72% (w/w) 2-octanol and 90.33% (w/w) 0.05 % TFA, pH 2.8. Conditions: Temperature 35°C, Flow rate 1 ml min<sup>-1</sup>, Injection volume 5 µl, Detection wavelength 267nm.

### 5.3.11.4 Precision and Repeatability

Precision and repeatability was assessed by preparing three replicates of three sample solutions. Five, six and seven ml of sample were transferred to 25 ml volumetric flasks and make up to the mark with microemulsion. Each of the nine sample solutions were run in triplicate. Repeatability was determined by calculating the relative standard deviation (RSD) of the determined vitamin concentrations. Intermediate precision was determined by running the samples on a different day and attaining the RSD of the calculated concentrations.

### **5.3.11.5 Accuracy**

The accuracy of the method was determined by preparing three known concentrations of each vitamin standard. Each standard was run in triplicate and the concentration determined from the calibration curve. Results were expressed as percent recovery of the known concentration.

### **5.3.11.6 Limit of Detection (LOD)**

The LOD for each vitamin was determined based on the calibration curve using equation 5.1.

$$\text{LOD} = 3.3\sigma/S \quad \text{Equation 5.1}$$

Where  $\sigma$  is the residual standard deviation of the regression line and S is the slope.  $\sigma$  was calculated using equation 5.2.

$$\sigma = \sqrt{\sum (y_i - \hat{y}_i)^2 / (n-2)} \quad \text{Equation 5.2}$$

### **5.3.11.7 Limit of Quantitation (LOQ)**

The LOD was calculated based on the calibration curve using Equation 5.3.

$$\text{LOQ} = 10\sigma/S \quad \text{Equation 5.3}$$

## **5.4 Results**

### **5.4.1 Solubility of vitamins and UV detection**

The lipophilic vitamins (A, D and E) were seen to be soluble in the standard microemulsion. Vitamins A and D were soluble at concentrations of 2 and 4 mg/ml respectively, while vitamin E had the poorest solubility with a maximum concentration of 0.5 mg/ml. All the hydrophilic vitamins (niacin, B<sub>6</sub>, B<sub>1</sub>, B<sub>2</sub> and C) were soluble at high concentrations. Table 5.3 shows the maximum solubility of each vitamin in the range of solvents examined. Other solvents examined included 1-butanol, 1-pentanol

and THF, however while these three solvents showed a good solubilisation capacity for the oil soluble vitamins they were incapable of dissolving vitamins B<sub>1</sub>, niacin, and C. From the UV spectrum of each vitamin it was seen that all vitamins absorbed at 267 nm except vitamin A which only absorbed at 345 and 285 nm.

**Table 5.3** Maximum solubility of vitamins in water, methanol and standard microemulsion

<i>Vitamin</i>	<i>Solvent</i>	<i>Max. solubility mg ml<sup>-1</sup></i>
A	Water	Insoluble
D	Water	Insoluble
E	Water	Insoluble
Niacin	Water	>18mg/ml
B <sub>6</sub>	Water	>18mg/ml
B <sub>1</sub>	Water	>18mg/ml
B <sub>2</sub>	Water	>18mg/ml
C	Water	>18mg/ml
A	Methanol	18.5mg/ml
D	Methanol	21.4mg/ml
E	Methanol	14.3mg/ml
Niacin	Methanol	>32mg/ml
B <sub>6</sub>	Methanol	>18mg/ml
B <sub>1</sub>	Methanol	>18mg/ml
B <sub>2</sub>	Methanol	>18mg/ml
C	Methanol	>18mg/ml
A	Standard Microemulsion	2mg/ml
D	Standard Microemulsion	4mg/ml
E	Standard Microemulsion	0.5mg/ml
Niacin	Standard Microemulsion	>36mg/ml
B <sub>6</sub>	Standard Microemulsion	>26mg/ml
B <sub>1</sub>	Standard Microemulsion	>26mg/ml
B <sub>2</sub>	Standard Microemulsion	>26mg/ml
C	Standard Microemulsion	>26mg/ml

#### 5.4.2 Analysis of vitamins using standard microemulsion

All vitamins except E were eluted and detected using the standard microemulsion. However, water soluble vitamins niacin, B<sub>6</sub> and B<sub>1</sub> co-eluted as did the oil soluble vitamins A and D.

### 5.4.3 Analysis of vitamin E on the 1050LC with traditional aqueous/organic solvents

Based on the Snyder polarity index [19] solvents of increasing hydrophobicity; methanol, 2-propanol, 1-propanol, and tetrahydrofuran (THF) were examined as described in section 5.3.5.1 to choose an organic modifier capable of eluting vitamin E. The results for the various compositions examined along with the flow rates are shown in Table 5.4.

**Table 5.4** Analysis of vitamin E using traditional HPLC

<i>Eluent composition</i>	<i>pH</i>	<i>Flow (ml min<sup>-1</sup>)</i>	<i>Sample solvent</i>	<i>Retention time (min)</i>
50/50 MeOH/H <sub>2</sub> O	6.25	1	MeOH	No peak
95/10 MeOH/H <sub>2</sub> O	6.25	2	MeOH	35
50/50 IPA/H <sub>2</sub> O	7.12	1	IPA	No Peak
50/50 nPA/H <sub>2</sub> O	6.90	1	nPA	78
50/50 THF/H <sub>2</sub> O	6.43	1	THF	68

From the results it could be seen that 50/50 THF/water gave the quickest elution time for vitamin E. It was therefore decided to modify the standard microemulsion with 50% THF in order to elute vitamin E.

### 5.4.4 Analysis of vitamins using THF modified microemulsion

All vitamin standards were analysed using the THF modified microemulsion at THF concentrations between 0-50% v/v. It was seen that changing the proportion of THF in the microemulsion had a large effect on the separation of the oil soluble vitamins. Baseline separation could be achieved for vitamins A, D and E from 50-5% v/v THF. However, only two of the five water soluble vitamins could be separated. Figure 5.3 shows a chromatogram of the separation at 10% THF.

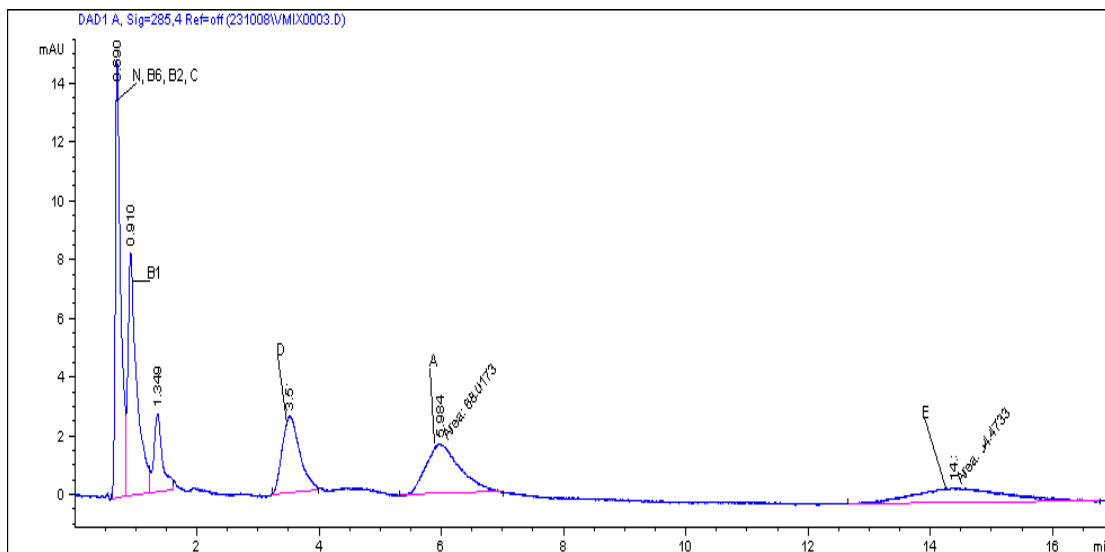


**Figure 5.3** Chromatogram of vitamin separation using standard microemulsion modified with 10% v/v THF. Conditions: C18 monolith column, Temperature 35°C, Flow rate 2 ml min<sup>-1</sup>, Injection volume 20 µl, Detection wavelength 285nm.

#### 5.4.5 Variation of oil phase for separation of water and oil- soluble vitamins

Changing the oil phase of the microemulsion had little effect on the separation of water soluble vitamins. Also, no oil phase examined was capable of separating vitamins A and D or eluting vitamin E. Examining just the water soluble vitamins, all oil phase microemulsions resulted in three peaks. 2-octanol, 1-pentanol and dodecane resulted in the co-elution of vitamins B<sub>2</sub>, niacin and B<sub>6</sub>. However when using hexane, a difference in selectivity was observed, vitamins C/B<sub>2</sub> and niacin/B<sub>6</sub> co-eluted. Figure 5.4 shows a graph illustrating the effect of oil phase on the capacity factors for each vitamin. In general the chromatography was poor with broad bands and peak tailing observed. Higher capacity factors were achieved with 2-octanol and it was used as the oil phase for the remainder of the study.

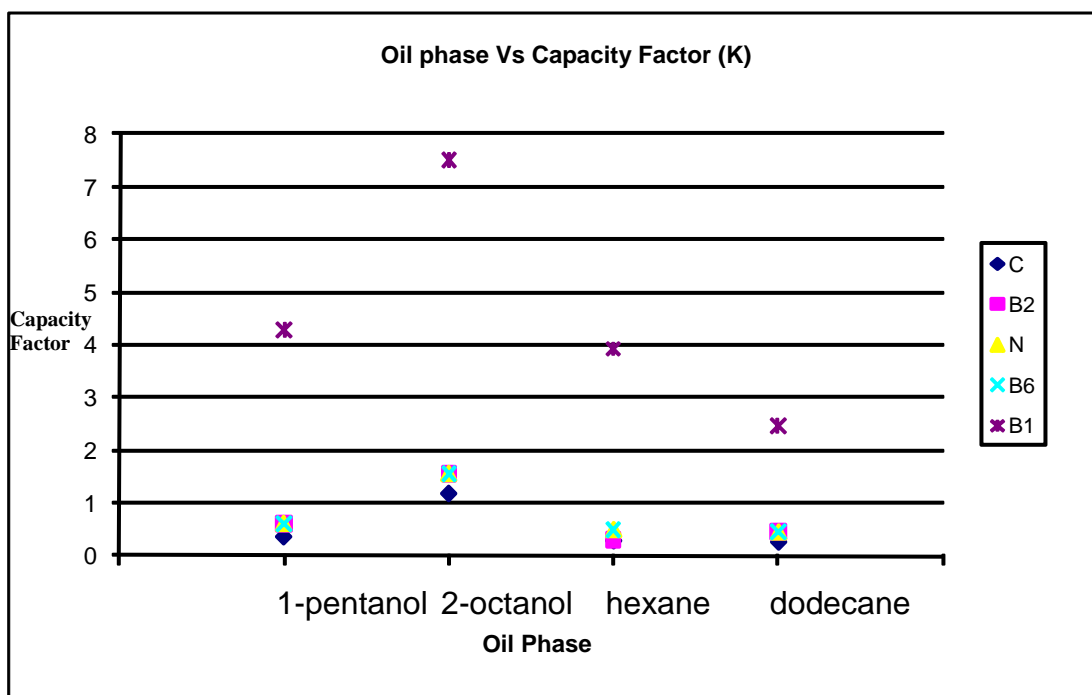
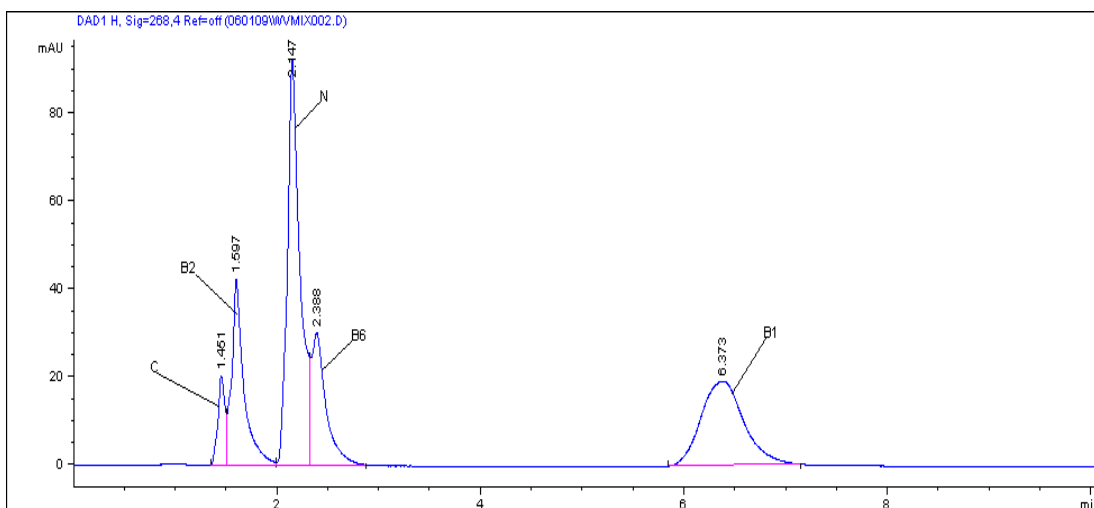


Figure 5.4: Change in capacity factor of water soluble vitamins with variation in microemulsion oil phase

#### 5.4.6 Effect of pH on the separation of water soluble vitamins

The pH of the microemulsion had a notable effect on the separation of the vitamins. Separation of all water soluble vitamins was achieved in pH range 2.87 to 4 with pH 2.87 the optimum (the natural pH of the microemulsion). From pH 4 to 9 vitamins B<sub>2</sub>, niacin and B<sub>6</sub> co-eluted. Increasing pH resulted in a reduction of retention time for all vitamins, especially B<sub>1</sub>. An increase in pH also led the band broadening and poorer peak shape for vitamin B<sub>1</sub>. Figure 5.5 shows a chromatogram of the separation at pH 2.86 while Figure 5.6 shows the effect of pH on the capacity factors. Efficiencies for the separation were still poor, with the maximum plate numbers between 1000 and 2500 recorded at pH 2.87. A drop in efficiency was observed in the pH range 4 to 8. Since a microemulsion pH of 2.8 proved beneficial in separating the water soluble vitamins, it was kept constant for the remainder of the study.



**Figure 5.5** Chromatogram of the water soluble vitamin separation at pH 2.86. Microemulsion composition: 2.98% w/w SDS, 5.96% w/w 1-butanol, 0.72% w/w 2-octanol and 90.33% aqueous buffer (0.05% TFA). Conditions: C18 monolith column, Temperature 35°C, Flow rate 1 ml min<sup>-1</sup>, Injection volume 20 µl, Detection wavelength 267nm.

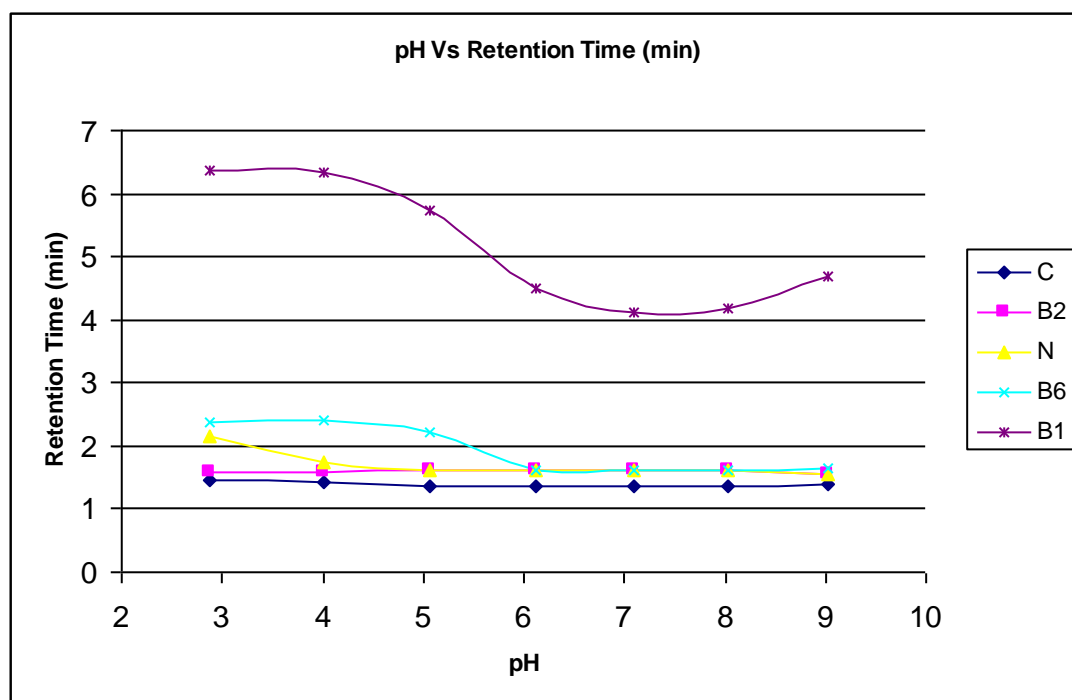


**Figure 5.6** Graph of pH vs capacity factor. Microemulsion composition: 2.98% w/w SDS, 5.96% w/w 1-butanol, 0.72% w/w 2-octanol and 90.33% w/w 0.05% TFA.

#### 5.4.7 Effect of co-surfactant on the separation of water and oil soluble vitamins

Replacing 1-butanol with 1-pentanol resulted in a dramatically improved separation. All vitamins were eluted and partially resolved except vitamins A and D which co-

eluted. Figure 5.7 shows a chromatogram of the water soluble vitamin separation while Figure 5.8 shows a chromatogram of the water and oil-soluble vitamin separation, when 1-pentanol was employed as the co-surfactant.

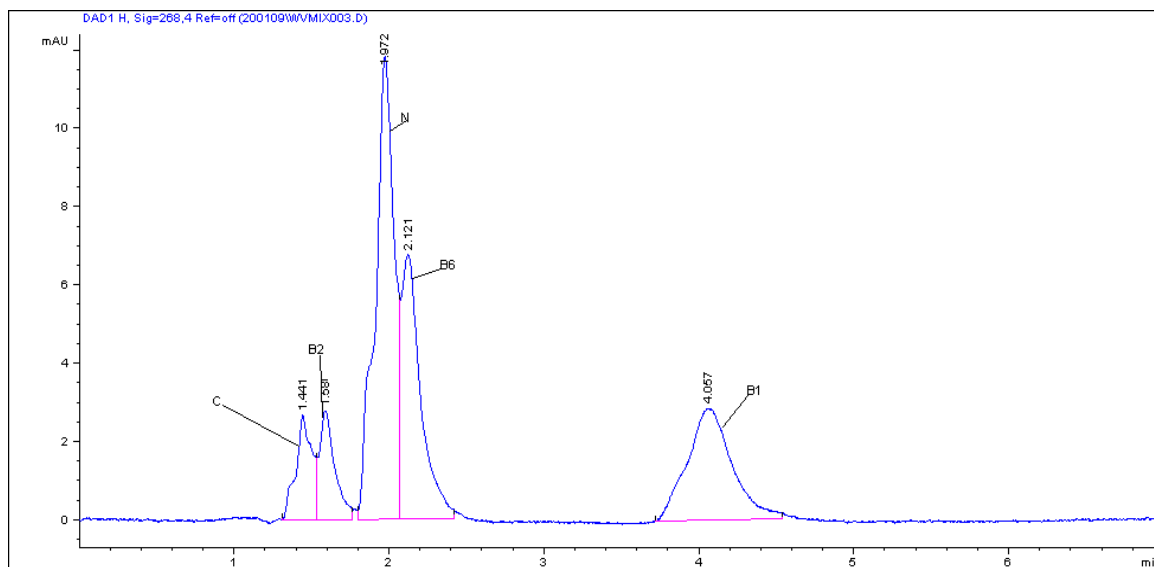


**Figure 5.7:** Separation of water soluble vitamins employing 1-pentanol as the co-surfactant. Conditions as in figure 5.5 except injection volume 5  $\mu$ L.

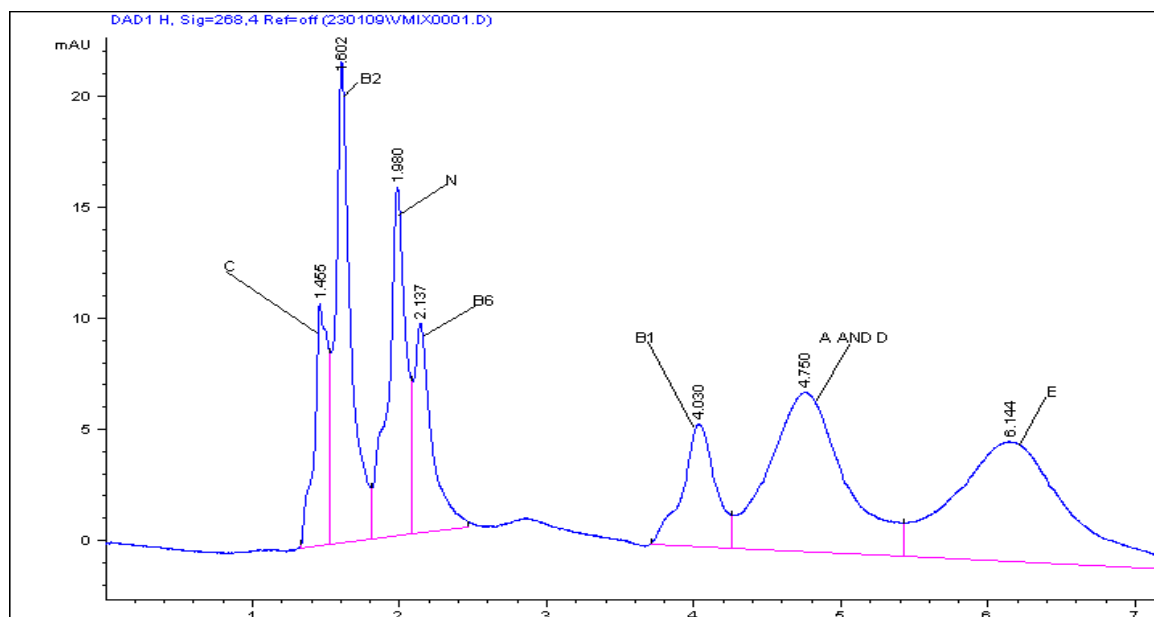


**Figure 5.8** Separation of water and oil soluble vitamins employing 1-pentanol as the co-surfactant. Conditions as described in figure 5.5 except injection volume 10  $\mu$ L.

The retention time of vitamin B<sub>1</sub> was reduced slightly in comparison to the same microemulsion using 1-butanol as the co-surfactant (4.03 vs 6.37 min). The retention time of all other water soluble vitamins was similar to the 1-butanol microemulsion. Efficiencies remained similar for both microemulsions.

### 5.4.8 Effect of column length on vitamin separation

Changing the column from 100 mm C18 monolith to 250mm C18 packed allowed baseline separation of all vitamins. Figure 5.9 shows the separation achieved using the 250mm packed column.

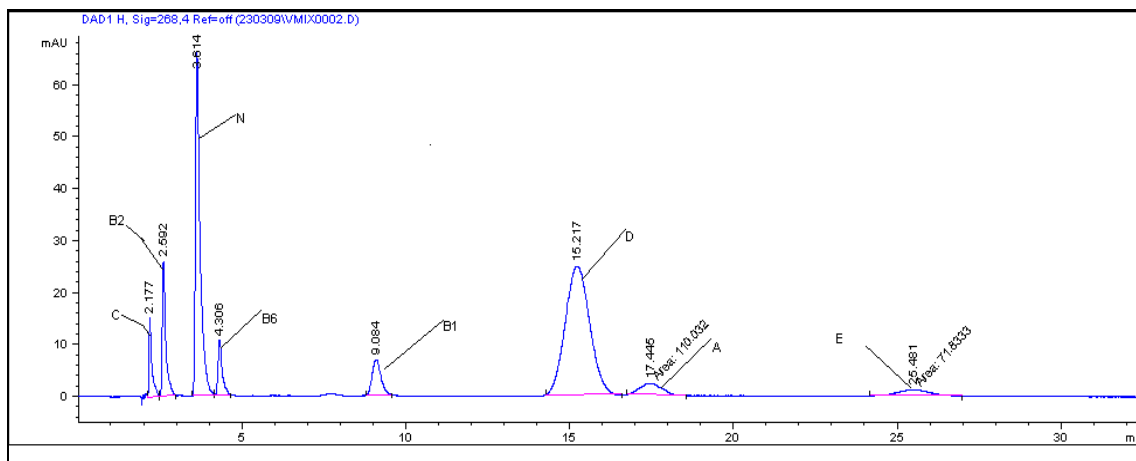


**Figure 5.9** Separation of oil and water soluble vitamins on 250mm C18 RP packed column. Microemulsion composition: 2.98% w/w SDS, 5.96% w/w 1-pentanol 0.72% w/w 2-octanol and 90.33% w/w 0.05% TFA, pH 2.8. Conditions: Temperature 35°C, Flow rate 1 ml min<sup>-1</sup>, Injection volume 5 µl, Detection wavelength 267nm.

Naturally column length had a significant effect on the peak efficiency of the vitamins. The 100 mm monolith column resulted in efficiencies between 520 and 2000 theoretical plates while the 250 mm packed column gave efficiencies between 1500 and 7000 theoretical plates. Also, there was a dramatic increase in retention time for all vitamins when separation was carried out on the 250mm packed column.

### 5.4.9 Validation

Due to the relatively high concentration of vitamin C and B<sub>2</sub> in the sample preparation and the minimum baseline resolution allowed by the method, full separation was not achieved. In addition, while vitamins A and D were separated their concentrations were below the LOQ. Due to these reasons method validation was applied only to vitamins B<sub>1</sub>, B<sub>6</sub>, niacin and E. Table 5.5 provides a summary of the data obtained for method validation.

**Table 5.5 Method validation data**

<b>Vitamin Niacin</b>			
Linearity	<i>Range (mg ml<sup>-1</sup>)</i> 0.8-1.44	<i>Regression equation</i> y = 10310x - 1300.8	<i>R<sup>2</sup></i> 0.9929
	<i>Residual Std. Dev. of the regression line (σ)</i> 202.28		
Accuracy (n = 3)	<i>Recovery</i> 102.92%	<i>Std. Dev.</i> 1.28	<i>RSD</i> 1.3%
Precision	<i>Repeatability (n = 9)</i> RSD = 0.65%	<i>Inter. Precision (n = 9)</i> RSD = 1.52%	
LOD	0.06 mg.ml <sup>-1</sup>		
LOQ	0.2 mg.ml <sup>-1</sup>		
Assay (% label claim)	<i>MELC Assay</i> 79.35		
<b>Vitamin B<sub>1</sub></b>			
Linearity	<i>Range (mg ml<sup>-1</sup>)</i> 0.04-0.08	<i>Regression equation</i> y = 6175.1x - 9.086	<i>R<sup>2</sup></i> 0.9998
	<i>Residual Std. Dev. of the regression line (σ)</i> 1.42		
Accuracy (n = 3)	<i>Recovery</i> 102.42%	<i>Std. Dev</i> 2.40%	<i>RSD</i> 2.34%
Precision	<i>Repeatability (n = 9)</i> RSD = 1.70%	<i>Inter. Precision (n = 9)</i> RSD = 3.32%	
LOD	0.000689 mg.ml <sup>-1</sup>		
LOQ	0.002299 mg.ml <sup>-1</sup>		
Assay (% label claim)	<i>MELC Assay</i> 66.71		
<b>Vitamin B<sub>6</sub></b>			
Linearity	<i>Range (mg.ml<sup>-1</sup>)</i> 0.02 - 0.12	<i>Regression equation</i> y = 8206.6x + 51.029	<i>R<sup>2</sup></i> 0.9932
	<i>Residual Std. Dev. of the regression line (σ)</i> 31.11		
Accuracy (n = 3)	<i>Recovery</i> 98.06%	<i>Std. Dev.</i> 0.98	<i>RSD</i> 1.0%
Precision	<i>Repeatability (n = 9)</i> RSD = 2.63	<i>Inter. Precision (n = 9)</i> RSD = 5.49	
LOD	0.01137 mg.ml <sup>-1</sup>		
LOQ	0.0379 mg.ml <sup>-1</sup>		
Assay (% label claim)	<i>MELC Assay</i> 62.54		

<b>Vitamin E</b>			
Linearity	Range (mg.ml <sup>-1</sup> ) 0.32 - 0.48 Residual Std. Dev. of the regression line ( $\sigma$ ) 41.46	Regression equation $y = 6150x - 73.14$	$R^2$ 0.9915
Accuracy (n = 3)	Recovery 101.04%	Std. Dev. 3.02	RSD 2.99%
Precision	Repeatability (n = 9) RSD = 2.45	Inter. Precision (n = 9) RSD = 3.75	
LOD	0.0202 mg.ml <sup>-1</sup>		
LOQ	0.067 mg.ml <sup>-1</sup>		
Assay (% label claim)	MELC Assay 59.62		

## 5.5 Discussion

### 5.5.1 Solubility of vitamins

The standard microemulsion proved to be effective in dissolving both water and oil soluble vitamins. In comparison to water, butanol, pentanol and THF, only the microemulsion could solubilise both vitamin types. However, it should be mentioned that aqueous/organic mixtures of water/2-propanol, water/acetonitrile and water/THF are also capable of dissolving all vitamins. These aqueous/organic mixtures are often relied upon to analyse vitamins in traditional HPLC [17] but require a large amount of organic phase to achieve separation of oil soluble vitamins (>95% v/v). By comparison the standard microemulsion only contained approximately 9% organic phase (butanol and octane). The fact that all vitamins showed a degree of solubility in the microemulsion allowed them to be run on the MELC system.

### 5.5.2 Analysis of vitamins using MELC with the standard microemulsion

Initial attempts to separate the oil and water soluble vitamins in MELC mode proved unsuccessful. Some water soluble vitamins co-eluted, as did vitamins A and D while vitamin E was not eluted. Vitamin E was the most hydrophobic of the oil soluble vitamins (log P = 10.8) and it was possible that E was heavily adsorbed onto the bonded phase of the C18 column. This indicated that the standard microemulsion mobile phase was not hydrophobic enough to elute vitamin E. An investigation was

carried out to find an appropriate modifier which would increase the overall hydrophobicity of the microemulsion and elute vitamin E.

### **5.5.3 Analysis of vitamin E on the HP 1050 with traditional aqueous/organic solvents**

In order to determine the most adequate organic modifier a range of solvents with increasing hydrophobicity were examined. Since the microemulsion was predominantly aqueous, only solvents which were miscible with water were used. The solvents examined included methanol, 2-propanol, 1-propanol, and THF. Only THF (most hydrophobic) was capable of eluting vitamin E at  $1 \text{ ml min}^{-1}$ , and in a reasonable time (68 min). Hence, THF was chosen as the microemulsion was relatively viscous in comparison to traditional HPLC mobile phases and the maximum flow rate was  $1 \text{ ml min}^{-1}$  on a C18 150mm packed column.

### **5.5.4 Analysis of vitamins using THF modified microemulsion**

Use of the monolith column with its large pore size drastically reduced the system back pressure and allowed flow rates of up to  $2 \text{ mL min}^{-1}$ . All vitamins were capable of being eluted at THF concentrations between 5 and 50% v/v. Since addition of THF increased the overall elution strength of the microemulsion eluent a large change in selectivity was observed for the oil soluble vitamins. At concentrations of 10% (v/v) the method was capable of eluting and separating all oil-soluble vitamins. Another possibility was that an increase in organic modifier would result in less surfactant being absorbed onto the stationary phase, hence reducing the amount of time the oil soluble vitamins would spend on the column.

Vitamins A and D were separated at THF concentrations between 5 and 40% v/v. All water soluble vitamins co-eluted with the solvent peak except vitamin B<sub>1</sub> which was separated with additions of THF from 5-50% v/v.

The use of THF as a modifier was questionable as it was miscible with all components of the microemulsion. For this reason it was difficult to postulate what role it actually played in the microemulsion. Given that THF has such a high capacity to solubilise; it may have solubilised the oil phase, surfactant and co-surfactant resulting in the formation of a modified solvent rather than any type of microemulsion. Before deciding to make a portion of THF constant in the method, the other components of the microemulsion were examined.

### **5.5.5 Variation of oil phase for separation of water soluble vitamins**

Analysis of the oil soluble vitamins with variation in the oil phase proved unsuccessful. All oil phases examined failed to elute vitamin E and while vitamins A and D were eluted they were not separated. It was possible that regardless of the oil phase employed the microemulsion was not hydrophobic enough to elute vitamin E. Changes to the oil phase resulted in a slightly better separation of the water soluble vitamins, although at best only three peaks were observed. Interestingly, a difference in selectivity occurred when hexane was used in place of the other oil phases which indicated the oil phase played a part in the separation of the water soluble vitamins. Also, there was an increase in retention of all vitamins when 2-octanol was employed as the oil phase. Given that an increase in retention of the water soluble vitamins may be exploited to improve selectivity 2-octanol was used as the oil phase for the remainder of the study.

### **5.5.6 Effect of pH on the separation of water soluble vitamins**

Since the oil soluble vitamins were not charged, changes in pH should not have presented an influence on their separation. Therefore, only the effect of pH on the water soluble vitamins was examined.

Adjusting the pH of the microemulsion had the most prominent effect on separation of the water soluble vitamins. Complete separation of the vitamins could only be achieved from pH 2.87-4, with vitamins B<sub>2</sub>, niacin and B<sub>6</sub> co-eluting in the 4-9 pH range. A decrease in retention time was observed for all vitamins with an increase in pH.

Looking at the pK<sub>a</sub> and Log P values of the vitamins helps elucidate some of these observations. At approximately pH 4 and above vitamins niacin and B<sub>6</sub> behaved as neutral analytes and were poorly retained. As these vitamins were highly water soluble they partitioned strongly with aqueous eluent. The retention time and charge of vitamins C and B<sub>2</sub> remained relatively unchanged across the pH range examined. Vitamin C had a negative charge and eluted first which may have been attributed to both its affinity for the aqueous phase and ion repulsion with the anionic surfactant coated column, while B<sub>2</sub> was neutral. Based on the Log P values, at pH 4 the three neutral vitamins eluted in increasing order of hydrophilicity. At pH 2.87 niacin and B<sub>6</sub> were protonated and carried a positive charge. While this may have resulted in an ion

pair interaction with the moving microemulsion droplet, it also facilitated the same interaction with the column and was responsible for their increased retention and separation. Vitamin B<sub>1</sub> remained positively charged throughout and was well retained and separated from the other vitamins.

### **5.5.7 Effect of co-surfactant on the separation of water and oil soluble vitamins**

Based on the concerns discussed in section 5.5.4 about the use of THF, it was decided to examine a co-surfactant which was more hydrophobic than 1-butanol while still being a short chain alcohol. Using an equal weight of 1-pentanol in place of 1-butanol had a very positive effect on the separation. All vitamins were eluted in less than seven minutes and while vitamins A and D co-eluted, all other vitamins were at least partially resolved. The retention time of all water soluble vitamins apart from vitamin B<sub>1</sub> (which was reduced by 2 minutes) remained similar to the 1-butanol microemulsion. It was apparent that 1-pentanol sufficiently increased the hydrophobicity/elution strength of the microemulsion allowing vitamin E to partition into the microemulsion droplet. From Figure 5.8 it could be seen that while all vitamins were detected, the peak shape was relatively poor, especially for vitamin E which eluted over 1.5 minutes.

Apart from being more hydrophobic than 1-butanol it was not clear why 1-pentanol improved the separation to such a degree. A possibility may have been that the components involved in the formation of the microemulsion droplet may have had a synergistic effect. It has been reported that when the carbon chain of the oil phase and co-surfactant added together is 1 carbon greater than the surfactant, a particularly stable microemulsion droplet results [20]. The 1-pentanol co-surfactant may have helped increase the elasticity of the surfactant film between the organic and aqueous part of the microemulsion droplet, hence improving the partitioning of the oil soluble vitamins into the droplet. However, this area will require further investigation.

### **5.5.8 Analytical column length**

It was not possible to directly compare the 100 mm monolith column and the 250 mm packed column due to the nature of the packing. Never the less, the longer column dramatically improved separation. Chromatographic resolution was increased due to the greater number of theoretical plates generated by the longer column. All vitamins were eluted and baseline separated.

### **5.5.9 Validation of vitamin preparation**

Minimum baseline resolution between the water-soluble vitamins proved problematic when validating the method for the vitamin preparation. Due to high concentration of vitamin C and B<sub>2</sub>, a masking effect was observed which made quantitative analysis difficult. This problem may have been circumnavigated by monitoring the respective vitamins at unique wavelengths of absorbance. In addition to the masking effect of water-soluble vitamins, interference from excipient peaks was also observed. However, these peaks did not interfere with the peaks of interest at the wavelengths examined for quantitation.

With respect to vitamins A and D their concentration in the vitamin preparation was below the methods LOQ.

Validation figures for the vitamins niacin, B<sub>6</sub>, B<sub>1</sub> and E showed reasonably good linearity ( $R^2 > 0.99$ ) in the ranges examined. Also, good results were obtained for accuracy (98.6% - 102.92) and precision (repeatability: RSD = 0.65 - 2.63%, int. prec. RSD = 0.98 - 3.75%). From the calibration curves modest LOQs and LODs were obtained. However, assay results for the vitamin preparation were very poor. This may have been attributed to two reasons. Firstly without a placebo of the vitamin preparation it was not feasible to do meaningful recovery studies and therefore not possible to analyse the microemulsions ability to extract the vitamins of interest. Also, the sample examined was aged and there may have been a degree of degradation. Further development work would be required for validation of this method including cross correlation with different sample extraction methods in conjunction with a formulation placebo. Overall results indicated that the method had the potential to be applied to the separation and quantitation of a limited number of oil- and water- soluble vitamins.

#### **5.5.9.1 Gradient Elution Option**

The use of gradient onset to increase retention of water soluble vitamins and improve the peak shape of oil-soluble vitamins was considered. However, previous investigations by this group concluded that MELC was not compatible with gradient elution. Work by McEvoy et al. [12] when separating paracetamol and its related substances showed that long equilibration times were required when using a SDS based microemulsion. Employing a gradient was seen to disrupt the steady state equilibration

between the surfactant molecules and stationary phase leading to irreproducible separations.

#### **5.5.9.2 Development of method for oil- or water- soluble vitamins**

Separating either vitamin set independently may have proved more successful. From figure 5.3 it could be seen that the standard microemulsion modified with 10% THF resulted in a relatively quick separation of the oil soluble vitamins with good resolution between vitamin A and D.

### **5.6 Conclusion**

A completely isocratic microemulsion method has been developed capable of simultaneously separating water and oil-soluble vitamins. While the method is far from optimised the results so far are promising. Only one HPLC method capable of analysing water and oil-soluble vitamins simultaneously has been reported [17], and while successful this method required gradient elution and large volumes of organic solvents. The only other comparable method in the literature utilised MLC for the separation of vitamins E and A [11]. This method required the addition of 12% v/v butanol and achieved separation on a 100 mm RP packed column in 17 minutes at a flow rate of 1.35 ml min<sup>-1</sup>. By comparison the method reported in this chapter can achieve separation of vitamins E and A in under seven minutes at a flow rate of 1 ml min<sup>-1</sup>, and less than 10% organic phase. Another report utilising micelles achieved separation of vitamins A, D and E in 23 minutes on a 250mm RP packed column and required 15% v/v butanol [21]. It is certainly clear that use of micelle and microemulsion eluents present a greener and more time efficient method for analysis of oil soluble vitamins.

## 5.7 References

- [1] Eitenmiller, R.R. and Landen, W.O. (1999) Vitamin Analysis for the Health and Food Sciences. CRC Press.
- [2] Bodson, C., Dewe, W., Hubert, P., Delattre, L., Journal of Pharmaceutical and Biomedical Analysis, 41 (2006) 783-790.
- [3] Lopez-de-Alba, P.L., Lopez-Martinez, L., Cerda, V., mador-Hernandez, J., Journal of the Brazilian Chemical Society, 17 (2006) 715-722.
- [4] Dilgin, Y., and Nisli, G., Chemical & Pharmaceutical Bulletin, 53 (2005) 1251-1254.
- [5] Du, Y.Y., Jia, L., Liu, H.Q., Xing, D., Analytical Letters, 40 (2007) 2005-2015.
- [6] Kvasnicka, F., Electrophoresis, 28 (2007) 3581-3589.
- [7] Presoto, A.E.F., and de Almeida-Muradian, L.B., Quimica Nova, 31 (2008), 498-U38.
- [8] Kostarnoi, A.V., Golubitskii, G.B., Basova, E.M., Budko, E.V., Ivanov, V.M., Journal of Analytical Chemistry, 63 (2008) 516-529.
- [9] Cheung, R.H.F., Marriott, P.J., Small, D.M., Electrophoresis, 28 (2007) 3390-3413.
- [10] Yin, C.N., Cao, Y.H., Ding, S.D., Wang, Y., Journal of Chromatography A, 1193 (2008) 172-177.
- [11] Momenbeik, F., Momeni, Z., Khorasani, J.H., Journal of Pharmaceutical and Biomedical Analysis, 37 (2005) 383-387.
- [12] McEvoy, E., Donegan, S., Power, J., Altria, K., Chromatographia, 68 (2008) 49-56.
- [13] Marsh, A., Clark, B., Altria, K., Chromatographia, 2004, 59, 531-542.
- [14] Marsh, A., Clark, B.J., Altria, K.D., Chromatographia, 61 (2005) 539-547.
- [15] McEvoy, E., Donegan, S., Power, J., Altria, K., Journal of Pharmaceutical and Biomedical Analysis, 44 (2007) 137-143.
- [16] Cheng, T.J., Zhao, Y., Li, X., Lin, F., Xu, Y., Zhang, X.L., Li, Y., Wang, R.X., Lai, L.H., Journal of Chemical Information and Modeling, 47 (2007) 2140-2148.
- [17] Klejdus, B., Petrlova, J., Potesil, D., Adam, V., Mikelova, R., Vacek, J., Kizek, R., Kuban, V., Analytica Chimica Acta, 520 (2004) 57-67.
- [18] Monferrer-Pons, L., Capella-Peiro, M.E., Gil-Agusti, M., Esteve-Romero, J., Journal of Chromatography A, 984 (2003) 223-231.

- [19] Snyder, L.R., *Journal of Chromatographic Science*, 16 (1978) 223-234.
- [20] Li, G.Z., and Friberg, S.E., *Journal of the American Oil Chemists Society*, 59 (1982) 569-572.
- [21] Kienen, V., Costa, W.F., Visentainer, J.V., Souza, N.E., Oliveira, C.C., *Talanta*, 75 (2008) 141-146.

## **Chapter Six**

### **Analysis of oil and water-soluble vitamins by MEEKC**

## **6.1 Introduction**

In chapter five both oil- and water-soluble vitamins were separated by HPLC using an O/W microemulsion. Utilising the microemulsion as the sample solvent and eluent allowed solubilisation and isocratic separation of these diverse analytes.

The aim of this experimental section was to separate the same range of oil- and water soluble vitamins using CE with an O/W microemulsion as the background electrolyte. Initial separation conditions were optimised in terms of buffer concentration, applied voltage, temperature and injection time. The microemulsion was optimised in terms of the type and concentration of surfactant, co-surfactant, oil and addition of modifiers. Changes in the microemulsion composition were evaluated with respect to migration time, separation and resolution. Also for comparison, separations were carried out in MEKC and modified MEKC mode.

Both micellar [1-3] and microemulsion [4;5] buffers have been used as background electrolytes in CE for the analysis of vitamins. The anionic surfactant, SDS, is the most common surfactant used in both systems. However, the cationic surfactant CTAB has also been utilised in MEEKC [6]. CTAB forms positively charged microemulsion droplets which generate a positively charged surfactant bilayer on the capillary wall which reverses the EOF direction. A negative polarity voltage was therefore required when working with cationic microemulsion. This study attempted to compare the benefits and drawbacks of both surfactant systems.

Similar to the MELC study, a previously reported microemulsion [7-9], hereafter referred to as the standard microemulsion, was chosen as the starting point for method development. The microemulsion consisted of 2.98% w/w SDS, 5.96% w/w 1-butanol, 0.72% w/w n-octane and 90.33% w/w of sodium tetraborate buffer pH 9.2.

## **6.2 Experimental**

### **6.2.1 Chemicals**

Vitamin standards retinol acetate (vitamin A), tocopherol acetate (vitamin E), cholecalciferol (vitamin D), thiamine hydrochloride (vitamin B<sub>1</sub>), riboflavin (vitamin B<sub>2</sub>), pyridoxine (vitamin B<sub>6</sub>), niacin and ascorbic acid (vitamin C) were purchased from

Sigma Aldrich (Ireland). Figure 6.1 shows the chemical structure of the water and oil-soluble vitamins, along with Log P and pKa values where available.

### 6.2.2 Microemulsion components

HPLC grade water, n-octane, trifluoroacetic acid (TFA), 1-butanol (all Romil) and 99% sodium dodecyl sulphate (SDS), sodium cholate (SC), cetyltrimethylammonium bromide (CTAB) and sodium tetraborate were obtained from Lennox Laboratory Supplies (Ireland). 2-octanol, 1-pentanol, hexane, nonane and dodecane were obtained from the chemical stores at WIT. Organic additives: tetrahydrofuran (THF), 1-propanol, 2-propanol and methanol were also obtained from Lennox.

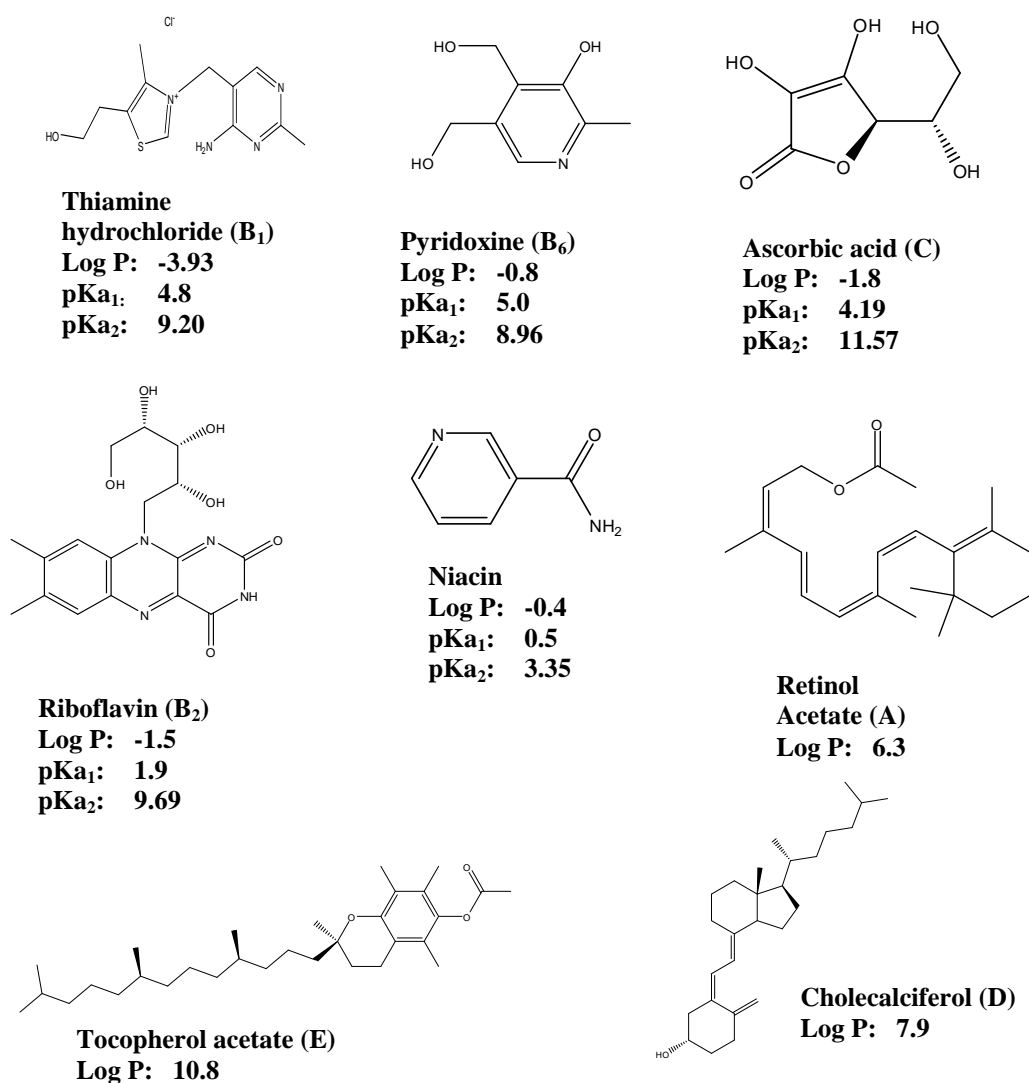


Figure 6.1 Structure and physical data of the water and oil-soluble vitamins [10-12].

### **6.2.3 Instrumentation**

MEEKC experiments were performed on an Agilent 3D-CE capillary electrophoresis instrument, (model G1600AX,) equipped with UV diode array detector and Agilent Chemstation software Rev A.08.03. All separations were performed on fused silica capillaries with 50  $\mu\text{m}$  ID, total length 35.5 cm with detection window at 26.5 cm. Injections were performed in hydrodynamic way at a pressure of 20 mbar.

## **6.3 Method development**

### **6.3.1 Microemulsion preparation**

The standard microemulsion was prepared by mixing 3.3 g of SDS, 6.6 g of 1-butanol, and 0.8 g of n-octane in a 200 ml duran bottle. This mixture was stirred for 10 minutes using a magnetic stirrer to ensure a homogenous solution was formed. 100 mL of 20 mM sodium borate pH 9.2 was then added, sonicated for 30 minutes and filtered.

### **6.3.2 Sample preparation**

Vitamin standards were prepared freshly each day by dissolving each sample in the microemulsion buffer. Standards were prepared qualitatively to a concentration of approximately 200 mg L<sup>-1</sup> and syringe filtered prior to injection.

### **6.3.3 Initial conditions**

Initial runs were performed using an applied voltage of +18 kV and a cassette temperature of 20 degrees with an injection time of ten seconds. The capillary was flushed between runs for 1 minute with 0.1 M NaOH followed by 1 minute with microemulsion. This separation generated a current in excess of 100  $\mu\text{A}$  and all vitamins migrated within 15 minutes. In order to determine the optimum initial conditions; the buffer concentration, applied voltage, cassette temperature and various rinse cycles were examined. The buffer concentration was assessed at 10 and 20 mM. Applied voltage was varied between 10 and 18 kV, while cassette temperature was examined between 10 and 20 °C. The optimum initial conditions were found to be a buffer concentration of 10 mM sodium tetraborate, an applied voltage of + 16 kV and a cassette temperature of 20 °C. In order to achieve reproducible migration times a rinse cycle of 3 minutes of 0.1 M NaOH, followed by 1 minute of de-ionised water and 3 minutes of separation buffer was implemented. [4]

#### **6.3.4 Variation of oil phase type**

In order to assess the effect of oil phase type equal weight % (0.72% w/w) of 1-pentanol, 2-octanol, hexane and dodecane were examined in place of n-octane. The separation was also carried out in modified MEKC mode with no oil phase present and by traditional MEKC, with neither oil nor co-surfactant. 2-Octanol was chosen as the optimum oil phase.

#### **6.3.5 Variation of co-surfactant type**

1-butanol was replaced with equal weight % (5.96% w/w) of 1-pentanol and 1-propanol to assess the effect of co-surfactant hydrophobicity on the separation of vitamins. 1-butanol proved to be the optimum co-surfactant.

#### **6.3.6 Variation of SDS concentration**

The concentration of SDS was varied between 1.92 and 3.50% w/w. 2.73% w/w of SDS was found to provide the best separation and this concentration was fixed for the remainder of the study.

#### **6.3.7 Co-surfactant concentration**

Since the co-surfactant appeared to have the most significant effect on separation, the concentration of 1-butanol was varied from 5.46 to 6.48% w/w. The initial concentration of 5.96% w/w was held constant for the remainder of the study.

#### **6.3.8 Addition of organic modifiers**

Acetonitrile, 1-propanol and methanol were examined as organic modifiers in the concentration ranges 5, 10 and 15% v/v. Also the addition of mixed modifiers was examined. Equal amounts of 1-propanol and acetonitrile were added in the concentration ranges 5, 10, 15, 20 and 30% v/v.

#### **6.3.9 Addition of $\alpha$ -cyclodextrin**

The effect of cyclodextrin was assessed by preparing a 10 mM  $\alpha$ -CD modified microemulsion.

### 6.3.10 Addition of sodium cholate

The effect of a secondary anionic surfactant was assessed by preparing a 50 mM SC modified microemulsion. Figure 6.2 shows the structure of the anionic sodium cholate.

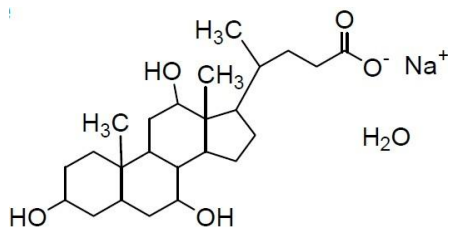


Figure 6.2 Structure of sodium cholate.

### 6.3.11 Variation of surfactant type

An alternative type of anionic surfactant was examined by replacing SDS with an equimolar (10.4 mmols) concentration of sodium cholate (4.47 g). The separation was also performed utilising the cationic surfactant CTAB in an equimolar concentration (3.79 g).

### 6.3.12 Mixed surfactant system

The influence of a mixed surfactant system was studied by preparing a microemulsion consisting of 1.35% w/w SDS and 2.01% w/w SC. The overall molar concentration was kept constant.

### 6.3.13 CTAB microemulsion with addition mixed of organic modifiers

Mixtures of acetonitrile and 1-propanol were examined as organic modifiers. Equal amounts of 1-propanol and acetonitrile were added to the ME buffer in the concentration ranges 5, 10, 15, 20 and 30% v/v.

### 6.3.14 Sodium cholate microemulsion

Use of sodium cholate as the surfactant was seen to provide promising results with an increased migration window for the water soluble vitamins while maintaining an overall short run time (12 mins). A minimum concentration of 5.68 % w/w (15.56 mM) was required to form the microemulsion.

#### **6.3.14.1 Sodium cholate microemulsion with the addition of organic modifiers**

IPA was added to the sodium cholate microemulsion buffer in the concentration range 5, 10 and 15% v/v.

#### **6.3.14.2 Sodium cholate ME with SDS and increased butanol concentration**

In order to swell the ME droplet and thereby facilitate mass transfer between the droplet and oil soluble vitamins, the level of butanol was increased from 5.97 % w/w to 11.94% w/w. However, in order to form the microemulsion while using the minimum amount of surfactant 0.99% w/w (1.2g) of SDS was added. A SC ME with 17.91% w/w of 1-butanol was also examined.

#### **6.3.14.3 Sodium cholate ME with increased butanol and addition of organic modifiers**

A microemulsion consisting of SC and SDS with 17.91% w/w of 1-butanol was modified with 10% IPA and 10% ACN respectively.

### **6.4 Results and discussion**

#### **6.4.1 Optimising initial conditions**

##### **6.4.1.1 Sodium tetraborate concentration**

The initial standard microemulsion had a sodium tetraborate concentration of 20 mM. This generated a current in excess of 100  $\mu$ A when run at 20 °C and an applied voltage of 18 kV. Separation was not repeatable and the current was deemed to be too high leading to joule heating. The buffer concentration was therefore reduced to 10 mM before further optimisation. At a concentration of 10 mM a current of 87  $\mu$ A was generated and migration time reproducibility improved. A relatively high pH (8-9.5) has been reported in the literature for the separation of water-soluble vitamins [1, 2, 4, 13]. The pH of the buffer was maintained at 9.2 as full separation of the water soluble vitamins was achieved.

##### **6.4.1.2 Applied voltage**

The effect of applied voltage on the separation was examined between 10 and 18 kV. Increasing the applied voltage resulted in shorter migration times for all vitamins. No effect on the separation of the oil-soluble vitamins was noted. Below 16 kV water-

soluble vitamins B<sub>1</sub> and B<sub>6</sub> co-migrated. The current generated was also monitored with respect to the applied voltage. Figure 6.3 shows the effect of applied voltage on current generated. 16 kV was chosen as the optimum as it allowed the quickest separation for the water-soluble vitamins with a corresponding current of 62  $\mu$ A. Figure 6.4 shows the effect of applied voltage on the migration time of water soluble vitamins while figure 6.5 shows the effect on oil-soluble vitamins.

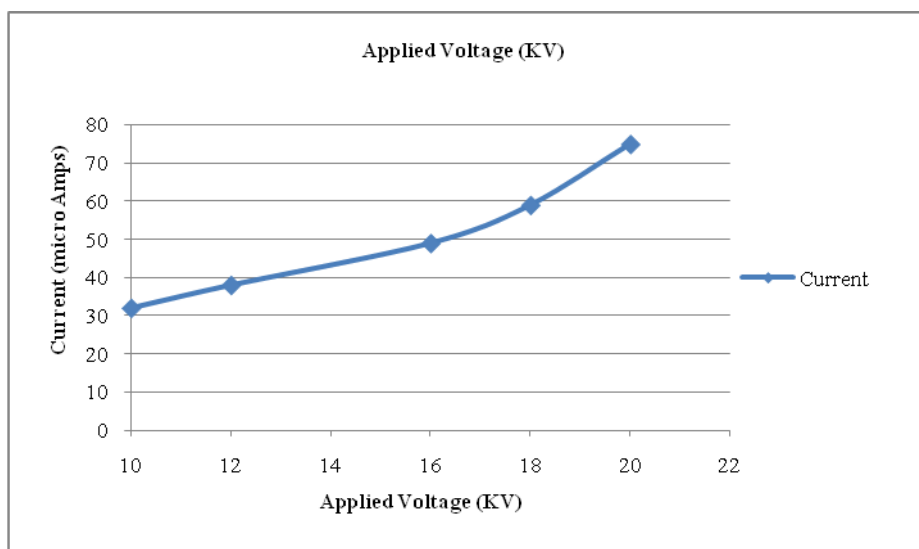


**Figure 6.3** Effect of applied voltage on current generated within the capillary during separation of water and oil-soluble vitamins. Buffer: 2.98% w/w SDS, 5.96% w/w 1-butanol, 0.72% w/w octane and 90.33% w/w 10 mM sodium borate buffer (pH 9.2) (standard microemulsion). Separation conditions; 50  $\mu$ M ID fused silica capillary length 35 cm, detection window at 26.5 cm, flush for 3 minutes with 0.1 M NaOH followed by 1 minute with microemulsion, capillary cassette temperature 20° C, sample injection 10 mbar for 10 seconds, UV detection at 267 nm.

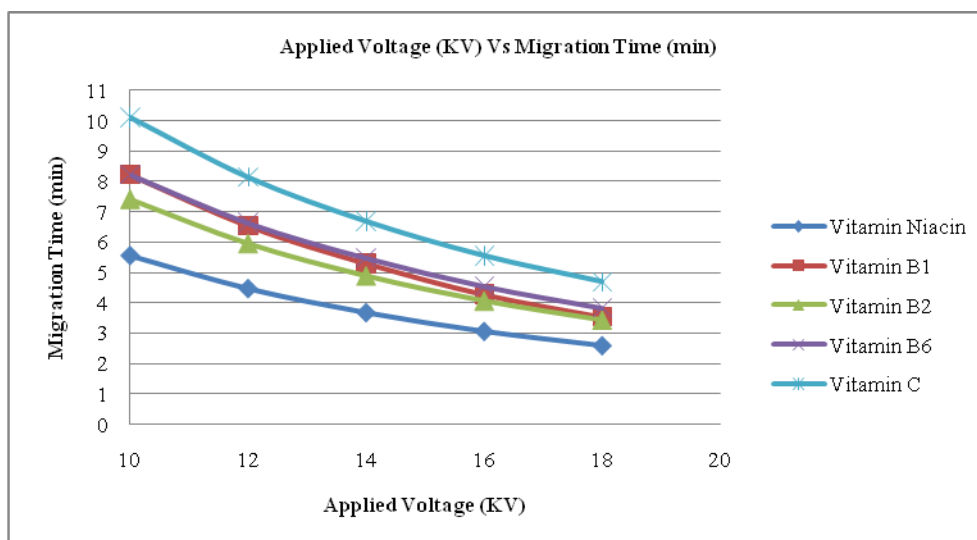


**Figure 6.4** Effect of applied voltage on migration time of water soluble vitamins. Conditions as in figure 6.3.

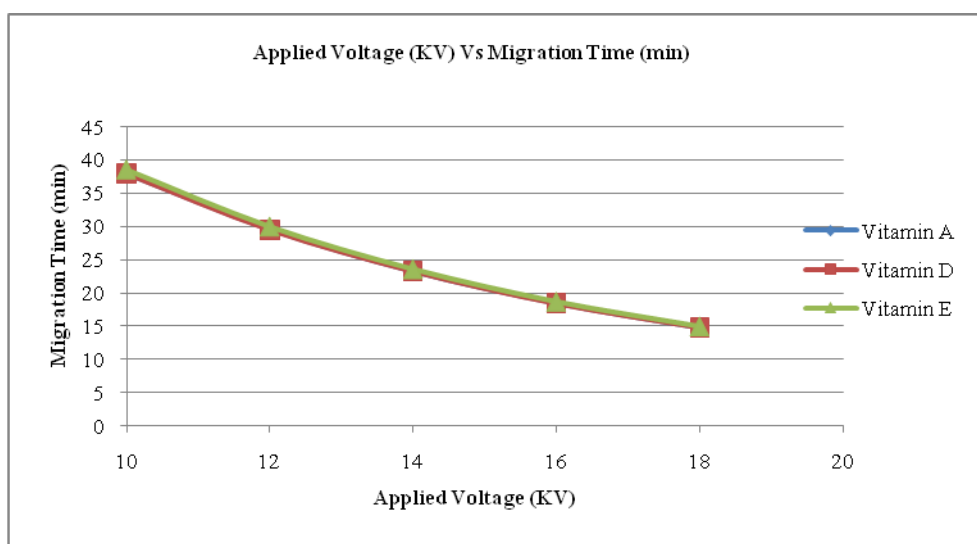


**Figure 6.5** Effect of applied voltage on migration time of oil soluble vitamins. Conditions as in figure 6.3.

### 6.4.1.3 Capillary cassette temperature

Varying the cassette temperature between 10 and 20 °C had little impact on the separation of either vitamin set. An increase in current from 50 to 59  $\mu$ A was noted. Figure 6.6 shows the effect of cassette temperature on current. Since vitamin A was heat sensitive (degrades quickly above 35 °C) a temperature of 20 °C was maintained for all experiments.

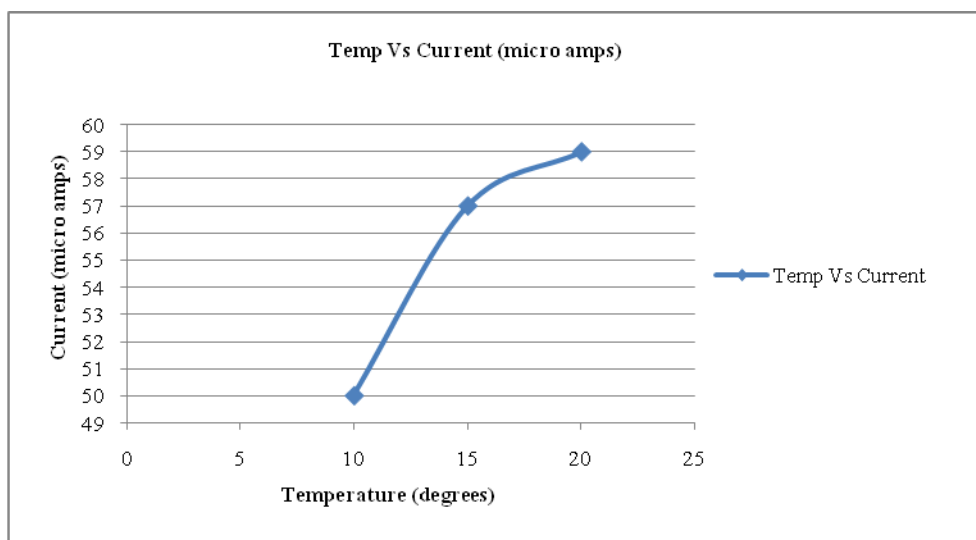


**Figure 6.6** Effect of cassette temperature on current. Conditions as in figure 6.3 except various cassette temperatures.

#### 6.4.1.4 Rinsing procedure

Authors separating vitamins with MEEKC have noted that the rinsing procedure between runs has to be optimised in order to achieve reproducible migration times [5;13]. A rinsing procedure was adapted from ref [5]. This involved the following steps:

- |        |                        |
|--------|------------------------|
| Step 1 | 3 min 0.1M NaOH        |
| Step 2 | 1 min de-ionised Water |
| Step 3 | 3 min buffer           |

Step 3 was carried out using buffer from a separate vial to the running buffers in order to avoid the risk of any siphoning effects.

In summary the optimum initial conditions were found to be a buffer concentration of 10 mM sodium tetraborate, an applied voltage of + 16 kV and a cassette temperature of 20 °C. In order to achieve reproducible migration times a flush cycle of 3 minutes of 0.1 M NaOH, followed by 1 minute of de-ionised water and 3 minutes of separation buffer was implemented. Figure 6.7 shows the separation achieved under optimum starting conditions using the standard microemulsion.

Full separation was achieved for the water soluble vitamins. However, vitamins A and D co-migrated. Based on their pKa values and buffer pH, the water soluble vitamins

migrated in the order of neutral (niacin), positively charged (B<sub>1</sub> and B<sub>2</sub>) and negatively charged (B<sub>6</sub> and C). It may have been expected that the positively charged analytes (B<sub>1</sub> and B<sub>2</sub>) would engage in an ion pairing interaction with the negatively charged ME droplet and migrate after the negatively charged vitamins (B<sub>6</sub> and C). However, on balance, vitamins B<sub>1</sub> and B<sub>2</sub> are very water soluble and may have partitioned more strongly in the aqueous phase and migrated towards the anode. The oil soluble vitamins migrated based on hydrophobicity and their affinity for the ME droplet. Vitamin E was the most hydrophobic (log P 10.8) and migrated last. Vitamins A and D possessed similar log P values (6.3 and 7.9 respectively) and may have had an equal affinity for the ME droplet, resulting in their co-migration.

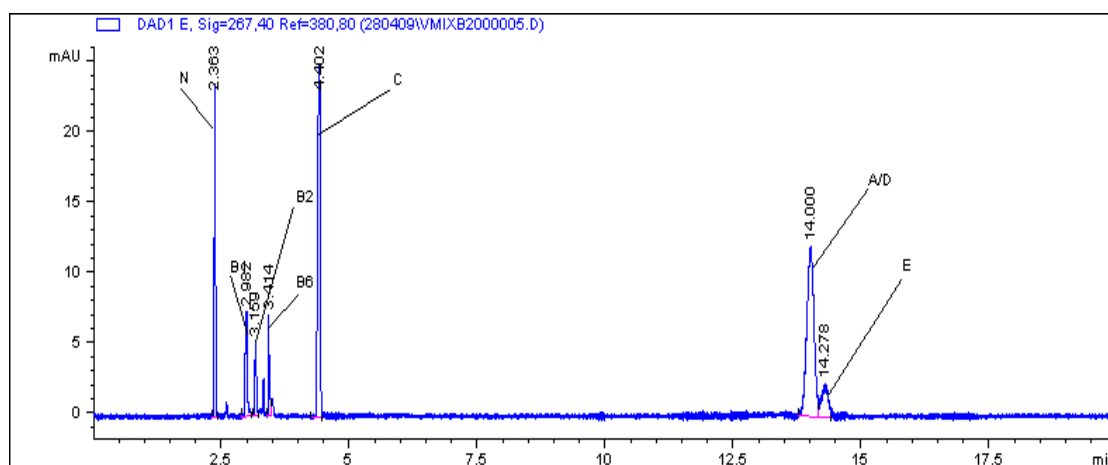


**Figure 6.7** Electropherogram of vitamin separation. Buffer: 2.98% (w/w) SDS, 5.96% w/w 1-butanol, 0.72% w/w octane and 90.33% w/w 10mm sodium borate buffer (pH 9.2) (standard microemulsion). Separation conditions; 50  $\mu$ M ID fused silica capillary length 35 cm, detection window at 26.5 cm, flush for 3 minute with 0.1 M NaOH followed by 1 minute with water and 3 minutes with microemulsion, capillary cassette temperature 20° C, applied voltage 16 kV, sample injection 10 mbar for 10 seconds, UV detection at 267 nm.

#### 6.4.2 Variation of oil phase type

Organic phases both greater and less hydrophobic than n-octane were examined to assess the impact of the internal oil phase type. The separation was also carried out in modified MEKC mode (with no internal oil phase) and in traditional MEKC mode (no oil phase or co-surfactant).

With respect to MEEKC separation, choice of oil phase type had little effect on the migration times of the water soluble vitamins; however an increase in separation between vitamins B<sub>1</sub> and B<sub>2</sub> was observed when an alkane was replaced with an alcohol

as the internal oil phase. Since these analytes carried a positive charge it was expected that they would have some interaction with the ME droplet.

The migration time of the oil soluble vitamins increased slightly with increasing hydrophobicity of the oil phase but no separation was observed between vitamins A and D. This result may have indicated a stronger partitioning between the ME droplet and oil soluble vitamins when an oil phase of higher hydrophobicity was used. Similar findings have been reported by other authors [4;5;13;14] indicating that the type or concentration of internal oil phase has little effect of separation selectivity. Figure 6.8 and figure 6.9 graph the changes in migration time of the water- and oil-soluble vitamins respectively.

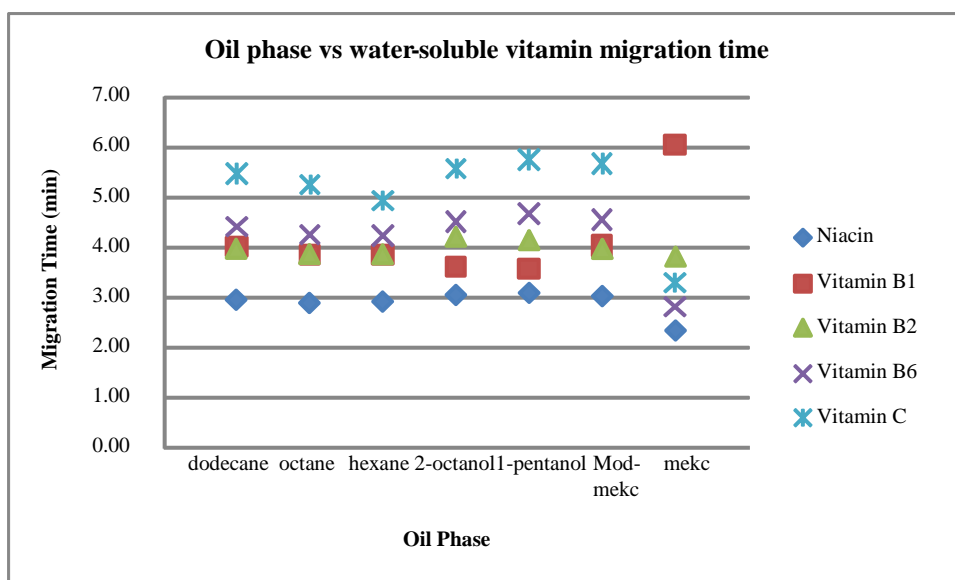


**Figure 6.8** Variation in the migration time of the water-soluble vitamins with changes in oil phase type. Buffer: 2.98% w/w SDS, 5.96% w/w 1-butanol, 0.72% w/w various oil phase and 90.33% w/w 10mm sodium borate buffer (pH 9.2). Separation conditions; 50  $\mu$ M ID fused silica capillary length 35 cm, detection window at 26.5 cm, flush for 3 minute with 0.1 M NaOH followed by 3 minutes with water and 3 minutes with microemulsion capillary cassette temperature 20° C, applied voltage 16 kV, sample injection 10 mbar for 10 seconds, UV detection at 267 nm.

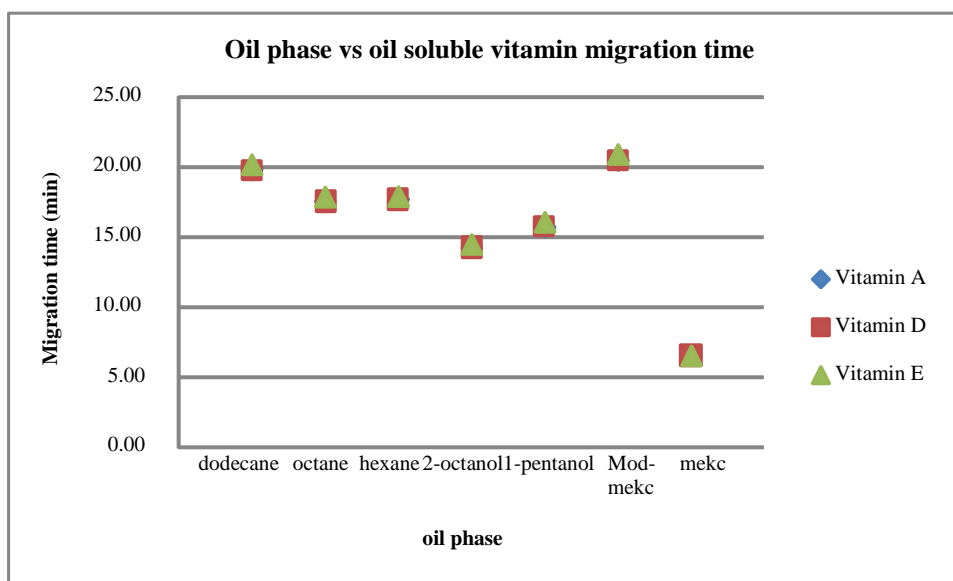


**Figure 6.9** Variation in migration time of the oil-soluble vitamins with changes in oil phase type. Conditions as in figure 6.8.

When the separation was carried out in modified MEKC mode the resolution between vitamins B<sub>1</sub> and B<sub>2</sub> was lost, however the migration time of the other water-soluble vitamins remained similar. An increase in the migration time for the oil-soluble vitamins was noted. It is possible that when operated in modified MEKC mode that the co-surfactant (1-butanol) may behave as an internal oil phase. Given that less organic phase was present, the negative charge on the micelle may be enhanced leading to an increased mobility towards the anode. As the oil-soluble vitamins partitioned with the micelle their migration times increased also.

The most dramatic changes were observed when the separation was carried out in traditional MEKC mode. A reversal in the migration of the charged vitamins was observed. The water-soluble vitamins migrated in the order of neutral (niacin), negatively charged (B<sub>6</sub> and C) and positively charged (B<sub>2</sub> and B<sub>1</sub>). The absence of either a co-surfactant or oil phase may have resulted in a densely negatively charged micelle. It appeared a strong ion-pair interaction may have formed between the micelle and positively charged analytes resulting in longer migration times. Interestingly the oil-soluble vitamins experienced no separation and all co-migrated in less than seven minutes. It appears the micelle may have been too rigid for the oil-soluble vitamins to penetrate or were highly bound to the interior of the micelle with very poor mass transfer. Sanchez and Salvado [13] reported that for SDS based MEKC, a modifier

such as butanol was necessary to achieve separation between oil-soluble vitamins. Also, it has been reported that the addition of a modifier was necessary to an SDS MEKC system to increase the lipophilicity of the electrolyte and prevent oil-soluble vitamins precipitating in the capillary [1].

It was concluded that the oil phase was necessary to enable full separation of the vitamins. Since 2-octanol gave full separation of the water-soluble vitamins and provided partial separation with a short migration time for the oil-soluble vitamins it was fixed for the remainder of the study.

### **6.4.3 Variation of co-surfactant type**

The presence of a co-surfactant in a MEEKC ME has the effect of lowering the surface tension between the oil and aqueous phase. The concentration of co-surfactant also influences the size and charge density on the ME which has an effect on analyte partitioning with the PSP. Furthermore, the co-surfactant can influence the viscosity of the ME buffer thereby affecting the velocity of the EOF.

In this experiment 1-butanol was replaced with 1-propanol (less hydrophobic) and 1-pentanol (more hydrophobic). The type of co-surfactant had a marked effect on separation. 1-propanol resulted in all water- and oil-soluble vitamins having a longer migration time with a reversal in migration order observed for vitamins B<sub>1</sub> and B<sub>2</sub>. Conversely, employing the more hydrophobic 1-pentanol resulted in a decrease in migration time for all vitamins, with co-migration of B<sub>1</sub>, B<sub>2</sub> and B<sub>6</sub>. Figure 6.10 and figure 6.11 graph the changes in migration time of the water- and oil-soluble vitamins, respectively, with changes in the co-surfactant type.

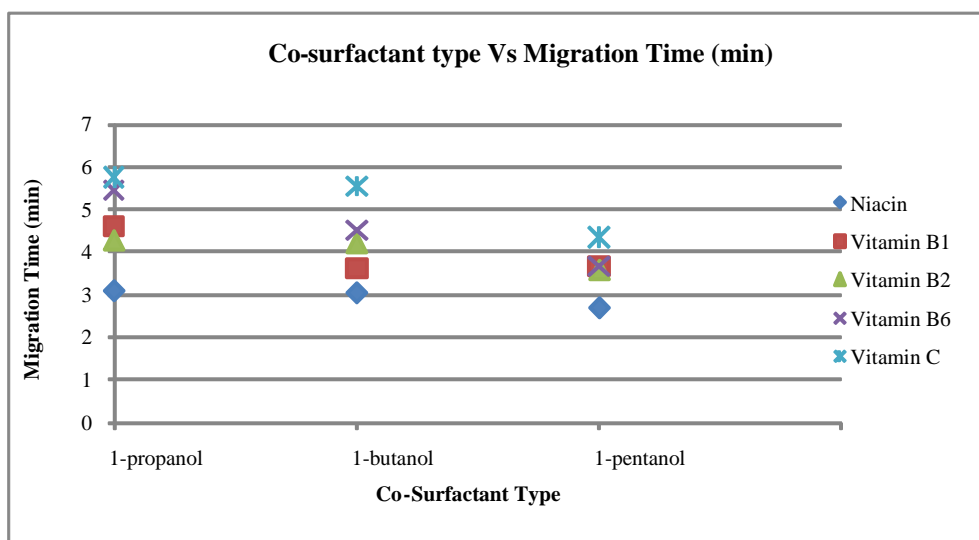


**Figure 6.10** Variation in the migration time of the water-soluble vitamins with changes in co-surfactant type. Buffer: 2.98% w/w SDS, 5.96% w/w various co-surfactants, 0.72% w/w 2-octanol and 90.33% w/w 10mm sodium borate buffer (pH 9.2). Separation conditions; 50  $\mu$ M ID fused silica capillary length 35 cm, detection window at 26.5 cm, flush for 3 minute with 0.1 M NaOH followed by 3 minutes with water and 3 minutes with microemulsion capillary cassette temperature 20° C, applied voltage 16 kV, sample injection 10 mbar for 10 seconds, UV detection at 267 nm.

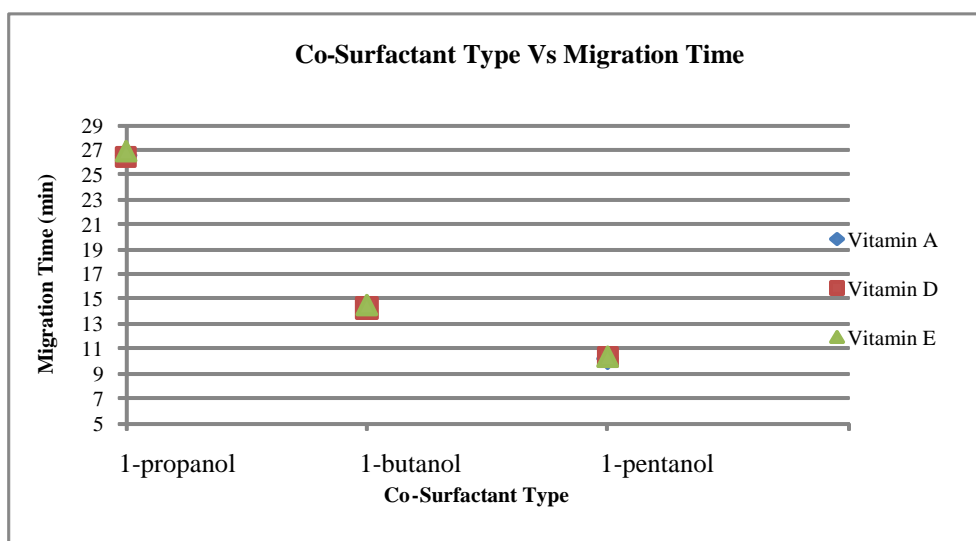


**Figure 6.11** Variation in the migration time of the oil-soluble vitamins with changes in co-surfactant type. Conditions as in figure 6.10.

1-Butanol (intermediate hydrophobicity) resulted in the migration of all vitamins within 14 minutes and full separation of the water soluble vitamins. 1-butanol was used as the co-surfactant for the rest of the study. The presence of a co-surfactant has been reported by various authors to have a significant effect on vitamin separation. Bustamante-Rangel et al. [4] stated that the presence of a co-surfactant (1-butanol)

reduced migration time and improved resolution for the separation of vitamins A, D and E, as well as being the most important factor in changing selectivity. Similar results were reported by Jensen et al. [14] for the separation of a range of neutral compounds. The authors noted that choice of co-surfactant had the greatest impact on selectivity.

The concentration of 1-butanol was varied from 5.46 to 6.48% w/w. It was postulated that the concentration of co-surfactant would influence the charge density on the ME droplet and hence its electrophoretic mobility towards the anode. Figures 6.12 and 6.13 demonstrate the effect of co-surfactant concentration on the migration time of the water- and oil-soluble vitamins respectively.

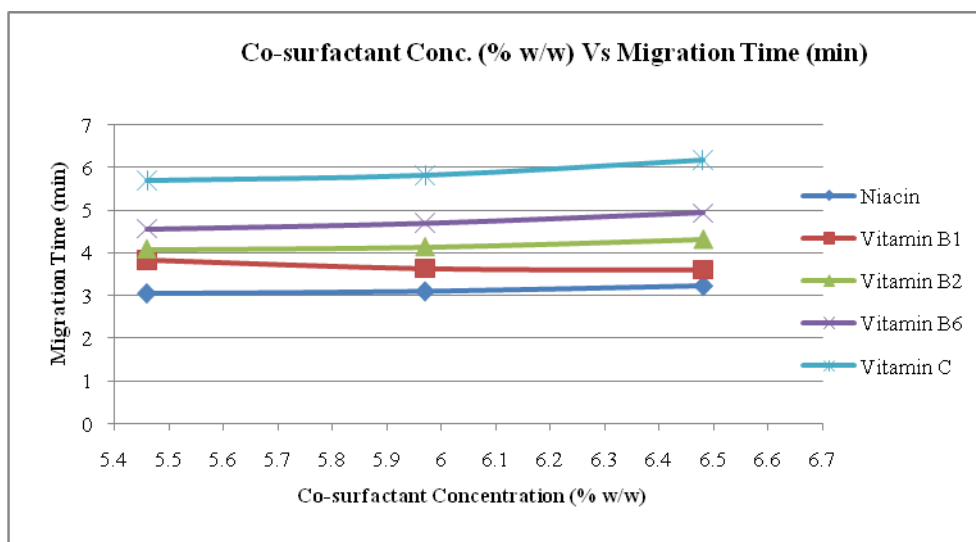


**Figure 6.12** Variation in the migration time of the water-soluble vitamins with changes in butanol concentration. Buffer: 2.98% w/w SDS, various co-surfactant concentrations, 0.72% w/w 2-octanol and 90.33% w/w 10mm sodium borate buffer (pH 9.2). Separation conditions; 50  $\mu$ M ID fused silica capillary length 35 cm, detection window at 26.5 cm, flush for 3 minute with 0.1 M NaOH followed by 3 minutes with water and 3 minutes with microemulsion capillary cassette temperature 20° C, applied voltage 16 kV, sample injection 10 mbar for 10 seconds, UV detection at 267 nm.

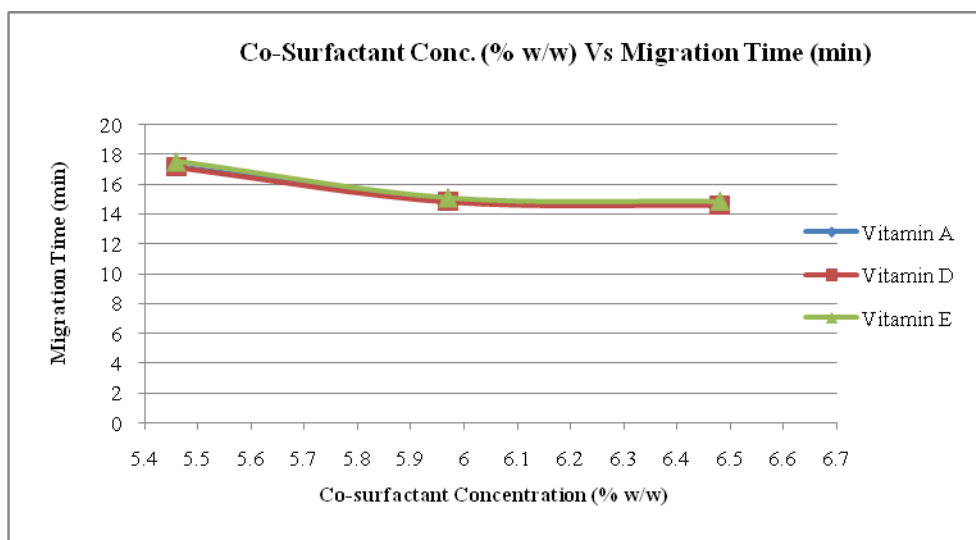


**Figure 6.13** Variation in the migration time of the oil-soluble vitamins with changes in butanol concentration. Conditions as in figure 6.12.

Increasing concentration of co-surfactant resulted in a slight increase in the migration time of the water soluble vitamins and a decrease in migration time of the oil soluble vitamins. An increase in co-surfactant concentration may have reduced the charge on the negatively charged ME droplet, thereby reducing its mobility towards the anode. Since the oil-soluble vitamins partition with the ME droplet, their migration time would be reduced. No improvement in separation was noted for the oil-soluble vitamins. A slight decrease in separation between B<sub>1</sub> and B<sub>2</sub> was observed at a 1-butanol concentration of 5.97% w/w. A concentration of 5.97% w/w was therefore kept constant for the remainder of the study.

#### 6.4.4 SDS concentration

Surfactant type plays a crucial role in any MEEKC separation since it influences not only solubility but governs the charge and size of the PSP. The nature of the surfactant effects selectivity through influences in partitioning and ion-pairing with charged analytes. Charged surfactants also contribute to the overall current generated in the capillary and have to be controlled in order to prevent joule heating.

Since SDS is the most commonly reported surfactant in literature [15] its concentration was examined to assess its effect on separation.

Concentration of SDS was varied between 1.92 to 3.50% w/w. Below 1.92% SDS the microemulsion became unstable and failed to form. Also baseline noise increased with a reduction in surfactant. Increasing SDS concentration had little effect on the

migration times or separation of the water-soluble vitamins. A slight increase in the migration time of the positively charged vitamins (B<sub>1</sub> and B<sub>2</sub>) was noted due to a possible increase in interaction with the ME droplet. With respect to the oil-soluble vitamins an increase in SDS concentration resulted in longer migration times but no improvement in separation. The increase in migration times could be attributed to the increase in the negative charge density on the ME droplet resulting in a greater mobility towards the anode. Separation of the water soluble vitamins was slightly better at 2.72% w/w SDS. Figure 6.14 and figure 6.15 graph the effect of SDS concentration on migration time. Yin et al [5] reported that a low concentration of SDS (1.2 g) achieved the best separation for a range of 13 water- and oil-soluble vitamins. However, the authors also noted that the microemulsion disintegrated at SDS concentrations below 3.3 g and a large concentration (21% v/v) of butanol was required to stabilise the system.

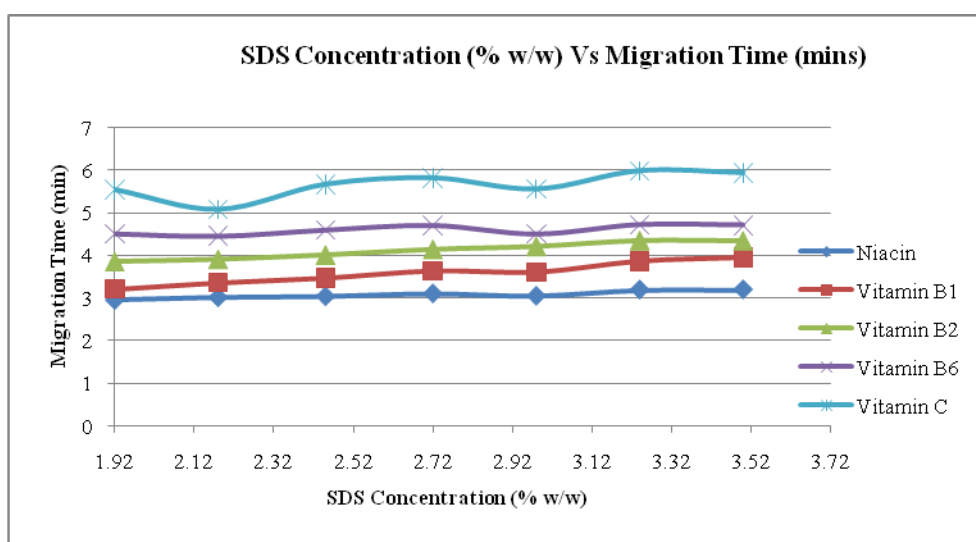


**Figure 6.14** Variation in the migration time of the water-soluble vitamins with changes in SDS concentration. Buffer: Various concentrations of SDS, 5.97% w/w 1-butanol, 0.72% w/w 2-octanol and 90.33% w/w 10mm sodium borate buffer (pH 9.2). Separation conditions; 50  $\mu$ M ID fused silica capillary length 35 cm, detection window at 26.5 cm, flush for 3 minute with 0.1 M NaOH followed by 3 minutes with water and 3 minutes with microemulsion capillary cassette temperature 20° C, applied voltage 16 kV, sample injection 10 mbar for 10 seconds, UV detection at 267 nm.

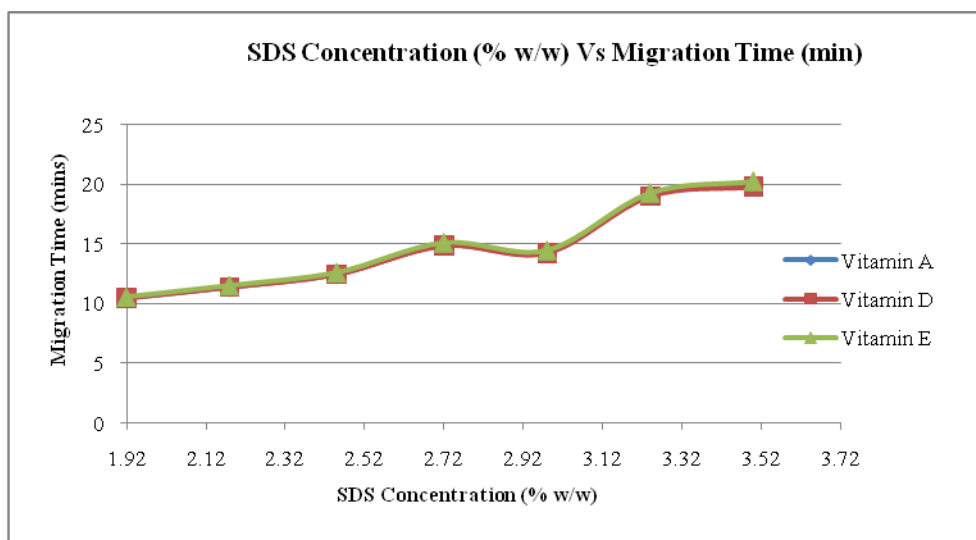


**Figure 6.15** Variation in the migration time of the oil-soluble vitamins with changes in SDS concentration. Conditions as in figure 6.14.

#### 6.4.5 Addition of organic modifiers

Addition of organic modifiers can affect the charge density and size of the ME droplet. This can play a crucial role in optimising the interaction between charged analytes and the ME droplet, thus influencing selectivity. Also, the addition of modifiers can change the viscosity of the buffer and affect the EOF. The addition of an organic modifier (also termed secondary co-surfactant) has been commonly reported for the successful separation of oil-soluble vitamins [4;5;13;16]. Bustamante-Rangel et al. [4] achieved full separation of A, D, and  $\alpha$ -tocopherols with the addition of 1-propanol and methanol to the ME buffer. Addition of 1-propanol (15% v/v) has also been reported for the separation of vitamins A, D and E [13] under suppressed EOF. A superior separation of oil-soluble vitamins (A, D, E and K) was also reported with the use of 15% v/v 2-propanol [1]. Yin et al [5] noted full baseline separation for a mixture of 13 vitamins was only achieved with the addition of 18 % v/v acetonitrile to the ME buffer. With respect to water-soluble vitamins the addition of a modifier was not necessary to achieve baseline separation [13;17;18]. However, in all cases it was noted that the addition of a modifier resulted in a longer migration time for all vitamins due to its effect on EOF and electrophoretic mobility.

In this experiment acetonitrile, 2-propanol and methanol were examined as organic modifiers in the concentration range 5, 10 and 15% v/v. The modifiers had a marked effect on the separation. Addition of each modifier at 5, 10 and 15% v/v increased the migration time of all vitamins with increasing resolution observed between B<sub>1</sub>, B<sub>2</sub> B<sub>6</sub>

and C. Importantly the addition of ACN or IPA increased the separation between vitamin A and E, however at all concentrations vitamins A and D co-migrated. Figures 6.16/6.17 and figures 6.18/6.19 graph the effect of ACN and IPA on vitamin migration times respectively.

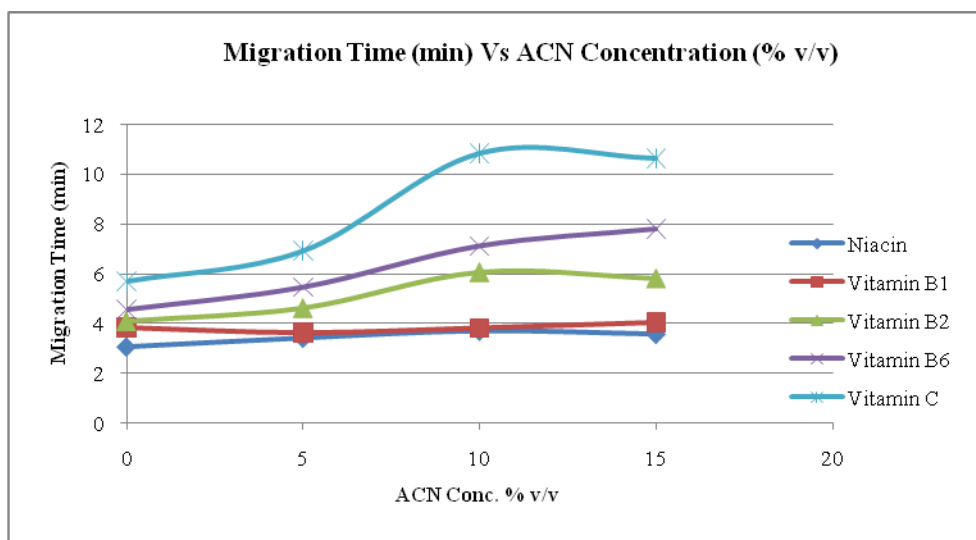


**Figure 6.16** Variation in the migration time of the water-soluble vitamins with the addition of 5, 10 and 15% v/v ACN to the microemulsion buffer. Buffer: 2.72% w/w SDS, 5.97% w/w 1-butanol, 0.72% 2-octanol and 90.58% w/w 10mM sodium tetraborate buffer (pH 9.2). Separation conditions; 50  $\mu$ M ID fused silica capillary length 35 cm, detection window at 26.5 cm, flush for 3 minute with 0.1 M NaOH followed by 3 minutes with water and 3 minutes with microemulsion capillary cassette temperature 20° C, applied voltage 16 kV, sample injection 10 mbar for 10 seconds, UV detection at 267 nm.

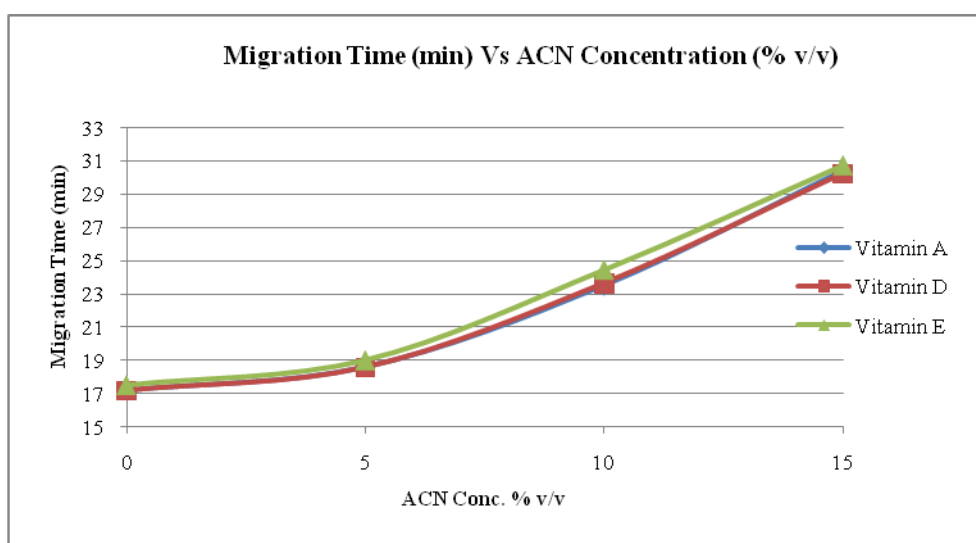


**Figure 6.17** Variation in the migration time of the oil-soluble vitamins with the addition of 5, 10 and 15% v/v ACN. Conditions as in figure 6.16.

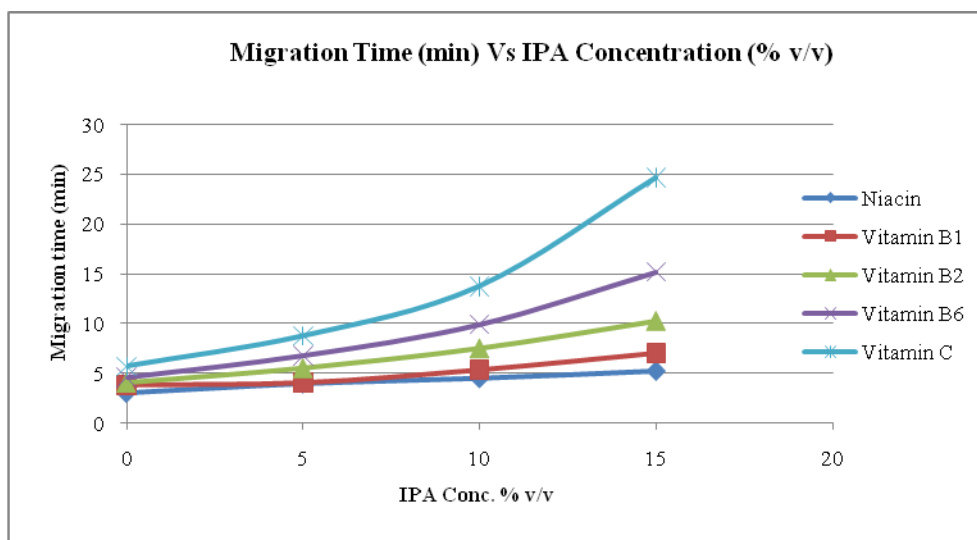


**Figure 6.18** Variation in the migration time of the water-soluble vitamins with the addition of 5, 10 and 15% v/v IPA. Conditions as in figure 6.16 except ACN was replaced with IPA.

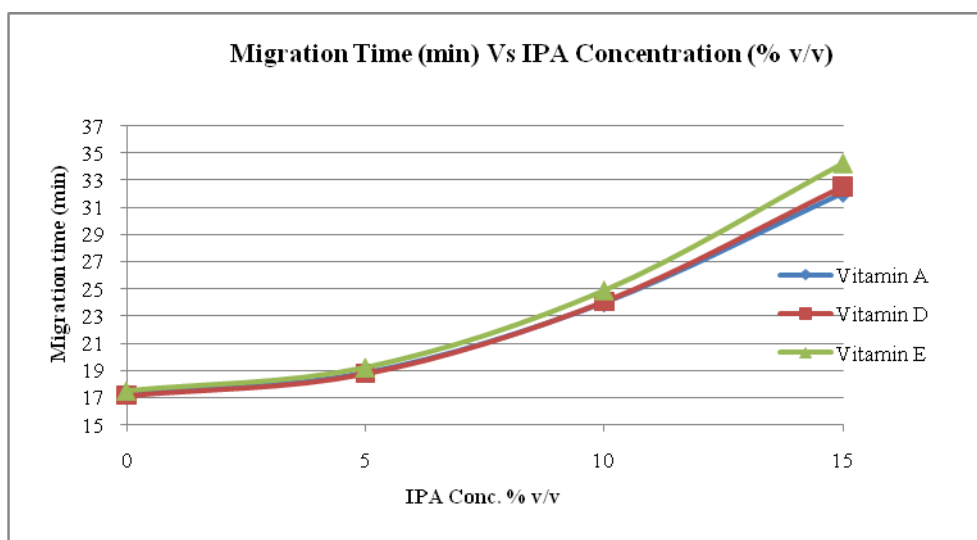


**Figure 6.19** Variation in the migration time of the oil-soluble vitamins with the addition of 5, 10 and 15% v/v IPA. Conditions as in figure 6.16 except ACN was replaced with IPA.

It has been reported that the addition of organic modifiers has an effect on both the EOF and analyte electrophoretic mobility in addition to analyte partitioning with the PSP [18]. The effect on EOF has been attributed to the increase in ME viscosity along with the fall in potential on the capillary wall. ACN, being less viscous than either the ME buffer or IPA was thought to have lowered the viscosity of the buffer while also reducing the EOF. Conversely IPA was more viscous and therefore increased both the viscosity and reduced the EOF. Figure 6.16 demonstrates the competing forces with respect to the water-soluble vitamins and the addition of ACN. Niacin, being water-soluble and neutral was taken to act as an indicator of EOF. It was seen that the

addition of ACN had little effect in its migration time indicating that any reduction in EOF was compensated for by the overall reduction in buffer viscosity. Conversely the addition of IPA resulted in a more linear increase in the migration time of niacin indicating any fall of in EOF was compounded by the increase in buffer viscosity. While both graphs demonstrate an increase in migration time for the addition of either ACN or IPA, there were some noticeable differences with regard to the water-soluble vitamins. Overall the addition of IPA resulted in much longer migration times compared to ACN. Also there is a clear difference in the behaviour of the charged analytes. For the addition of either IPA or ACN the negatively charged analytes (B<sub>6</sub> and C) experienced the most remarkable increase in migration time. Since these analytes possessed a negative charge at pH 9.2, it was expected that they would have had little interaction with the anionic ME droplet and their increase in migration time was based on changes in their electrophoretic mobility and the EOF.

With respect to the oil soluble vitamins, there was a similar increase in migration times with the addition of either ACN or IPA. This result indicated that both modifiers affected the electrophoretic mobility of the ME droplet to a similar degree. Interestingly an increase in resolution between E and the A/D pair was noted with the addition of IPA. It was apparent that IPA, having a higher hydrophobicity than ACN may have increased the rate of mass transfer between the aqueous buffer and ME droplet.

#### **6.4.6 Addition of mixed modifiers**

Since the addition of organic modifiers improved the separation of the oil-soluble vitamins and it was previously reported that the addition of more than one modifier was required for full separation [4], ACN and IPA were added to the buffer. 10 % v/v ACN and 10 % v/v IPA were added to the ME buffer. As with the addition of single modifiers, migration times increased and full separation of oil-soluble vitamins was observed. Unfortunately, these separations were not reproducible. It was possible that the addition of modifiers above a certain level caused instability in the microemulsion system.

#### **6.4.7 Addition of $\alpha$ -CD**

Cyclodextrins have been used in MEEKC for the separation of oil-soluble vitamins [1;19]. Addition of CDs to the ME buffer create a secondary PSP and modify the distribution of analytes between the aqueous and ME droplet through inclusion complexes with the CD cavity. In this study the ME buffer was prepared with 10 mM  $\alpha$ -CD and its effect on separation assessed. The addition of  $\alpha$ -CD slightly increased the migration time of all vitamins but had no dramatic effect on separation, particularly between vitamins A and D. It was possible that the  $\alpha$ -CD cavity was too small to incorporate A or D and therefore did not induce adequate selectivity. Similar results were reported by Delgado-Zamarreno et al. [1], where the addition of CD was not seen to improve resolution.

#### **6.4.8 Surfactant type**

The use of various surfactant types was investigated in order to change the nature of the ME droplet and assess its effect on vitamin separation. Surfactants examined included sodium cholate (anionic), CTAB (cationic) and a mixture of SDS and SC.

##### **6.4.8.1 Sodium cholate**

A sodium cholate (SC) ME was prepared by replacing SDS with an equimolar (10.4 mmols) quantity of SC (4.47 g). However, 15.56 mmols (6.7 g) of SC was the minimum required to form the ME. The SC ME provided excellent separation of the water soluble vitamins when compared to SDS and the overall run time was five minutes faster. Since SC is an anionic surfactant no change in the migration order of the vitamins was observed. As with the SDS ME vitamins A and D co-migrated. Interestingly, the SC ME provided better separation between D and E. Furthermore the negatively charged vitamin B<sub>6</sub> and vitamin C showed a large increase in migration time although they were not expected to partition with the SC ME droplet. The shape of the SC molecule, which is based around three fused cyclohexane rings and has a larger molecular volume than the C12 alkyl chain of SDS, may explain these results. The SC ME droplet may have had a larger organic core and a reduced anionic charge, due to its bulky structure and the negative ions remaining further apart. The larger droplet size would have allowed greater partitioning of the oil-soluble vitamins and the reduced anionic charge would have resulted in less opposition to the EOF, thus reducing the overall migration time. The negatively charged water-soluble vitamins would continue

to migrate towards the anode under their own charge. The SC ME had a poorer baseline than the corresponding SDS ME. This may have been due to the amount of surfactant in the system and increasing the amount of sodium cholate may improve the baseline resolution. Figure 6.20 shows the separation achieved using the SC ME.

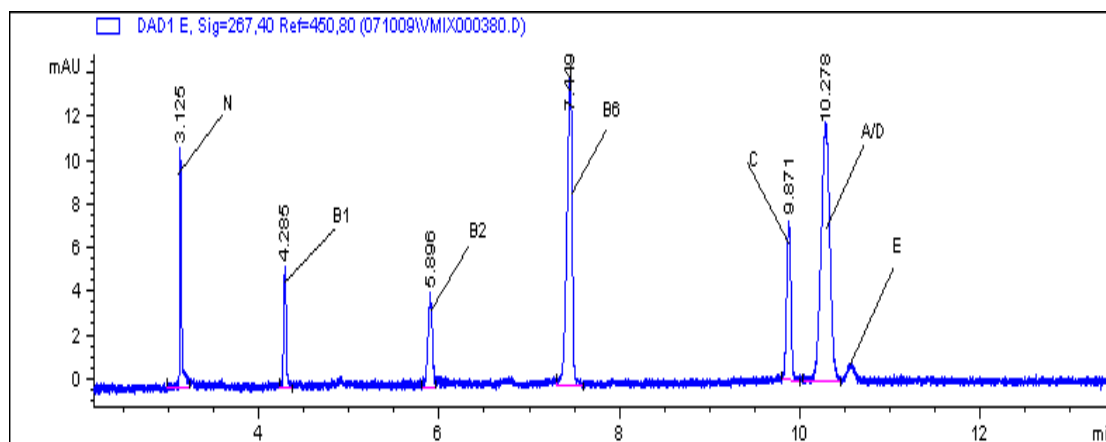


**Figure 6.20** Electropherogram of vitamin separation. Buffer: 5.68% w/w SC, 5.80% w/w 1-butanol, 0.70% w/w 2-octanol and 87.82% w/w 10mm sodium borate buffer (pH 9.2). All other conditions as in figure 6.16.

#### 6.4.8.2 Mixed surfactant system

Combining SDS and SC resulted in all vitamins migrating within 10 minutes. While all water soluble vitamins were separated, oil soluble vitamins A and D continued to co-migrate. In comparison to the SDS ME the migration times of the oil-soluble vitamins was decreased while the migration time of the water-soluble vitamins was increased.

#### 6.4.8.3 CTAB

SDS was replaced with an equi-molar quantity of the cationic surfactant CTAB. The polarity of the applied voltage was reversed to -16 kV and under the standard conditions all vitamins eluted in less than seven minutes. A change in migration order was noted for the water soluble vitamins with the negatively charged vitamins (C and B<sub>6</sub>) migrating ahead of neutral niacin, and then followed by the positively charged B<sub>2</sub> and B<sub>1</sub>. Apart from the neutral niacin the migration order was an exact reversal of that obtained using the SDS ME. No separation was observed for the oil soluble vitamins. Figure 6.21 shows an electropherogram of the separation achieved with the CTAB ME.

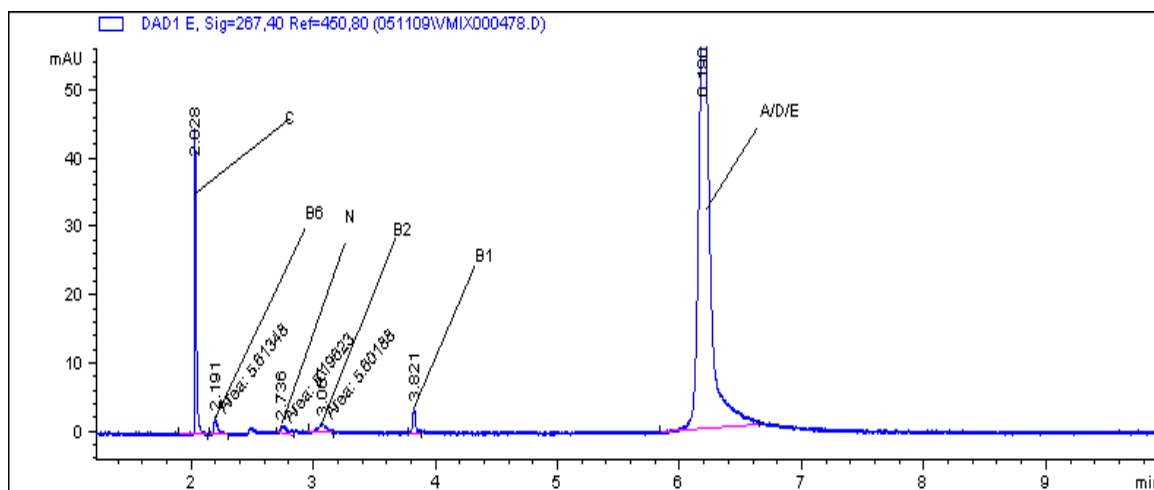


**Figure 6.21** Electropherogram of vitamin separation. Buffer: 3.41% w/w CTAB, 5.93% w/w 1-butanol, 0.72% w/w 2-octanol and 89.94% w/w 10mM sodium tetraborate buffer (pH 9.2). Applied voltage -16 kV and all other conditions as in Figure 6.16.

#### 6.4.8.4 CTAB microemulsion with addition of organic modifiers

Addition of 2-propanol/acetonitrile mixtures to the ME buffer had little effect on the water soluble vitamins and increased the migration time of the oil soluble vitamins. Full separation was achieved for the oil soluble vitamins with 15% ACN + 15% IPA. Unfortunately, similar to the addition of mixed organic modifiers to the SDS ME separations were irreproducible.

#### 6.4.8.5 Sodium cholate microemulsion with the addition of organic modifiers

Modifying the SC ME with the addition of 5, 10 and 15 % v/v IPA resulted in similar trends to those observed with the SDS ME. An increase in migration time was noted for all vitamins with the exception of the neutral niacin. However there were some notable differences between modifying both microemulsion types. A dramatic increase in migration time and change in selectivity was observed for the negatively charged vitamins B<sub>6</sub> and C. At 10% v/v IPA vitamin B<sub>6</sub> migrated just before the oil soluble vitamins A, D and E with vitamin C migrating after the oil soluble vitamins. This trend became even more pronounced at 15% v/v IPA where vitamin B<sub>6</sub> migrated after the oil soluble analytes and vitamin C was undetected. With respect to separation, all water soluble vitamins remained well resolved from each other at all IPA concentrations with an increasing migration window. Vitamin C migrated close to vitamin A at 5% IPA, while vitamin B<sub>6</sub> co-migrated with vitamin A at 10% IPA. A slight increase in separation was observed between the oil soluble vitamin E and the A/D pair with increasing IPA concentration. Similar to the SDS microemulsion it seemed apparent

that addition of IPA had the most pronounced effect on electrophoretic mobility of the negatively charged water soluble vitamins. Figure 6.22 graphs the effect of increasing IPA concentration on the migration time of vitamins.

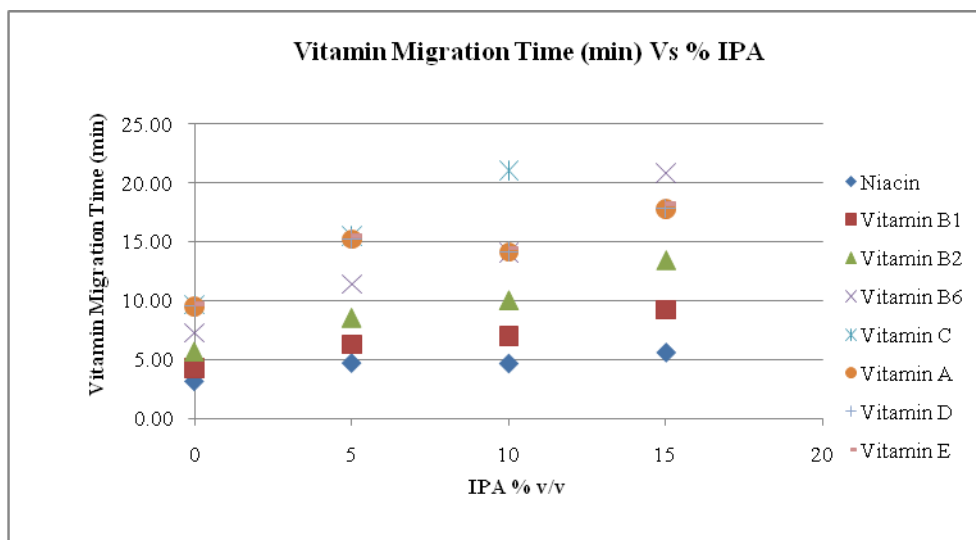


**Figure 6.22** Variation in the migration time of vitamins with the addition of 5, 10 and 15% v/v IPA to running buffer. Buffer: 5.68% w/w SC, 5.89% w/w butanol, 0.70% w/w 2-octanol and 87.82% w/w 10mm sodium borate buffer (pH 9.2).

#### 6.4.8.6 Sodium cholate ME with increased butanol concentration

Since addition of IPA to the SC ME did not contribute to the separation of vitamins A and D it was decided to use higher concentrations of co-surfactant. It has been reported that an increased concentration of co-surfactant may swell the ME droplet [5], thereby allowing greater mass transfer between analytes. The butanol concentration was increased from 5.80% w/w (6.6 g) to 10.85% (13.2 g). However, the ME did not form at this concentration. In order to facilitate the highest concentration of co-surfactant and therefore larger droplets, a minimum amount (0.99% w/w (1.2 g)) of SDS was added to form the microemulsion. In comparison to the standard SC ME an increase in migration time was observed for all vitamins, and while a slight increase in separation between the E and the A/D pair was seen no further discrimination between A and D was achieved.

A further increase in butanol from 10.85% w/w (13.2 g) to 15.44% w/w (19.8 g) was examined. Further SDS did not have to be added to form the microemulsion. Similar results were obtained and no further separation was observed between the oil-soluble vitamins. However, vitamin C was better resolved from the oil soluble vitamins and

migrated after vitamin E. From these experiments it was concluded that while increasing the co-surfactant concentration may have swelled the microemulsion droplet no improvement in discrimination between A and D was realised. The change in migration order for vitamin C may have been the result of a similar mechanism seen with the addition of organic modifiers, i.e. a change in the vitamin's electrophoretic mobility rather than a significant change in the interaction with the microemulsion droplet.

#### **6.4.8.7 Sodium cholate ME with increased butanol and addition of organic modifiers**

As previously reported in the literature, the addition of organic modifiers to the microemulsion was examined. Since the ME containing 5.04% w/w (6.47 g) SC, 0.93% w/w SDS, 0.62% w/w 2-octanol and 15.44% w/w 1-butanol and 77.96% w/w 10 mM sodium tetraborate buffer gave the greatest degree of separation, it was modified with 10 % v/v IPA and ACN respectively.

As seen with the addition of IPA or ACN to other microemulsions mentioned in this chapter, an increase in migration time for all vitamins was observed. Similar to the SDS based buffers, IPA resulted in a greater increase in migration time for the water-soluble vitamins. However, the addition of 10% ACN in this case caused a slightly greater increase in the migration time of the oil-soluble vitamins and more importantly resulted in a repeatable separation between A, D and E. Unfortunately the addition of either modifier resulted in a failure of vitamin C to be detected, even after 120 minutes. It may have been possible that changes to the electrolyte resulted in the EOF not being strong enough to sweep the vitamin towards the cathode and through the detector. Alternatively, the vitamin may have degraded in the capillary when in a basic pH for a prolonged amount of time. Figure 6.23 shows an electropherogram of the separation achieved with the addition of 10% ACN.

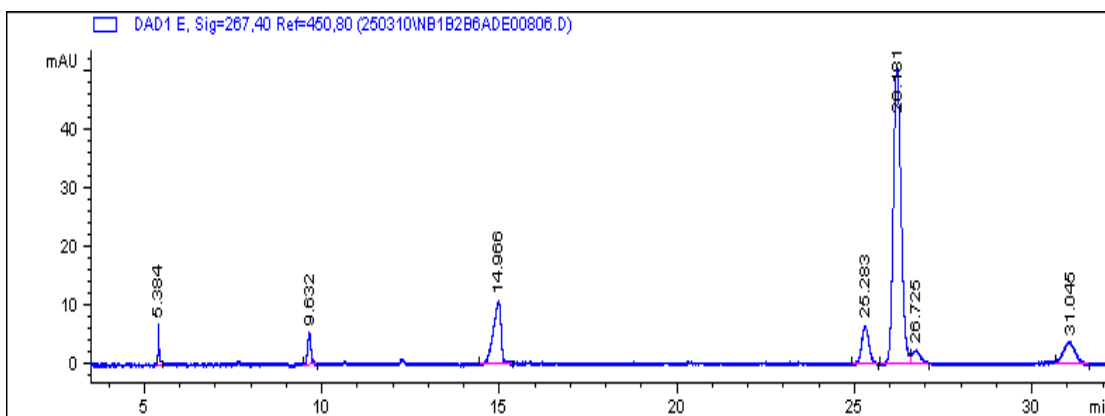


**Figure 6.23** Electropherogram of vitamin separation. Buffer: 5.04% w/w SC, 0.93% w/w SDS 15.44% w/w 1-butanol, 0.62% w/w 2-octanol and 77.96% w/w 10 mM sodium tetraborate buffer pH 9.2 with addition of 10 % v/v ACN. All other conditions as in Figure 6.15.

## 6.5 Conclusion

A microemulsion composed of 5.04% w/w SC, 0.93% w/w SDS 15.44% w/w 1-butanol, 0.62% w/w 2-octanol and 77.96% w/w 10 mM sodium tetraborate buffer pH 9.2 with addition of 10 % v/v ACN was developed for the simultaneous separation of oil- and water-soluble vitamins. With the exception of vitamin C all analytes were baseline separated with good peak shape within 31 minutes.

There was a clear compromise between optimising the microemulsion for either vitamin set and creating a microemulsion capable of separating both vitamin types. From the results it could be seen that the use of SC as the surfactant played a crucial role in improving the separation of the water-soluble vitamins. All water-soluble vitamins were well resolved in less than ten minutes without the addition of modifiers. Separation was five minutes longer when compared to the SDS based ME; however the increased separation window and greater resolution would prove beneficial when applied to a vitamin preparation. The addition of organic modifiers to either SDS or SC based MEs served only to increase separation at the expense of longer migration times; no change in selectivity was noted.

With respect to the oil/soluble vitamins, separation of E from either A or D was readily achieved, possibly due to the large difference in log P. However separation of vitamins A and D proved extremely difficult. It was worth noting only three reports have been published in MEEKC reporting the separation of vitamin A and D along with other water-soluble vitamins [5;13;16]. Separation of the oil-soluble vitamins required a relatively high organic content (15.44% w/w 1-butanol, 0.62% w/w 2-octanol and 10% v/v ACN). It was noted that separation could not just be achieved with high

concentrations of organic modifiers. SDS based microemulsion with up to 30 % IPA and ACN failed to give an acceptable separation. Also, it was seen that simply swelling the microemulsion with co-surfactant did not seem to increase the analyte partitioning with the droplet. It was clear that choice and concentration of surfactant, co-surfactant and type of modifier was important. The increased organic content of the ME would also prove useful for extracting and solubilising oil-soluble vitamins in real samples.

## 6.6 References

- [1] Delgado-Zamarreno, M.M., Gonzalez-Maza, I., Sanchez-Perez, A. and Carabias-Martinez, R., *Journal of Chromatography A*, 953 (2002) 257-262.
- [2] Gong, S., Liu, F., Li, W., Gao, F., Gao, C., Liao, Y. and Lui, H., *Journal of Chromatography A*, 1121 (2006) 274-279.
- [3] Okamoto, H., Nakajima, T. and Ito, Y., *Journal of Pharmaceutical and Biomedical Analysis*, 30 (2002) 815-822.
- [4] Bustamante-Rangel, M., Delgado-Zamarreno, M.M., Sanchez-Perez, A. and Carabias-Martinez, R., *Journal of Chromatography A*, 1125 (2006) 270-273.
- [5] Yin, C., Cao, Y., Ding, S. and Wang, Y., *Journal of Chromatography A*, 1193 (2008) 172-177.
- [6] McEvoy, E., Donegan, S., Power, J. and Altria, K.D., *Chromatographia*, 68 (2008) 56-59.
- [7] Marsh, A., Clark, B. and Altria, K., *Chromatographia*, 59 (2004) 531-542.
- [8] Marsh, A., Clark, B.J. and Altria, K.D., *Chromatographia*, 61 (2005) 539-547.
- [9] McEvoy, E., Donegan, S., Power, J. and Altria, K., *Journal of Pharmaceutical and Biomedical Analysis*, 44 (2007) 137-143.
- [10] Cheng, T.J., Zhao, Y., Li, X., Lin, F., Xu, Y., Zhang, X.L., Li, Y., Wang, R.X. and Lai, L.H., *Journal of Chemical Information and Modelling*, 47 (2007) 2140-2148.

- [11] Klejdus, B., Petrlova, J., Potesil, D., Adam, V., Mikelova, R., Vacek, J., Kizek, R. and Kuban, V., *Analytica Chimica Acta*, 520 (2004) 57-67.
- [12] Monferrer-Pons, L., Capella-Peiro, M.E., Gil-Agusti, M. and Esteve-Romero, J., *Journal of Chromatography A*, 984 (2003) 223-231.
- [13] Sanchez, J.M. and Salvado, V., *Journal of Chromatography A*, 950 (2002) 241-247.
- [14] Gabel-Jensen, C., Hansen, S.H. and Pedersen-Bjergaard, S., *Electrophoresis*, 22 (2001) 1330-1336.
- [15] Ryan, R., Donegan, S., Power, J., McEvoy, E. and Altria, K., *Electrophoresis*, 30 (2008) 65-82.
- [16] Svidritskii, E.P., Pashkova, E.B., Pirogov, A.V. and Shpigun, O.A., *Journal of Analytical Chemistry*, 65 (2009) 292-287.
- [17] Hu, Q., Zhou, T., Zhang, L., Li, H. and Fang, Y., *Analytica Chimica Acta*, 437 (2001) 125-129.
- [18] Schreiner, M., Razzazi, E. and Luf, W., *Food*, 47 (2003) 243-247.
- [19] Chang, L.C., Chang, H.T. and Sun, S.W., *Journal of Chromatography A*, 1110 (2006) 227-234.

## **Chapter Seven**

### **Characterisation of microemulsions for the MEEKC separation of oil-and water-soluble vitamins**

## **7.1 Introduction**

Throughout the many reported separations utilising CE and microemulsions as the background electrolytes [1], few papers have correlated changes in composition with microemulsion microstructure and effect on separation [2,3].

Cao et al. [2] characterised a microemulsion consisting of a 3.3% (w/v) SDS, 6.6% (w/v) 1-butanol and 0.8% (w/v) n-octane in 50 ml of 10 mM borate buffer (pH 9.2). The authors varied the concentration of each microemulsion component in a one-factor effect experiment and assessed the droplet size and zeta potential of the resultant system. The group also referenced their results to the separation of oil soluble vitamins (A and E) and to a previously reported successful analysis of water- and oil soluble vitamins [4].

The only other work relating microemulsion structure to chromatography was a microemulsion liquid chromatography (MELC) separation reported by Andelija et al. [3]. The group calculated the predicted droplet radii, area per surfactant, film thickness and bending moment for various microemulsion compositions used in the separation of simvastatin and its related substances. The starting microemulsion composition was 2% (w/w) SDS, 6.6% (w/w) 1-butanol, 1% (w/w) diisopropyl ether and 90.4% 25 mM disodium phosphate buffer (pH 7.0).

Chapter four gave an account of the many characterisation tools available to investigate the influences of composition on microstructure. The aim of this chapter was to assess a range of microemulsion compositions utilised in developing the MEEKC vitamin separation in chapter six. Microemulsions were examined by performing measurements on; conductivity, surface tension, refractive index, and droplet size.

In all cases the results were compared to the respective vitamin separations obtained in chapter six and an attempt was made to rationalise any correlations.

## **7.2 Experimental**

### **7.2.1 Microemulsion components**

HPLC grade water, n-octane, sodium tetraborate, 1-butanol (all Romil) and 99% sodium dodecyl sulphate (SDS), sodium cholate (SC), cetyltrimethylammonium bromide (CTAB) and sodium tetraborate were obtained from Lennox Laboratory Supplies (Ireland). 2-octanol, 1-pentanol, hexane, nonane, dodecane, 1-propanol, 2-propanol and methanol were also obtained from Lennox.

## **7.2.2 Microemulsion preparation**

The standard microemulsion was prepared by mixing 3.3 g of SDS, 6.6 g of 1-butanol, and 8 g of n-octane in a 200 ml duran bottle. This mixture was stirred for 10 minutes using a magnetic stirrer to ensure a homogenous solution was formed. 100 mL of 10 mM sodium borate pH 9.2 was then added, sonicated for 30 minutes and filtered.

### **7.2.2.1 Variation of oil phase type**

In order to assess the effect of oil phase type equal weight % (0.72% w/w) of 1-pentanol, 2-octanol, hexane and dodecane were examined in place of n-octane. The separation was also carried out in modified MEKC mode with no oil phase present and by traditional MEKC, with neither oil nor co-surfactant. 2-Octanol was chosen as the optimum oil phase.

### **7.2.2.2 Variation of co-surfactant type**

1-butanol was replaced with equal weight % (5.96% w/w) of 1-pentanol and 1-propanol to assess the effect of co-surfactant hydrophobicity on the separation of vitamins. 1-butanol proved to be the optimum co-surfactant.

### **7.2.2.3 Variation of SDS concentration**

The concentration of SDS was varied between 1.92 and 3.50% w/w. 2.73% w/w of SDS was found to provide the best separation and this concentration was fixed for the remainder of the study.

### **7.2.2.4 Co-surfactant concentration**

Since the co-surfactant appeared to have the most significant effect on separation, the concentration of 1-butanol was varied from 5.46 to 6.48% w/w. The initial concentration of 5.96% w/w was held constant for the remainder of the study.

### **7.2.2.5 Addition of organic modifiers**

Acetonitrile, 1-propanol and methanol were examined as organic modifiers in the concentration ranges 5, 10 and 15% v/v. Also the addition of mixed modifiers was examined. Equal amounts of 1-propanol and acetonitrile were added in the concentration ranges 5, 10, 15, 20 and 30% v/v.

### **7.2.2.6 Variation of surfactant type**

An alternative type of anionic surfactant was examined by replacing SDS with an equimolar (10.4 mmols) concentration of sodium cholate (4.47 g). The separation was also performed utilising the cationic surfactant CTAB in an equimolar concentration (3.79 g).

### **7.2.2.7 Mixed surfactant system**

The influence of a mixed surfactant system was studied by preparing a microemulsion consisting of 1.35% w/w SDS and 2.01% w/w SC. The overall molar concentration was kept constant.

## **7.2.3 Instrumentation**

### **7.2.3.1 Droplet Size**

Droplet size measurements were performed on Malvern DTS dynamic light scattering nanosizer, equipped with a temperature controlled sample compartment, a helium-neon laser at 632.8 nm and an optical detector. The intensity of scattered light was measured at an angle of  $178^\circ$ . Data was analysed using Malvern zetasizer software, version 6.01. Approximately 3 mL of microemulsion sample was placed in a quartz cuvette. The cuvette was placed in the sample compartment and allowed to equilibrate at  $25^\circ\text{C}$  before the measurement was performed. All measurements were carried out in triplicate. The RSD for all measurements was less than 5%. The polydispersion index (PDI) for all measurements was less than 0.2 indicating relatively monodisperse systems.

### **7.2.3.2 Conductivity**

Conductivity measurements were performed using a bench-top WTW LF538 dual pH/conductivity meter.

### **7.2.3.3 Surface Tension**

Surface tension measurements were performed on a Kruss G10 contact angle/surface tension meter, equipped with a stage, syringe and camera. Calculations were performed based on the shape of a hanging pendent drop according to the Young-Laplace equation using DSA 10.1 software. Measurements were conducted in triplicate. The RSD of all measurements was less than 3%.

#### **7.2.3.4 Refractive Index**

Refractive index measurements were carried out using a Bellingham Stanley RFM340 refractometer.

All refractive index measurements had an RSD less than 0.1%. The refractive index of all systems showed little variation with values of approximately 1.34.

### **7.3 Results and discussion**

#### **7.3.1 Variation of oil phase type**

##### **7.3.1.1 Surface tension**

A slight difference in surface tension was obtained with variation in oil phase type. The three alkane oils resulted in a similar surface tension of approximately 29 dynes  $\text{cm}^{-1}$ . When the alkanes were replaced by the alcohols, a drop in surface tension was recorded. 2-octanol and 1-pentanol gave surface tensions of 26.1 and 27.1 dynes  $\text{cm}^{-1}$  respectively. Apparently, the alcohols with their lower interfacial tension allowed an overall reduction in surface tension. The modified MEEKC system in which no oil was present had a surface tension of 28.85 dynes  $\text{cm}^{-1}$  which was closer to the alkane MEs than the alcohol MEs. Interestingly, the MEKC composition had a surface tension of 34 dynes  $\text{cm}^{-1}$  which was considerably higher than either the MEEKC or modified MEKC system. The MEKC result indicated that the co-surfactant (1-butanol) played a significant role in lowering interfacial tension. Figure 7.1 shows the effect of oil type on surface tension.

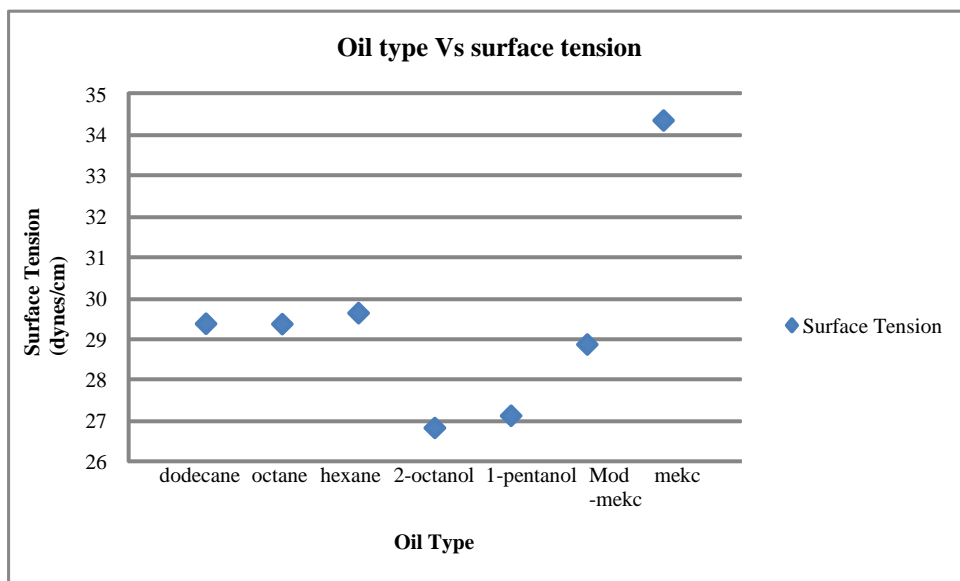


**Figure 7.1** Effect of oil phase type on microemulsion surface tension

### 7.3.1.2 Droplet size

Variation in the type of oil phase resulted in all droplets having a size of approximately 1.5 nm with two significant exceptions. Replacing alkanes or 1-pentanol with 2-octanol resulted in a droplet size of 1.8 nm. This increase in droplet size may have been due to the branched nature of the alcohol. Also, the MEKC system had the smallest micelle size of 0.9 nm, which was possibly the result of the surfactant heads residing much closer together due to the absence of co-surfactant. Figure 7.2 shows the effect of oil phase type on droplet size, conductivity and refractive index.

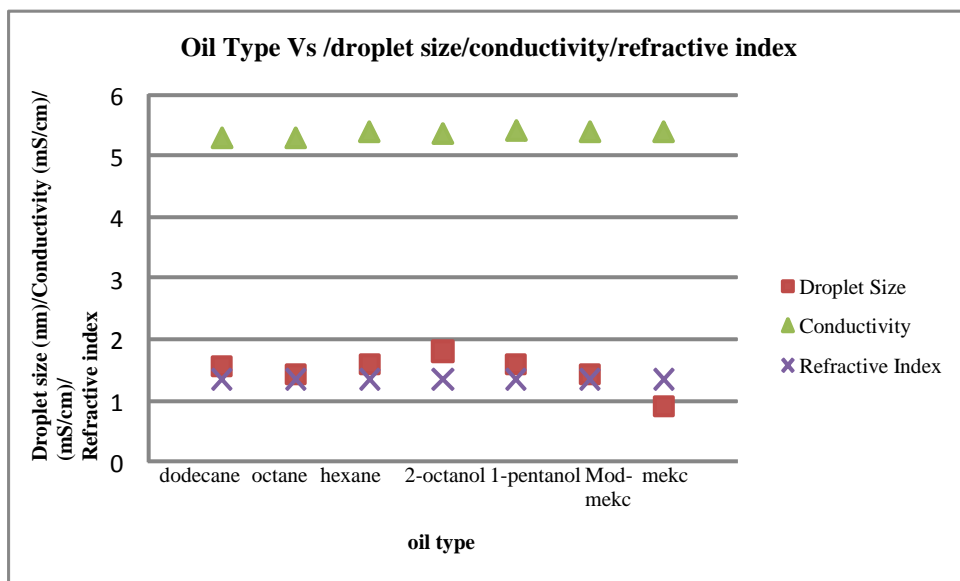


**Figure 7.2** Effect of oil phase type on microemulsion droplet size, conductivity and refractive index

### 7.3.1.3 Conductivity

The overall conductivity of each system was around 5.4 mS/cm and was independent of the type of oil phase employed. This result was expected, as the oil type would not have contributed to the overall charge in the system.

### 7.3.1.4 Correlation with separation

Interestingly the oil phase chosen for further development was 2-octanol, which resulted in the optimum separation and had the largest droplet size. Resolution between the positively charged vitamins ( $B_1$  and  $B_2$ ) was poor when alkanes were employed as the oil phase. The larger droplet may have facilitated a more selective interaction between the positively charged vitamins and ME droplet. However, it may also have been due to interaction with the  $-OH$  group on the alcohol, as 1-pentanol also improved separation between  $B_1$  and  $B_2$ , but did not show a substantial change in droplet size. The dramatic reduction in migration time for the oil soluble vitamins in MEKC mode correlates well with the decreased micelle size which would prove difficult to penetrate and thereby reduce the overall migration window. The presence of co-surfactant and oil resulted in a larger droplet and a larger separation window. No definitive correlation was observed with respect to surface tension, conductivity or refractive index.

## 7.3.2 Variation of co-surfactant type

### 7.3.2.1 Surface tension

Increasing chain length of co-surfactant resulted in a decrease in surface tension from 27.99 to 23.78 dynes  $\text{cm}^{-1}$  respectively. The longer chain length co-surfactants seemed to be more efficient in penetrating the interface between oil and water droplet while the alcohol groups reduced electrostatic attraction between the surfactant head groups. The length of co-surfactant which would be anchored in the organic phase of the oil droplet may have had an influence on how effectively the alcohol group on the co-surfactant positioned itself at the interface and further lowered interfacial tension. It has previously been reported that when the total number of carbons in the co-surfactant and the oil is one carbon greater than the surfactant, an optimally stable microemulsion is formed [5]. Figure 7.3 shows the effect of co-surfactant type on surface tension.

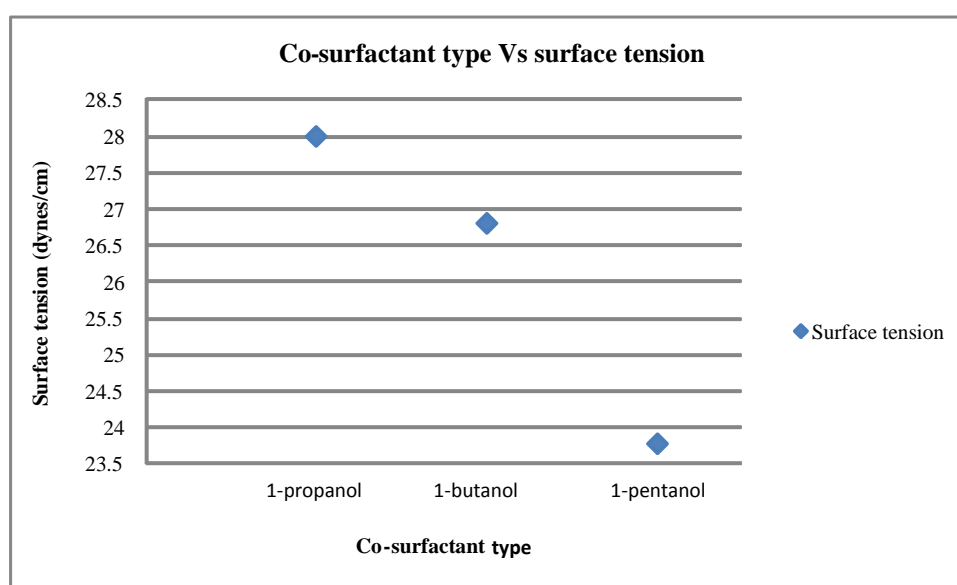
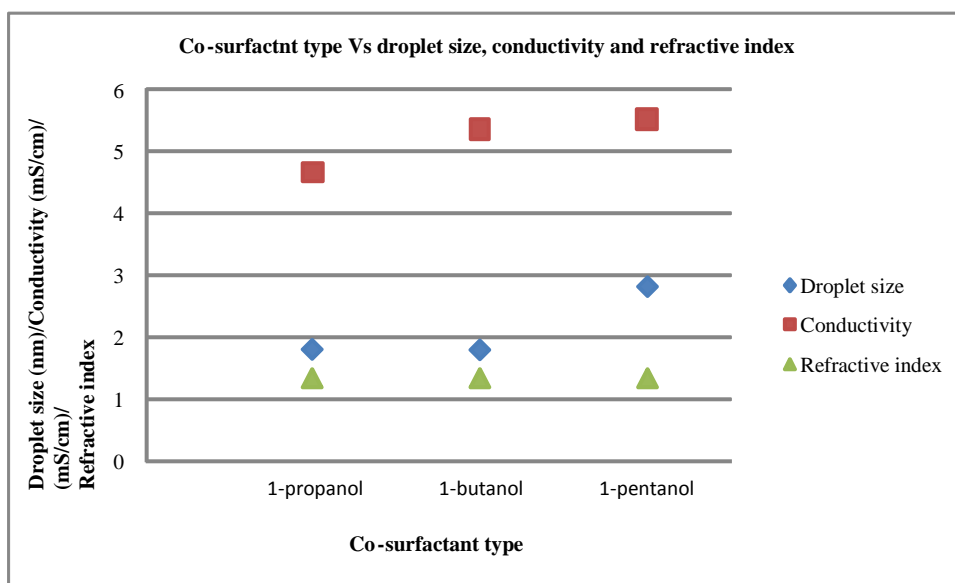


Figure 7.3 Effect of co-surfactant type on microemulsion surface tension

### 7.3.2.3 Droplet size

While microemulsions composed of 1-propanol and 1-butanol had a similar droplet size of 1.8 nm, 1-pentanol resulted in a droplet size of 2.8 nm. This was a relatively large increase and may have been correlated with the positioning of the alcohol mentioned in the surface tension section. The decreased electrostatic charge between the surfactant head groups may have allowed a swelling of the ME droplet. Figure 7.4 shows the effect of co-surfactant type on droplet size, conductivity and refractive index.



**Figure 7.4** Effect of co-surfactant type on droplet size, conductivity and refractive index

### 7.3.2.4 Conductivity

A slight increase from 4.67 to 5.53 mS/cm was observed with increasing co-surfactant chain length. This increase, while small, showed no correlation with droplet size or surface tension.

### 7.3.2.5 Correlation with separation

The type of co-surfactant had a marked effect on the vitamin separation and overall migration window. With respect to migration window, 1-pentanol resulted in all vitamins migrating in around 10 minutes compared to 1-propanol where vitamins A, D and E migrated at approximately 27 minutes. It has previously been stated that the nature of the co-surfactant can affect the charge density on the ME droplet [1,2]. Given the increase in the droplet size for the 1-pentanol ME, compared to 1-propanol and 1-butanol, a decrease in charge density could be expected. This would have resulted in the ME droplet having a decreased electrophoretic mobility towards the anode and hence resulted in a shorter migration window. The shortening of the migration window would also have been responsible for the decreased separation of the water-soluble vitamins, in addition to poorer interaction between the positively charged vitamins and ME droplet. It is also noteworthy that a larger droplet should have allowed greater partitioning with the oil-soluble vitamins which should have improved their separation.

It seems apparent that increasing droplet size and maintaining an appropriate charge on the ME droplet may involve a significant trade-off with respect to co-surfactant type. While an increase in co-surfactant chain length resulted in a decreased surface tension, no significant correlation with the separations was observed.

### 7.3.3 SDS concentration

#### 7.3.3.1 Surface tension

It was seen that for increasing concentrations of SDS, incrementally from 1.92 and 3.50% w/w, an unusual surface tension profile was obtained. While a narrow range of values were obtained between 1.92 and 2.72% w/w (25.4-25.9 dynes  $\text{cm}^{-1}$ ), further increases resulted in an increased surface tension (25.9-26.9 dynes  $\text{cm}^{-1}$ ). Figure 7.5 graphs the effect of SDS on surface tension.

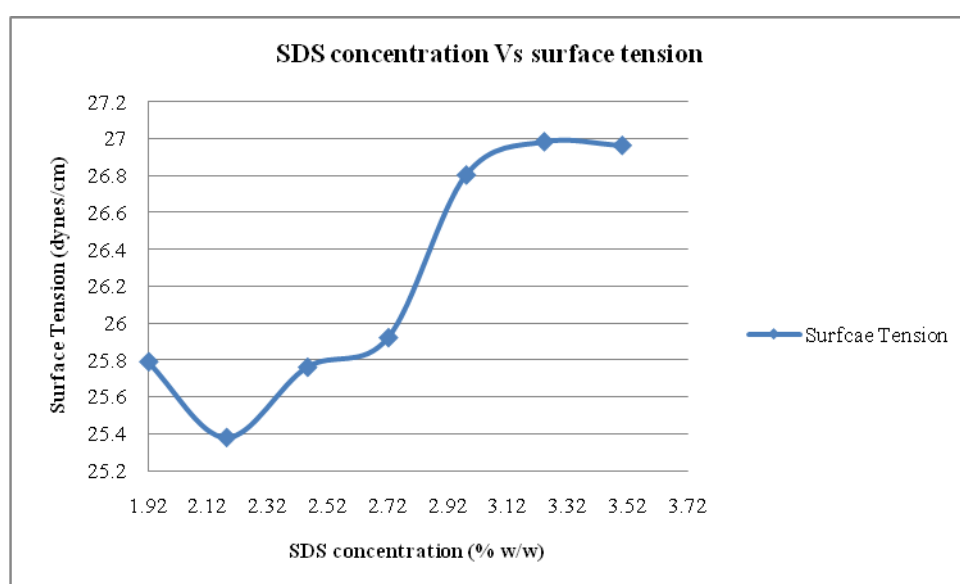


**Figure 7.5** Effect of SDS concentration on microemulsion surface tension

#### 7.3.3.2 Droplet size

For all but one SDS concentration (2.18% w/w) a slightly decreasing droplet size was obtained over the concentration range examined. The decreasing droplet size was most likely due to the dispersion of internal oil phase between greater numbers of ME droplets. The increased concentration of SDS may have directly affected the aggregation number of surfactant molecules at the oil-aqueous interface due to electrostatic repulsion between the head groups. It has been reported in the use of MELC that an increased number of ME droplets results in an increase in separation

efficiency [3]. Figure 7.6 graphs the influence of SDS concentration on droplet size, conductivity and refractive index.

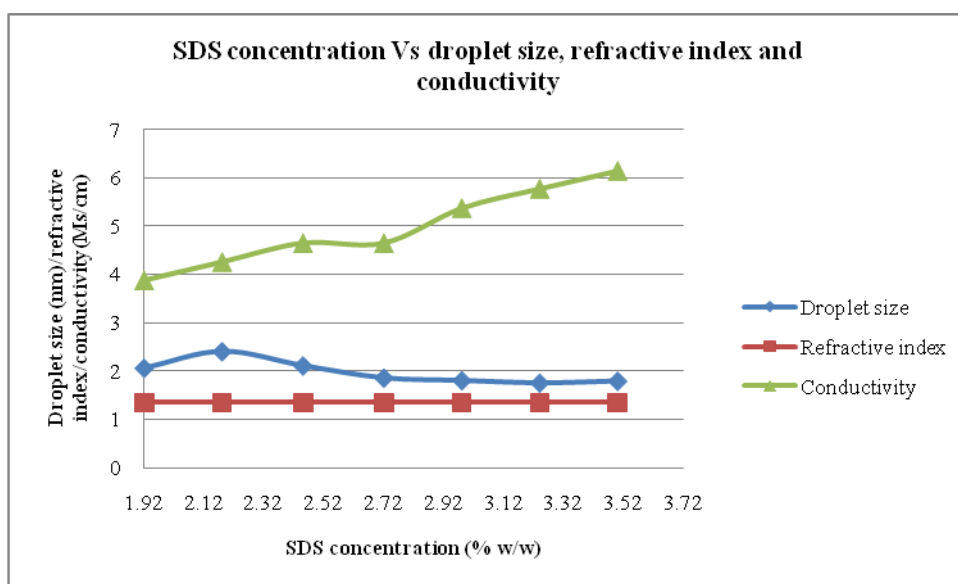


**Figure 7.6** Effect of SDS concentration on droplet size, surface tension and refractive index.

### 7.3.3.3 Conductivity

As expected, a relatively proportional increase in conductivity was noted for increasing concentrations of SDS. During separations this was also accompanied by an increase in current which would facilitate joule heating and above a certain level may have a detrimental effect on separations.

### 7.3.3.4 Correlation with separation

While the level of baseline noise was reduced with an increase in surfactant concentration, this was not reflected by a decrease in the surface tension of each system examined.

Separation of the water soluble-vitamins remained relatively unchanged, with only a slight increase in the migration time of the positively charged vitamins ( $B_1$  and  $B_2$ ). However, the migration time of the oil-soluble vitamins almost doubled when SDS concentration increased from 1.92 to 2.98% w/w. While no improvement in separation was achieved, and the decrease in droplet size was modest (2.06-1.79 nm), results indicated that the oil soluble vitamins were interacting with the ME droplets.

An increase in conductivity corresponded to the increased migration time of the oil-soluble vitamins.

### 7.3.4 Co-surfactant concentration

#### 7.3.4.1 Surface tension

A slight decrease in surface tension from 26.97 to 25.92 dynes  $\text{cm}^{-1}$  was seen when increasing 1-butanol concentration from 5.46 to 6.48% w/w. Further increases in concentration from 5.97 to 6.48% w/w resulted in a slightly higher surface tension of 26.21 dynes  $\text{cm}^{-1}$ . While the presence of a co-surfactant plays an important role in helping to increase the stability of the system, no significant difference in surface tension could be observed in the concentration range examined. Figure 7.7 shows the effect of 1-butanol concentration on surface tension.

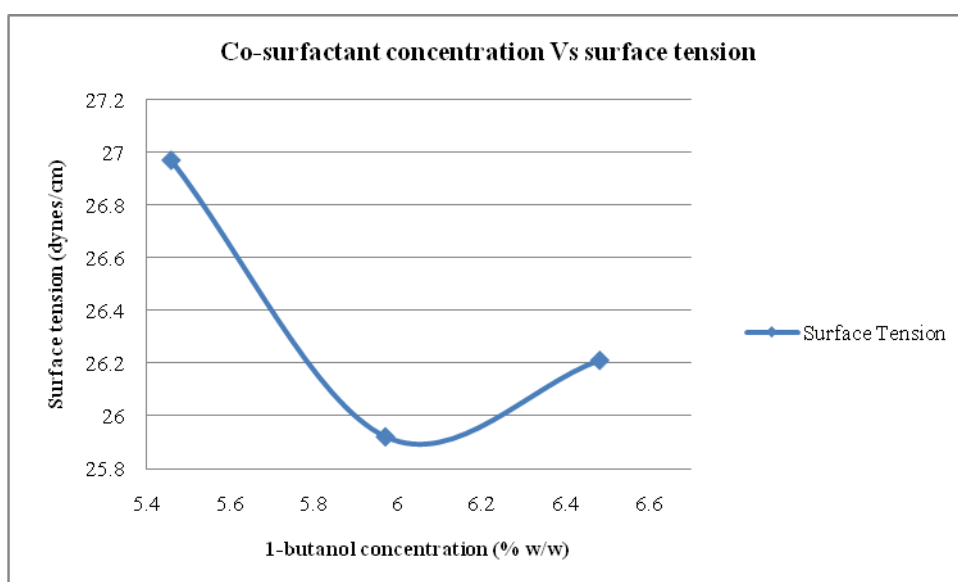


**Figure 7.7** Effect of 1-butanol concentration on surface tension

#### 7.3.4.2 Droplet size

Microemulsion droplet sizes fell within a narrow range for the 1-butanol concentrations examined. However, a slight decrease in droplet size from 1.8 to 1.7 nm was observed when the concentration was reduced from 5.97 to 5.46% w/w respectively. Figure 7.8 shows the influence of 1-butanol concentration on droplet size, conductivity and refractive index.

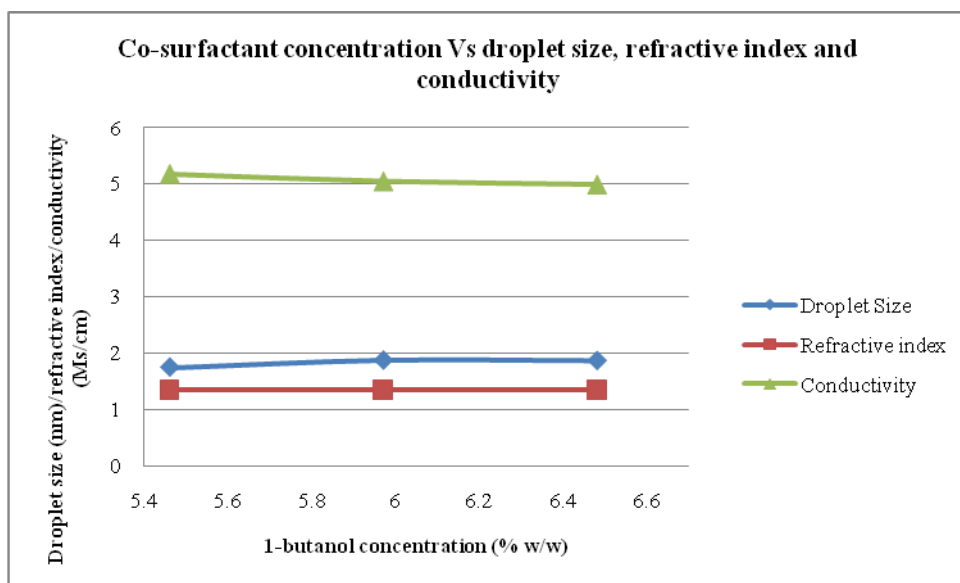


Figure 7.8 Effect of 1-butanol on droplet size, conductivity and refractive index.

### 7.3.4.3 Conductivity

In a similar trend to droplet size, conductivity remained relatively constant, showing only a slight decrease from 5.18 to 4.99 mS/cm with increasing 1-butanol concentration.

### 7.3.4.4 Correlation with separation

A loss of separation between the positively charged vitamins ( $B_1$  and  $B_2$ ) and an overall decrease in migration time for the water-soluble vitamins was observed with decreasing 1-butanol concentration. In parallel, an increase in migration time for the oil-soluble vitamins was noted with decreasing 1-butanol concentration, particularly between 5.97 and 5.46% w/w. While the decrease in droplet size was very small, it correlated with an overall increase in conductivity. The smaller droplet size may have indicated an increase in negative charge density on the ME droplet which would have increased the droplets electrophoretic mobility towards the anode, hence an increase in the oil-soluble vitamins migration time.

## 7.3.5 Addition of ACN

### 7.3.5.1 Surface Tension

On addition of ACN at the 5% level there was an increase in surface tension from 25.92 to 26.96 dynes  $\text{cm}^{-1}$ . No change in surface tension was observed on addition of 10% ACN, and only a modest increase to 27.31 dynes  $\text{cm}^{-1}$  was seen on addition of 15%.

With respect to the apparent stability of the microemulsion, the addition of ACN was well tolerated. Figure 7.9 graphs the effect of ACN concentration on surface tension.

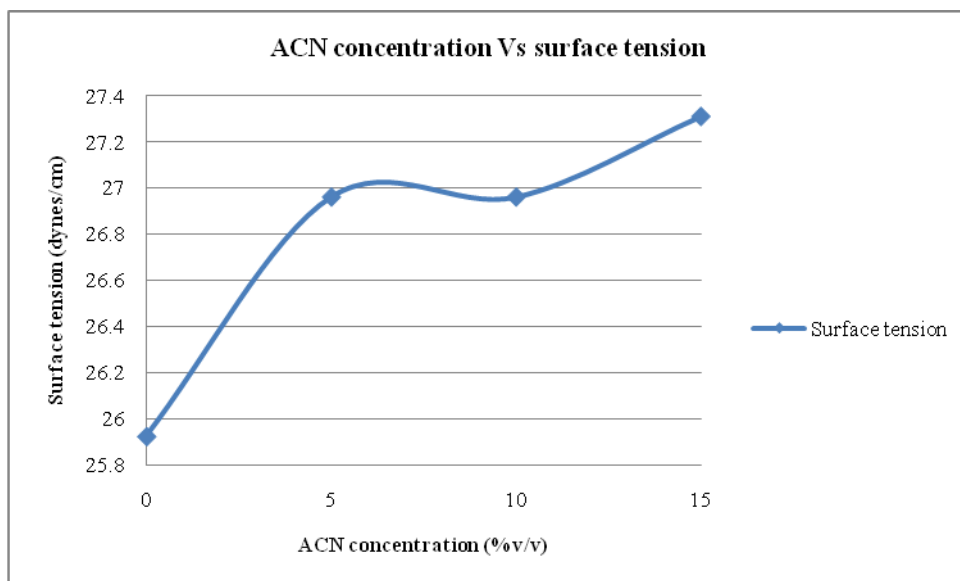


**Figure 7.9** Effect of ACN concentration on microemulsion surface tension

### 7.3.5.2 Droplet size

Addition of ACN from 0-15% v/v resulted in a slight decrease in droplet size from 1.8 nm to 1.6 nm. Figure 7.10 demonstrates the effect of ACN concentration on droplet size, conductivity and refractive index.

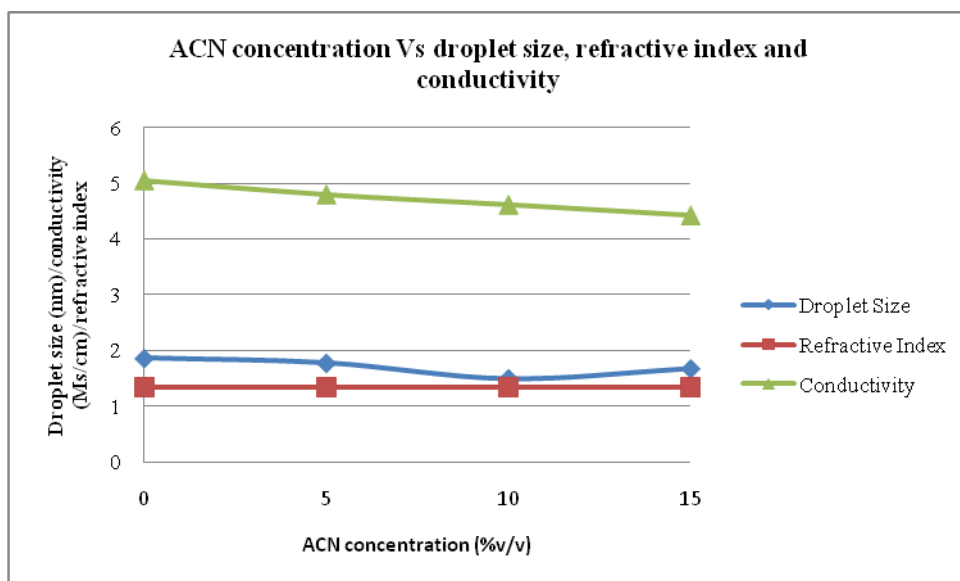


**Figure 7.10** Effect of ACN concentration on microemulsion droplet size, conductivity and refractive index

### 7.3.5.3 Conductivity

Additions of ACN naturally reduced the overall conductivity of the medium in a linear fashion from 5.05-4.43 mS/cm.

### 7.3.5.4 Correlations with separation

Looking solely at surface tension, droplet size and conductivity there was no distinct correlation apart from the reduction in conductivity and the increased migration time of all vitamins. While, as described in the chapter six, ACN may have played a significant role with respect to viscosity and EOF.

## 7.3.6 Addition of methanol

### 7.3.6.1 Surface Tension

Addition of MeOH from 0-15% v/v resulted in an increase in surface tension from 25.92 to 28.11 dyne  $\text{cm}^{-1}$ . Similar to the addition of 5% ACN, the initial addition of 5% methanol resulted in a 1 dyne  $\text{cm}^{-1}$  increase. However, further additions continued to increase surface tension. Figure 7.11 shows the effect of methanol concentration on surface tension.

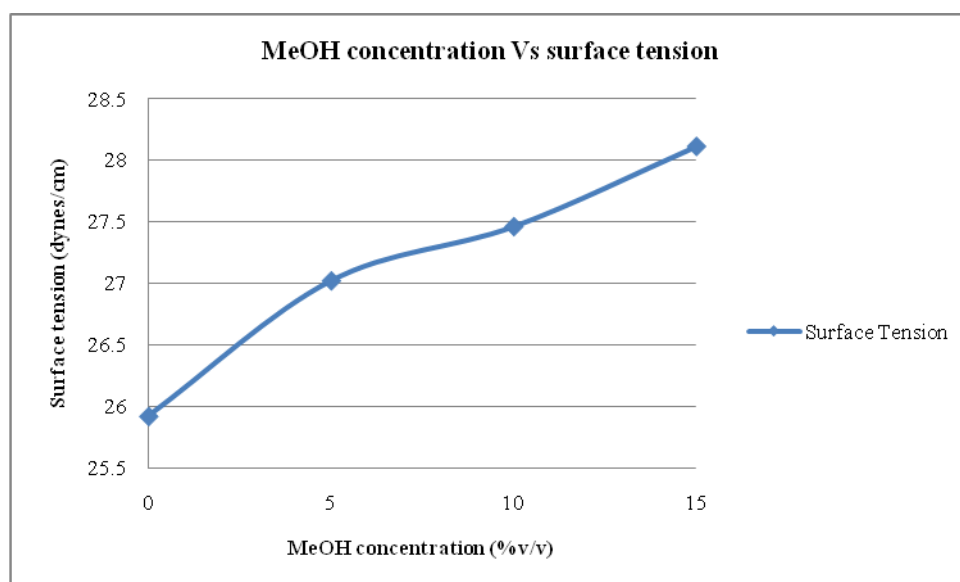
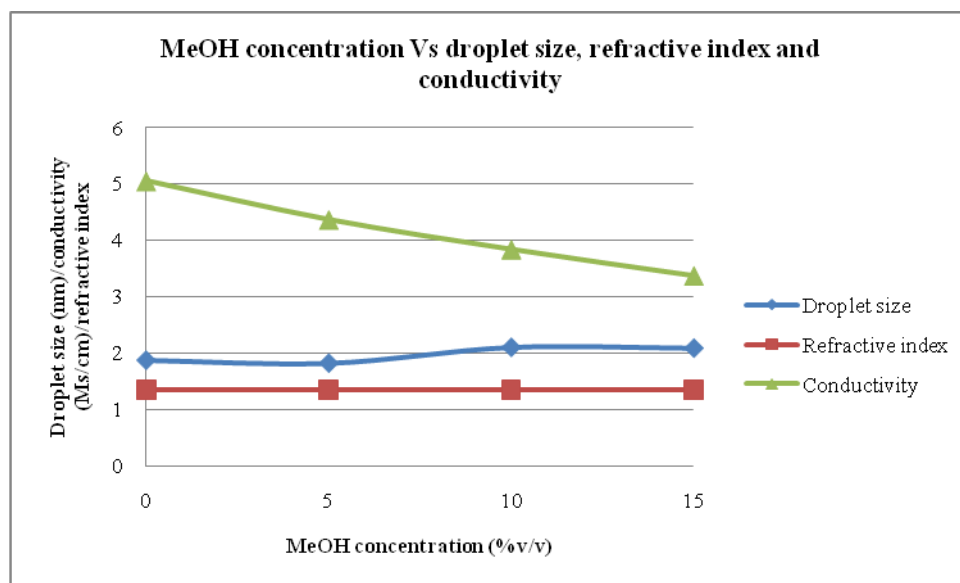


Figure 7.11 Effect on methanol concentration on surface tension

### 7.3.6.2 Droplet size

The initial 5% addition of methanol had little effect on the observed droplet size (1.8 nm), while increases to 15% resulted in slight increase to 2.0 nm. Figure 7.12 shows the effect on methanol concentration on droplet size, conductivity and refractive index.



**Figure 7.12** Effect of methanol concentration on microemulsion droplet size, conductivity and refractive index

### 7.3.6.3 Conductivity

Compared to modification with ACN, the fall in conductivity was greater with addition of methanol, and a reduction from 5.05 to 3.36 mS/cm was observed.

### 7.3.6.4 Correlations with separation

Modification with methanol above 5% resulted in very poor solubility of the oil-soluble vitamins and migration time for the water-soluble vitamins became excessively long (> 30 minutes after the addition of 10% v/v methanol).

## 7.3.7 Addition of IPA

### 7.3.7.1 Surface Tension

Addition of 5% IPA had no effect on surface tension and it remained constant at 25.92 dynes  $\text{cm}^{-1}$ . However, when 10% and 15% IPA was added, the surface tension increased to 26.85 and 27.40 dynes  $\text{cm}^{-1}$  respectively. Figure 7.13 graphs the effect of IPA concentration on surface tension.

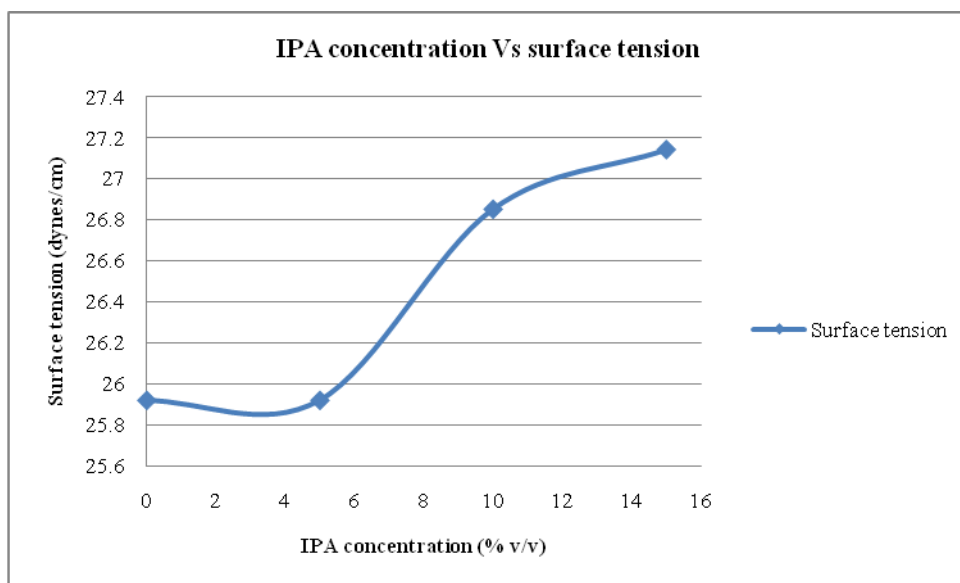


**Figure 7.13** Effect of IPA concentration on microemulsion surface tension.

### 7.3.7.2 Droplet size

An initially small increase in droplet size from 1.8 to 1.9 nm was observed on addition of 5% IPA. By comparison, additions of 10 and 15% IPA resulted in substantial increases in droplet size to 2.4 and 2.6 nm respectively. Figure 7.14 demonstrates the influence of IPA concentration on microemulsion droplet size, conductivity and refractive index.

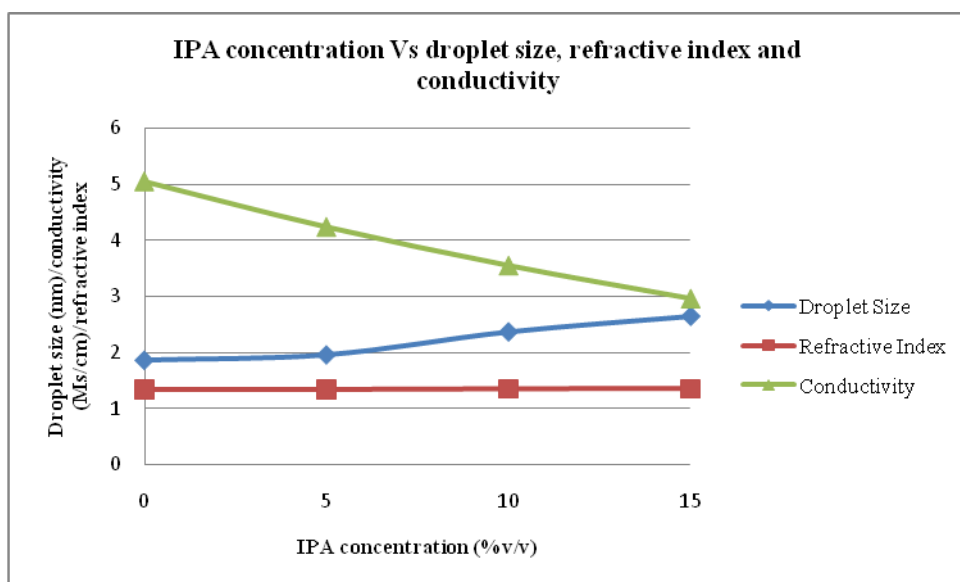


**Figure 7.14** Effect of IPA concentration on microemulsion droplet size, conductivity and refractive index.

### **7.3.7.3 Conductivity**

Compared to the additions of either ACN or methanol, IPA had the largest impact on conductivity. A fall in conductivity from 5.05 to 2.96 mS/cm was realised on increasing the concentration of IPA from 0 to 15% v/v.

### **7.3.7.4 Correlations with separation**

Compared to the other modifiers, addition of IPA at the 10 and 15% level appeared to improve separation between oil-soluble vitamin E and the A/D pair. While IPA was more hydrophobic and therefore would have increased the overall hydrophobicity of the ME droplet, it also increased the size of the droplet. A larger droplet would also have enabled a greater degree of interaction and therefore improved selectivity.

### **7.3.8 Addition of mixed modifiers**

It had been noted that addition of 10% ACN and 10 % IPA resulted in full separation of all vitamins including A, D and E. However, these separations were not reproducible. It had been postulated that addition of these mixed modifiers, particularly above a certain level, may result in an unstable system and may in turn have caused the irreproducible separations. Figure 7.15 and figure 7.16 show the effect of mixed modifier concentration on surface tension, droplet size, conductivity and refractive index respectively. As can be seen from the graphs, the addition of mixed modifiers at the 10 and 20% level showed similar trends to that observed in the addition of neat modifiers. Surface tension increased, but was still within the same range as that seen for the addition of neat IPA. Conductivity was reduced, but again its reduction was similar to that previously observed. While droplet sizes were also similar; there was a decrease in size from 2.3 to 1.8 nm with an increase in concentration from 10 to 20%. As noted with the addition of neat modifiers, ACN decreases droplet size while IPA serves to increase the droplet size. It appeared that addition of the modifiers together may have cancelled each other out with respect to droplet size. Overall, there was no evidence to suggest a less stable system and the poor reproducibility of the separation may have been the result of capillary conditioning.

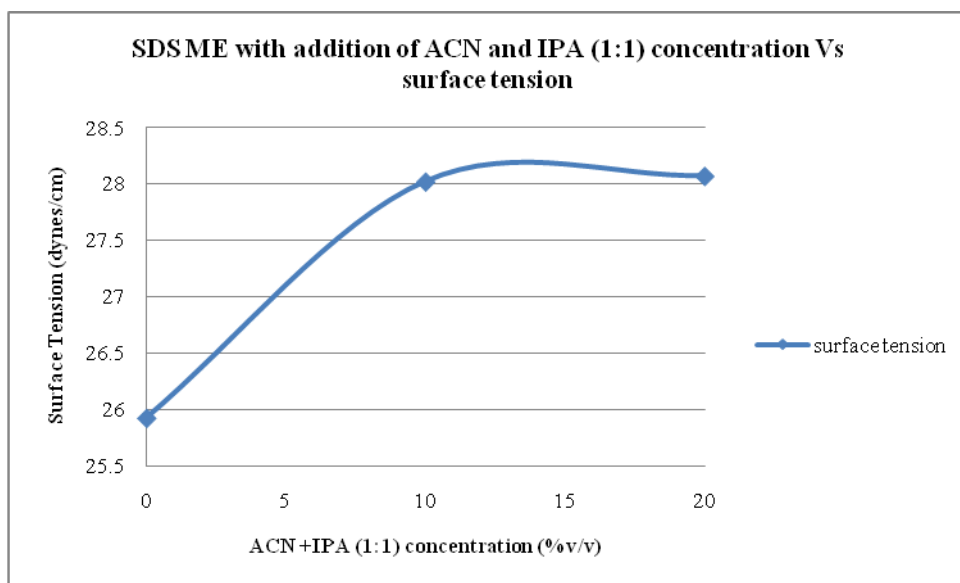


**Figure 7.15** Effect of mixed modifier concentration on surface tension of SDS based microemulsion.

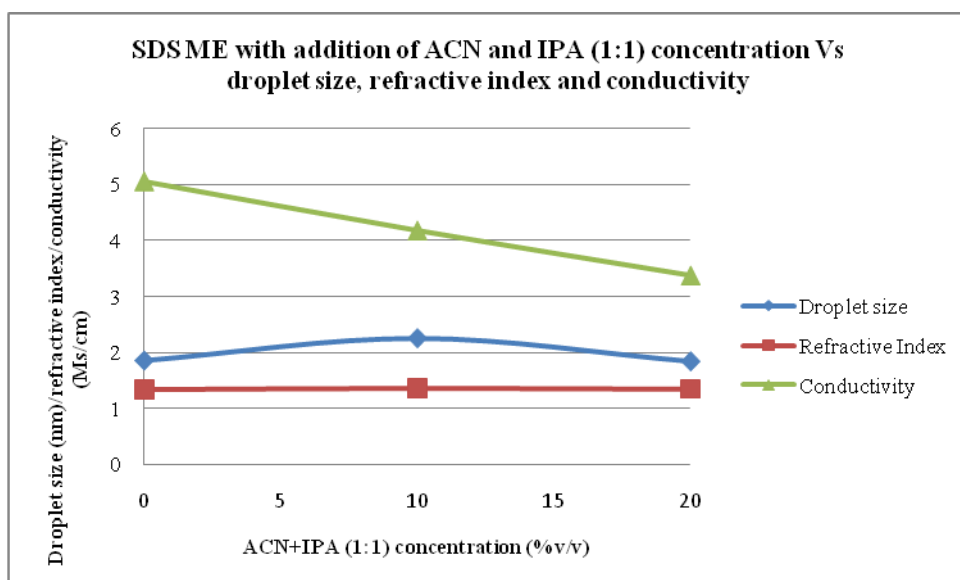


**Figure 7.16** Effect of mixed modifier concentration on droplet size, conductivity and refractive index of SDS based microemulsion.

### 7.3.9 Surfactant type

#### 7.3.9.1 Surface tension

Figure 7.17 graphs the effect of surfactant type on the on surface tension of each microemulsion. As can be seen in the graph, all values were within a relatively narrow range. SDS appeared to be the most efficient at lowering surface tension, followed by CTAB and SC. It was noteworthy that SC had the highest surface tension, although it was present at a higher concentration (15.56 mmols Vs 10.4 mmols for SDS and CTAB). Equimolar concentrations of SDS and SC combined, resulted in a similar

surface tension to that obtained for the SDS microemulsion. It was clear that above a certain concentration of surfactant, further increases would have little impact on interfacial tension.

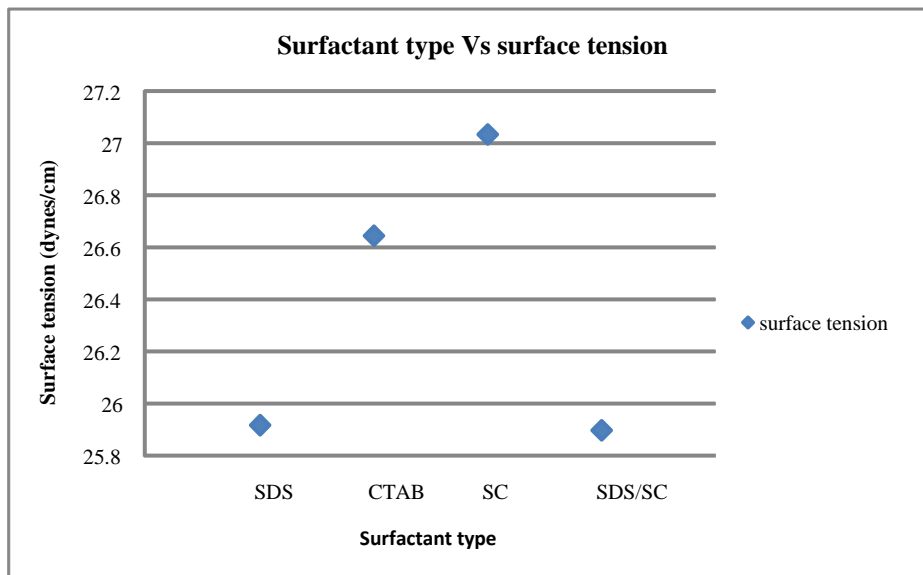


**Figure 7.17** Effect of surfactant type on microemulsion surface tension

### 7.3.9.2 Droplet size

Use of CTAB as the surfactant resulted in the largest droplet size (3.0 nm) of any microemulsion system examined in the study. Given its longer alkyl chain (C-14) compared to that of SDS (C-12) it was not a surprise that its microemulsion droplet would occupy a greater volume. Also, the SC microemulsion had a significantly larger droplet size (2.3 nm) compared to SDS (1.8 nm). As postulated in chapter six, due to the shape of the SC molecule, it would have occupied a larger molecular volume and this was evident from its measured droplet size. Taking into account the larger and somewhat bulky shape of SC, it may also have been responsible for the surfactants inferior ability to reduce the interfacial tension between the oil and aqueous domains. Hence, the higher surface tension value and greater quantity required to form the microemulsion. Interestingly, when SC and SDS were used in combination, the droplet size was similar to that of the SDS microemulsion. Figure 7.18 shows the effect of surfactant type on droplet size, conductivity and refractive index.

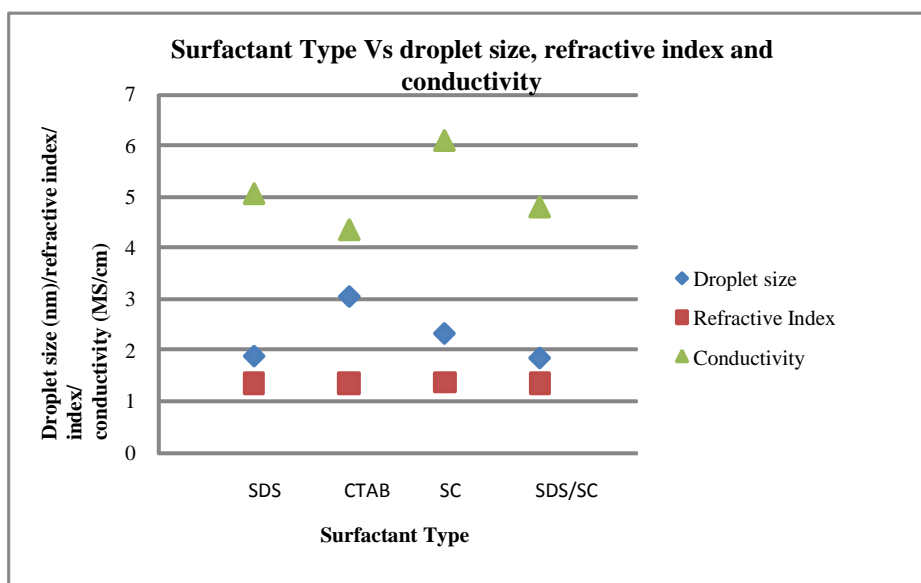


**Figure 7.18** Effect of surfactant type on microemulsion droplet size, conductivity and refractive index

### 7.3.9.3 Conductivity

The microemulsion formed by the combination of SC and SDS had only slightly lower conductivity than that of the SDS system (5.0 mS/cm). This was an unusual result, in that the overall concentration of surfactant was highest of all systems examined. As seen when examining the SDS concentration, an increased surfactant level results in an overall increased conductivity. The microemulsion composed of SC had the highest conductivity value (6.08 mS/cm), while having an overall lower concentration of surfactant than the SC/SDS system. These results indicated that, microemulsion formation and structure may also play a part in the overall charge of the microemulsion system.

### 7.3.9.4 Correlations with separation

As expected there was a change in migration order for the water soluble vitamins when separated using the CTAB buffer under a reversed polarity. However, despite the largest droplet size of any system examined, the CTAB system failed to produce any resolution between the oil soluble vitamins. This may have indicated that the larger droplet size did not aid mass transfer/partitioning between the analytes or droplet effectively. However, given that the separation was conducted under in reversed voltage, there was a significant decrease in migration time of the CTAB droplet and hence shortening of the migration window, which would have impeded separation.

While all parameters measured with respect to the SDS/SC microemulsion were analogous to the SDS system, the overall migration time was quite different. The

mixed surfactant resulted in all vitamins migrating within 10 minutes, compared to the SDS microemulsion buffer (approximately 17 minutes). While it was apparent that the mixture of SC and SDS affected the overall migration window, only a slight difference in conductivity was observed between the two systems.

The optimum separation was achieved when SC was employed as the surfactant. Resolution between the water-soluble vitamins was improved and the vitamin E remained well resolved from the A/D pair. Overall, the separation was approximately five minutes shorter than the SDS based system. Compared to the SDS microemulsion, the SC system possessed a larger droplet size which may have increased partitioning with the oil-soluble vitamins. Also, the increased conductivity seemed to correlate with the overall reduced migration window. Importantly, the influence of SC on the microemulsion droplet may have helped increase resolution between the water-soluble vitamins.

## **7.4. Conclusion**

### **7.4.1 Surface tension**

For all microemulsion systems examined, surface tension remained within a relatively narrow range (23.8-28 dynes  $\text{cm}^{-1}$ ) and all systems appeared stable. The greatest influence on the surface tension (apart from the minimum concentration of surfactant required for formation) was the presence of a co-surfactant. The presence of 1-pentanol as a co-surfactant resulted in the lowest surface tension observed for any system (23.8 dynes  $\text{cm}^{-1}$ ). By comparison, the MEKC system yielded the highest surface tension (34 dynes  $\text{cm}^{-1}$ ). The co-surfactant concentration had little effect on surface tension in the range examined.

Variation of oil phase type played a subtle role in surface tension, with the alkanes resulting in higher values than the alcohols.

The effect of SDS concentration in the range examined showed an interesting trend. While the range was narrow (25.4-27 dynes  $\text{cm}^{-1}$ ), at concentrations above 2.72% w/w surface tension increased.

Apart from the addition of 5% v/v IPA to the microemulsion system, additions of organic modifier up to 15% v/v (IPA, ACN or MeOH) gradually increased the surface tension of each system. While addition of 15% MeOH resulted in the highest surface tension of any single modifier examined (28 dynes  $\text{cm}^{-1}$ ), it was still considerably lower than the micellar system.

In general, no correlation could be made with any vitamin separation. As long as a stable microemulsion was formed, the effect on separation seemed independent of surface tension.

#### **7.4.2 Droplet size**

The components and their concentration used in the formation of each microemulsion resulted in some definite trends in the measured droplet size. Droplet sizes for the microemulsion compositions examined ranged from 1.5 to 3.0 nm, with the SDS micellar system measured at 0.9 nm.

Similar to surface tension, the type of co-surfactant played a substantial role in droplet size with 1-pentanol resulting in a size of 2.8 nm. In the range examined (5.46-6.48% w/w) co-surfactant concentration did not have a significant effect on droplet size.

While not a substantial increase, the type of oil phase was also seen to have an effect on droplet size. Replacing the linear alcohol 1-pentanol with the branch chained 2-octanol resulted in an increase in droplet size from 1.5 to 1.8 nm. Together with the nature of the oil phase, size and shape may have a significant effect on how analytes interact and partition with droplet.

Increasing concentrations of SDS resulted in a slightly decreasing droplet size. This decrease in droplet size was most likely due to the fixed oil phase being distributed among a greater number of smaller droplets. Surfactant type had a more marked influence on droplet size, with CTAB having a droplet of 3.0 nm and an equimolar concentration of SDS having a droplet size of 1.8 nm. The SC microemulsion, although present in a higher concentration, had an intermediate droplet size of 2.3 nm. With respect to separation, the SC microemulsion provided superior resolution between the water-soluble vitamins and equivalent resolution between the oil soluble vitamins, when compared to SDS. While the size and charge ratio on the droplet would have influenced the interaction with the water-soluble vitamins, the droplet size would have been crucial in allowing partitioning with the oil soluble vitamins.

Addition of modifiers to the microemulsion buffers had an interesting effect on droplet size. While ACN resulted in smaller droplets (1.8-1.6 nm), the addition of IPA increased droplet size (1.8-2.6 nm). The use of MeOH as a modifier resulted in a slight increase in droplet size (1.8-2.0 nm). The discrepancy in size trends between modifier type may have resulted from where they were located within the microemulsion. While all modifiers were capable of partitioning in the oil or aqueous phase, their polarity may

influence where they reside. The measured droplet size may be used to infer the degree of inclusion in the droplet or presence in the aqueous bulk phase. It was apparent that IPA, with its ability to increase droplet size, may have partitioned closer to the oil/water interface compared to ACN or MeOH. However, it should also be noted that in addition to partitioning to a greater degree in the droplet, the branched structure of IPA may also have served to increase droplet size. Given the difference in polarity (Snyder index [6]) between ACN (6.2), MeOH (6.6) and IPA (4.3), the ACN and MeOH would naturally partition in the aqueous phase to a greater extent than IPA. Never the less, it was interesting to note the effect on droplet size, as many reports have indicated that successful separation of oil soluble vitamins may be based on their ability to penetrate the microemulsion droplet. With respect to correlating the effect of droplet size on separation, some observations were made but in all cases the effect on conditions such as droplet charge density, EOF strength buffer viscosity and electrophoretic mobility would also have to be taken into account. Addition of ACN and IPA, while frequently reported in the literature for the successful separation of oil soluble vitamins appeared in this study to have had opposite effects on droplet size. In either case, the addition of ACN or IPA improved separation between vitamin E and the A/D pair. While droplet size may play a role, the nature of the modifier and its effect on droplet hydrophobicity, EOF, etc would be of greater influence.

### **7.4.3 Conductivity**

The surfactant type and its concentration, and the level of organic modifier, had the greatest impact on the conductivity of the microemulsion buffer. Increasing the concentration of SDS raised the overall conductivity of the system. Since the increase in surfactant concentration served to increase the negative charge density on the microemulsion droplet, a corresponding increase in the migration time of the oil soluble vitamins was observed. Also, an increase in the migration time of the positively charged water soluble vitamins (B<sub>1</sub> and B<sub>2</sub>) was observed, due possibly to ion-pairing. In all cases the addition of modifiers lowered the conductivity of the system. This decrease could in part be attributed to overall dilution of the buffer. Similar to droplet size, the addition of modifiers did not affect all microemulsions to the same degree. While addition of IPA and MeOH resulted in a decrease in conductivity from 5.05-2.96 and 5.05-3.36 mS/cm respectively, addition of ACN resulted in a modest decrease from 5.05-4.43 mS/cm. With respect to separation, the addition of modifiers increased the

migration time of all vitamins. While the increase in conductivity obtained through increasing SDS concentration could be correlated with an increase in the negative charge density on the droplet, the effect of modifiers was more complicated. In addition to reducing the negative charge density on the microemulsion droplet, the presence of modifiers would have a large influence on EOF and viscosity. Of interest was the comparison of ACN and IPA. While IPA greatly reduced the overall conductivity, ACN had a more modest effect.

#### **7.4.4 General correlations and limitations**

While definite correlations between surfactant components and the measured characteristics could be observed, it was not possible to directly attribute these measurements with specific effects on vitamin separations.

Comparing results obtained in this chapter to similar work yielded some interesting findings. While one of the microemulsions examined in this study was similar to that of Cao et al. [2], a large discrepancy in droplet sizes was observed. The authors reported that a microemulsion composed 3.3% (w/v) SDS, 6.6% (w/v) 1-butanol and 0.8% (w/v) n-octane in 10 mM borate buffer (pH 9.2) had a droplet size approximately 130 nm. However, a droplet size of 1.42 nm was recorded in this chapter. This was a large discrepancy, given that microemulsion droplets are generally perceived to range from a couple of nanometres to less than 100 nm [7]. The results obtained by Cao et al. [2] are more associated with nano emulsions [8]. Both techniques employed dynamic light scattering (DLS) to measure droplet size, albeit using instrumentation from different manufacturers. The only substantial difference between the two systems was the angle at which the scattered light was measured. While the work reported in this chapter measured the scattered light at  $178^\circ$ , Cao et al. measured at an angle of  $90^\circ$ . As discussed in the characterisation review, the angle at which scattered light is measured can have an effect on the size result obtained. In spite of the stark difference in actual values, there was some similarity in the trends observed between both studies. Cao et al. [2] noted a decreasing particle size with an increase in surfactant concentration. Also, the addition of ACN up to 10% did not significantly affect droplet size, but had a marked effect on increasing the migration window and reducing EOF. Interestingly, Cao et al. [2] observed an increase in droplet size on increasing co-surfactant concentration from 2 to 12%. While this result was not mirrored in this chapter, a decrease in migration window was observed in both systems indicating a reduction in

the droplets' negative charge density. Measurement of zeta potential provided accurate information on the droplets charge density and it would be useful to conduct similar measurements for all microemulsions used in this work.

In characterising the microemulsion utilised in the MELC separation Andelija et al. [3] noted the best separation in terms of resolution and efficiency was achieved when the microemulsion had the smallest droplets, thinnest film thickness and lowest interfacial tension. However, the separation mechanism in MELC is very different to CE. While theoretically a greater number of small droplets should have increased separation and efficiency for the oil soluble vitamins, it was not observed. The principal reason for this was the inability of oil soluble vitamins to penetrate the smaller droplets, coupled with an increase in peak broadening due to joule heating and longer migration times.

## 7.5 References

- [1] Ryan, R., Donegan, S., Power, J., McEvoy, E., Altria, K., *Electrophoresis*, 30 (2009) 65-82.
- [2] Cao, Y., Sheng, J., *Electrophoresis*, 31 (2010) 672-678.
- [3] Anđelića, M., Darko, I., Mirjana, M., Biljana, J., Slavko, M., *Journal of Chromatography A*, 1131 (2006) 67-73.
- [4] Yin, C.N., Cao, Y.H., Ding, S.D., Wang, Y., *Journal of Chromatography A*, 1193 (2008), 172-177.
- [5] Li, G.Z., Friberg, S.E., *Journal of the American Oil Chemists Society*, 59 (1982) 569-572.
- [6] Snyder, L.R., *Journal of Chromatographic Science*, 16 (1978) 223-234.
- [7] Flanagan, J., Singh, H., *Critical reviews in food science and nutrition*, 46 (2006) 221-237.
- [8] Shafiq, S., Shakeel, F., Talegaonkar, S., Ahmad, F.J., Khar, R.K., Ali, M., *Journal of Pharmaceutical and Biopharmaceutical*, 66 (2006) 227-243.

## **Chapter Eight**

### **Characterisation of SDS based microemulsion**

## **8.1 Introduction**

As discussed in chapter four, there are many techniques available with which to characterise microemulsions. While few reports related to separation methodologies, an aim of this chapter was to use a range of techniques to examine the physicochemical properties of microemulsions within an SDS based system. In addition to physicochemical properties, all microemulsions were used as background electrolytes in MEEKC for the separation of acidic and neutral analytes.

The majority of microemulsion compositions utilised for MEEKC separations make little reference to their overall position within a phase diagram. Based on the concentration of components, it is assumed they are either O/W or W/O in type. A further aim of this chapter was to employ routine characterisation techniques to determine phase types and track changes in phase with respect to composition.

The microemulsion system investigated was composed of SDS, 1-butanol, octane and tetraborate buffer pH 9.2. Initially a pseudoternary phase diagram was constructed to determine the composition of all possible microemulsion regions. Phases of interest included O/W, bicontinuous and W/O. Based upon the microemulsion region obtained, an area was chosen whereby the surfactant to co-surfactant ratio was held constant and a hypnotised region from O/W, through a bicontinuous phase, to W/O was investigated. The aqueous concentration was varied from 8 to 63% w/w. In addition to a reference standard microemulsion [1], eight compositions were examined with respect to droplet size, surface tension, conductivity, refractive index, and DSC profile. All compositions were utilised as a CE buffer for the separation of thiourea, sorbic acid, paracetamol and butyl paraben.

## **8.2 Experimental**

### **8.2.1 Phase Diagram**

A pseudoternary phase diagram was constructed using the titration method to ascertain the concentration range of all components (SDS/1-butanol, octane and aqueous buffer) which formed a microemulsion. The SDS and 1-butanol (surfactant mixture) were mixed in a 2 to 1 weight ratio. This ratio was chosen as quite a number of reports utilised this composition for the successful separation of pharmaceutical analytes [2-4]. Samples of octane and surfactant mixture were prepared in weight ratios of 1:9, 2:8, 3:7, 4:6, 1:1, 6:4, 7:3, 8:2 and 9:1. These samples were then titrated dropwise with aqueous buffer under moderate stirring in order to identify the microemulsion regions.

Figure 8.1 shows the pseudoternary phase diagram and the microemulsion regions obtained. Also, Table 8.1 details the composition of the samples chosen for further examination.

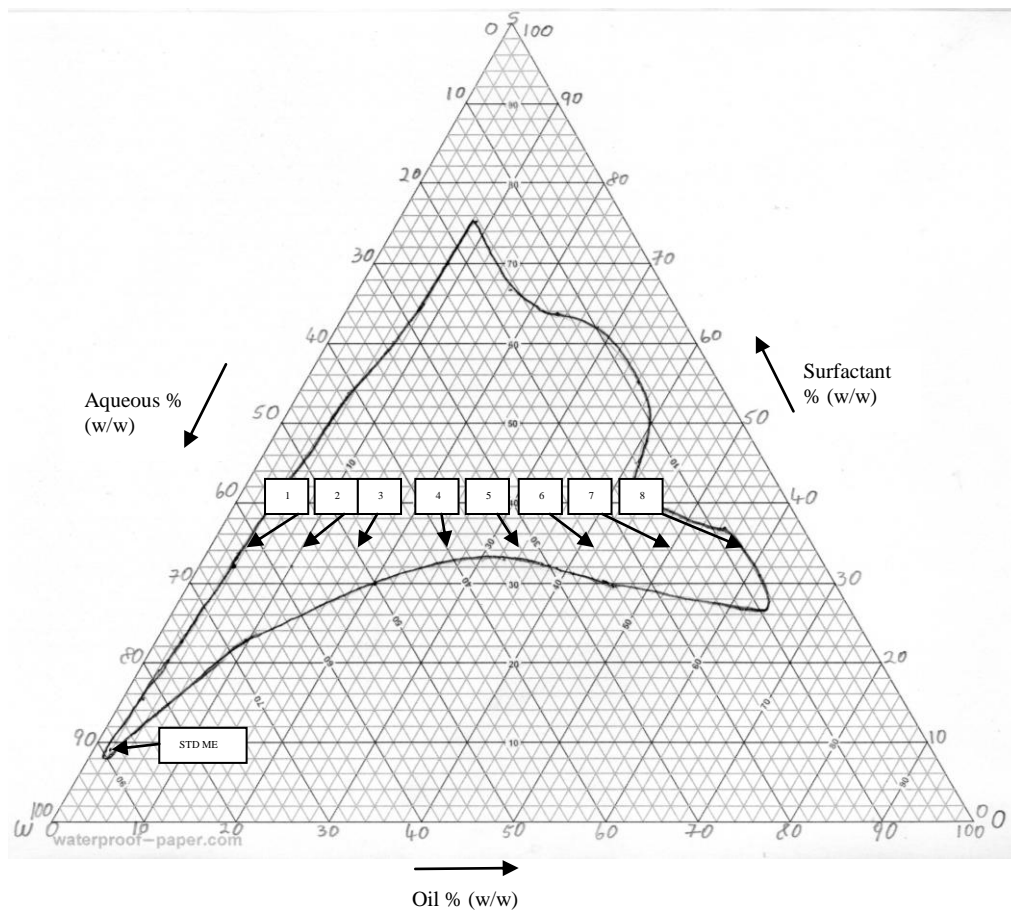


**Figure 8.1** Pseudoternary phase diagram indicating the standard microemulsion and regions examined.

**Table 8.1**                      **Composition of all microemulsions examined within the pseudoternary phase diagram.**

<i>Microemulsion</i>	<i>Oil (% w/w)</i>	<i>Surfactant (% w/w)</i>	<i>Aqueous Buffer (%w/w)</i>
ME1	3	34	63
ME2	10	34	56
ME3	18	34	48
ME4	26	34	40
ME5	34	34	32
ME6	42	34	24
ME7	50	34	16
ME8	58	34	8
Standard Microemulsion	0.8	9.9	89.3

### 8.2.2 Sample preparation

Samples were chosen from the pseudoternary phase diagram maintaining a surfactant mixture concentration of 34 % w/w, while water concentration was varied from 8 to 63 % w/w. The region was judiciously chosen as it allowed examination of compositions within the microemulsion from the water to oil rich phases and all points in between. As a reference point, a typical standard microemulsion region was also examined. Microemulsions were prepared by mixing SDS, 1-butanol, and n-octane in a 200 ml duran bottle. This mixture was stirred for 10 minutes using a magnetic stirrer to ensure a homogenous solution was formed. 10 mM sodium borate pH 9.2 was then added, sonicated for 30 minutes and filtered.

### 8.2.3 Droplet Size

Droplet size measurements were performed on Malvern HPPS 5001 dynamic light scattering apparatus, equipped with a temperature controlled sample compartment, a helium-neon laser at 632.8 nm and an optical detector. The intensity of scattered light was measured at an angle of 178°. Approximately 3 mL of microemulsion sample was placed in a quartz cuvette. The cuvette was placed in the sample compartment and allowed to equilibrate at 25°C before the measurement was performed. All measurements were carried out in triplicate. The RSD for all measurements was less

than 5%. The polydistribution index (PDI) for all measurements was less than 0.2 indicating relatively monodisperse systems.

#### **8.2.4 Surface Tension**

Surface tension measurements were performed on a Kruss G10 contact angle/surface tension meter, equipped with a stage, syringe and camera. Calculations were performed based on the shape of a hanging pendent drop according to the Young-Laplace equation and DSA 10.1 software. Measurements were conducted in triplicate. The RSD of all measurements was less than 3%.

#### **8.2.5 Conductivity**

Conductivity measurements were performed using a bench-top WTW LF538 dual pH/conductivity meter.

#### **8.2.6 Refractive index**

Refractive index measurements were performed on a Bellingham Stanley RFM340 refractometer. All refractive index measurements had an RSD less than 0.1%. The refractive index of all systems showed little variation with values of approximately 1.34.

#### **8.2.7 DSC**

DSC measurements were performed on a TA instruments DSC Q2000 equipped with a refrigerated cooling system. Nitrogen with a flow rate of 50 ml/min was used as the purge gas. Approximately 10 mg of sample was precisely weighted into a hermetically sealed aluminium pan. An empty hermetically sealed pan was used as a reference. Samples were cooled from 25°C to -95 °C at a rate of 5°C/min, held at three minutes at -95 °C for 3 minutes before heating at a rate of 10°C /min. Data was analysed using TA instruments universal analysis software version 4.7A.

#### **8.2.8 MEEKC separation**

MEEKC experiments were performed on an Agilent 3D-CE capillary electrophoresis instrument, (model G1600AX,) equipped with UV diode array detector and Agilent Chemstation software Rev A.08.03. All separations were performed on fused silica

capillaries with 50  $\mu\text{m}$  ID, total length 35.5 cm with detection window at 26.5 cm. Injections were performed in hydrodynamic way at a pressure of 20 mbar.

### **8.3 Results and discussion**

#### **8.3.1 Particle size**

Compared to the standard microemulsion (1.54 nm), located at the edge of the water rich single phase region, microemulsions spanning across the phase diagram had an increased droplet size. This result was attributed to the small concentration of oil (0.8 %) and relatively large concentration of aqueous buffer (89.3%). However, the microemulsion ME1 (aqueous buffer 63% w/w), at the aqueous dominant side of the phase diagram, with a particle size of 3.26 nm, was thought to form an O/W type microemulsion based on the composition in Table 8.1.

Figure 8.2 graphs the obtained droplet size against an increasing concentration of aqueous buffer (%w/w). A sharp increase in droplet size from (4.48 to 9.43 nm) was observed with an increase in aqueous buffer from 24% to 32%. Thereafter, further increases in aqueous buffer resulted in a reduced droplet size (from 9.43 to 1.96 nm). The sharp change in droplet size may have inferred a change in phase.

Comparison of the droplet size ranges obtained for the standard microemulsion (1.96 nm) to that obtained across the dilution line (3.26-9.43 nm) indicate the small size of droplets present in routine MEEKC separations.

While a size was obtained throughout the microemulsion region examined, meaningful results may have been limited due to the nature of the measurement system. All sizes reported were calculated based on hypothetical spheres and therefore no information on dimension was attained. Also, as with any light scattering experiment, the presence of extraneous particles or contamination would contribute to a result. However, the polydispersity index (PDI) for all measurements was no greater than 0.2 indicating a relatively monodisperse system.

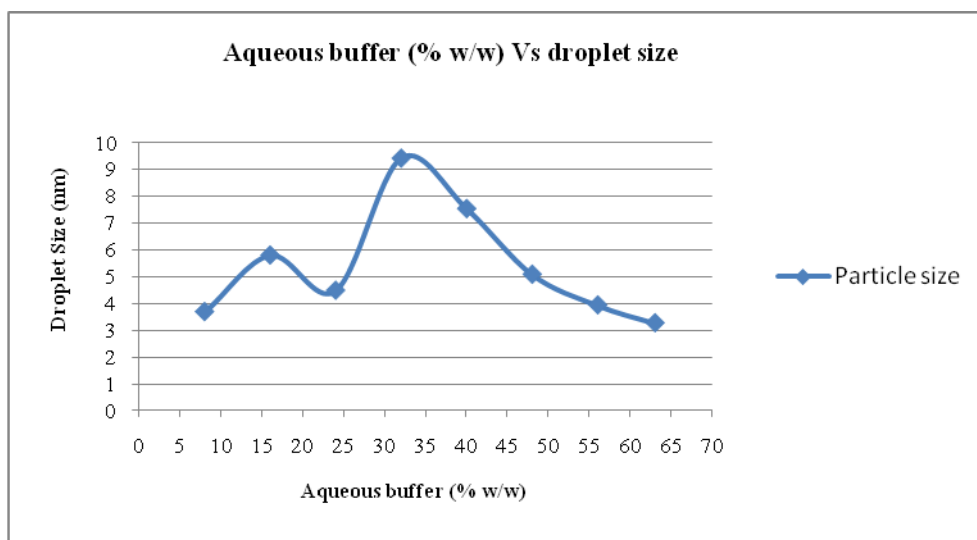


**Figure 8.2** Effect of aqueous buffer concentration on microemulsion droplet size

### 8.3.2 Surface Tension

Across the chosen dilution line ME8-ME1, a decrease in surface tension (26.85-22.32 dynes  $\text{cm}^{-1}$ ) was seen with an increase in aqueous content (8-63% w/w). A slight plateau of approximately 24 dynes  $\text{cm}^{-1}$  was noted at aqueous concentrations between 32 and 40%. The surface tension either side of the plateau had similar slopes. The plateau may have represented a change in phase when compared to the microemulsions on either side. The overall decrease in surface tension could also be attributed to the increase in aqueous buffer concentrations, which had a lower surface tension than n-octane. Figure 8.3 shows a graph demonstrating the effect of aqueous buffer concentration on microemulsion surface tension. On comparison to the standard microemulsion which had a surface tension of 27 dyne  $\text{cm}^{-1}$ , values across the dilution line were consistently lower. This may have resulted from the increase in surfactant mixture concentration, which was 9.9 % w/w for the standard microemulsion compared to 34% w/w across the dilution line.

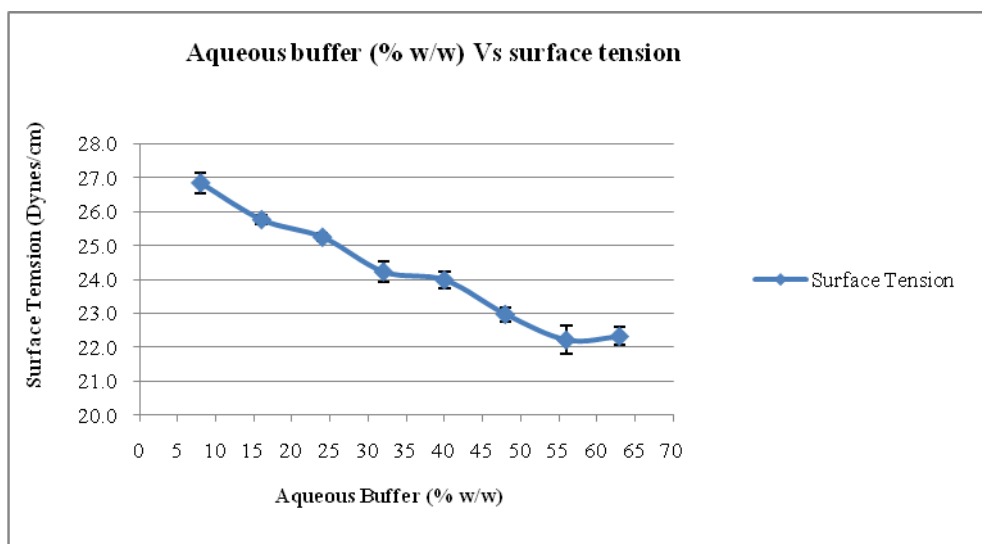


**Figure 8.3:** Effect of aqueous buffer concentration on microemulsion surface tension

### 8.3.3 Refractive index

All refractive index measurements obtained across the dilution line were within a narrow range. ME8 with an aqueous concentration of 8% had a refractive index of 1.4020 while ME1 with an aqueous concentration of 63% had a refractive index of 1.3704. Figure 8.4 shows the effect of aqueous buffer concentration on refractive index. The changes in the slope of the refractive index graph were similar to those obtained when the concentration of aqueous phase was graphed against surface tension. A plateau was noted at aqueous concentrations between 32 and 40%. The standard microemulsion had a refractive index of 1.3438.

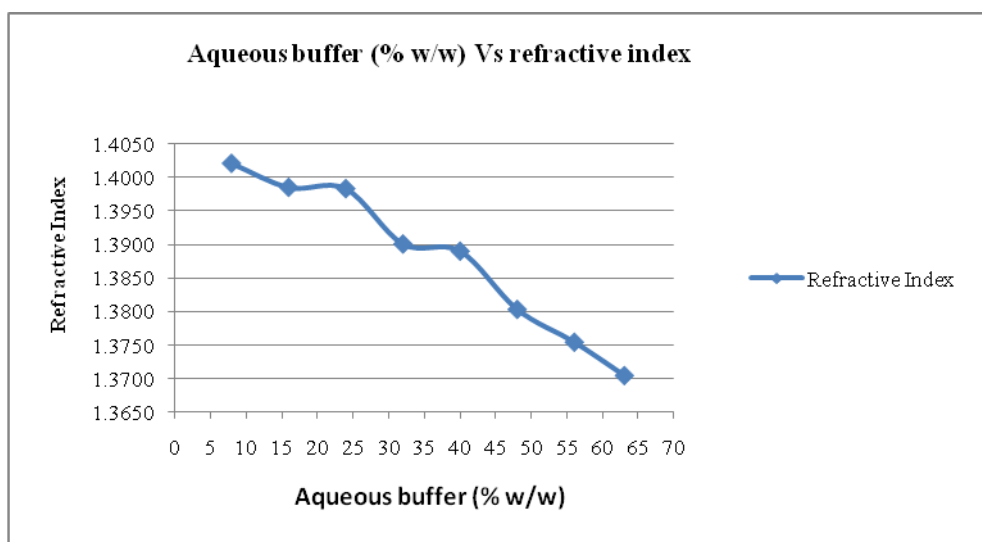


**Figure 8.4** Effect of aqueous buffer concentration on microemulsion refractive index

### 8.3.4 Conductivity

Increasing aqueous buffer concentration across the dilution line from ME8 to ME1 revealed a sharp change in measured conductivity. Figure 8.5 graphs the effect of aqueous buffer concentration on the conductivity values obtained. At aqueous concentrations above 24% a dramatic increase in conductivity was noted. Taken with the change in droplet size, in figure 8.2, this may have correlated with a change in phase. Above 32% aqueous buffer, the conductivity appeared to increase in a linear fashion. The standard microemulsion had a conductivity of 5.42 mS/cm, and while its value was lower with respect to its aqueous concentration, this was attributed to its reduced SDS concentration.

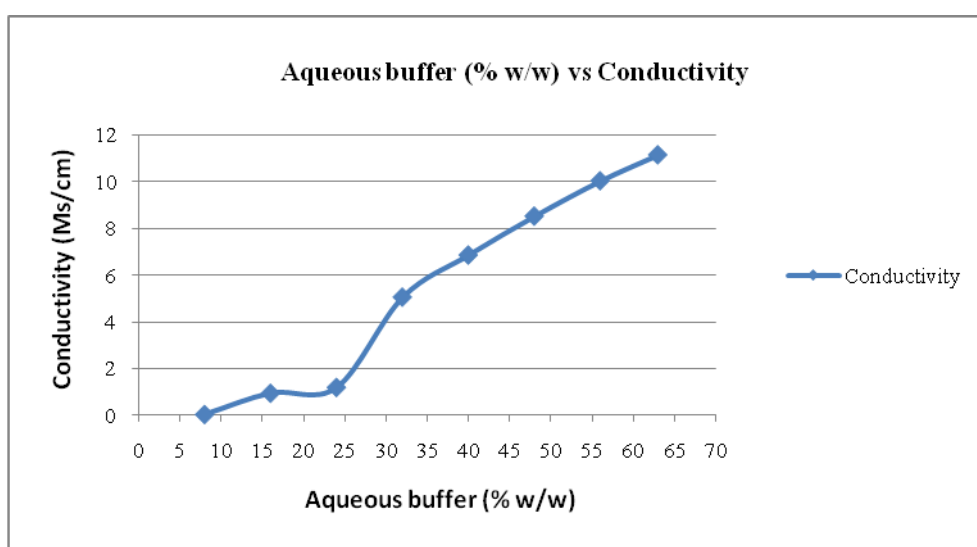
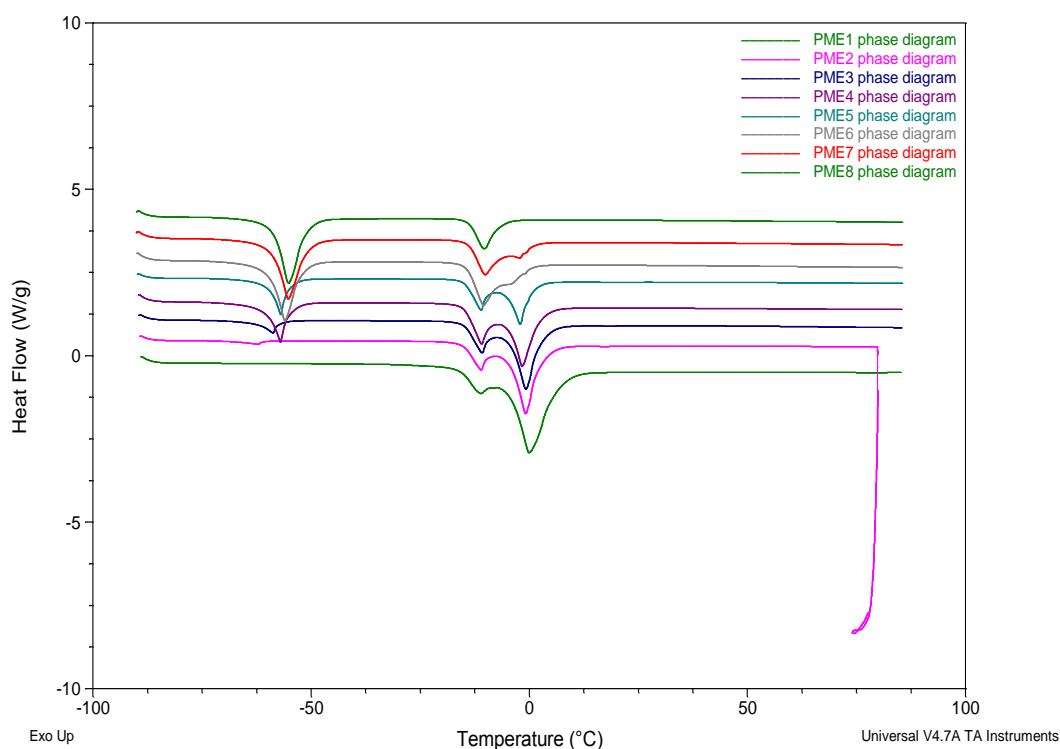


Figure 8.5 Effect of aqueous buffer concentration on microemulsion conductivity

### 8.3.5 DSC

Analysis of DSC curves for all microemulsions was conducted with a view to understanding the behaviour of water (aqueous buffer) within the system and hence determining any phase transitions. The water in all systems was deemed to behave either as bound, interphasal or free/bulk water. Bound or interphasal water results from its interaction between the surfactant hydrophilic head groups and alcohol group on the co-surfactant which reside in or around the amphiphilic film. Literature suggests [5-7] the melting point of interphasal water is approximately  $-10^{\circ}\text{C}$ , while bound water has a melting point of less than  $-10^{\circ}\text{C}$ . By contrast free water has a melting point closer to that of pure water at  $0^{\circ}\text{C}$ . Figure 8.6 shows a graph containing the DSC curves for all regions examined within the phase diagram.

Starting at the oil rich side of the phase diagram (ME8) where the aqueous concentration was 8 % w/w, two principal peaks corresponding to bound water at -10.42 °C and n-octane at -55.27 °C were observed. No endothermic peak for free water was detected, which indicated the system was possibly W/O in nature. Increases in aqueous concentration to 16 and 24% w/w (ME7 and ME6, respectively) resulted in similar thermographs. However, a slight shoulder was observed on the bound water peak at approximately -2.29 °C. This peak may have corresponded to interfacial water or free water depending on definition. It has previously been reported that the interfacial water and bound water may be indistinguishable for microemulsion systems [5]. Taking the shoulder on the peak as interfacial water may indicate the microemulsion was still W/O in nature. However, if the peak was taken to correspond to free water, it may indicate a bicontinuous type phase. When the aqueous concentration was increased to 40% a very distinctive peak corresponding to free water was observed at approximately -1 °C. The peaks corresponding to bound water and n-octane were also present at -11 and -57 °C respectively. The appearance of the peak corresponding to free water was indicative of a phase change. However, since a peak corresponding to n-octane was also present, it was difficult to determine if this represented an O/W or bicontinuous phase. Similar curves were observed with increases in aqueous concentration up to 56% w/w, with three peaks corresponding to free water, bound water and n-octane. While the n-octane peak decreased in size, this was attributed to the dilution effect. When the aqueous concentration reached 56% w/w (ME1), only two peaks corresponding to free and bound water were detected. At this point, it was likely that a definite O/W microemulsion was formed. A similar thermograph was obtained for the standard microemulsion.



**Figure 8.6** DSC curves for microemulsions regions within phase diagram. Refer to table 8.1 for compositions.

### 8.3.6 MEEKC separation

An initial set of starting conditions were chosen using the standard microemulsion as the background electrolyte. A voltage of 10 KV in positive polarity was applied across the capillary and the cassette temperature was held at 20°C. Peaks were detected for thiourea, paracetamol and sorbic acid with migration times of 5.2, 6.8 and 13.7 minutes respectively. However, the more hydrophobic butyl paraben, which had the greatest affinity for the negatively charged microemulsion droplet, was not detected. It was apparent that the EOF was not strong enough to sweep butyl paraben towards the cathode for detection. Increasing the applied voltage to 12 KV allowed detection of all analytes, with butyl paraben migrating in 26 minutes. Figure 8.7 shows an electropherogram of the separation carried out employing the standard microemulsion with an applied voltage of 12 KV.

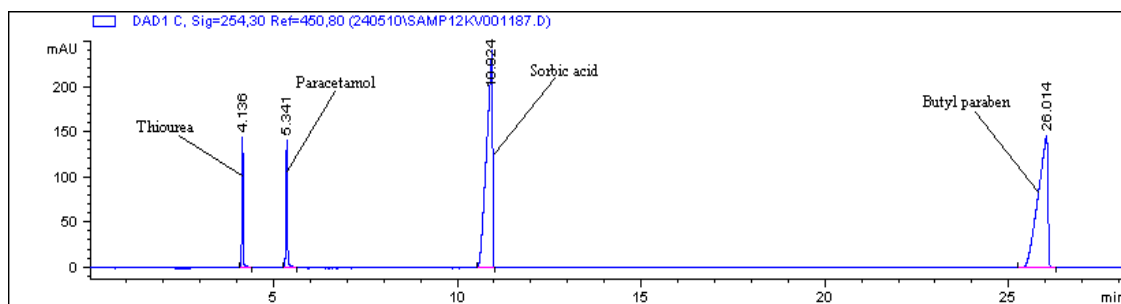


**Figure 8.7** Electropherogram of analyte separation using standard microemulsion. **Buffer:** 9.9% w/w SDS, 5.9/1-butanol, 0.8% w/w octane and 89.3% w/w 10mm sodium tetraborate buffer (pH 9.2). Separation conditions; 50  $\mu$ M ID fused silica capillary length 35 cm, detection window at 26.5 cm, flush for 3 minute with 0.1 M NaOH followed by 1 minute with water and 3 minutes with microemulsion, capillary cassette temperature 20° C, applied voltage 12 kV, sample injection 10 mbar for 10 seconds, UV detection at 254 nm.

With respect to microemulsions ME1 to ME8, It was initially attempted to carry out the separation in positive polarity using an applied voltage of 12 KV. Starting with ME1, which was the nearest composition to the standard microemulsion, the current generated was excessive (125 amps) and no peaks were observed. This result was not surprising as the higher level of SDS in microemulsion ME1 would have strongly contributed to the overall ionic strength. When the separation was carried out with an applied voltage of 10 KV, the current was acceptable (77 $\mu$ A). However, no peaks were observed and it appeared the EOF was not sufficient to facilitate a separation. It was decided to conduct the separation under a suppressed EOF by reversing the polarity of the applied voltage (-10 KV) and allowing analytes to migrate under electrophoretic mobility alone. Figure 8.8 graphs the effect of aqueous buffer concentration on the migration times of all analytes.

Above 24% w/w aqueous buffer, the migration time of thiourea and paracetamol increased and an improvement in separation was noted. Above 40% w/w aqueous buffer, a sharp increase in the migration time of paracetamol was observed. While butyl paraben and sorbic acid also showed an increase in migration time, the change was not as dramatic.

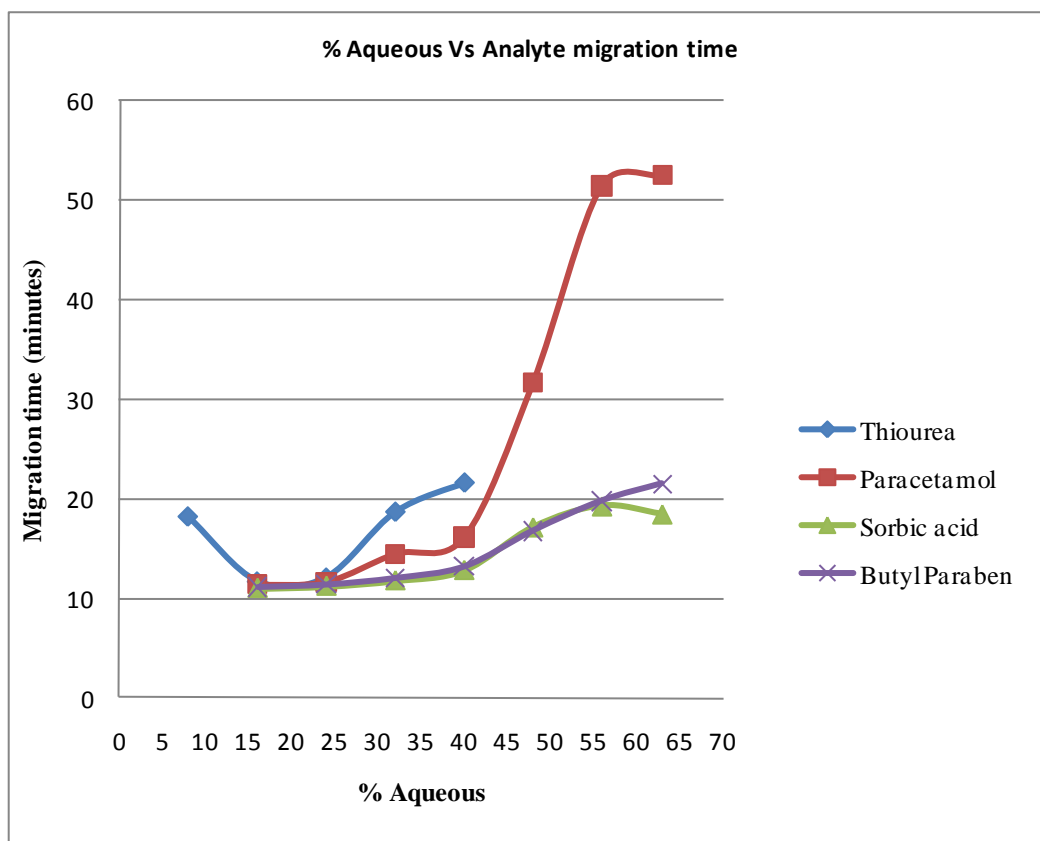


**Figure 8.8** Effect of aqueous buffer concentration on migration time of thiourea, paracetamol, sorbic acid and butyl paraben. Separation conditions; applied voltage -10 KV, cassette temperature 20°C, all other conditions as described in figure 8.7.

Below 32% aqueous buffer, the separation was rapid, and while all peaks were separated the resolution was poor. At 6% aqueous buffer, it appeared that only thiourea migrated past the detector. The behaviour of thiourea was most interesting. Above 40% aqueous phase it was not detected. Since thiourea was a neutral analyte, it would have no electrophoretic mobility of its own and therefore would have to interact with a microemulsion droplet in order to possess a pseudo negative charge and migrate towards the detector. Given that thiourea was highly hydrophilic, it would possibly not interact with an O/W microemulsion droplet and therefore not be detected. Conversely, it would be expected to interact strongly with a W/O microemulsion droplet. The migration behaviour of thiourea suggests a possible change in microemulsion phase at or around a concentration of 40% aqueous buffer. The dramatic increase in migration time for the weakly acidic paracetamol may also suggest a change in the microemulsion buffer. When present within a W/O microemulsion droplet, its migration time would decrease due to its increased negative charge. However, when present in an O/W

microemulsion environment, it would migrate under its own electrophoretic mobility. According to the graph the migration time of paracetamol time levelled out above 55% aqueous buffer, possibly indicating the formation of a stable O/W droplet system.

#### **8.4 Conclusions**

Refractive index, droplet size, conductivity, calorimetry and MEEKC separation suggested a significant change in the nature of the microemulsion system above 24% w/w aqueous phase. The noted shifts in trend may have inferred a change in phase type. However it was not obvious if this change in phase was from W/O to bicontinuous or O/W. A second possible change in phase was observed at aqueous concentrations above 40%. This change was most apparent in droplet size, refractive index and MEEKC separation. Taking the phase transition at 24% to represent W/O to bicontinuous, the transition at 40% may have been bicontinuous to O/W. While surface tension measurements did not imply a clear phase transition at either 24 or 40%, a plateau was noted at aqueous concentrations in between. This plateau was also noted in refractive index, conductivity and in the MEEKC separation (particularly for paracetamol). While no definite conclusions could be made, the plateau may represent a bicontinuous region. Each technique on its own merit may not describe such transitions. However, in combination good agreement was observed.

Further investigations would be useful to test the conclusions drawn above, particularly the use of NMR or small angle scattering. Cross correlation by substituting the microemulsion components with different surfactants, oils etc would be beneficial in determining the capability of the techniques to distinguish and characterise different phase transitions. Interestingly, a very simple technique such as measurement of refractive index, in certain cases, may be capable of indicating complicated phase transitions.

A significant drawback of this work was the fact it was conducted in a region of the phase diagram where microemulsions are unlikely to find use either as mobile phases in HPLC or background electrolytes in CE. It was clear from the phase diagram that the traditional MEEKC microemulsion was in a very small highly aqueous region. While conducting MEEKC under suppressed EOF may possess some advantages for particularly hydrophobic analytes, the majority of applications employ highly aqueous O/W type buffers.

The characterisation of microemulsions discussed in this chapter may be of greater relevance to solubilisation or inclusion of either aqueous or organic components in applications such as drug delivery.

## 8.5 References

- [1] McEvoy, E., Donegan, S., Power, J. and Altria, K., *Journal of Pharmaceutical and Biomedical Analysis*, 44 (2007) 137-143.
- [2] Marsh, A., Clark, B., Broderick, M., Power, J., Donegan, S. and Altria, K., *Electrophoresis*, 25 (2004) 3970-3980.
- [3] McEvoy, E., Marsh, A., Altria, K., Donegan, S. and Power, J., *Electrophoresis*, 28 (2007) 193-207.
- [4] Ryan, R., Donegan, S., Power, J., McEvoy, E. and Altria, K., *Electrophoresis*, 30 (2009) 65-82.
- [5] Boonme, P., Krauel, K., Graf, A., Rades, T. and Junyaprasert, V.B., *Aaps Pharmscitech*, 7 (2006).
- [6] Garti, N., Aserin, A., Tiunova, I. and Fanun, M., *Colloids and Surfaces A- Physicochemical and Engineering Aspects*, 170 (2000) 1-18.
- [7] Spornath, A., Aserin, A. and Garti, N., *Journal of Thermal Analysis and Calorimetry*, 83 (2006) 297-308.

## **Chapter Nine**

### **Conclusions/Future Work**

## 9.1 Microemulsion liquid chromatography (MELC)

The use of microemulsions as eluents and sample diluents in liquid chromatography was presented. Chapter two briefly introduced the advantages and disadvantages of microemulsion use in HPLC. In addition to offering alternative selectivity approaches, microemulsions can be used as sample extraction solvents for a diverse range of analytes and sample matrices. In a typical O/W type system, the oil core can incorporate organic analytes while water soluble analytes are dissolved by the aqueous portion of the microemulsion. Extraction with such solvents may allow reduced sample pre-treatment and higher sample throughput. However, such a technique may still lead to the injection matrix interferences which may complicate chromatography. Also, sample concentration for related substance assays would prove difficult in such a highly aqueous extraction solvent. In general, microemulsions utilise less organics in the mobile phase and thereby present a greener way to conduct HPLC analysis. The inability to perform repeatable gradient separation with MELC is a significant drawback and may limit its application in the pharmaceutical industry.

A microemulsion HPLC eluent was developed for the separation of a range of water- and oil-soluble vitamins. Simultaneous separation of such a diverse range of analytes was conducted to stretch the capabilities of O/W MELC. Up to this point MELC simultaneous separation was only reported for intermediately hydrophobic analytes (e.g. parabens). In the course of method development, the effects of concentration and type of microemulsion components was investigated. It was seen that the co-surfactant type and pH had the greatest effect on the separation. Replacing 1-butanol with 1-pentanol as the co-surfactant increased both the elution strength and solubilisation capacity of the microemulsion, thereby enabling the separation and elution of the oil-soluble vitamins. Conversely, pH had the greatest effect on the separation of the water-soluble vitamins. Given that the separation had to be conducted in isocratic mode, it was quite a challenge to elute and separate such a diverse range of analytes. The use of organic modifiers, while aiding the elution of oil-soluble vitamins, resulted in the co-elution of water-soluble analytes. While baseline separation was achieved for all analytes, the oil soluble vitamins eluted as broad peak over a long time and this impacted on sensitivity. However, the use of gradient conditions would greatly have improved the separation. The method was validated for the assay of vitamin B<sub>1</sub>, C, E and niacin in a pharmaceutical vitamin supplement.

## 9.2 Microemulsion electrokinetic chromatography (MEEKC)

A comprehensive review detailing the methodology and application of microemulsions in CE was reported. MEEKC has proven to be capable of providing fast and efficient separations for a wide range of acidic, basic and neutral, water-soluble and -insoluble compounds. ME composition offers several optimisation options in terms of surfactant/co-surfactant concentration and type, pH and oil type. While SDS remains the most common surfactant in use, there has been an increase in number of reports utilising alternative types of surfactant, such as non-ionic, bile salts and mixed surfactant systems. Enantioseparation had been achieved through the use of chiral ME components as well as through the addition of CDs.

MEEKC has shown good quantitative results when cross-validated with other techniques such as HPLC. With advances in online sample concentration and MEEKC-MS the sensitivity for the detection of trace solutes has been greatly improved.

MEEKC has also found use in predicting brain tissue binding of central nervous system (CNS) drugs based on the relationship between analyte lipophilicity and migration time.

From an analytical standpoint HPLC remains the technique of choice for the majority of pharmaceutical applications. Conversely, CE inhabits a niche area with the majority of applications relating to protein analysis, drug research and chiral separation. CE possesses a number of significant advantages such as low solvent consumption, cheaper consumables (silica capillary vs analytical LC column) and alternative selectivity options. However, the uptake of CE techniques as an alternative methodology to LC continues to face challenges on a number of fronts. In addition to the cost of equipment, analyst retraining and downtime, technique issues such as migration time reproducibility, injection reproducibility and sensitivity also serve to stilt uptake. However, in comparison to the slow uptake of MELC in routine LC applications, the use of microemulsions has fit comfortably into routine CE use. The ability to separate non-polar analytes and the wide range of options for adjusting selectivity has proven very useful. With a wide range of applications, and advances in the theory and methodology, the area of MEEKC is expected to continue growing.

The use of a microemulsion as a background electrolyte in CE was investigated for vitamin analysis through optimisation of microemulsion composition and component concentration. The surfactant type had the greatest affect on the separation of the

water-soluble vitamins. Replacing SDS with sodium cholate as the surfactant greatly improved resolution between the water-soluble vitamins. While separation of water-soluble vitamins was readily achieved using a 'standard microemulsion (SDS, butanol, octane and tetraborate buffer)', a considerable degree of optimisation was required to separate all oil soluble vitamins. In order to achieve separation of the oil-soluble vitamins, the use of mixed surfactant system (SC and SDS) and a significant increase in co-surfactant (1-butanol) concentration with the addition of an organic modifier (IPA) was necessary.

### **9.3 Comparison of MELC and MEEKC**

Compared to MELC, a large concentration of organic modifier could be employed in MEEKC to enhance selectivity without reducing separation between the water-soluble vitamins. Also, while the MELC separation was governed predominantly by the stationary phase interactions, the use of MEEKC allowed a greater number of separation possibilities. Analytes were separated based upon their charge, number of charges, interaction with the microemulsion droplet and electrophoretic mobility. Therefore, it could be concluded that MEEKC presents a greater number of method development options compared to MELC. In the past number of years MEEKC has gained considerable interest with the number of published applications steadily rising, while no more than twelve no new MELC applications have been reported in the same time.

### **9.4 Microemulsion characterisation**

All microemulsion compositions employed in the MEEKC vitamin separation were characterised in terms of droplet size, surface tension, refractive index and conductivity. Results of these measurements were then correlated with respect to changes in composition and the effect on separation. Physical measurements showed a good correlation with changes in ME composition. A notable difference was observed when the droplet size of an SDS micellar system (0.9 nm) was compared to a microemulsion system (1.5 nm). Increasing the SDS concentration corresponded to a decrease in microemulsion droplet size, while replacing SDS with the longer chain cationic surfactant CTAB resulted in an increase in droplet size (1.5 to 3.0 nm respectively). Employing SC as the surfactant resulted in a droplet size of 2.3 nm. Replacing the straight chain internal oil phases with a branched chain 2-octanol was

seen to increase droplet size from 1.5 to 1.8 nm. While variation of co-surfactant concentration did not have a dramatic effect on the droplet size, replacing 1-butanol with 1-pentanol resulted in an increase from 1.8 to 2.8 nm. The inclusion of organic modifiers such as methanol, acetonitrile and isopropyl alcohol had contradicting effects on droplet size. Use of methanol and IPA served to increase droplet size, while ACN resulted in a slight decrease in droplet size. While an increase in droplet size could be seen to improve the vitamin separation (particularly for oil-soluble vitamins), possibly on account of greater partitioning with the oil droplet, direct correlations with respect to composition may also be attributed to changes in charge density, EOF and analyte electrophoretic mobility. In terms of surface tension and inferred stability, the microemulsion had a significantly lower surface tension compared to a micellar (34 and 29 dynes/cm respectively) system. However, in all cases once the micellar system or microemulsion was formed stability was not seen to be an issue. Conductivity measurements were mostly impacted by the type and concentration of surfactant and organic modifier. Increasing the concentration of SDS raised the overall conductivity of the system. Since the increase in surfactant concentration served to increase the negative charge density on the microemulsion droplet, a corresponding increase in the migration time of the oil soluble vitamins was observed. Changes in refractive index across all compositions were small and did not correspond to any significant changes in separation.

A pseudoternary phase diagram was also constructed for an SDS based microemulsion system. Based upon the available single phase region, a number of points were chosen along an aqueous dilution line. The microemulsions phases in this region were then characterised through measurements in droplet size, surface tension, conductivity, refractive index and DSC profile. The microemulsion compositions were also employed as a CE buffer for the separation of acidic, basic and neutral analytes. Through graphing physicochemical measurements across the chosen dilution line changes in microemulsion phase could be inferred. Refractive index, droplet size, conductivity, calorimetry and MEEKC separation suggested a significant change in the nature of the microemulsion system above 24% (w/w) aqueous phase. The noted shifts in trend may have inferred a change in phase type. However it was not obvious if this change in phase was from W/O to bicontinuous or O/W. A second possible change in phase was observed at aqueous concentrations above 40 %. This change was most

apparent in droplet size, refractive index and MEEKC separation. Correlations between inferred phase type and CE separation were also noted.

## **9.5 Future Work**

### **9.5.1 MELC**

#### **9.5.1.2 Gradient onset**

While previous reports have demonstrated the incompatibility of microemulsions with gradient onset, the area may well justify further research. As a means of simplification, initial studies could be conducted using micellar mobile phases in both the aqueous and organic solvents. Separation could proceed initially with the aqueous micellar phase before gradient onset using the organic micellar phase. While the organic phase would disrupt the stationary phase adsorbed layer, the presence of surfactant may allow for quicker equilibration. Such a proposal has not yet appeared in the literature.

#### **9.5.1.3 Robustness testing Experimental design (QbD)**

Given the range of composition variables, robustness testing for a MELC method can be time consuming. A design of experiments using statistical analysis to map and predict critical composition parameters could greatly facilitate method validation. Approaches such as artificial neural networks (ANNs) have been reported.

#### **9.5.1.4 Compatibility of MELC with different stationary phases**

While compatibility with C18 reverse phase and normal phase columns has been reported, it may be of interest to examine different stationary phase types such as Hydrophilic interaction liquid chromatography (HILIC). HILIC is a technique that is complementary to reversed-phase liquid chromatography (RPLC) which utilises a blend of water (aqueous) with a miscible organic solvent to insure the proper interaction of the sample compounds with a polar particle surface. Water competes effectively with polar analytes for the stationary phase. HILIC may be run in either isocratic or gradient elution modes. Polar compounds that are initially attracted to the polar packing material particles can be eluted as the polarity [strength] of the mobile phase is increased [by adding more water]. HILIC allows the separation of very polar analytes that cannot be retained on an RP column and analytes are eluted in order of increasing

hydrophilicity. However, despite its suitability to separate highly polar molecules, HILIC fails to adequately retain more strongly hydrophobic APIs. Moreover, HILIC requires an organic solvent-rich mobile phase, which is undesirable from cost and environmental-sustainability standpoints. While HILIC is often useful for hydrophilicity-based class separation, its flexibility in method development is limited. Employing W/O MELC may present unique selectivity options in addition improving the retention of more hydrophobic analytes.

#### **9.5.1.5 Rapid Resolution MELC**

The area of rapid resolution liquid chromatography has attracted much attention in recent years due to its capacity for increased sample throughput. The methodology involves the use of shorter columns packed with smaller particles and pumps capable of higher back pressures. The reduced particle size (5 to 1.8  $\mu\text{m}$ ) dramatically improves efficiency thereby allowing the use of shorter columns and increased flow rate which improves sample throughput. The reduced particle size coupled with increased flow rate also causes a dramatic increase in system back pressure which necessitates the use of higher specification pumps. The use of MELC has to date not been reported for such a system and may present a useful application.

#### **9.5.1.6 Method for extremes or intermediate polarity analytes**

The development of a LC method for simultaneously separating water- and oil-soluble vitamins demonstrated the working limits of the O/W MELC methodology. There is always a risk when developing a LC technique for two diverse analyte sets that the end result is a method which is suitable for neither. While the method reported in this work was capable of separating both water and oil-soluble vitamins, the chromatography was not ideal. The water-soluble vitamins eluted rather quickly with poor peak capacity and the oil-soluble vitamins were quite broad which impacted sensitivity. It would be of interest to develop and optimise a related substance method for some particular vitamins within each class. Solid phase extraction could be employed as a means for extraction and sample concentration while the O/W microemulsion eluent could be optimised to give maximum separation in a reasonable time. Separation and peak shape of the oil-soluble vitamins could possibly be improved by employing a C8 RP column to reduce retention.

## **9.5.2 MEEKC**

### **9.5.2.1 Online sample concentration/MS/fluorescence**

Sensitivity continues to remain an area of interest for CE methodologies using UV detection, particularly for related substances assays. The reporting of API impurities to 0.1 % places a high demand on sensitivity. While the use of fluorescence detection and the coupling of CE to MS offer a significant advantage, the area of online sample concentration continues to attract attention. Use of online sample concentration enables a cost effective improvement in sensitivity but places an increased demand on the injection repeatability.

### **9.5.2.2 Streamlining method development**

While the variety of composition options available for MEEKC separation offers great opportunity to fine tune selectivity, it can add extra time and cost method development. Similar to the use of ANNs in MELC the creation of predictive modelling software would be a distinct advantage. The work reported in chapters five and six generated data examining microemulsion separation and physicochemical properties. Such data would require further statistical analysis to probe more definite correlations. However, once generated the existing data may prove useful as a training set for predictive modelling software.

### **9.5.3 Microemulsion characterisation**

Further work in the characterisation of microemulsions for separation science is strongly recommended. As discussed in chapter four techniques such as NMR and small angle scattering can investigate microstructure on the nano level. Similar work has been conducted for pharmaceutically useful microemulsions, so the methods could be applied and correlated to better understand separation mechanisms.

The SDS based system examined in chapter eight demonstrated the finite useful region in which such microemulsions employed in MELC or MEEKC may exist. Further investigation into different compositions which expand the area may be beneficial.

## **Appendix**

### **Publications**